

Environmental Drivers of Benthic Community Structure and Function in Fjords of the West Antarctic Peninsula

A Dissertation Submitted to the Graduate Division of the University of Hawai'i at Mānoa in Partial Fulfillment of the Requirements for Degree of

DOCTOR OF PHILOSOPHY
IN
OCEANOGRAPHY

DECEMBER 2019

By
Amanda Fern Ziegler

Dissertation Committee:

Craig Smith (Chairperson)

Jeffrey Drazen

Kyle Edwards

Brian Powell

Amy Moran

Les Watling

Keywords: Antarctic, fjord, diversity, ecosystem function, export flux, larval dispersal

© Copyright 2019 - Amanda Ziegler

All Rights Reserved

To my parents who always encouraged me to strive toward my dreams.

Acknowledgements

I would like to whole-heartedly thank my advisor, Dr. Craig Smith, for his support and guidance throughout this dissertation work. Your passion for and pride in your work is truly inspiring. I am honored to have learned how to be a sea-going oceanographer from you. Thank you for providing me with many amazing opportunities and for your understanding during this long process. I would also like to thank Drs. Kyle Edwards, Jeff Drazen, Brian Powell, Amy Moran, Les Watling and Margaret McManus who contributed so much to my education and each provided unique insights into my work. You have all held me to a high standard which has made me a better scientist.

My dissertation research spanned several branches of oceanography and I am indebted to several collaborators with whom I have been fortunate to learn from. I thank all involved in the FjordEco project who made this dissertation possible. I thank Drs. Øyvind Lundesgaard and Lisa Hahn-Woernle for your intellectual contributions and sincere friendship. I would go to sea with you both again any day. I would like to thank Drs. Mattias Cape and Maria Vernet for their collaboration and mentorship during many phases of my research. As most of my research utilized samples and data collected at sea, I would like to thank the Captains, crews and support staff of the *Nathaniel B. Palmer*, *Laurence M. Gould*, *Thomas G. Thompson*, *Oceanus*, and the *Araon*. The expeditions aboard these vessels not only provided me with priceless scientific data but also experiences that I will remember for a lifetime.

I am deeply thankful to my friends and family who have supported me through the exciting times as well as my struggles. My Oceanography 'Ohana have been by my side celebrating each other's successes. I want to extend my deepest gratitude to Dr. Mackenzie Gerringer for being a wonderfully supportive office mate and inspiration. Thank you for always caring and joining me on coffee dates. I have been surrounded by amazing role models in academia including Drs. Diva Amon, Jennifer Durden and Mackenzie Gerringer. You all inspire me and continue to be my cheerleaders in life. My family have supported my love of the ocean from a very young age and I would not be where I am today without their sacrifices and love. To my parents, Sally and Lon Ziegler, thank you for instilling the courage and

determination to follow my dreams. You've endured my time in Hawai'i which required far fewer visits and calls than I preferred, but your never-ending support, love and encouragement was felt across the thousands of miles of land and sea. I love you. Thank you Patrick A'Hearn for your unconditional love and willingness to stand by my side through this challenging process. Your curiosity of the natural world is admirable, but your silliness and love of life reminds me why I did all of this. I am honored to have all of you in my life and could not have accomplished any of this without you.

Abstract

The West Antarctic Peninsula (WAP) is a unique ecosystem in which harsh environmental conditions influence benthic community assembly processes from dispersal to the development of a complex community. The coastline of the WAP is lined with deep, glaciomarine fjords in which glacial processes affect stratification, sedimentation, and biological productivity which in turn affect the benthos. The environmental background and context of WAP fjords is provided in chapter I. The chapters that follow explore the roles of habitat heterogeneity, larval dispersal, and food availability as drivers of benthic community structure and function in WAP fjords. In chapter II, photographic surveys of WAP fjord and shelf habitats quantify the distribution of hard substrate in the form of glacial dropstones. The inclusion of this substrate type enhances the species richness of WAP benthos by 20% as well as the functional diversity by supporting an abundance of hard-substrate obligate fauna that are predominantly suspension feeders. Colonization patterns of dropstones are consistent with recruitment-limitation rather than by the availability of dropstones suggesting that dispersal processes constrain dropstone colonization. Chapter III explores patterns of larval dispersal and settlement of benthic organisms with varying life-history traits during the austral summer using coupled hydrodynamic and particle-tracking models. Results show that connectivity between neighboring fjords < 50 km apart is lacking for organisms producing larvae with demersal swimming behavior and short development times. > 98% of these larvae were retained within natal fjords indicating that self-recruitment processes are important for maintaining fjord populations. Larvae with long development times that lack swimming abilities were transported away from natal fjords, especially in surface layers (< 100 m) that were affected by episodic Katabatic winds. Connectivity to the broader WAP shelf was increased for these organisms with larval export from our study region reaching up to 39%. While chapters II and III explored the influence of environmental conditions on spatial patterns of community structure, chapter IV investigated the influence of short-term changes in food availability on the function of benthic organisms within a glaciomarine fjord of the WAP. Benthic time-lapse photography was used to quantify the accumulation and utilization of phytodetritus by detritivores. Phytodetritus arrived in a singular pulse in summer which overwhelmed benthic detritivores and developed a sediment food bank storing labile organic matter throughout the winter. Phytodetritus was consumed rapidly by

detritivores which fed throughout the winter months when overlying productivity was absent. The formation of the sediment food bank decoupled detritivore feeding from variability in surface productivity and aids in maintaining high abundances of large detritivores inside the fjord. As fjord productivity is regularly observed to be greater than that of the outer WAP shelf, it is likely that these results are representative of most WAP fjords highlighting the importance of detritivores in the regional carbon cycle. Finally, chapter V summarizes the main findings of this dissertation research, discusses these results in the context of future climatic changes on the WAP and identifies outstanding research questions stimulated from this work. This dissertation provides the first focused study of dropstone communities in the Antarctic, the first modelling study of benthic larval dispersal from WAP fjords and presents a methodology for quantifying seafloor phytodetritus using oblique time-lapse imagery of the seafloor.

Table of Contents

Acknowledgements	i
Abstract	iii
List of Tables	vii
List of Figures	viii
Chapter I Introduction: The West Antarctic Peninsula Ecosystem	1
Broad Hydrographic Context of the West Antarctic Peninsula	1
Detailed Hydrography of Andvord Bay.....	4
Biological Context	5
Fjord Ecosystems.....	9
Reproductive Characteristics of Antarctic Benthic Communities.....	11
Climate Change on the West Antarctic Peninsula	17
References	19
Chapter II Glacial dropstones: islands enhancing seafloor species richness of benthic megafauna in West Antarctic Peninsula fjords	37
Abstract	37
Introduction	38
Materials and Methods.....	41
Results	45
Discussion.....	55
Conclusions.....	61
References	62
Chapter III Dispersal of Antarctic Fjord Benthic Fauna: A Modeling Study	68
Abstract	68
Introduction	68
Methods	73
Results	80
Discussion.....	91
References	98
Chapter IV Intense deposition and rapid processing of seafloor phytodetritus in a glaciomarine fjord, Andvord Bay (Antarctica).....	114

Abstract	114
Introduction	115
Methods	118
Results	134
Discussion	137
Conclusion	141
References	142
Chapter V Conclusion: Community Structure and Function of West Antarctic Peninsula	
Benthos	159
References	168
Appendix: Supplementary Material	177
References	198

List of Tables

Table 1.1 Reproductive characteristics of Antarctic benthic fauna	16
Table 2.1 Summary of dropstone measurements by sampling location	47
Table 2.2 Morphotypes present in groups identified by canonical analysis of principal coordinates	53
Table 2.3 Summary of diversity indices	55
Table 3.1 Life history traits of Antarctic organisms with high and low dispersal potential	78
Table 3.2 Modeling scenario details	80
Table 4.1 Phytodetritus definitions in HSV color-space	127
Table 4.2 Correlation table of environmental data, fecal pellet production and phytodetritus cover	136
Table 4.3 Deposit-feeding rates of benthic taxa	140

List of Figures

Figure 1.1 The Antarctic Peninsula region and detailed bathymetry for the region of study.....	1
Figure 1.2 Circulation surrounding the Antarctic Peninsula.....	3
Figure 1.3 Inter-annual variability in magnitude and timing of seafloor phytodetritus flux along the West Antarctic Peninsula.....	8
Figure 1.4 Community assembly processes.....	9
Figure 1.5 Spatial model of Arctic fjord benthic community structure and disturbance gradient.....	10
Figure 1.6 Contrasting down-fjord species richness patterns in Arctic and Antarctic fjords.....	11
Figure 1.7 Relationships of larval development time vs temperature and dispersal distance vs pelagic larval duration.....	13
Figure 1.8 Trends in temperature and sea ice extent along the Antarctic Peninsula.....	18
Figure 2.1 Photographic transect locations and bathymetry.....	42
Figure 2.2 Colonization proportion of dropstones	48
Figure 2.3 Examples of colonized dropstones from <i>in situ</i> photographs	49
Figure 2.4 Non-metric multidimensional scaling analysis visualization.....	51
Figure 2.5 Canonical analysis of principal coordinates visualization.....	52
Figure 2.6 Morphotype groupings from canonical analysis of principal coordinates.....	53
Figure 2.7 Chao 1 species richness estimates for fjord and shelf phototransects.....	54
Figure 2.8 Examples of dropstone use by <i>Ptychogastria polaris</i> and <i>Chaenodraco wilsoni</i> in <i>in situ</i> photographs.....	60
Figure 3.1 Detailed bathymetry of the model domain.....	75

Figure 3.2 Settled particle distribution heatmaps for low dispersal potential model simulations.....	81
Figure 3.3 Recirculation features visible in particle trajectories	83
Figure 3.4 Settled particle distribution heatmaps for Andvord Bay high dispersal simulations	85
Figure 3.5 Settled particle distribution heatmaps for Flandres Bay high dispersal simulations	86
Figure 3.6 Percentage of particles settling in neighboring fjord across all pre-competency periods	87
Figure 3.7 Mean dispersal distance of high dispersal potential simulations	88
Figure 3.8 Time series of environmental conditions and particle transport for Andvord Bay releases	90
Figure 3.9 Time series of environmental conditions and particle transport for Flandres Bay releases	91
Figure 3.10 Conceptual connectivity diagram of low dispersal model simulations.....	94
Figure 3.11 Conceptual connectivity diagram of high dispersal model simulation.....	96
Figure 4.1 Time-lapse camera deployment location in Andvord Bay	119
Figure 4.2 The time-lapse camera system with components labeled	121
Figure 4.3 An oblique image from the time-lapse camera with Canadian perspective grid overlaid	122
Figure 4.4 Example time-lapse camera images from across the entire time series	124
Figure 4.5 Seafloor regions quantified for phytodetritus cover and fecal pellet production	125
Figure 4.6 Identification of <i>Amythas membranifera</i> tubes, fecal pellets and sinking particles	128
Figure 4.7 Comparison of sinking particle abundances	130
Figure 4.8 Time series of phytodetritus cover, environmental conditions and fecal pellet production	133

Chapter I Introduction: The West Antarctic Peninsula Ecosystem

Broad Hydrographic Context of the West Antarctic Peninsula

The West Antarctic Peninsula (WAP) is a mountainous spine extending northward approximately 1300 km from 75°S, on West Antarctica, to the South Shetland Islands (Figure 1.1). The coastline is a rugged network of glacially carved fjords and channels with steep topography rising rapidly to summits of over 2000 m. The Antarctic continent is nearly entirely covered by massive ice sheets reaching up to 4 km thick, which depresses the continental shelf to an anomalously deep ~ 500 m on average (Ducklow et al. 2007). The Antarctic Peninsula Ice Sheet, however, is substantially thinner than that of either the West or East Antarctic Ice Sheets and at the coast of the peninsula, this ice flows as hundreds of glaciers and few small ice shelves that terminate in the ocean (i.e. they are glaciomarine). Glaciomarine fjords, therefore, provide conduits between the terrestrial cryosphere and the oceanic realm, and this relationship has implications for both the physics and biology of this ecosystem that will be discussed further. The latitudinal extent of the WAP generates a natural laboratory for research involving gradients of temperature, light and sea ice as the climate ranges from sub-polar at the northern tip to fully polar at its base (Martinson et al. 2008).

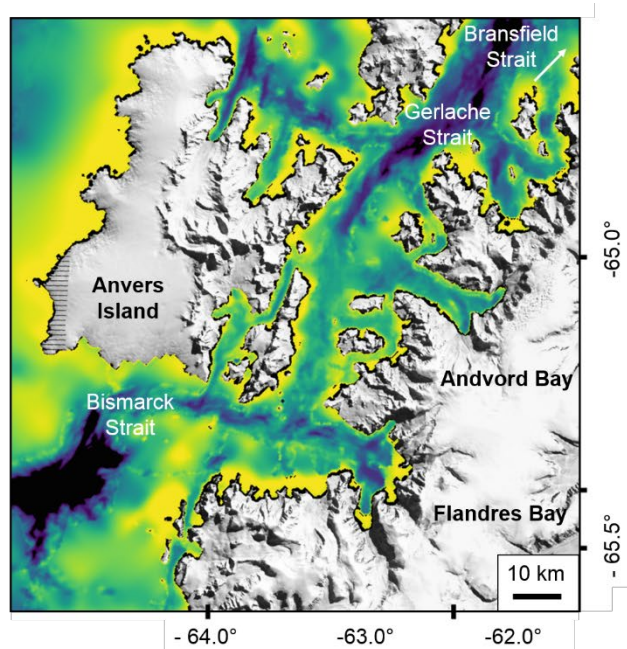
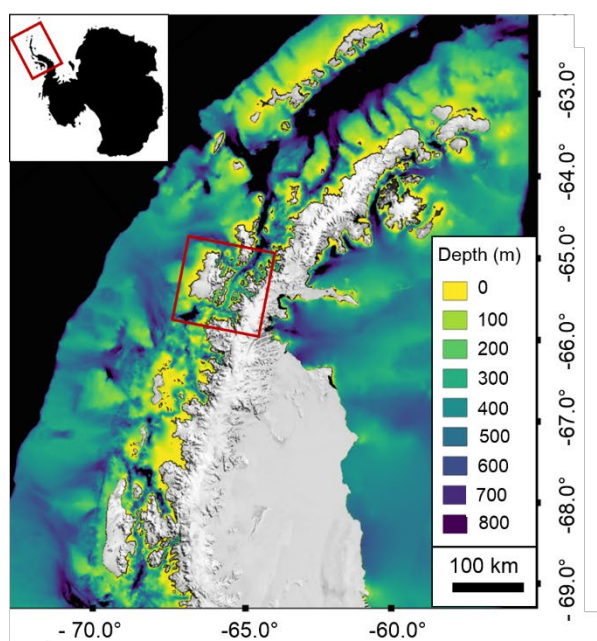


Figure 1.1 The Antarctic Peninsula (left). The WAP region encompassing Andvord and Flandres Bays is shown in greater detail on the right. Bathymetry (depth in m) is provided in color for both regions.

Circulation around Antarctica is dominated by the Antarctic Circumpolar Current (ACC); a narrow, deep, cyclonic current that circumnavigates the continent along the shelf break driven by strong, consistent westerly winds (Nowlin and Klinck 1986). The establishment of the ACC nearly 35 MYA led to the geographic isolation and glaciation of Antarctica (Barker et al. 2007), the biological implications of which are discussed on pg. 8. Interaction between the ACC and the Antarctic Peninsula forms a recirculation gyre in the Weddell Sea and a current transporting Weddell Sea Water southwestward through the Bransfield Strait (Figure 1.2). Inland along the coast of the Antarctic Peninsula, there are observations of an Antarctic Peninsula Coastal Current (APCC) seaward of Anvers Island and around Adelaide Island (Dinniman et al. 2011). These circulation features dictate the water mass properties along the Antarctic Peninsula. At the tip of the peninsula, Weddell Sea Water cools the surrounding Bransfield Strait Water (BSW), creating a cold, saline water mass with a characteristic temperature and salinity of $< 0^{\circ}\text{C}$ and 34.45-34.6 PSU (Hofmann et al. 1996). At the surface, Antarctic Surface Water (AASW) is defined by a thermal minimum of $< -1^{\circ}\text{C}$ and moderate salinity around 34 PSU (Hofmann et al. 1996). This water mass is the result of atmospheric cooling during the winter and may appear as an isolated water mass centered at approximately 100 m during the summer (Winter Water, Hofmann *et al.*, 1996). Along the continental shelf break, the dominant water mass is Circumpolar Deep Water (CDW), with a characteristically warm and saline signature ($> 1^{\circ}\text{C}$, 34.6-34.73 PSU). Modifications of CDW exist (e.g. Upper Circumpolar Deep Water and Lower Circumpolar Deep Water) depending on the contribution of AASW, the season, and location along the peninsula (Moffat et al. 2008). The hydrographic structure of the WAP region changes substantially in a pronounced seasonal cycle due to sea-ice formation/melt and wind-driven mixing processes (Moffat et al. 2008). In addition, the extent to which CDW crosses the shelf-break to influence inland water masses varies substantially along the peninsula with topographic pathways along some canyons such as at Marguerite Trough (Couto et al. 2017; Moffat et al. 2009; Klinck et al. 2004; Dinniman

et al. 2011). These intrusions increase water temperatures locally and increase glacial basal melt rates in some locations (Dinniman et al. 2012; Pritchard et al. 2012). Cryosphere-ocean interactions within glaciomarine fjords globally have been linked to glacial ice loss (Mortensen et al. 2011; Rignot et al. 2013; Rignot et al. 2015) and sea-level changes (Straneo and Cenedese 2015). The confluence of warmer CDW-dominated waters and colder BSW-dominated waters occurs around Anvers Island between Flandres Bay and Andvord Bay; two glaciomarine fjords (black box in Figure 1.1). Bottom water temperatures (~ 500 m) in these fjords can differ by 1°C (Smith, unpub. data) and a modified CDW signature was recently observed seasonally within Andvord Bay (Lundesgaard et al., in press). Typically, shallow sills at fjord mouths prevent exchange of deep external waters, but reasonably deep sills in Andvord and Flandres Bays makes these fjords particularly susceptible to future intrusions as the extent of CDW expands vertically, water masses warm ubiquitously, and intrusions increase in frequency and duration. The impacts of these intrusions is not well known; however, increased exchange with deeper nutrient-rich waters could provide an additional nutrient source supporting productivity.

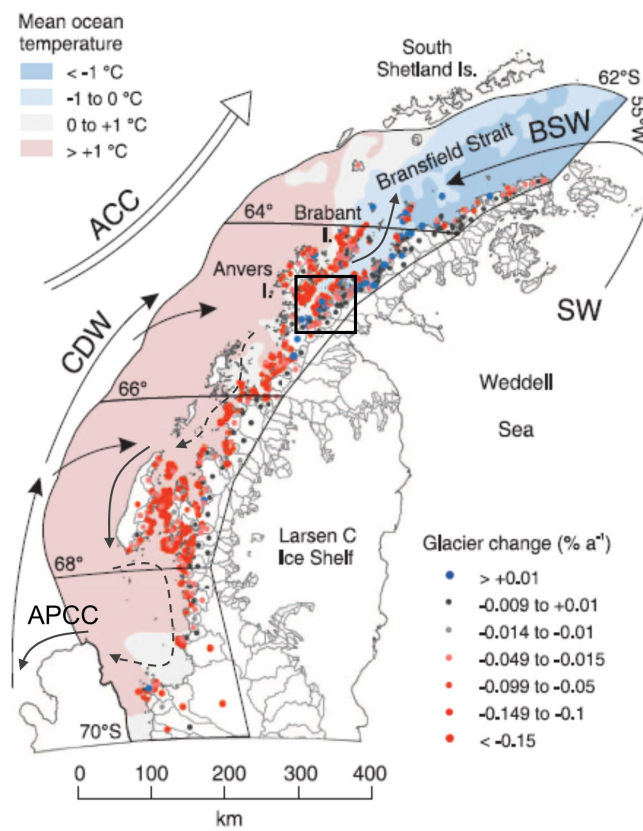


Figure 1.2 Circulation of the Antarctic Peninsula (modified from Cook et al. 2016). Solid lines represent currents supported by substantial observational data while dashed lines represent inferred current pathways. Water mass temperatures are shown in color and colored dots represent glacial advance/retreat rates. Current and water mass abbreviations: Antarctic Circumpolar Current (ACC), Antarctic Peninsula Coastal Current (APCC), Bransfield Strait Water (BSW), Shelf Water (SW), and Circumpolar Deep Water (CDW). The boxed region is the focus of this dissertation.

Detailed Hydrography of Andvord Bay

Andvord Bay is bordered by several fast-flowing glaciers ($> 7 \text{ m d}^{-1}$) which produce $\sim 2 \times 10^{12} \text{ kg y}^{-1}$ of solid ice, with the largest source from Bagshawe Glacier (Lundesgaard et al., in press) in the innermost SW basin of Andvord Bay. Waters within Andvord Bay are dominated by BSW with temperatures $< 0.5^{\circ}\text{C}$ at depths $> 300 \text{ m}$, and though there is substantial seasonal temperature variability, especially in surface waters ($-1.4 - +1.2^{\circ}\text{C}$), this is not caused by the import of warmer water from the Gerlache Strait but from solar heating during summer (Lundesgaard et al., in press). The consistently cold deep waters of Andvord Bay maintain glaciers which are not rapidly retreating (Cook et al. 2016) and meltwater input is estimated to be substantially lower than the contribution of solid ice (Lundesgaard et al., in press). Weak plumes of slightly colder water, presumably from subsurface glacial melt, were observed near Bagshawe Glacier (50-200 m) during the early fall (April, 2016) and have been observed previously (Domack and Williams 1990; Domack and Ishman 1993) but this melting appears to be too weak to drive significant circulation in the fjord (Lundesgaard et al., in press). Surface salinity variability is low in Andvord Bay with minimum values observed around 33.5 PSU; not characteristic of strong meltwater input as is observed for the WAP (Lundesgaard et al., in press). Sea ice concentrations within Andvord Bay are typically low throughout the spring and summer months (Nov. - Mar.) and observations show increasing concentrations by early fall (end April), but full coverage did not occur until August and the fjord remained completely covered for only 1-2 months during winter.

Andvord Bay is a quiescent, low-energy fjord with current velocities of only a few cm s^{-1} , low turbulent kinetic energy dissipation ($\epsilon \sim 10^{-9} \text{ W kg}^{-1}$), and low tidal energy (amplitudes $\sim 1 \text{ cm s}^{-1}$) (Lundesgaard et al., in press). The bordering Gerlache Strait is more energetic, despite similarly weak tides, but substantially higher current velocities (Lundesgaard et al., in press). The greatest turbulence was measured at the mouth of Errera Channel on the northeast coast of Andvord Bay and is attributed to tidal interaction within the channel (Lundesgaard et al., in press). Circulation in Andvord Bay is weakly layered with a northward (down-fjord) flow $< 300 \text{ m}$ and southward (up-fjord) flow in the deep water $> 300 \text{ m}$ (Lundesgaard et al., in press). Flow in the Gerlache Strait is predominantly to the northeast driven by consistent northeasterly winds and intensifies toward its main channel near the South Shetland Islands in the Bransfield Strait with a surface velocity of $\sim 30 \text{ cm s}^{-1}$ (Zhou et al. 2002). Circulation within Andvord Bay is generally decoupled from that of the Gerlache Strait and water mass distribution suggests isolation of fjord waters, despite the lack of a shallow sill as is characteristic of temperate and boreal fjords. Exchange with Gerlache Strait waters and *in situ* mixing ventilates the deep waters of Andvord Bay maintaining high concentrations of oxygen (Lundesgaard et al., in press). It is possible that deep water oxygen content is restored via the transport of Gerlache Strait waters during strong Katabatic wind events, which have been documented in other fjord systems (Spall et al. 2017; Moffat 2014; Klinck and O'Brien 1981; Svendsen and Thomsson 1978). These winds originate from the dry, cold plateaus surrounding fjords and travel rapidly down the glaciers at the head of the fjord to impart strong wind forcing on surface waters. Recent modeling suggests that these wind events can rapidly export the upper 35 m of water from Andvord Bay during the summer (Lundesgaard et al. 2019).

Biological Context

The Antarctic Peninsula is a hotspot of biological productivity with primary production of up to $2 \text{ g C m}^{-2} \text{ d}^{-1}$ (Ducklow et al. 2008; Smith et al. 1996; Karl et al. 1987) and an annual average of $182 \text{ g C m}^{-2} \text{ y}^{-1}$ (Vernet et al. 2008), which maintains high standing stocks of all trophic levels (Ducklow et al. 2007; Nowacek et al. 2011; Santora and Veit 2013). The coastal WAP is also important for Antarctic krill (*Euphusia*

superba), a keystone species, which performs onshore-offshore ontogenetic migrations (Nicol 2006), forming enormous aggregations in WAP fjords including Andvord Bay (Espinasse et al. 2012; Nowacek et al. 2011). Extreme seasonality in light intensity, day length and sea-ice concentration results in high variability of productivity throughout the year. During the fall months (Apr. - Jun.), sea ice formation begins, and as light intensity and day length decrease below levels required for photosynthesis, phytoplankton growth ceases. In the early spring (Oct. - Nov.), light intensity and day length increases causing the retreat of sea ice. Reduced nutrient uptake during winter and an increase in mixing following the retreat of sea ice stimulates rapid phytoplankton growth (Ducklow et al. 2007; Vernet et al. 2008). Chlorophyll-*a* concentrations have been observed to increase from $< 0.5 \text{ mg m}^{-3}$ to $> 15 \text{ mg m}^{-3}$ during blooms (Smith et al. 2008). Phytoplankton growth continues throughout the summer months (Dec. - Mar.) until light and sea ice again become growth-limiting. There is a consistent offshore decrease in chlorophyll-*a* concentration, phytoplankton abundance, and phytoplankton biomass of an order of magnitude (Vernet et al. 2008) making the inshore waters of the WAP significantly more productive than even the nearby outer shelf waters. The phytoplankton community along the coastal WAP is dominated by diatoms and cryptomonads with substantial spatio-temporal variability (Vernet et al. 2008; Smith et al. 1998; Schofield et al. 2017). In Andvord Bay, diatoms are typically present in the earliest spring bloom period and succeeded by microplankton such as cryptomonads (Vernet, pers. comm.). The seasonal cycle of productivity and succession of the phytoplankton community can dramatically affect carbon export from the euphotic zone. Carbon flux may be influenced by processes favoring aggregation (e.g. turbulence or mixing, Levy, 2008), the presence of sea ice from which ice algae melt (Smith et al. 2006a), the size of dominant phytoplankton species (Vernet et al. 2008), and grazing by zooplankton (Gleiber et al. 2012). Long-term studies of particle export show high variability across repeat sampling locations as well within a site and even within a single growing season (Holm-Hansen et al. 1987; Karl et al., 1987; Wefer et al., 1988; Karl et al. 1991; Ducklow et al., 2006; Buesseler et al., 2010, Figure 1.3).

Surface productivity and organic carbon flux to the seafloor provides a connection between pelagic and benthic habitats that has been shown to result in a coupling between pelagic and benthic processes (i.e. pelagic-benthic coupling). For instance, the amount of detritus delivered to the seafloor limits the biomass and activity of the seafloor community such that a relationship between particulate organic carbon (POC) flux, benthic respiration and nutrient cycling is observed (Hartnett et al. 2008; Jahnke 1996). Pelagic-benthic coupling can occur in either a “top-down” or “bottom-up” direction, but the most prominent coupling for benthic systems is the top-down influence of POC flux described above. In fact, POC flux influences the abundance, biomass and respiration of all organismal size classes as well as sedimentary processes in abyssal oceans (Smith et al. 2008). In detritus-based food webs of the deep ocean (> 200 m), POC flux represents food availability which imposes direct limitations on growth, reproduction and recruitment with community and population level consequences. On the WAP shelf, however, seafloor community processes (e.g. recruitment) are surprisingly decoupled due to an accumulation of labile organic matter (i.e. sediment food bank) which supports the community throughout the winter season (Mincks et al. 2005; Mincks and Smith 2007; Smith et al. 2008). Food availability, however, is not the only control on abundance, biomass, community structure and diversity of Antarctic benthic communities. In shallow regions of the shelf < 200 m, disturbance by ice scour is one of the most influential processes driving the colonization and succession of the benthos (Barnes and Conlan 2007; Gutt 2001; Gutt and Piepenburg 2003). From an ecological perspective, these processes and other environmental conditions act as “filters” selecting successful fauna for a particular habitat and ultimately assemble (and maintain) local benthic communities (Figure 1.4). This “filtering” occurs during the dispersal process (in the larval phase or with immigrating adults) as well as within local communities over longer timescales through processes such as competition for space or food. The community composition one observes at a given point in time integrates these processes over a variety of timescales. It is important, therefore, to consider how environmental conditions affect the different aspects of community assembly so we may better understand the changes these communities may face in the future.

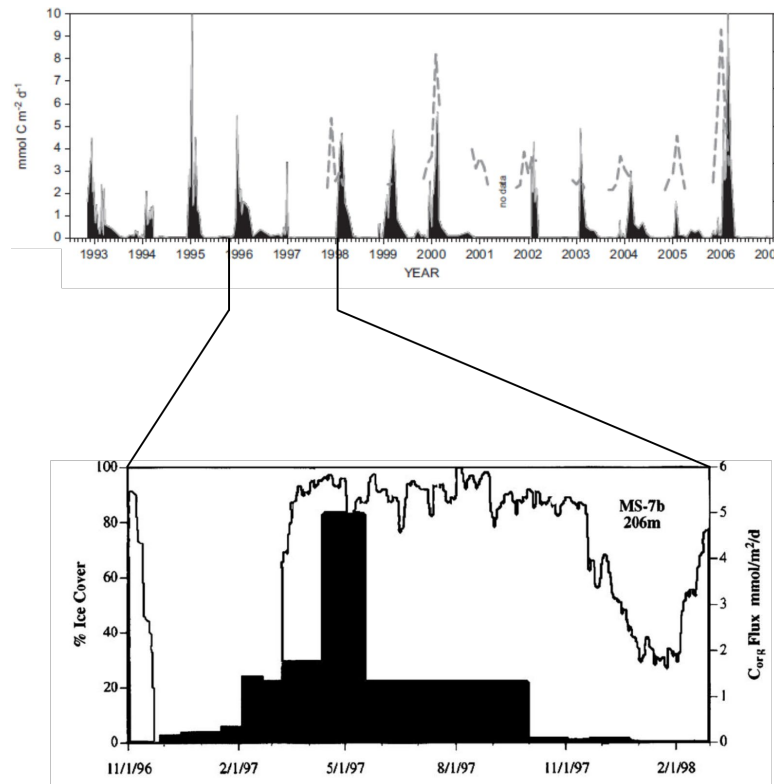


Figure 1.3 Inter-annual variability in the magnitude of carbon flux on the WAP (top panel) as well as the within-season timing of carbon flux compared with the seasonal cycle of sea-ice cover (bottom panel). In the bottom panel, ice cover is provided by the solid line while carbon flux is given by solid black bars. Dashed lines in the top panel show surface chlorophyll-*a* concentration from SeaWiFS when data are available. Modified from Ducklow et al. 2008 (top) and Smith et al. 2006 (bottom).

Historically, the Antarctic shelf was assumed to harbor a low diversity of organisms because of intense disturbance regime and physiological limitation from temperature (Clarke 2008a). Ice scour disturbance, however, is restricted to depths of < 200 m, and early work by Dell (1972) and later by many others (e.g. (Arntz et al. 1994; Clarke and Johnston 2003; Brandt et al. 2007; Gutt and Starmans 2003; Piepenburg et al. 2002) has shown diversity of even deep Antarctic communities to be substantially higher than previously hypothesized (reviewed by Clarke, 2008).

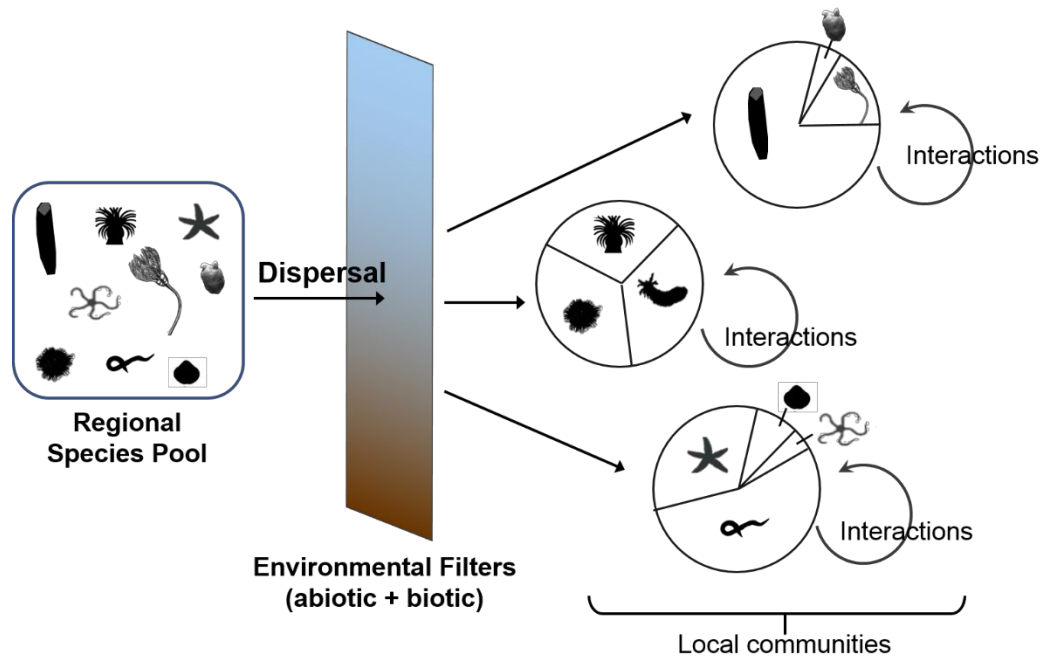


Figure 1.4. Community assembly processes diagram modified from Mittelbach and Schemske 2015. In this diagram, the pool of species in a region are subject to the process of dispersal where they interact with their environment (including biotic environment of other organisms) and undergo a selection process or “filtering” to form various local communities in the larger region. Within these local communities, additional interactions among species occur (e.g. competition for space and food) and results in the community composition we observe at a given point in time.

Fjord Ecosystems

Given the observed onshore trend of increasing phytoplankton biomass along the WAP and efficient export of this material to depth, it may not be surprising that benthic megafauna in WAP fjords are more abundant than on the adjacent shelf (Grange and Smith 2013). However, what is particularly surprising about these communities, is that they are up to 38 times more abundant and there is no reduction in species richness or total biomass toward the head of the fjords in proximity to active glacial fronts (Grange and Smith 2013). This is contrary to substantial work conducted in temperate and Arctic glaciomarine fjord systems (Holte and Gulliksen 1998; Kedra et al. 2010; Maria and Weslawski 2008;

Renaud et al. 2007; Renaud et al. 2007; Syvitski 1989; Włodarska-Kowalczyk et al. 2012; Włodarska-Kowalczyk and Pearson 2004; Włodarska-Kowalczyk et al. 2005). These studies all conformed to the paradigm that glacial sedimentation causes severe burial and ice scour disturbance yielding depauperate benthic communities dominated by few, opportunistic mobile species near the glacial front and a general increase in diversity, biomass, community complexity and sedimentary processes (e.g. bioturbation) with increasing distance from the glacial front out to the open shelf (Włodarska-Kowalczyk et al. 2012; Włodarska-Kowalczyk et al. 2005, Figure 1.5).

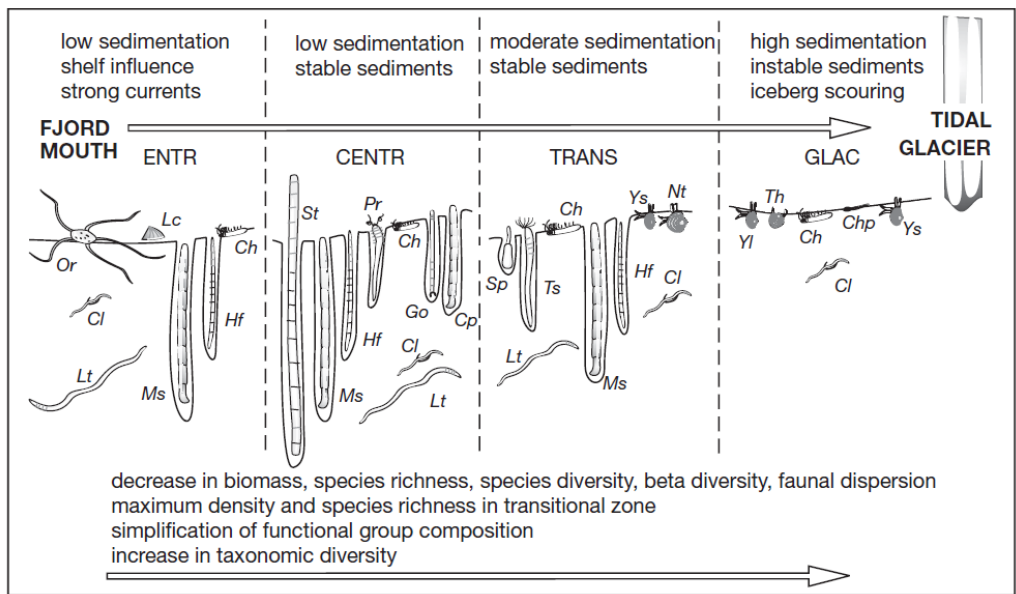


Figure 1.5 Spatial model of Arctic fjord benthic community structure in response to gradients of glacial sedimentation and disturbance (Włodarska-Kowalczyk et al. 2005).

Though Arctic and temperate glaciomarine fjords follow this model very well, Antarctic fjords do not. Glaciers in fjords along the WAP, though many are in a state of retreat, are not melting in the same manner as in Arctic fjords. Many WAP glaciers shed predominantly solid ice and experience basal melting from interactions with the ocean. Arctic and temperate glaciers, however, melt predominantly from surface heating and carry significantly more terrigenous sediments in subglacial flows into the surrounding

waters, imparting a much greater sedimentation disturbance (Domack and Williams 1990; Grange and Smith 2013; Lundesgaard et al. 2019).

Opposing patterns of Arctic/temperate and Antarctic fjord benthos is illustrated in Figure 1.6. Grange and Smith (2013) found that the community composition of WAP fjords was distinct even from neighboring fjords separated by < 50 km (e.g. Flandres and Andvord Bays) as well as from the adjacent shelf. These findings suggest that there are processes unique to the fjords which enhance local benthic abundance, species richness, diversity and body size compared to the shelf and that there are processes potentially limiting the exchange of these organisms between neighboring fjord habitats.

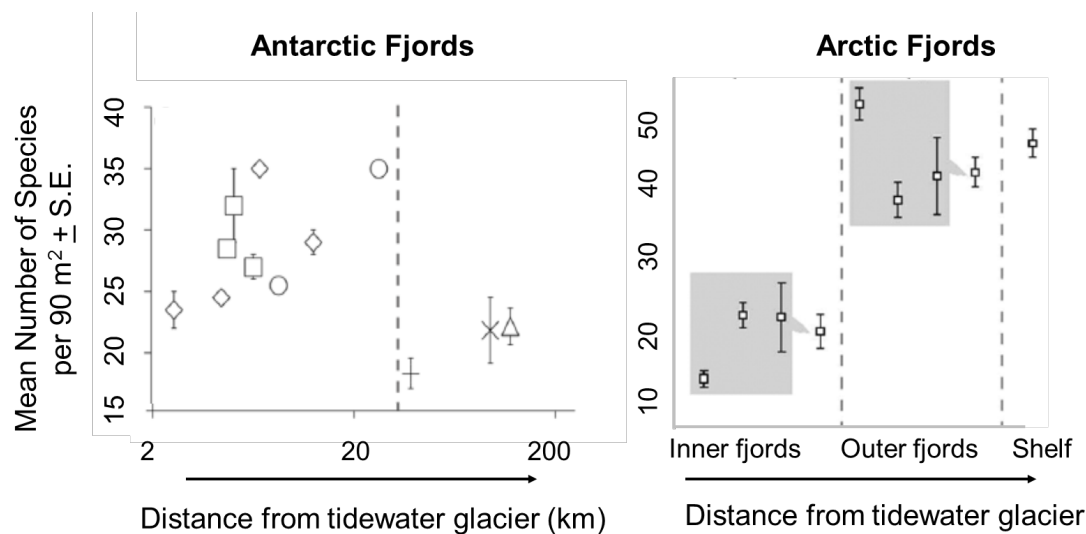


Figure 1.6 Species richness along a down-fjord gradient for Antarctic fjords (from Grange and Smith, 2013) and Arctic fjords (modified from Włodarska-Kowalczyk et al., 2012).

Reproductive Characteristics of Antarctic Benthic Communities

The harsh environmental conditions and isolation of the Antarctic have served as selective pressures since the continent's glaciation (~ 35 MYA) and shape the characteristics of extant fauna (see review by Brandt, 2005). In general, Antarctic benthos are K-selected; they are slow-growing, long-lived, mature later in life, exhibit low fecundity, and grow to large adult sizes (Clarke 1979). Many of these characteristics are related to low temperature and the energetic tradeoffs of reproduction. First, tradeoffs

between adult body size and egg size and fecundity mean adult females grow to larger sizes and produce more or larger eggs than low latitude relatives. Second, the seasonality of food availability acts as a selective pressure for organisms with planktotrophic (feeding) larvae such that spawning times are expected to align with spring blooms, so larvae emerge during peak phytoplankton production (Pearse et al. 1991). This requires spawning typically in the late winter, spring or early summer (Oct. - Jan.). Low temperature also increases the development time of larvae because of physiological kinetics. Because of the consistently low water temperatures in Antarctica, even a 2°C increase reduces the development time of echinoids (Bosch et al. 1987) and krill (Ross and Quetin 1986) by half and causes a shift in the timing of reproduction in the benthic shrimp *Notocrangon antarcticus* (Lovrich et al. 2005). The characteristics described above led to the hypothesis that organisms which brood young, exhibit direct development, or produce fewer and larger lecithotrophic (non-feeding) larvae would dominate at high latitudes (Thorson 1950a). This hypothesis was supported by observations of declining proportions of planktotrophy with increasing latitude attributed to cold temperatures and low food availability and the relationship was later coined “Thorson’s Rule” (Mileikovsky 1971a). While this trend is observed in many groups (e.g. echinoids), there are numerous exceptions and planktotrophy is now recognized as a prominent reproductive strategy of Antarctic fauna (Mileikovsky, 1971; Bosch and Pearse, 1990; Pearse et al. 1991; Clarke, 1992; Pearse, 1994; Poulin and Féral, 1996, Table 1.1). Planktotrophic larvae require a minimum developmental period in the water column, known as the pre-competency period, which is generally longer for high-latitude species than for low-latitude species (i.e. longer development time, Bosch et al., 1987; Stanwell-Smith and Clarke, 1998; Peck, Convey and Barnes, 2006, Figure 1.7 a). The larvae are dispersed via ocean currents for some period and once competent to settle, larval behavior may be altered to promote settlement (e.g. downward swimming), and larvae either contact suitable substrate to metamorphose or they perish in the plankton.

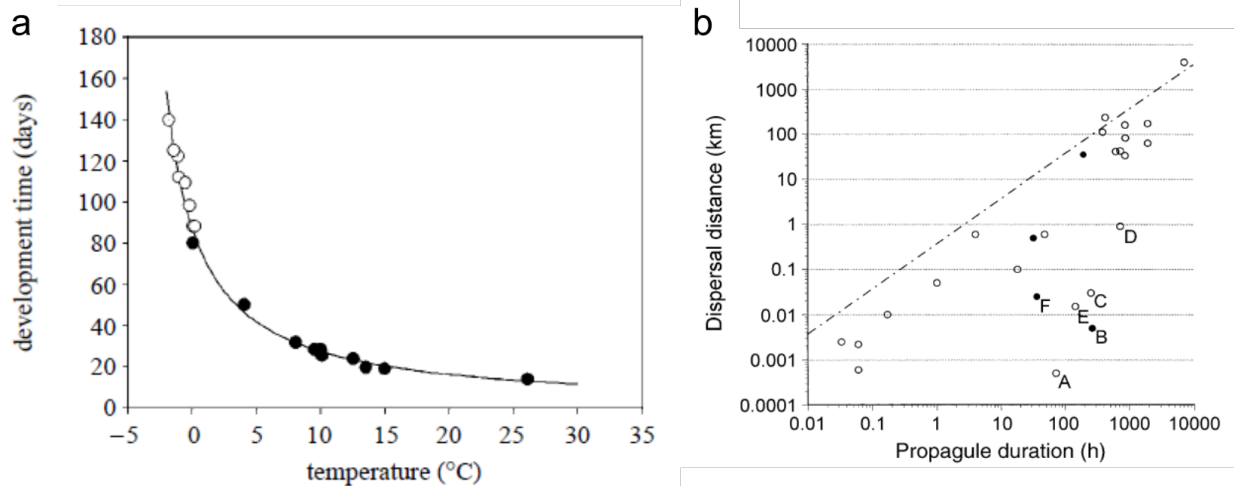


Figure 1.7 (a) The relationship between development time and temperature for echinoderms from tropical to polar habitats (Clarke et al. 2007, from Bosch et al. 1987 and Stanwell-Smith and Peck, 1998). (b) A linear relationship between dispersal distance and PLD (propagule duration) for a wide range of species reported in the literature (Shanks et al. 2003).

The total time spent in the water column until settlement is referred to as the pelagic larval duration (PLD). It is extremely difficult to determine accurate PLDs for invertebrates because their larvae are small, occur at low densities in the water column, and are difficult to identify even to higher taxonomic levels. These characteristics preclude the use of traditional methods such as mark and recapture as well as *in situ* larval tracking. Therefore, PLDs are often reported in the literature from laboratory studies that monitor the survival of larvae until settlement and may better represent the pre-competency period and provide a conservative estimate of true PLD. The pre-competency period is the minimum time required for larvae to develop in the water column prior to settlement. Regardless, pre-competency period and PLD data are difficult to obtain and are lacking for most Antarctic benthos. Table 1.1 provides the life-history traits of some common Antarctic benthic organisms for which data are available. Determination of accurate PLDs and pre-competency periods is very important as organisms with sessile adult forms rely on the pelagic larval stage for wide ranging dispersal. Long distance dispersal is advantageous because it

maintains greater genetic variation, thus improving long-term fitness of a population and the potential for range expansions which could be important for organisms experiencing habitat shifts from climate change. The assumption underpinning this strategy is a causal relationship between PLD (or pre-competency period in the water column) and dispersal distance (Figure 1.7 b) which varies among taxa (Selkoe and Toonen 2011; Shanks et al. 2003; Siegel et al. 2003; Weersing and Toonen 2009).

The development of molecular techniques to measure genetic connectivity of organisms and infer dispersal has revealed many instances of population genetic structure which seem otherwise capable of long-distance dispersal (e.g. Sköld et al. 2003; Paris et al. 2007; Siegel et al. 2008; Cunningham *et al.*, 2009; Ledoux *et al.*, 2012; Riesgo et al. 2015). Retentive circulation features, PLD and larval behavior have now been acknowledged as major factors affecting the true dispersal of marine larvae (Bilton et al. 2002; Bingham and Young 1991; Breusing et al. 2016; Cunningham et al. 2009; Mullineaux and Mills 1997; North 2008; North et al. 2008; Palumbi 1994, 2003; Paris et al. 2007; Siegel et al. 2003; Thornhill et al. 2008; Woodson et al. 2012; Woodson and McManus 2007; Wright 1943; Xu et al. 2018). One way to incorporate both circulation and larval behavior into the determination of dispersal distances is through coupled hydrodynamic and particle tracking models (e.g. Döös et al. 2013; North 2008; Bidegain et al. 2013; Thorpe et al. 2004; Paris et al. 2013). These models utilize 3-dimensional parameter predictions of hydrodynamic models (e.g. ROMS, HYCOM, MITgcm) in space and time to calculate the 3-dimensional trajectories of simulated larvae with a variety of optional characteristics including buoyancy, swimming velocity, or more advanced behavior such as diel vertical migrations and ontogenetic behavior shifts. Data processing capabilities now allow for very high-resolution hydrodynamic models optimized for a specific region and subsequent particle tracking on very small scales. Studies using these models have investigated dispersal in the deep ocean where it is otherwise difficult to collect larval samples (e.g. Young et al. 2012; Arellano et al. 2014) or track larvae for species for which little is known about PLD or behavior (Hilario et al. 2015). In the Antarctic, dispersal-driven modeling studies are still few and mostly focus on krill or commercially important fish species to inform fisheries management (Thorpe et al. 2004,

289 2007; Piñones et al. 2013; Fach and Klinck, 2006; Hofmann and Murphy, 2004; Ashford et al. 2010, 2012;
290 La Mesa et al. 2015). These modeling methods could prove useful when applied to ecological questions
291 regarding the dispersal of benthic fauna, especially in regions facing significant climate changes.

292 **Table 1.1** Reproductive characteristics of Antarctic organisms with high and low dispersal potential from the literature.

Organism	Larval Mode	Larval Release Time	Pre-Competency Period	Pelagic Larval Duration	Fecundity	References
Low Dispersal Potential						
Tunicata *						
<i>Cnemidocarpa verrucosa</i> *	lecithotrophic	June - July / Oct. - Nov.	~ 2 weeks, 8-16 days	~ 8 days		12, 13
Porifera *	lecithotrophic		Hours	12 hours - 2 weeks		14, 15, 16
High Dispersal Potential						
Brachiopoda *						
<i>Liothyrella uva</i>	lecithotrophic	Jan.	70 - 115 days (brooded)	≥ 45 days	20-4,000	7, 8, 9
Echinodermata: Crinoidea *						
<i>Promachorcinus kergulensis</i>	lecithotrophic?	Oct. - Nov.	60 - 90 days		29,000	5
Echinodermata: Echinoidea *						
<i>Sterechinus neumayeri</i> *	planktotrophic	Nov. - Dec.	115 days		12,700	1, 3, 19
Echinodermata: Asteroidea *						
<i>Porania antarctica</i> *	planktotrophic	Nov. - Jan.	65 - 78 days		35,000	2, 6, 17
Asteroidea sp.	planktotrophic / lecithotrophic		150 - 180 days / 60 - 90 days			?
<i>Lophaster gaini</i> *	lecithotrophic	Feb. - Mar.			3,000 - 5,000	11
<i>Diplasterias brucei</i> * / <i>Notasterias armata</i>	brooding		165 days ^a		< 300	17
<i>Psilaster charcoti</i> *	lecithotrophic	Nov. - Dec.			10,000	17
<i>Odontaster validus</i> * / <i>O. meridionalis</i>	planktotrophic	Sept. - Nov.	167 days			10, 11, 18
<i>Acodontaster conspicuus</i> / <i>A. hodgsoni</i>	lecithotrophic	Nov. - May	91 - 100 days			5, 13, 17
Echinodermata: Holothuroidea *						
<i>Protelpidia murrayi</i> / <i>Peniagone vignoni</i>	lecithotrophic		60-90 days		1498-9986	4

* species that have been observed in Andvord and/or Flandres Bays. Larval release time was based on literature or estimation from literature report of spawning time (or report of gravid females) + development time.

^a takes place internally within female not in water column.

References: [1] Bosch et al. 1987; [2] Bosch 1989; [3] Galley 2005; [4] Galley et al. 2008; [5] McClintock and Pearse, 1987; [6] McClintock and Pearse, 1990; [7] Meidlinger et al. 1998; [8] Peck and Robinson, 1994; [9] Peck et al. 1997; [10] Pearse and Bosch, 1986; [11] Pearse et al. 1991; [12] Sahade et al. 2004; [13] Strathmann et al. 2006; [14] McClintock et al. 2005; [15] Maldonado, 2006; [16] Leys and Ereskovsky, 2006; [17] Bosch and Pearse, 1990; [18] Stanwell-Smith and Clarke, 1998; [19] Stanwell-Smith and Peck, 1998;

294 *Climate Change on the West Antarctic Peninsula*

295 As greenhouse gas concentrations continue to rise at an unprecedented rate, atmospheric and ocean
296 temperatures are also rising (Pachauri et al. 2014). In the Antarctic, this warming has been most
297 pronounced on the West Antarctic Peninsula where air temperatures have risen 3.7 ± 1.6 °C century⁻¹,
298 several times that of the global average of 0.6 ± 0.2 °C during the 20th century (Vaughan et al. 2003) and
299 sea surface temperatures have increased by > 1°C since 1951 (Meredith and King 2005). Temperature
300 and sea-ice extent trends for the LTER study region are shown in Figure 1.8. Though there has been a
301 hiatus in warming over the last decade (Cook et al. 2016; Turner et al. 2016), it is undeniable that the
302 Antarctic Peninsula region has changed and that it is projected to warm substantially by the year 2100.
303 Increased air and sea temperatures have been linked to a multitude of cascading effects including
304 reduced winter sea ice concentration and duration (Stammerjohn et al. 2008; Turner et al. 2017),
305 increased surface snow melt (Barrand et al. 2013), the melt and retreat of glaciers (Cook et al. 2016;
306 Pritchard and Vaughan 2007), and the collapse of ice-shelves (e.g. Wordie, Larsen A and B Ice Shelves).
307 In turn, these trends are linked to an overall decrease in chlorophyll-a concentration and size structure of
308 phytoplankton communities (Montes-Hugo et al. 2009), a reduction in krill biomass in exchange for salps (
309 Atkinson et al. 2004; Loeb et al. 1997; Trivelpiece et al. 2011), shifts in the age-structure of krill
310 populations and a subsequent reduction in penguin foraging efficiency (Fraser and Hofmansn 2003). We
311 do not yet understand how most climatic stressors will affect WAP benthic ecosystems or how
312 interactions between stressors may be synergistic or antagonistic (Griffiths et al. 2017; Gutt et al. 2015). It
313 is clear, however, that changes to water properties that affect circulation, productivity or changes to
314 seafloor properties (e.g. sediment grain size, organic carbon content) could change benthic community
315 structure or function.

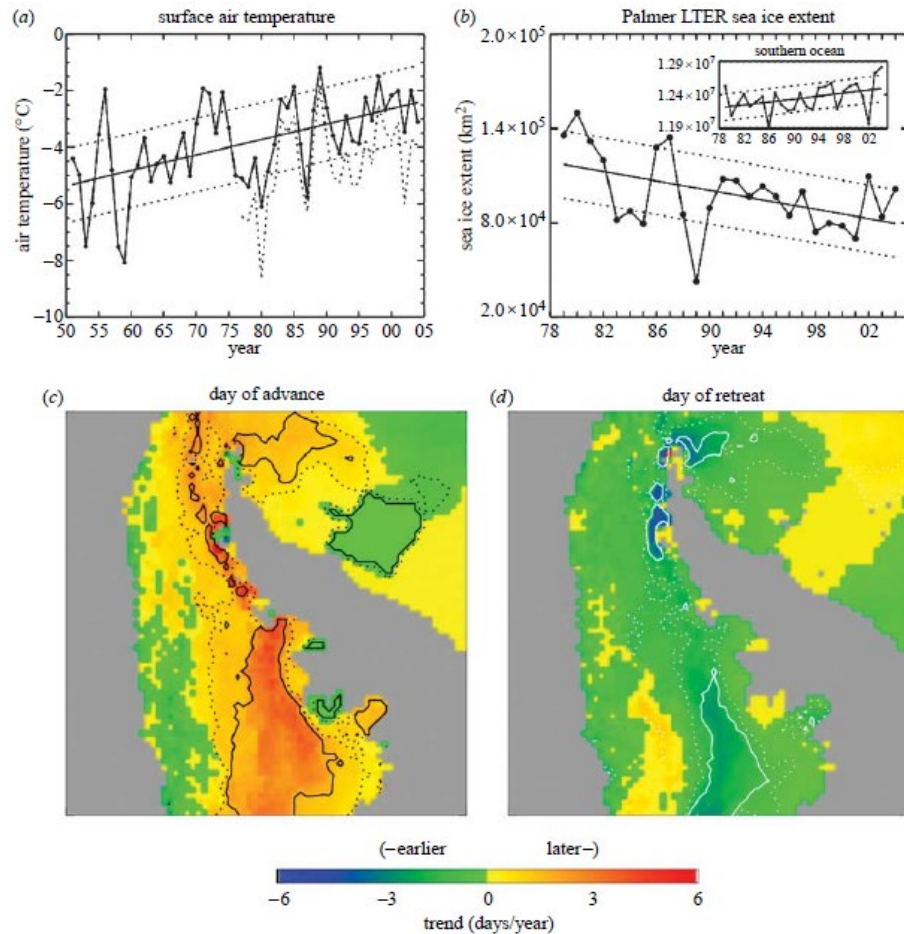


Figure 1.8 Trends in surface air temperature (a) and sea ice extent (b) in the Palmer LTER study region. (c) and (d) show trends in sea ice advance and retreat along the peninsula. (Ducklow et al. 2007).

The chapters that follow explore environmental drivers of benthic community structure and function in glaciomarine fjords (esp. Andvord Bay) of the West Antarctic Peninsula. These fjords are currently regions of high productivity and biodiversity but are expected to face dramatic environmental changes in the future. It is important, therefore, to understand how environmental conditions affect community assembly processes and ecosystem functions prior to substantial environmental changes. **Chapter II** investigates the influence of habitat heterogeneity, generated by glacial dropstones, on benthic community composition, species richness and diversity. This study asks whether the abundance and size

of dropstones is greater in glaciomarine fjords as compared to the adjacent shelf, if the distribution of dropstones increases local species richness and abundance of hard-substrate fauna, and whether dropstones function as island habitats. **Chapter III** asks whether previously observed differences in neighboring fjord communities can be attributed (at least in part) to larval dispersal. This study utilizes a modeling approach to test the hypothesis that fjords act to retain larvae, resulting in limited connectivity between fjords and increased self-recruitment within individual fjords. We also investigate the potential for these fjords to be substantial sources of larvae to the greater West Antarctic Peninsula shelf. **Chapter IV** explores the temporal deposition and consumption of phytodetritus on the seafloor via color-recognition using time-lapse imagery. We investigate the relationship between phytodetritus deposition and overlying oceanic conditions such as sea-ice cover and surface wind speed. The fate of this material is further explored in a detailed study of the response of a key deposit-feeder to increased food availability. Finally, **Chapter V** summarizes the results of this research and identifies future research goals.

References

- Arellano, S. M., Van Gaest, A. L., Johnson, S. B., Vrijenhoek, R. C., & Youn, C. M. (2014). Larvae from deep-sea methane seeps disperse in surface waters. *Proceedings of the Royal Society B: Biological Sciences*, 281(1786), 1–8. <https://doi.org/10.1098/rspb.2013.3276>
- Arntz, W. E., Brey, T., & Gallardo, V. A. (1994). Antarctic Zoobenthos. *Oceanography and Marine Biology: An Annual Review*, 32, 241–304.
- Atkinson, A., Siegel, V., Pakhomov, E., & Rothery, P. (2004). Long-term decline in krill stock and increase in salps within the Southern Ocean. *Nature*, 432, 100–103. <https://doi.org/10.1038/nature02950.1>.
- Barker, P. F., Filippelli, G. M., Florindo, F., Martin, E. E., & Scher, H. D. (2007). Onset and role of the Antarctic Circumpolar Current. *Deep-Sea Research Part II: Topical Studies in Oceanography*, 54(21–22), 2388–2398. <https://doi.org/10.1016/j.dsr2.2007.07.028>
- Barnes, D. K. A., & Conlan, K. E. (2007). Disturbance, colonization and development of Antarctic benthic

communities. *Philosophical Transactions of the Royal Society B: Biological Sciences*, 362(1477),
11–38. <https://doi.org/10.1098/rstb.2006.1951>

Barrand, N. E., Vaughan, D. G., Steiner, N., Tedesco, M., Kuipers Munneke, P., Van Den Broeke, M. R.,
& Hosking, J. S. (2013). Trends in Antarctic Peninsula surface melting conditions from observations
and regional climate modeling. *Journal of Geophysical Research: Earth Surface*, 118(1), 315–330.
<https://doi.org/10.1029/2012JF002559>

Bidegain, G., Bárcena, J. F., García, A., & Juanes, J. A. (2013). LARVAHS: Predicting clam larval
dispersal and recruitment using habitat suitability-based particle tracking model. *Ecological
Modelling*, 268, 78–92. <https://doi.org/10.1016/j.ecolmodel.2013.07.020>

Bilton, D. T., Paula, J., & Bishop, J. D. D. (2002). Dispersal, genetic differentiation and speciation in
estuarine organisms. *Estuarine, Coastal and Shelf Science*, 55(6), 937–952.
<https://doi.org/10.1006/ecss.2002.1037>

Bingham, B. L., & Young, C. M. (1991). Larval behavior of the ascidian *Ecteinascidia turbinata* Herdman;
an in situ experimental study of the effects of swimming on dispersal. *Journal of Experimental
Marine Biology and Ecology*, 145(2), 189–204. [https://doi.org/10.1016/0022-0981\(91\)90175-V](https://doi.org/10.1016/0022-0981(91)90175-V)

Bosch, I., Beauchamp, K. A., Steele, M. E., & Pearse, J. S. (1987). Development , Metamorphosis , and
Seasonal Abundance of Embryos and Larvae of the Antarctic Sea Urchin *Sterechinus neumayeri*.
Biological Bulletin, 173(1), 126–135.

Bosch, I., & Pearse, J. S. (1990). Developmental types of shallow-water asteroids of McMurdo Sound,
Antarctica. *Marine Biology*, 104(1), 41–46. <https://doi.org/10.1007/BF01313155>

Bosch, Isidro. (1989). “Contrasting Modes of Reproduction in Two Antarctic Asteroids of the Genus
Porania, With a Description of Unusual Feeding and Non-Feeding Larval Types.” *The Biological
Bulletin* 177 (1): 77–82. <https://doi.org/10.2307/1541836>.

Brandt, A. (2005). Evolution of Antarctic biodiversity in the context of the past: The importance of the

376 Southern Ocean deep sea. *Antarctic Science*, 17(4), 509–521.
 377 <https://doi.org/10.1017/S0954102005002932>

378 Brandt, A., Gooday, A. J., Brandão, S. N., Brix, S., Brökeland, W., Cedhagen, T., ... Vanreusel, A. (2007).
 379 First insights into the biodiversity and biogeography of the Southern Ocean deep sea. *Nature*,
 380 447(7142), 307–311. <https://doi.org/10.1038/nature05827>

381 Breusing, C., Biastoch, A., Drews, A., Metaxas, A., Jollivet, D., Vrijenhoek, R. C., ... Reusch, T. B. H.
 382 (2016). Biophysical and Population Genetic Models Predict the Presence of “Phantom” Stepping
 383 Stones Connecting Mid-Atlantic Ridge Vent Ecosystems. *Current Biology*, 26(17), 2257–2267.
 384 <https://doi.org/10.1016/j.cub.2016.06.062>

385 Buesseler, K. O., McDonnell, A. M. P., Schofield, O. M. E., Steinberg, D. K., & Ducklow, H. W. (2010).
 386 High particle export over the continental shelf of the west Antarctic Peninsula. *Geophysical*
 387 *Research Letters*, 37(22), 1–5. <https://doi.org/10.1029/2010GL045448>

388 Clarke, A. (1979). On Living in Cold Water: K-Strategies in Antarctic Benthos. *Marine Biology*, 55, 111–
 389 119.

390 Clarke, A. (1992). Reproduction in the cold: Thorson revisited. *Invertebrate Reproduction & Development*,
 391 22(1–3), 175–183. <https://doi.org/10.1080/07924259.1992.9672270>

392 Clarke, A. (2008). Antarctic marine benthic diversity: patterns and processes. *Journal of Experimental*
 393 *Marine Biology and Ecology*, 366(1–2), 48–55. <https://doi.org/10.1016/j.jembe.2008.07.008>

394 Clarke, A., & Johnston, N. M. (2003). Antarctic Marine Benthic Diversity. *Oceanography and Marine*
 395 *Biology : And Annual Review*, 41, 47–114.

396 Cook, A. J., Holland, P. R., Meredith, M. P., Murray, T., Luckman, A., & Vaughan, D. G. (2016). Ocean
 397 forcing of glacier retreat in the western Antarctic Peninsula. *Science*, 353(6296), 283–286.
 398 <https://doi.org/10.1126/science.aae0017>

399 Couto, N., Martinson, D. G., Kohut, J., & Schofield, O. (2017). Distribution of Upper Circumpolar Deep

Water on the warming continental shelf of the West Antarctic Peninsula. *Journal of Geophysical Research: Oceans*, 1–15. <https://doi.org/10.1002/2016JC012335>. Received

Cunningham, K. M., Canino, M. F., Spies, I. B., & Hauser, L. (2009). Genetic isolation by distance and localized fjord population structure in Pacific cod (*Gadus macrocephalus*): limited effective dispersal in the northeastern Pacific Ocean. *Canadian Journal of Fisheries and Aquatic Sciences*, 66(1), 153–166. <https://doi.org/10.1139/F08-199>

Dell, R. (1972). Antarctic Benthos. *Advances in Marine Biology*, 10, 1–216.

Dinniman, M. S., Klinck, J. M., & Hofmann, E. E. (2012). Sensitivity of circumpolar deep water transport and ice shelf basal melt along the west antarctic peninsula to changes in the winds. *Journal of Climate*, 25(14), 4799–4816. <https://doi.org/10.1175/JCLI-D-11-00307.1>

Dinniman, M. S., Klinck, J. M., & Smith, W. O. J. (2011). A model study of circulation and cross-shelf exchange on the west Antarctic Peninsula continental shelf. *Deep-Sea Research Part II: Topical Studies in Oceanography*, 58, 1508–1523.

Domack, E.W., & Williams, C. R. (1990). Fine structure and suspended sediment transport in three Antarctic fjords. *Antarctic Research Series*, 50, 71–89.

Domack, Eugene W., & Ishman, S. (1993). Oceanographic and physiographic controls on modern sedimentation within Antarctic fjords. *Geological Society of America Bulletin*, 105, 1175–1189.

Döös, K., Kjellsson, J., & Jonsson, B. (2013). TRACMASS - A lagrangian trajectory model. In *Preventive Methods for Coastal Protection: Towards the Use of Ocean Dynamics for Pollution Control* (pp. 225–249). <https://doi.org/10.1007/978-3-319-00440-2>

Ducklow, H. W., Baker, K., Martinson, D. G., Quetin, L. B., Ross, R. M., Smith, R. C., ... Fraser, W. (2007). Marine pelagic ecosystems: The West Antarctic Peninsula. *Philosophical Transactions of the Royal Society B: Biological Sciences*, 362(1477), 67–94. <https://doi.org/10.1098/rstb.2006.1955>

Ducklow, H. W., Erickson, M., Kelly, J., Montes-Hugo, M., Ribic, C. A., Smith, R. C., ... Karl, D. M. (2008).

- Particle export from the upper ocean over the continental shelf of the west Antarctic Peninsula: A long-term record, 1992-2007. *Deep-Sea Research Part II: Topical Studies in Oceanography*, 55(18–19), 2118–2131. <https://doi.org/10.1016/j.dsr2.2008.04.028>
- Ducklow, H. W., Fraser, W., Karl, D. M., Quetin, L. B., Ross, R. M., Smith, R. C., ... Daniels, R. M. (2006). Water-column processes in the West Antarctic Peninsula and the Ross Sea: Interannual variations and foodweb structure. *Deep-Sea Research Part II: Topical Studies in Oceanography*, 53(8–10), 834–852. <https://doi.org/10.1016/j.dsr2.2006.02.009>
- Espinasse, B., Zhou, M., Zhu, Y., Hazen, E. L., Friedlaender, A. S., Nowacek, D. P., ... Carlotti, F. (2012). Austral fall-winter transition of mesozooplankton assemblages and krill aggregations in an embayment west of the Antarctic Peninsula. *Marine Ecology Progress Series*, 452, 63–80. <https://doi.org/10.3354/meps09626>
- Fraser, W. R., & Hofmann, E. E. (2003). A predators perspective on causal links between climate change physical forcing and ecosystem response. *Marine Ecology Progress Series*, 265, 1–15.
- Galley, E. A., P. A. Tyler, C. R. Smith, and A. Clarke. (2008). “Reproductive Biology of Two Species of Holothurian from the Deep-Sea Order Elaspoda, on the Antarctic Continental Shelf.” *Deep-Sea Research Part II: Topical Studies in Oceanography* 55 (22–23): 2515–26. <https://doi.org/10.1016/j.dsr2.2008.07.002>.
- Galley, Elizabeth A., Paul A. Tyler, Andrew Clarke, and Craig R. Smith. (2005). “Reproductive Biology and Biochemical Composition of the Brooding Echinoid *Amphipneustes lorioli* on the Antarctic Continental Shelf.” *Marine Biology* 148 (1): 59–71. <https://doi.org/10.1007/s00227-005-0069-3>.
- Gleiber, M. R., Steinberg, D. K., & Ducklow, H. W. (2012). Time series of vertical flux of zooplankton fecal pellets on the continental shelf of the western Antarctic Peninsula. *Marine Ecology Progress Series*, 471, 23–36. <https://doi.org/10.3354/meps10021>
- Grange, L. J., & Smith, C. R. (2013). Megafaunal communities in rapidly warming fjords along the West Antarctic Peninsula: Hotspots of abundance and beta diversity. *PLoS ONE*, 8(12).

<https://doi.org/10.1371/journal.pone.0077917>

Griffiths, H. J., Meijers, A. J. S., & Bracegirdle, T. J. (2017). More losers than winners in a century of future Southern Ocean seafloor warming. *Nature Climate Change*, 7(10), 749–754.

<https://doi.org/10.1038/nclimate3377>

Gutt, J. (2001). On the direct impact of ice on marine benthic communities, a review. *Polar Biology*, 24(8), 553–564. <https://doi.org/10.1007/s003000100262>

Gutt, Julian, Bertler, N., Bracegirdle, T. J., Buschmann, A., Comiso, J., Hosie, G., ... Xavier, J. C. (2015). The Southern Ocean ecosystem under multiple climate change stresses - an integrated circumpolar assessment. *Global Change Biology*, 21(4), 1434–1453. <https://doi.org/10.1111/gcb.12794>

Gutt, Julian, & Piepenburg, D. (2003). Scale-dependent impact on diversity of Antarctic benthos caused by grounding of icebergs. *Marine Ecology Progress Series*, 253, 77–83.

<https://doi.org/10.3354/meps253077>

Gutt, Julian, & Starmans, Æ. A. (2003). Patchiness of the megabenthos at small scales: ecological conclusions by examples from polar shelves, *Polar Biology*, 276–278.

<https://doi.org/10.1007/s00300-002-0468-6>

Hartnett, H., Boehme, S., Thomas, C., DeMaster, D., & Smith, C. (2008). Benthic oxygen fluxes and denitrification rates from high-resolution porewater profiles from the Western Antarctic Peninsula continental shelf. *Deep-Sea Research Part II: Topical Studies in Oceanography*, 55(22–23), 2415–2424. <https://doi.org/10.1016/j.dsr2.2008.06.002>

Hofmann, E. E., Klinck, J. M., Lascara, C. M., & Smith, D. A. (1996). Water mass distribution and circulation west of the Antarctic Peninsula. *Antarctic Research Series*, 70, 61–80.

Holm-Hansen, O., Letelier, R., & Mitchell, B. G. (1987). RACER: Temporal and spatial distribution of phytoplankton biomass and primary production. *Antarctic Journal of the United States*, 22, 142–145.

Holte, B., & Gulliksen, B. (1998). Common macrofaunal dominant species in the sediments of some north

473 Norwegian and Svalbard glacial fjords. *Polar Biology*, 19(6), 375-382.

474 Jahnke, R. A. (1996). The global ocean flux of particulate organic carbon: Areal distribution and
475 magnitude. *Global biogeochemical cycles*, 10(1), 71–88.

476 Karl, D.M., Tien, G., Jones, D., Tilbrook, B., Bailiff, M. D., Nawrocki, M., ... Haberstroh, P. (1987).
477 RACER : Seasonal changes in the downward flux of biogenic matter RACER: Feeding and egg
478 production rates of some antarctic copepods. *Antarctic Journal*, 157–158.

479 Karl, David M., Tilbrook, B. D., & Tien, G. (1991). Seasonal coupling of organic matter production and
480 particle flux in the western Bransfield Strait, Antarctica. *Deep Sea Research*, 38(89), 1097–1126.

481 Kedra, M., Wlodarska-Kowalczyk, M., & Weslawski, J. M. (2010). Decadal change in macrobenthic soft-
482 bottom community structure in a high Arctic fjord (Kongsfjorden, Svalbard). *Polar Biology*, 33, 1–11.
483 <https://doi.org/10.1007/s00300-009-0679-1>

484 Klinck, J. M., Hofmann, E. E., Beardsley, R. C., Salihoglu, B., & Howard, S. (2004). Water-mass
485 properties and circulation on the west Antarctic Peninsula Continental Shelf in Austral Fall and
486 Winter 2001. *Deep-Sea Research Part II: Topical Studies in Oceanography*, 51(17–19), 1925–1946.
487 <https://doi.org/10.1016/j.dsr2.2004.08.001>

488 Klinck, J. M., & O'Brien, J. J. (1981). A simple model of fjord and coastal circulation interaction. *Journal of*
489 *Physical Oceanography*, 11, 1612–1626.

490 Ledoux, J. B., Tarnowska, K., Gérard, K., Lhuillier, E., Jacquemin, B., Weydmann, A., ... Chenuil, A.
491 (2012). Fine-scale spatial genetic structure in the brooding sea urchin *Abatus cordatus* suggests
492 vulnerability of the Southern Ocean marine invertebrates facing global change. *Polar Biology*, 35(4),
493 611–623. <https://doi.org/10.1007/s00300-011-1106-y>

494 Levy, M. (2008). The Modulation of Biological Production by Oceanic Mesoscale Turbulence. In *Transport*
495 *and Mixing in Geophysical Flows* (pp. 219–261). Springer-Verlag Berlin Heidelberg.
496 <https://doi.org/10.1007/978-3-540-75215-8>

497 Leys, S P, and A V Ereskovsky. (2006). "Embryogenesis and Larval Differentiation in Sponges."
 498 *Canadian Journal of Zoology* 84 (2): 262–87. <https://doi.org/10.1139/z05-170>.

499 Loeb, V., Siegel, V., Holm-Hansen, O., Hewitt, R., Fraser, W., Trivelpiece, W., & Trivelpiece, S. (1997).
 500 Effects of sea-ice extent and krill or salp dominance on the Antarctic food web. *Nature*, 387(6636),
 501 897–900. <https://doi.org/10.1038/43174>

502 Lovrich, G. A., Romero, M. C., Tapella, F., & Thatje, S. (2005). Distribution, reproductive and energetic
 503 conditions of decapod crustaceans along the Scotia Arc (Southern Ocean). *Scientia Marina*, 69(1),
 504 183–193.

505 Lundesgaard, Ø., Powell, B., Merrifield, M., Hahn-Woernle, L., & Winsor, P. (2019). Response of an
 506 Antarctic Peninsula fjord to summer katabatic wind events. *Journal of Physical Oceanography*,
 507 49(6), 1485–1502. <https://doi.org/10.1175/jpo-d-18-0119.1>

508 Włodarska-Kowalczyk, M. and Weslawski, J. M. (2008). Mesoscale spatial structures of soft-bottom
 509 macrozoobenthos communities: effects of physical control and impoverishment. *Marine Ecology*
 510 *Progress Series*, 356, 215–224. <https://doi.org/10.3354/meps07285>

511 Martinson, D. G., Stammerjohn, S. E., Iannuzzi, R. A., Smith, R. C., & Vernet, M. (2008). Western
 512 Antarctic Peninsula physical oceanography and spatio-temporal variability. *Deep-Sea Research Part*
 513 *II: Topical Studies in Oceanography*, 55(18–19), 1964–1987.
 514 <https://doi.org/10.1016/j.dsr2.2008.04.038>

515 McClintock, J. B., and J. S. Pearse. (1987). "Reproductive Biology of the Common Antarctic Crinoid
 516 *Promachocrinus kerguelensis* (Echinodermata: Crinoidea)." *Marine Biology* 96 (3): 375–83.
 517 <https://doi.org/10.1007/BF00412521>.

518 McClintock, James B, Charles D Amsler, Bill J Baker, and Rob W.M. van Soest. (2005). "Ecology of
 519 Antarctic Marine Sponges: An Overview." *Integrative and Comparative Biology* 45 (2): 359–68.

520 Meidlinger, K, P.A. Tyler, and L.S. Peck. (1998). "Reproductive Patterns in the Antarctic Brachiopod
 521 *Liothyrella uva*." *Marine Biology* 132 (1): 153–62. <https://doi.org/10.1007/s002270050381>.

522 Meredith, M. P., & King, J. C. (2005). Rapid climate change in the ocean west of the Antarctic Peninsula
 523 during the second half of the 20th century. *Geophysical Research Letters*, 32(19), 1–5.
 524 <https://doi.org/10.1029/2005GL024042>

525 Mileikovsky, S. A. (1971). Types of larval development in marine bottom invertebrates, their distribution
 526 and ecological significance: a re-evaluation. *Marine Biology*, 10(193–213), 193–213.

527 Mincks, S. L., & Smith, C. R. (2007). Recruitment patterns in Antarctic Peninsula shelf sediments:
 528 Evidence of decoupling from seasonal phytodetritus pulses. *Polar Biology*, 30(5), 587–600.
 529 <https://doi.org/10.1007/s00300-006-0216-4>

530 Mincks, S. L., Smith, C. R., & DeMaster, D. J. (2005). Persistence of labile organic matter and microbial
 531 biomass in Antarctic shelf sediments: Evidence of a sediment "food bank." *Marine Ecology Progress*
 532 *Series*, 300, 3–19. <https://doi.org/10.3354/meps300003>

533 Mittelbach, G. G., & Schemske, D. W. (2015). Ecological and evolutionary perspectives on community
 534 assembly. *Trends in Ecology and Evolution*, 30(5), 241–247.
 535 <https://doi.org/10.1016/j.tree.2015.02.008>

536 Moffat, C., Owens, B., & Beardsley, R. C. (2009). On the characteristics of Circumpolar Deep Water
 537 intrusions to the west Antarctic Peninsula Continental Shelf. *Journal of Geophysical Research:*
 538 *Oceans*, 114(5), 1–16. <https://doi.org/10.1029/2008JC004955>

539 Moffat, Carlos. (2014). Wind-driven modulation of warm water supply to a proglacial fjord, Jorge Montt
 540 Glacier, Patagonia. *Geophysical Research Letters*, 41, 3943–3950.
 541 <https://doi.org/10.1002/2014GL060071.1>.

542 Moffat, Carlos, Beardsley, R. C., Owens, B., & van Lipzig, N. (2008). A first description of the Antarctic
 543 Peninsula Coastal Current. *Deep-Sea Research Part II: Topical Studies in Oceanography*, 55(3–4),

544 277–293. <https://doi.org/10.1016/j.dsr2.2007.10.003>

545 Montes-Hugo, M., Doney, S. C., Ducklow, H. W., Fraser, W., Martinson, D., Stammerjohn, S. E., &
546 Schofield, O. (2009). Recent changes in phytoplankton communities associated with rapid regional
547 climate change along the western Antarctic Peninsula. *Science*, 323(5920), 1470–1473.
548 <https://doi.org/10.1126/science.1164533>

549 Mortensen, J., Lennert, K., Bendtsen, J., & Rysgaard, S. (2011). Heat sources for glacial melt in a sub -
550 Arctic fjord (Godthåbsfjord) in contact with the Greenland Ice Sheet. *Journal of Geophysical*
551 *Research*, 116, 1–13. <https://doi.org/10.1029/2010JC006528>

552 Mullineaux, L. S., & Mills, S. W. (1997). A test of the larval retention hypothesis in seamount-generated
553 flows. *Deep-Sea Research I*, 44(5), 745–770.

554 Nicol, S. (2006). Krill, currents, and Sea Ice: *Euphausia superba* and its Changing Environment.
555 *BioScience*, 56(2), 111–120.

556 North, E. (2008). LTRANS Model Description. *Continental Shelf Research*, (April), 1–6.

557 North, E. W., Schlag, Z., Hood, R. R., Li, M., Zhong, L., Gross, T., & Kennedy, V. S. (2008). Vertical
558 swimming behavior influences the dispersal of simulated oyster larvae in a coupled particle-tracking
559 and hydrodynamic model of Chesapeake Bay. *Marine Ecology Progress Series*, 359(Leis 2007),
560 99–115. <https://doi.org/10.3354/meps07317>

561 Nowacek, D. P., Friedlaender, A. S., Halpin, P. N., Hazen, E. L., Johnston, D. W., Read, A. J., ... Zhu, Y.
562 (2011). Super-aggregations of krill and humpback whales in Wilhelmina Bay, Antarctic Peninsula.
563 *PloS One*, 6(4), e19173. <https://doi.org/10.1371/journal.pone.0019173>

564 Nowlin, W. D., & Klinck, J. M. (1986). The physics of the Antarctic Circumpolar Current. *Reviews of*
565 *Geophysics*, 24(3), 469–491. <https://doi.org/10.1029/RG024i003p00469>

566 Pachauri, R. K., Allen, M. R., Barros, V. R., Broome, J., Cramer, W., Christ, R., ... Hallegatte, S. (2014).
567 *Climate Change 2014 Synthesis Report. IPCC, 2014*. <https://doi.org/10.1046/j.1365->

2559.2002.1340a.x

Palumbi, S. R. (1994). Genetic divergence, reproductive isolation, and marine speciation. *Annual Review of Ecology and Systematics*, 25, 547–572.

<https://doi.org/10.1146/annurev.es.25.110194.002555>

Palumbi, S. R. (2003). Ecological subsidies alter the structure of marine communities. *PNAS*, 100(21), 11927–11928. <https://doi.org/10.1073/pnas.2335832100>

Paris, C. B., Chérubin, L. M., & Cowen, R. K. (2007). Surfing, spinning, or diving from reef to reef: Effects on population connectivity. *Marine Ecology Progress Series*, 347, 285–300.

<https://doi.org/10.3354/meps06985>

Paris, C. B., Helgers, J., van Sebille, E., & Srinivasan, A. (2013). Connectivity Modeling System: A probabilistic modeling tool for the multi-scale tracking of biotic and abiotic variability in the ocean.

Environmental Modelling and Software, 42, 47–54. <https://doi.org/10.1016/j.envsoft.2012.12.006>

Pearse, John S., and McClintock James B. (1990). “A Comparison of Reproduction by the Brooding Spatangoid Echinoids *Abatus shackletoni* and *A. nimrodi* in McMurdo Sound, Antarctica.”

Invertebrate Reproduction & Development 17 (3): 181–91.

<https://doi.org/10.1080/07924259.1990.9672110>.

Pearse, J. S. (1994). Cold-water echinoderms break “Thorson’s Rule.” In *Reproduction, Larval Biology, and Recruitment of the Deep-sea Benthos* (pp. 26–43).

Pearse, J. S., McClintock, J. B., & Bosch, I. (1991). Reproduction of Antarctic benthic marine invertebrates: Tempos, modes, and timing. *American Zoologist*, 31(1), 65–80.

<https://doi.org/10.1093/icb/31.1.65>

Pearse, John S, and Isidro Bosch. (1986). “Are the Feeding Larvae of the Commonest Antarctic Asteroid Really Demersal?” *Bulletin of Marine Science* 39 (2): 477–84.

Peck, L. S., Convey, P., & Barnes, D. K. A. (2006). Environmental constraints on life histories in Antarctic

592 ecosystems: Tempos, timings and predictability. *Biological Reviews of the Cambridge Philosophical*
593 *Society*, 81(1), 75–109. <https://doi.org/10.1017/S1464793105006871>

594 Peck, Lloyd S., Simon Brockington, and Thomas Brey. (1997). “Growth and Metabolism in the Antarctic
595 Brachiopod *Liothyrella uva*.” *Philosophical Transactions of the Royal Society B: Biological*
596 *Sciences* 352 (1355): 851–58. <https://doi.org/10.1098/rstb.1997.0065>.

597 Peck, Lloyd S., and K. Robinson. (1994). “Pelagic Larval Development in the Brooding Antarctic
598 Brachiopod *Liothyrella uva*.” *Marine Biology* 120 (2): 279–86.
599 <https://doi.org/10.1007/BF00349689>.

600 Piepenburg, D., Schmid, K., & Gerdes, D. (2002). The benthos off King George Island (South Shetland
601 Islands, Antarctica): further evidence for a lack of a latitudinal biomass cline in the Southern Ocean,
602 146–158. <https://doi.org/10.1007/s003000100322>

603 Poulin, É., & Féral, J.-P. (1996). Why are there so many species of brooding antarctic echinoids?
604 *Evolution*, 50(2), 820–830. <https://doi.org/10.1111/j.1540-6237.2012.00858.x>

605 Pritchard, H. D., Ligtenberg, S. R. M., Fricker, H. A., Vaughan, D. G., van den Broeke, M. R., & Padman,
606 L. (2012). Antarctic ice-sheet loss driven by basal melting of ice shelves. *Nature*, 484, 502–505.
607 <https://doi.org/10.1038/nature10968>

608 Pritchard, H. D., & Vaughan, D. G. (2007). Widespread acceleration of tidewater glaciers on the Antarctic
609 Peninsula. *Journal of Geophysical Research*, 112(3), 1–10. <https://doi.org/10.1029/2006JF000597>

610 Renaud, P. E., Riedel, A., Michel, C., Morata, N., Gosselin, M., Juul-Pedersen, T., & Chiuchiolo, A.
611 (2007). Seasonal variation in benthic community oxygen demand: A response to an ice algal bloom
612 in the Beaufort Sea, Canadian Arctic? *Journal of Marine Systems*, 67(1–2), 1–12.
613 <https://doi.org/10.1016/j.jmarsys.2006.07.006>

614 Renaud, P. E., Włodarska-Kowalczyk, M., Trannum, H., Holte, B., Węśławski, J. M., Cochrane, S., ...
615 Gulliksen, B. (2007). Multidecadal stability of benthic community structure in a high-Arctic glacial

- fjord (van Mijenfjord, Spitsbergen). *Polar Biology*, 30(3), 295–305. <https://doi.org/10.1007/s00300-006-0183-9>
- Riesgo, A., Taboada, S., & Avila, C. (2015). Evolutionary patterns in Antarctic marine invertebrates: An update on molecular studies. *Marine Genomics*, 23, 1–13. <https://doi.org/10.1016/j.margen.2015.07.005>
- Rignot, E., Jacobs, S., Mouginot, J., & Scheuchl, B. (2013). Ice-shelf melting around antarctica. *Science*, 341(6143), 266–270. <https://doi.org/10.1126/science.1235798>
- Rignot, Eric, Fenty, I., Xu, Y., Cai, C., & Kemp, C. (2015). Undercutting of marine-terminating glaciers in West Greenland. *Geophysical Research Letters*, 42(14), 5909–5917. <https://doi.org/10.1002/2015GL064236>
- Ross, R. M., & Quetin, L. B. (1986). How Productive Are Antarctic Krill? *BioScience*, 36(4), 264–269.
- Santora, J. A., & Veit, R. R. (2013). Spatio-temporal persistence of top predator hotspots near the Antarctic Peninsula. *Marine Ecology Progress Series*, 487, 287–304. <https://doi.org/10.3354/meps10350>
- Schofield, O., Saba, G., Coleman, K., Carvalho, F., Couto, N., Ducklow, H., ... Waite, N. (2017). Decadal variability in coastal phytoplankton community composition in a changing West Antarctic Peninsula. *Deep-Sea Research Part I: Oceanographic Research Papers*, 124(March), 42–54. <https://doi.org/10.1016/j.dsr.2017.04.014>
- Selkoe, K. A., & Toonen, R. J. (2011). Marine connectivity: A new look at pelagic larval duration and genetic metrics of dispersal. *Marine Ecology Progress Series*, 436, 291–305. <https://doi.org/10.3354/meps09238>
- Shanks, A. L., Grantham, B. A., & Carr, M. H. (2003). Propagule dispersal distance and the size and spacing of marine reserves. *Ecological Applications*, 13(1), 159–169.
- Siegel, D. A., Fields, E., & Buesseler, K. O. (2008). A bottom-up view of the biological pump: Modeling

640 source funnels above ocean sediment traps. *Deep-Sea Research Part I: Oceanographic Research*
641 *Papers*, 55(1), 108–127. <https://doi.org/10.1016/j.dsr.2007.10.006>

642 Siegel, D. A., Kinlan, B. P., Gaylord, B., & Gaines, S. D. (2003). Lagrangian descriptions of marine larval
643 dispersion. *Marine Ecology Progress Series*, 260, 83–96. <https://doi.org/10.3354/meps260083>

644 Sköld, M., Wing, S. R., & Mladenov, P. V. (2003). Genetic subdivision of a sea star with high dispersal
645 capability in relation to physical barriers in a fjordic seascape. *Marine Ecology Progress Series*,
646 250(Palumbi 1994), 163–174. <https://doi.org/10.3354/meps250163>

647 Smith, C. R., De Leo, F. C., Bernardino, A. F., Sweetman, A. K., & Arbizu, P. M. (2008). Abyssal food
648 limitation, ecosystem structure and climate change. *Trends in Ecology and Evolution*, 23(9), 518–
649 528. <https://doi.org/10.1016/j.tree.2008.05.002>

650 Smith, C. R., Mincks, S., & DeMaster, D. J. (2006). A synthesis of benthic-pelagic coupling on the
651 Antarctic shelf: Food banks, ecosystem inertia and global climate change. *Deep-Sea Research Part*
652 *II: Topical Studies in Oceanography*, 53(8–10), 875–894. <https://doi.org/10.1016/j.dsr2.2006.02.001>

653 Smith, R. C., Baker, K. S., & Vernet, M. (1998). Seasonal and interannual variability of phytoplankton
654 biomass west of the Antarctic Peninsula. *Journal of Marine Systems*, 17(1–4), 229–243.
655 [https://doi.org/10.1016/S0924-7963\(98\)00040-2](https://doi.org/10.1016/S0924-7963(98)00040-2)

656 Smith, Raymond C., Dierssen, H. M., & Vernet, M. (1996). Phytoplankton biomass and productivity in the
657 Western Antarctic Peninsula region. *Antarctic Research Series*, 70, 333–356.
658 <https://doi.org/10.1029/ar070p0333>

659 Smith, Raymond C., Martinson, D. G., Stammerjohn, S. E., Iannuzzi, R. A., & Ireson, K. (2008).
660 Bellingshausen and western Antarctic Peninsula region: Pigment biomass and sea-ice
661 spatial/temporal distributions and interannual variability. *Deep-Sea Research Part II: Topical Studies*
662 *in Oceanography*, 55(18–19), 1949–1963. <https://doi.org/10.1016/j.dsr2.2008.04.027>

663 Spall, M. A., Jackson, R. H., & Straneo, F. (2017). Katabatic Wind-Driven Exchange in Fjords. *Journal of*

664 *Geophysical Research: Oceans*, 8246–8262.

665 Stammerjohn, S. E., Martinson, D. G., Smith, R. C., & Iannuzzi, R. A. (2008). Sea ice in the western
666 Antarctic Peninsula region: Spatio-temporal variability from ecological and climate change
667 perspectives. *Deep-Sea Research Part II: Topical Studies in Oceanography*, 55(18–19), 2041–
668 2058. <https://doi.org/10.1016/j.dsr2.2008.04.026>

669 Stanwell-Smith, D., & Clarke, A. (1998). Seasonality of reproduction in the cushion star *Odontaster*
670 *validus* at Signy Island, Antarctica. *Marine Biology*, 131(3), 479–487.
671 <https://doi.org/10.1007/s002270050339>

672 Stanwell-Smith, Damon, and Lloyd S. Peck. (1998). “Temperature and Embryonic Development in
673 Relation to Spawning and Field Occurrence of Larvae of Three Antarctic Echinoderms.” *Biological*
674 *Bulletin* 194 (1): 44–52. <https://doi.org/10.2307/1542512>.

675 Straneo, F., & Cenedese, C. (2015). The Dynamics of Greenland's Glacial Fjords and Their Role in
676 Climate. *Annual Review of Marine Science*, 7, 89–112. [https://doi.org/10.1146/annurev-marine-](https://doi.org/10.1146/annurev-marine-010213-135133)
677 010213-135133

678 Strathmann, Richard R., Lindsay R. Kendall, and Adam G. Marsh. (2006). “Embryonic and Larval
679 Development of a Cold Adapted Antarctic Ascidian.” *Polar Biology* 29 (6): 495–501.
680 <https://doi.org/10.1007/s00300-005-0080-7>.

681 Svendsen, H., & Thomsson, R. O. R. Y. (1978). Wind-driven circulation in a fjord. *Journal of Physical*
682 *Oceanography*, 8, 703–712.

683 Syvitski, J. P. M. (1989). Glacier-Influenced Fjords : Oceanographic Controls. *Marine Geology*, 85(2–4),
684 301–329.

685 Thornhill, D. J., Mahon, A. R., Norenburg, J. L., & Halanych, K. M. (2008). Open-ocean barriers to
686 dispersal: A test case with the Antarctic Polar Front and the ribbon worm *Parborlasia corrugatus*
687 (Nemertea: Lineidae). *Molecular Ecology*, 17(23), 5104–5117. <https://doi.org/10.1111/j.1365->

294X.2008.03970.x

- Thorpe, S. E., Heywood, K. J., Stevens, D. P., & Brandon, M. A. (2004). Tracking passive drifters in a high resolution ocean model: Implications for interannual variability of larval krill transport to South Georgia. *Deep-Sea Research Part I: Oceanographic Research Papers*, 51(7), 909–920. <https://doi.org/10.1016/j.dsr.2004.02.008>
- Thorson, G. (1950). Reproductive and larval ecology of marine bottom invertebrates. *Biological Reviews*, 25(1), 1–45. <https://doi.org/https://doi.org/10.1111/j.1469-185X.1950.tb00585.x>
- Trivelpiece, W. Z., Hinke, J. T., Miller, A. K., Reiss, C. S., Trivelpiece, S. G., & Watters, G. M. (2011). Variability in krill biomass links harvesting and climate warming to penguin population changes in Antarctica. *Proceedings of the National Academy of Sciences*, 108(18), 7625–7628. <https://doi.org/10.1073/pnas.1016560108>
- Turner, J., Lu, H., White, I., King, J. C., Phillips, T., Hosking, J. S., ... Deb, P. (2016). Absence of 21st century warming on Antarctic Peninsula consistent with natural variability. *Nature*, 535(7612), 411–415. <https://doi.org/10.1038/nature18645>
- Turner, J., Phillips, T., Marshall, G. J., Hosking, J. S., Pope, J. O., Bracegirdle, T. J., & Deb, P. (2017). Unprecedented springtime retreat of Antarctic sea ice in 2016. *Geophysical Research Letters*, 44(13), 6868–6875. <https://doi.org/10.1002/2017GL073656>
- Vaughan, D. G., Marshall, G. J., Connolley, W. M., Parkinson, C., Mulvaney, R., Hodgson, D. A., ... Turner, J. (2003). Recent rapid regional climate warming on the Antarctic Peninsula. *Climatic Change*, 60(3), 243–274. <https://doi.org/10.1023/A:1026021217991>
- Vernet, M., Martinson, D., Iannuzzi, R., Stammerjohn, S., Kozlowski, W., Sines, K., ... Garibotti, I. (2008). Primary production within the sea-ice zone west of the Antarctic Peninsula: I-Sea ice, summer mixed layer, and irradiance. *Deep-Sea Research Part II: Topical Studies in Oceanography*, 55(18–19), 2068–2085. <https://doi.org/10.1016/j.dsr2.2008.05.021>

712 Weersing, K., & Toonen, R. J. (2009). Population genetics, larval dispersal, and connectivity in marine
 713 systems. *Marine Ecology Progress Series*, 393, 1–12. <https://doi.org/10.3354/meps08287>

714 Wefer, G., Fisher, G., Fuetterer, D., & Gersonde, R. (1988). Seasonal particle flux in the Bransfield Strait,
 715 Antarctica. *Deep Sea Research*, 35(6), 891–898.

716 Włodarska-Kowalczyk, M., & Pearson, T. H. (2004). Soft-bottom macrobenthic faunal associations and
 717 factors affecting species distributions in an Arctic glacial fjord (Kongsfjord, Spitsbergen). *Polar*
 718 *Biology*, 27(3), 155–167. <https://doi.org/10.1007/s00300-003-0568-y>

719 Włodarska-Kowalczyk, M., Pearson, T. H., & Kendall, M. A. (2005). Benthic response to chronic natural
 720 physical disturbance by glacial sedimentation in an Arctic fjord. *Marine Ecology Progress Series*,
 721 303(Hall 1994), 31–41. <https://doi.org/10.3354/meps303031>

722 Włodarska-Kowalczyk, M., Renaud, P. E., Węśławski, J. M., Cochrane, S. K. J., & Denisenko, S. G.
 723 (2012). Species diversity, functional complexity and rarity in Arctic fjordic versus open shelf benthic
 724 systems. *Marine Ecology Progress Series*, 463(Pearson 1980), 73–87.
 725 <https://doi.org/10.3354/meps09858>

726 Woodson, C. B., & McManus, M. A. (2007). Foraging behavior can influence dispersal of marine
 727 organisms. *Limnology and Oceanography*, 52(6), 2701–2709.
 728 <https://doi.org/10.4319/lo.2007.52.6.2701>

729 Woodson, C. B., McManus, M. A., Tyburczy, J. A., Barth, J. A., Washburn, L., Caselle, J. E., ... Palumbi,
 730 S. R. (2012). Coastal fronts set recruitment and connectivity patterns across multiple taxa.
 731 *Limnology and Oceanography*, 57(2), 582–596. <https://doi.org/10.4319/lo.2012.57.2.0582>

732 Wright, S. (1943). Isolation by Distance. *Genetics*, 28(2), 114–138.

733 Xu, G., McGillicuddy Jr., D. J., Mills, S. W., & Mullineaux, L. S. (2018). Dispersal of Hydrothermal Vent
 734 Larvae at East Pacific Rise 9 – 10 ° N Segment. *Journal of Geophysical Research: Oceans*, 123,
 735 7877–7895. <https://doi.org/10.1029/2018JC014290>

736 Young, C. M., He, R., Emlet, R. B., Li, Y., Qian, H., Arellano, S. M., ... Rice, M. E. (2012). Dispersal of
737 deep-sea larvae from the intra-American seas: Simulations of trajectories using ocean models.
738 *Integrative and Comparative Biology*, 52(4), 483–496. <https://doi.org/10.1093/icb/ics090>

739 Zhou, M., Niiler, P. P., & Hu, J. H. (2002). Surface currents in the Bransfield and Gerlache Straits,
740 Antarctica. *Deep-Sea Research Part I: Oceanographic Research Papers*, 49(2), 267–280.
741 [https://doi.org/10.1016/S0967-0637\(01\)00062-0](https://doi.org/10.1016/S0967-0637(01)00062-0)

742

**Chapter II Glacial dropstones: islands enhancing seafloor species richness of benthic
megafauna in West Antarctic Peninsula fjords**

Ziegler, A.F.¹, Smith, C.R.¹, Edwards, K.F.¹, and Vernet, M.²

¹University of Hawai'i at Mānoa, Department of Oceanography, Honolulu, HI 96822, USA

²Integrative Oceanographic Division, Scripps Institution of Oceanography, La Jolla, CA, 92093, USA

Abstract

The West Antarctic Peninsula (WAP) margin is dominated by glaciomarine fjords and has experienced rapid climate warming in recent decades. Glacial calving along the peninsula delivers ice-rafted debris (e.g. dropstones) to heavily-sedimented fjord basins and the open continental shelf. Dropstones provide hard substrate, increase habitat heterogeneity, and may function as island habitats surrounded by mud. We used seafloor photographic transects to evaluate the distribution and community structure of Antarctic hard-substrate megafauna and the role of dropstones as island habitats in 3 WAP fjords and at 3 nearby shelf stations. Several lines of evidence indicate that dropstones function as island habitats; their communities adhere to principles of island biogeography theory with (1) a positive correlation between dropstone size and species richness, (2) an increase in the proportion of colonized dropstones with increasing dropstone size, and (3) a species–area scaling exponent consistent with island habitats measured globally. Previous work on the soft-sediment megafauna of this region found strong differences in community composition between fjord and shelf sites, whereas we found that dropstone communities differed within sites at small scales (1 km and smaller). We identified 73 megafaunal morphotypes associated with dropstones, 29 of which were not previously documented in the soft-sediment megafauna. While dropstones constituted <1% of the total seafloor area surveyed, they contributed 20% of the overall species richness of WAP megabenthos at depths of 437–724 m. WAP dropstone

communities adhere to key principles of island biogeography theory, contribute environmental heterogeneity, and increase biodiversity in the WAP region.

Introduction

The West Antarctic Peninsula (WAP) spans a transition between polar and subpolar climates and has experienced significant recent warming, i.e. a 6°C rise in mean winter air temperatures (Vaughan et al. 2001, Cook et al. 2005) and a 1°C increase in sea surface temperature since the 1950s (Vaughan et al. 2001, Cook et al. 2005, Meredith 2005). This warming, and changes in ocean circulation, have contributed to the retreat of 87% of glaciers along the WAP (Cook et al. 2005, 2016, Pritchard and Vaughan 2007). Glaciomarine fjords (i.e. fjords with glaciers terminating in the ocean) dominate the WAP margin and are common in other polar regions. In Arctic glaciomarine fjords, e.g. on Baffin Island and Svalbard, plumes of fine-grained terrigenous sediments from tidewater glaciers cause burial disturbance, reducing the abundance, biomass, and functional diversity of macrobenthos (Włodarska-Kowalczyk et al. 2005). Sedimentation rates within WAP fjords, measured on 100 yr time scales, appear to be ~1–7 mm yr⁻¹ (Domack and Ishman 1993, Domack and McClennen 1996, Boldt et al. 2013) and are approximately an order of magnitude lower than estimated for inner Svalbard fjords over similar time scales (Elverhøi and Seland 1983). Low rates of burial disturbance in WAP fjords allows an unexpectedly high diversity and abundance of megabenthos close to glacial termini (Grange and Smith 2013). In addition, lower turbidity from glacial outflow compared to Arctic fjords may result in higher primary production and detrital food availability, increasing benthic abundance and diversity via pelagic–benthic coupling (Smith et al. 2006, 2012, Grange and Smith 2013). These fjords are considered ‘biodiversity hotspots’ since they contain 3–38 times greater benthic megafaunal abundances than the adjacent continental shelf at similar depths and add substantially to the regional species pool (Grange and Smith 2013). While soft-sediment megafaunal communities in WAP fjords have recently been assessed (Grange and Smith 2013), hard-substrate communities in these fjords remain unexplored.

Subpolar conditions in the northern WAP favor glacier calving, delivering ice-rafted sediments to the seafloor, including dropstones (Domack and Ishman 1993, Syvitski et al. 1996). Dropstones are ice-rafted debris in the pebble to boulder size range, i.e. >2 mm diameter (Wentworth 1922, Bennett et al. 1996). Icebergs can have highly variable residence times within high-latitude fjords, ranging from 1 to >12 mo. (Syvitski et al. 1996, Sutherland et al. 2014), suggesting a stochastic deposition of dropstones as icebergs drift through fjords and across the continental shelf. The addition of hard substrata, in the form of dropstones, to soft-sediment dominated benthic landscapes at fjord and shelf floors enhances habitat heterogeneity, potentially influencing biodiversity. Habitat heterogeneity has been shown to increase diversity in many ecosystems, ranging from forests to abyssal plains (MacArthur and Wilson 1967, Simberloff 1974, Huston 1979, McClintock et al. 2005, Schönberg and Fromont 2012, Amon et al. 2016), but the contribution of glacial debris to habitat heterogeneity has been assessed at only a few locations on continental shelves (Oschmann 1990, Starmans et al. 1999, Schulz et al. 2010, Meyer et al. 2015, 2016, Lacharité and Metaxas 2017). On the Antarctic shelf, the most influential factors affecting benthic biodiversity are postulated to be disturbance (e.g. iceberg scour, burial from glacial sedimentation), sea-ice duration, productivity, and habitat heterogeneity (Gutt 2001, Gutt and Piepenburg 2003, Cummings et al. 2006, Thrush et al. 2010). In Svalbard fjords and in the Weddell Sea, heterogeneity provided by dropstones enhances functional and taxonomic diversity (Meyer et al. 2015, Post et al. 2017), and similar patterns may exist for other soft-sediment habitats containing dropstones, including within Antarctic glaciomarine fjords.

A stochastic delivery of dropstones to the seafloor implies a heterogeneous distribution of fragmented hard substrata, forming island habitats. When considering the scale of single dropstones, the theory of island biogeography suggests that the species diversity on dropstones, if they function as habitat islands, will depend on the rates of faunal colonization and local mortality (MacArthur and Wilson 1967, Rosenzweig 1995). Due to small island size and low dispersal abilities of most megabenthos, recruitment of megabenthos to dropstones is likely to be predominantly non-local (i.e. little self-recruitment). Therefore, the balance between colonization and mortality will control local population dynamics on individual islands, while colonization and extinction rates will define the dynamics of the entire

metapopulation. For obligate hard-substrate fauna, community structure on an island will further be constrained by island size (which limits colonization rates and maximum population sizes) and the distance between neighboring islands (which limits dispersal rates) (MacArthur and Wilson 1967, Rosenzweig 1995). The balance of these processes leads to different dynamic equilibria on islands of varying size and/or distance to source populations (Rosenzweig 2003). Application of island biogeography theory to WAP fjord dropstones predicts a positive relationship between dropstone size and species richness for obligate hard-substrate fauna. The absence of such a relationship might indicate the influence of additional abiotic factors such as sedimentation disturbance or dispersal limitation from isolating circulation features. Characteristics of the environment, such as the magnitude of overlying productivity which controls the flux of organic matter to the seafloor, may influence the community structure and especially the functional diversity of the communities between sites. The extent to which dropstone communities function as habitat islands has recently been investigated in Svalbard fjords (Meyer et al. 2016) but remains unassessed in most glaciomarine fjords, including along the WAP, which harbors novel patterns of biodiversity and community structure. While a positive correlation was found between dropstone size and species richness in Svalbard fjords, the mechanisms behind this island-like phenomenon are likely to be related to dispersal and not the same mechanisms that produce these patterns in terrestrial island communities, such as disturbance and competition (Meyer et al. 2016).

In this study, we quantified the distribution and megafaunal community structure of dropstones in 3 fjords and at 3 open-shelf stations along the WAP. With these data, we tested the predictions of island biogeography theory, explored the influence of various abiotic factors on dropstone community structure, and evaluated the contribution of dropstone assemblages to regional diversity along the deep WAP continental shelf. We found support for several predictions of island biogeography theory, and that dropstones provide an important habitat for a variety of megafaunal species, including many morphotypes that were not detected in diversity assessments of soft-sediment habitats in WAP fjords.

844 *Materials and Methods*

845 Study sites and data collection

846 Digital still images of the seafloor were collected in 2010 during LARISSA Project cruise NBP10-01
847 aboard the RVIB 'Nathaniel B. Palmer' in 3 glaciomarine fjords along the WAP: Andvord, Barilari, and
848 Flandres Bays. Additional images were obtained during FOODBANCS2 Project cruises LMG08-08 and
849 LMG09-02 at the 3 shelf sites (referred to as stations B, E, and F) aboard the ASRV 'Laurence M. Gould'
850 in 2008 and 2009 (Fig. 2.1). All fjord-basin and shelf stations fell within depths of 436–725 m
851 (Supplementary Table 2.1, also available at www.int-res.com/articles/suppl/m583p001_supp.pdf).
852 Seafloor images in phototransects were collected using the 'yo-yo camera' system with methods detailed
853 by Grange and Smith (2013). At each site (fjord basin or shelf station), 2 randomized 1 km phototransects
854 were conducted (except in Outer Barilari Bay, where weather and sea-ice conditions allowed only 1
855 transect). Fjord transects were conducted within sediment-floored basins in the inner, middle, outer,
856 and/or mouth of fjords (Fig. 2.1). Each phototransect produced approximately 100 images, from which 50
857 images of high quality were randomly selected for analysis. The images in this study were selected, color-
858 corrected, and analyzed for soft-sediment fauna reported by Grange and Smith (2013); we reanalyzed the
859 same images for dropstones and associated fauna. Environmental data were also collected on each
860 cruise. Bottom-water temperatures were extracted from CTD casts deeper than 350 m, and all were
861 conducted within 5.5 km and 36 h of phototransects.

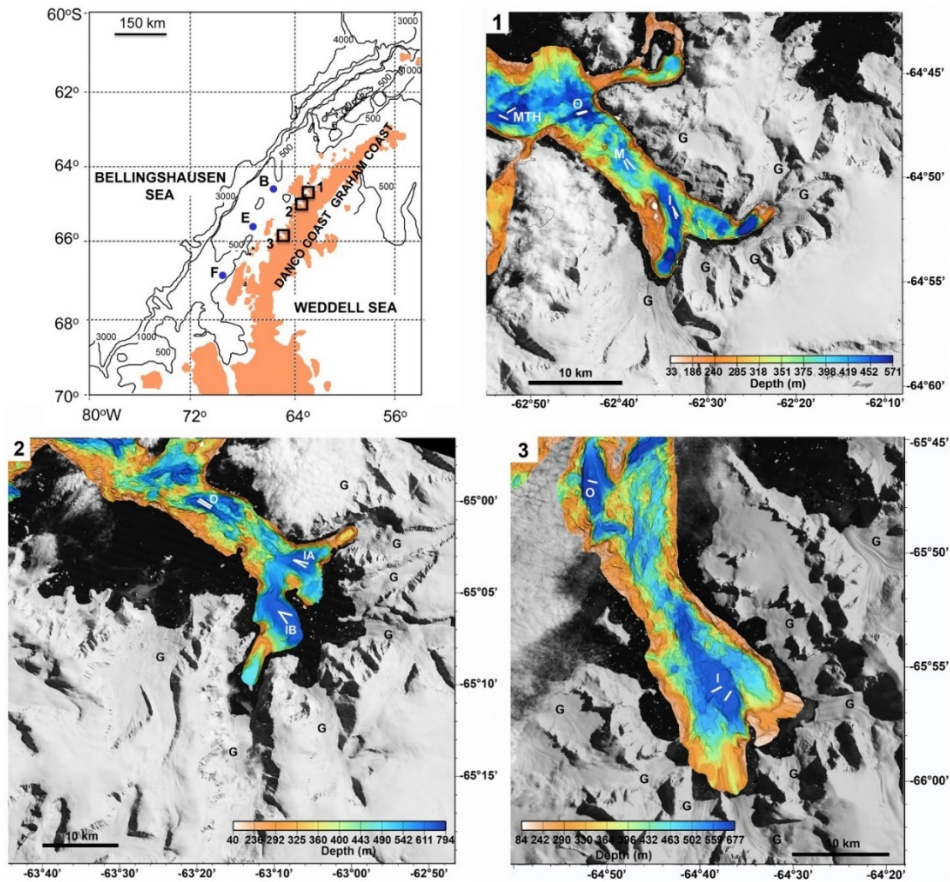


Figure 2.1 Study area along the West Antarctic Peninsula. Bathymetry and glacial satellite imagery overlaid for (1) Andvord Bay, (2) Flandres Bay, and (3) Barilari Bay. White lines show phototransects in fjord basins; I: inner, M: middle, O: outer, MTH: mouth. G denotes major tidewater glaciers entering the fjords. B, E, and F correspond to shelf sampling stations (Grange and Smith 2013)

To relate the variability in community composition between dropstones, sites, and habitats to the variability in the surrounding abiotic environment, we assessed a range of environmental parameters at our study sites (Supplementary Table 2.2). Where possible, environmental data were paired with phototransects by time of collection such that a single bottom-water temperature record corresponded to a single phototransect. Annual primary production ($\text{mg C m}^{-2} \text{ yr}^{-1}$) was derived from concentrations of silicic acid and nitrate in surface waters above the pycnocline. We assumed that winter nutrient

concentrations above the pycnocline were representative of the nutrient concentrations at the start of the summer phytoplankton growth season. Annual production was calculated based on conversion of these nutrients to biomass, assuming no additional nutrient input during the summer growth season, which is a reasonable assumption given the stratification observed during summer months. Therefore, the annual production values presented here are conservative and could underestimate the true production in the fjords. To obtain better estimates of production within a fjord basin, we averaged production estimates derived from multiple nutrient measurements in each fjord. This is appropriate because water-column mixing integrates primary production at the scale of fjord basins, or larger (M. Vernet et al. unpubl. data).

Dropstone and megafauna analyses

In this study, 'dropstone' refers to rocks that were visible at the seafloor and were ≥ 3 cm in 2 minimum dimensions normal to one another. Dropstones and megafauna (animals > 1 cm in largest dimension) were counted within a clear and well illuminated 1.8 m² area in the center of each selected image. In total, 1430 seafloor images were analyzed for dropstones and their associated megafauna. Megafauna were grouped into morphotypes, i.e. putative species, based on Grange and Smith (2013), identification literature (Brueggeman et al. 1998), and feedback from taxonomists. Each morphotype represents the lowest level of identification possible within images and is therefore probably a minimum estimate of true taxonomic diversity. Megafaunal functional groups were assigned as per Grange and Smith (2013) and included surface deposit feeders, suspension feeders, and predators/scavengers. Dropstones were manually outlined to measure total plan area (i.e. the top-down area of the dropstone surface), and the plan area of each stone covered by sediment, using ImageJ®. These measurements also provided calculations of dropstone density and the percentage of exposed hard substrate within each image.

Statistical analyses

898 The Kolmogorov-Smirnov test was used to determine whether the size–frequency distributions differed
899 between 2 groups; colonized and uncolonized dropstones. Mann-Whitney tests were conducted after
900 significant Kolmogorov-Smirnov tests for pairwise comparisons of dropstone parameters (e.g. area and
901 sediment cover) between the 2 groups. Kruskal-Wallis tests were used to test for between-site differences
902 in plan area, percent of exposed hard substrate, and dropstone density. Pairwise comparisons of these
903 parameters between groups (e.g. fjord vs. shelf) were conducted using *t*-tests. To avoid Type II error and
904 over-testing, only differences between the 2 groupings (fjord and shelf) were conducted for a total of only
905 3 *t*-tests. To further assess the contribution of various abiotic parameters to the total variation in
906 megafaunal abundance and species richness, generalized linear mixed models (GLMMs) were created
907 and compared using the ‘glmer’ function in the R package lme4 (Bates et al. 2015). GLMMs allow
908 simultaneous testing of the role of predictors that vary at different scales: area and sediment cover vary at
909 the dropstone scale, while density and percentage of hard substrate vary at the frame scale. Random
910 effects for dropstone frame, transect, and/or site were included. These terms account for the hierarchical
911 spatial structure of the data and quantify which spatial scales hold the greatest variation in megafaunal
912 abundance and species richness. Additionally, a ‘habitat’ fixed effect was included, which accounted for
913 whether observations originated from a fjord or the open shelf. A full model with all fixed and random
914 effects contained too many parameters to be fit by the observational data available; therefore, some
915 random effects were sequentially removed. Versions of the GLMMs with different random effects were
916 assessed by comparing Akaike’s information criterion (AIC) as well as the random-effects estimates
917 themselves. Effects that equaled zero were eliminated first, and AIC comparisons determined which near-
918 zero effects did not significantly improve model fit and could therefore be removed. The final model for
919 megafaunal abundance included random effects for dropstone and transect, while the model for species
920 richness included a random effect for site. Both models included a fixed effect accounting for the different
921 habitats in which these dropstones occurred, i.e. fjord or shelf. Additionally, a binomial GLMM was
922 created to explore the relationship between dropstone colonization (presence/absence) and dropstone
923 sediment cover.

Patterns of community composition were explored through non-metric multidimensional scaling (nMDS) and Bray-Curtis similarity analyses using PRIMER® v6, as well as a canonical analysis of principal coordinates (CAP) using the 'capscale' function in the R package 'vegan' (Oksanen et al. 2017). nMDS analysis used square-root transformed abundance data pooled at the transect level for fjord sites. The square-root transformation reduces the range of abundances so that species with abnormally high abundances do not drive community patterns. The number of individuals observed per transect at shelf sites was much lower than within the fjords, so shelf abundances of megafauna were pooled by site to provide similar numbers of individuals to fjord transects. CAP analysis related community composition at the transect level to dropstone parameters and abiotic factors in the fjords. Dropstone measurements used are thus transect means. The total variability in community composition that could be attributed to each parameter alone was determined using the 'adonis' function in R. This is a multivariate permutation test similar to PERMANOVA with permutations constrained within each sampling site. Finally, Chao 1 species-richness and rarefaction estimates were calculated using PRIMER®v6 for fjord and shelf habitats, both individually and pooled, to determine the contribution of dropstones and fjord ecosystems to WAP regional (γ) diversity.

Results

Dropstone size–frequency distribution

In total, we measured 2972 dropstones, of which 467 were colonized by at least 1 megafaunal individual, and a total of 1766 individual megafauna were counted and identified. Dropstone plan area ranged from 4.6 to 4936.9 cm², with an overall mean \pm SE of 67.0 \pm 3.9 cm² (Table 2.1).

The distribution of dropstone area was highly right-skewed, with 95% of dropstones <250 cm² and a few outliers >2000 cm² (maximum size = 4936.9 cm²). Mean dropstone area varied significantly by site (Kruskal-Wallis $\chi^2 = 91.108$, $p < 0.001$), although size did not vary significantly between fjord and shelf habitats (t -test, $p > 0.05$). Shelf Stn B had significantly smaller dropstones than any other site confirmed by non-overlapping 95% confidence intervals (Supplementary Figure 2.1). The percentage of seafloor

area comprising exposed hard substrate differed by site (Kruskal-Wallis $\chi^2 = 191.95$, $p < 0.001$) but, again, differences did not simply represent a fjord–shelf distinction (t -test, $p > 0.05$). The total seafloor area occupied by dropstones was only 0.77% of the entire surveyed area (2574 m²). Dropstone density was significantly higher within fjords compared to the open shelf (t -test, $p = 0.013$), with maximum fjord densities 70-fold greater than minimum shelf densities (Table 1). The proportion of dropstones colonized by megafauna increased with increasing dropstone size (Fig. 2.2). The size–frequency distributions of colonized and uncolonized dropstones differed significantly (Kolmogorov-Smirnov test, $D = 0.50$, $p < 0.001$), with colonized dropstones having larger median size (Mann-Whitney $p < 0.001$) and significantly higher sediment cover (Mann-Whitney $p < 0.001$) than uncolonized dropstones.

Table 2.1 Summary of dropstone measurements by sampling location. Mean area: average dropstone plan area, mean sediment cover: average percentage cover of dropstone area by sediment, dropstone density: total number of dropstones per seafloor area, hard substrate area: total percentage of seafloor area that is exposed hard substrate, abundance: number of megafauna per seafloor area, species richness: total number of species.

	Images Analyzed	Mean Area (cm ² ± SE)	Mean Sediment Cover (% ± SE)	Total Dropstones	Dropston e Density (m ⁻²)	Hard Substrate (%)	Total Individuals (N)	Abundance (m ⁻²)	Species Richness (S)
Fjord									
Andvord	399	48.1 ± 4.4	66.1 ± 1.4	1502	2.09	0.34	1170	1.63	40
Inner	99	45.9 ± 7.1	61.4 ± 2.7	366	2.05	0.33	75	0.42	17
Middle	100	46.9 ± 9.3	68.0 ± 2.8	776	4.31	0.61	954	5.30	27
Mouth	100	66.8 ± 13.2	64.9 ± 2.9	101	0.56	0.19	71	0.39	18
Outer	100	47.4 ± 6.4	67.4 ± 2.9	259	1.44	0.23	70	0.39	20
Flandres	295	94.3 ± 17.8	56.6 ± 1.8	1096	2.06	0.48	440	0.83	47
InnerA	100	108.8 ± 36.3	63.6 ± 2.6	224	1.24	0.28	132	0.73	16
InnerB	96	87.2 ± 29.9	55.4 ± 3.3	825	4.77	0.99	264	1.53	38
Outer	99	150.6 ± 20.6	44.80 ± 3.27	47	0.26	0.19	44	0.25	6
Barilari	150	46.4 ± 4.1	77.2 ± 2.1	173	0.64	0.06	40	0.15	12
Inner	100	45.2 ± 5.4	78.1 ± 2.5	131	0.73	0.07	29	0.16	8
Outer	50	50.0 ± 4.7	74.3 ± 3.9	42	0.47	0.05	11	0.12	7
Shelf									
St. B	200	25.9 ± 0.8	85.8 ± 1.7	44	0.12	0.01	12	0.03	7
St. E	198	73.5 ± 6.3	64.9 ± 2.2	21	0.06	0.02	20	0.06	8
St. F	188	93.2 ± 26.5	57.3 ± 1.8	136	0.40	0.14	84	0.25	25

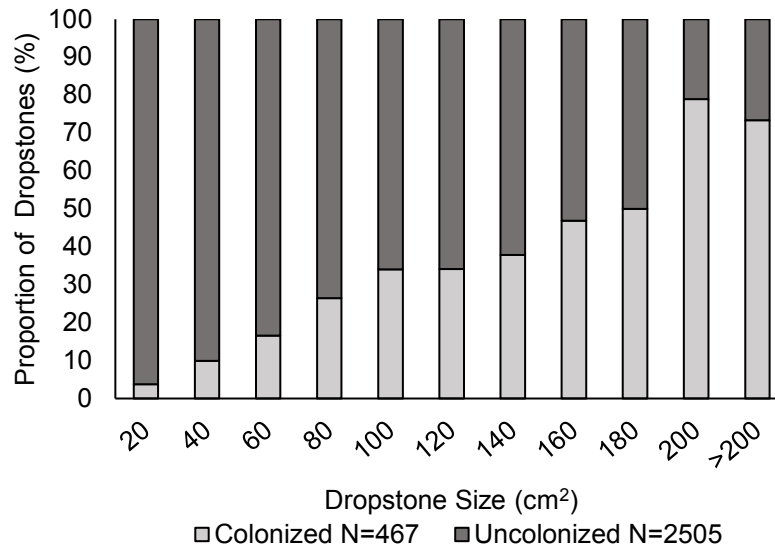
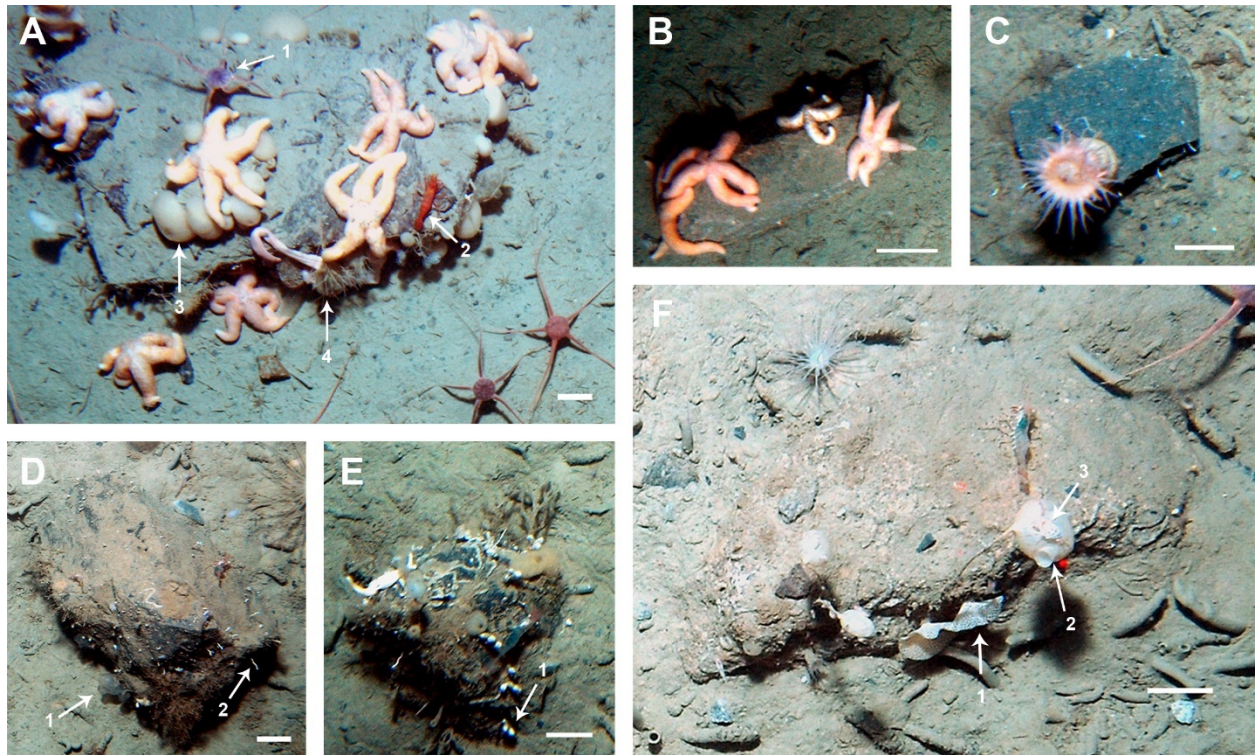


Figure 2.2 Proportion of all dropstones that were colonized by at least 1 individual (light grey), and uncolonized dropstones (dark grey) binned by dropstone plan area. N indicates total observations.

Dropstone megafauna

In total, we observed 73 megafaunal morphotypes within 10 phyla on dropstones (Supplementary Table 2.3). The most diverse phylum was Porifera, followed by Chordata (mostly tunicates), Echinodermata, and Cnidaria. Examples of morphotypes and dropstone assemblages are shown in Fig. 2.3. Of the 73 morphotypes, 28 (38%) were sessile and occurred only on hard substrates (called obligate hard-substrate fauna here), and of those, 66% were suspension feeders. The remaining 45 morphotypes were mobile deposit feeders and predators/scavengers that may use the dropstones opportunistically. Twenty-seven morphotypes were present at both fjord and shelf sites, while 9 morphotypes were unique to the shelf stations and 37 were unique to the fjords. Considering only obligate hard-substrate fauna, 15 morphotypes were common to both fjord and shelf stations, 11 were unique to the fjords, and 1 was unique to the shelf stations. Rank abundance revealed the dominance of a single morphotype, Bryozoan sp. 5, especially within the middle basin of Andvord Bay (Supplementary Table 2.4), which was more than 8 times more abundant than the second most abundant morphotype overall. However, species

983 accumulation curves show that fjord and shelf sites remain under-sampled since they do not reach an
 984 asymptote (Supplementary Figure 2.2), indicating that the number of unique morphotypes within fjord and
 985 shelf habitats may be overestimated.



986
 987 **Figure 2.3** Examples of dropstone megafaunal communities from different sites: (A, D) Flandres Bay and
 988 (B, C, E, F) Andvord Bay. All scale bars represent 5 cm. In panel A: (1) *Ophionotus victoriae*, (2)
 989 *Notocrangon antarcticus*, (3) Porifera sp. 3, (4) Bryozoan sp. 1 (*Cellaria* sp.). Panels B and C show
 990 *Diplasterias brucei* and *Anemone* sp. 1, respectively. In panel D: (1) Tunicate sp. 2 and (2) Bryozoan sp.
 991 5. Panel E shows (1) Scalpelliformes sp. 1, and panel F shows (1) *Reteporella* sp. 1, (2) *Pyura*
 992 *bouvetensis*, and (3) Amphipod sp. 1 (eusirid)

993 994 Modeling megafaunal abundance and species richness on dropstones

995 The GLMM for megafaunal abundance indicated a significant effect only for dropstone area ($p < 0.001$),
 996 and non-significant effects for dropstone sediment cover, density, and the percentage of available hard

substrate (all $p > 0.05$) (Supplementary Table 2.5). The random effect variance for 'stone,' a dropstone-level predictor accounting for over-dispersion (variability greater than expected for the Poisson distribution, i.e. a clumped dispersion pattern), was the greatest at 0.407, suggesting that abundance varied greatly between dropstones due to unknown cause(s). Overall, the parameters in this model explained 38.5% of the variability in megafaunal abundance with 29.2% attributed to fixed effects. Similarly, dropstone area was a significant predictor of species richness ($p < 0.001$) and the random effect estimate for 'site' suggested no significant variation across sampling locations. Overall, parameters in the species-richness model captured 23.4% of the variation, with 21.8% of the variation attributed to fixed effects. A binomial GLMM was used to assess the relationship between presence/absence of any morphotype and dropstone parameters. In this model, both dropstone area and the percentage of dropstone area covered by sediment were significant predictors of presence ($p < 0.01$).

Megafaunal community structure and diversity

Bray-Curtis similarity and nMDS analyses revealed high transect-level variability in community structure and weak clustering at the fjord level. Generally, transects within fjords were 20–40% similar (Fig. 2.4), with some basins within Flandres Bay <20% similar. There was no distinct separation between Barilari Bay and shelf samples. Because spatial clustering by community composition was relatively weak, we explored how much of the variability could be attributed to abiotic factors using CAP. Individually, each abiotic factor could explain only 5.3–19.8% of the variability (Supplementary Table 2.6), but considered together, these parameters explained over 65% of the total variability in community composition.

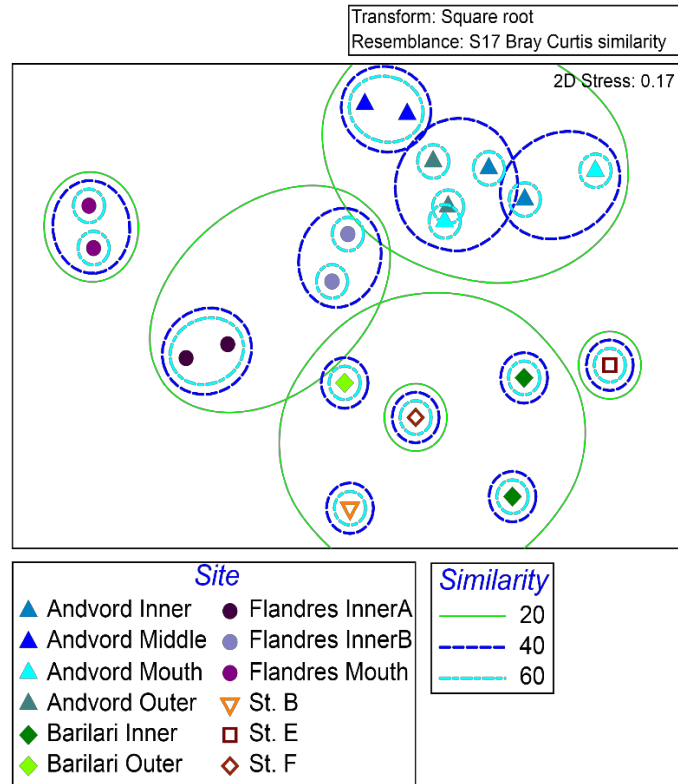


Figure 2.4 Non-metric multidimensional scaling analysis from square-root transformed megafaunal abundances. Points represent communities at the transect level. Bray-Curtis similarity thresholds of 20, 40, and 60% are shown with colored lines. Station locations are given in Fig. 2.1

Dropstone density was most strongly correlated with the first axis of variation in community composition (Fig. 2.5). Several other environmental factors were moderately correlated with the first axis; these were bottom-water temperature, diatom primary production as estimated from silicic acid drawdown, and dropstone area. The second major axis of variation in this analysis can be attributed to differences in dropstone sediment cover.

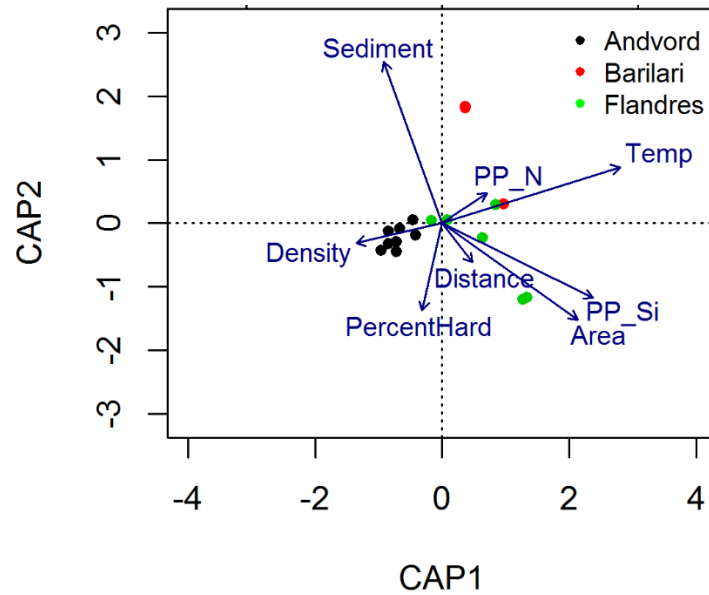
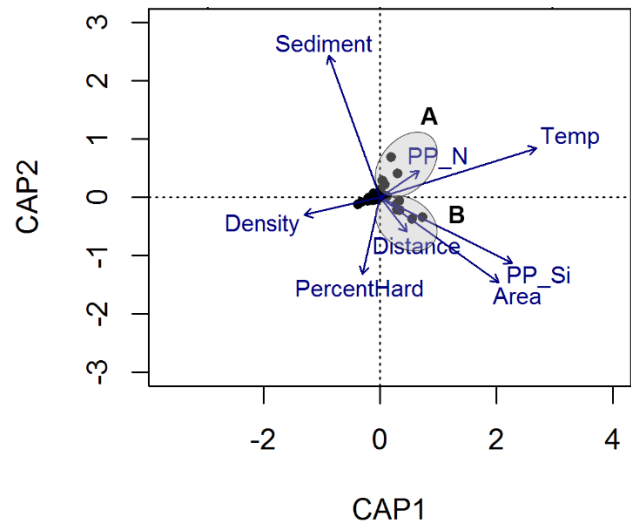


Figure 2.5 Canonical analysis of principal coordinates (CAP) showing alignment of ordinated data (points colored by sampling site) with environmental predictors (vectors). PP_Si and PP_N: mean productivity estimates based on silicic acid and nitrate drawdown, respectively, and summarized at the basin level; Sediment: sediment cover (%) on dropstones summarized at the transect level; PercentHard: percentage of hard substrate available (m^{-2}) summarized at the transect level; Distance: distance from the nearest glacial terminus summarized at the basin level; Area: plan area of a dropstone summarized at the transect level; Density: abundance (m^{-2}) of dropstones summarized at the transect level; Temp: mean bottom water (>350 m) temperature measured *in situ* via CTD as close in space and time to phototransects as possible summarized at the basin level. Note that only data for fjord sampling locations are included. The length of the vector represents the strength of the correlation between that parameter and the community composition.

The percentage of available hard substrate (PercentHard) also correlated moderately with the second axis, but oppositely to dropstone sediment cover. The distribution of morphotypes in the CAP analysis (Fig. 2.6) revealed 2 groups, A and B, which both included predatory/scavenging and suspension-feeding morphotypes. Morphotypes in group A were more positively correlated with silicic acid-derived production

estimates and dropstone size, while those in group B were more positively correlated with temperature or dropstone sediment cover, although these appear to be weak associations. Morphotypes present in clusters A and B are summarized in Table 2.2.



Morphotype	Feeding Group
Group A	
Pycnogonida sp. 4	PS
<i>Cnemidocarpa verrucosa</i>	
Bryozoan sp. 2 (<i>Camptoplites</i> sp.)	SF
Tunicate sp. 5	
Bivalve sp. 2	
Group B	
Amphipod sp. 1 Eusirid	
<i>Pryonosyllis kerguelensis</i>	PS
<i>Parborlasia corrugatus</i>	
Demospongiae sp. 7	SF
Porifera spp. 2 and 7	

Figure 2.6 Canonical analysis of principal coordinates (CAP) displaying ordinated megafaunal abundance data by morphotype (circles) correlated with environmental predictors (vectors). Vector labels are as in Fig. 2.5. The morphotypes present in groups A and B are provided in the table (2.2) on the right.

Species accumulation curves show that fjord and shelf sites remain under-sampled since they do not reach an asymptote (Fig. 2.7, observed), precluding direct comparisons of total species richness. Instead, rarefaction estimates are calculated by randomly re-sampling the pool of samples while accounting for the increase of species richness with an increasing number of samples. Direct comparison of the species richness for a given number of sampled individuals is then possible. Rarefaction estimates for these data compared at the lowest number of individuals collected at the basin, site, and habitat levels ($Es_{(11)}$, $Es_{(12)}$, and $Es_{(116)}$, respectively) revealed that shelf locations exhibited higher rarefaction diversity than fjord locations. At the site level, Stn F, Flandres InnerA, and Andvord Outer had the highest rarefaction

diversity, due to both high evenness (Pielou's J') and species richness (S) (Supplementary Figure 2.2 and Supplementary Table 2.2).

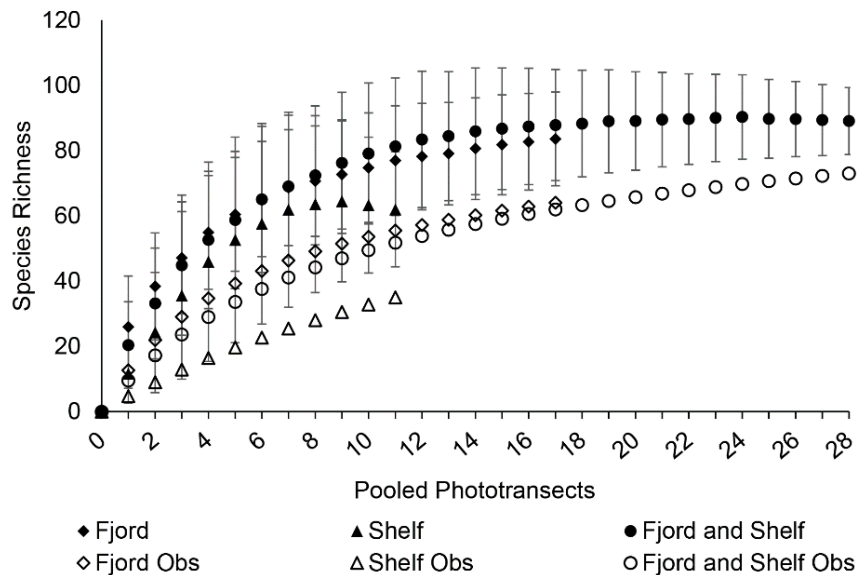


Figure 2.7 Chao 1 species richness estimates (\pm SD) and observed species richness (species accumulation) for fjord and shelf phototransects combined (solid and open circles), fjord phototransects only (solid and open diamonds), and for shelf phototransects (solid and open triangles).

Flandres Outer and Andvord Middle stations had the lowest rarefaction diversity of all basins, again due to low evenness and richness (Table 2.2). Andvord Bay exhibited the lowest evenness overall of any site, likely due to a dominance of a single morphotype (Bryozoan sp. 5) present in very high abundances in the middle fjord which may have reduced overall diversity measures (H' and E_s) and may have contributed to reduced similarity to other regions within Andvord Bay (Table 2.2, Fig. 2.4). Shannon diversity estimates for these data indicate comparable diversity in both fjord and shelf habitats, but these estimates are sensitive to sample size (Magurran 2004) which was highly variable. Relatively high Shannon diversity was maintained even in the innermost regions of Andvord and Flandres Bays, where glacial disturbance was expected to be greatest. Using Chao 1, total species richness for pooled fjord and shelf

phototransects was estimated to be $89 (\pm 10)$ (Fig. 2.7). The fjord sites contributed most to the total estimated species richness (83 ± 14); however, the shelf remains under-sampled, with Chao 1 suggesting there are approximately 27 additional species expected in this habitat.

Table 2.3 Summary of diversity indices. *S*: total richness, *J'*: Pielou's evenness, *Es*_(min): rarefaction, *H'*: Shannon-Weiner diversity index. Rarefaction estimates were assessed at the minimum number of individuals for the level of comparison (*Es*₍₁₁₎ for basin-level comparisons, *Es*₍₁₂₎ for site-level comparisons, and *Es*₍₁₁₆₎ for habitat-level comparisons). The number of individuals, *n*, sampled for each site at these various levels of comparison is provided for reference.

	S	N	J'	Es₍₁₁₎	Es₍₁₂₎	Es₍₁₁₆₎	H'
Fjord	64	1650	0.5977	-	-	28.13	2.486
Andvord Bay	40	1170	0.4439	-	4.530	-	1.637
Inner	17	75	0.8248	6.771	-	-	2.337
Middle	27	954	0.6543	3.468	-	-	1.238
Outer	20	70	0.8968	7.934	-	-	2.687
Mouth	18	71	0.6543	5.395	-	-	1.891
Flandres Bay	47	440	0.7557	-	8.076	-	2.910
Inner A	16	264	0.9028	7.259	-	-	2.751
Inner B	38	132	0.9456	4.671	-	-	1.701
Outer	6	44	0.9076	3.758	-	-	1.173
Barilari Bay	12	40	0.7327	-	5.759	-	1.821
Inner	8	29	0.9277	4.653	-	-	1.510
Outer	7	11	0.9800	7.000	-	-	1.768
Shelf	35	116	0.8661	-	-	3.5	3.079
Stn B	7	12	0.8730	-	7.000	-	1.699
Stn. E	8	20	0.9220	-	6.536	-	1.917
Stn. F	25	84	0.8661	-	8.496	-	2.788

Discussion

Island biogeography and species–area relationships

Dropstones constitute a small fraction (<1%) of the seafloor in this region, and their patchy distribution reflects a heterogeneous delivery mechanism which creates a mosaic of isolated hard-substrate habitat patches. The community patterns observed in this study mirror those of classic island communities, conforming to predictions of island biogeography theory. The correlations between dropstone area and species richness and abundance, and the increase in the proportion of dropstones colonized with increasing dropstone size, match the predicted island-versus-size relationships of island biogeography. Recent investigations of Arctic dropstone communities in Svalbard yielded similar relationships between dropstone size and species richness (Meyer et al. 2016). It is clear from our study that dropstone communities in fjords along the WAP and on the open Antarctic shelf were not space-limited; all dropstones contained open space, and uncolonized stones often were covered with sediment, indicating they had been at the seafloor for a relatively long time. In addition, we found a weak, positive relationship between colonization and dropstone sediment cover, and the binomial model indicates that dropstone sediment cover is a significant predictor of colonization ($p < 0.05$); this suggests that longer exposure time increases the chances of colonization, a pattern consistent with recruitment limitation. Thus, on WAP dropstones, community composition and species richness are controlled, at least in part, by the arrival of colonists rather than by density-dependent processes (e.g. competition) within 'island' assemblages, as originally postulated in island biogeography theory. The insignificance of dropstone density as a predictor of either species richness or megafaunal abundance does not support an effect of distance between individual dropstones. Improved fit of the mixed models with the inclusion of sampling site suggests, instead, differences between sites in the distance to large source populations (e.g. fjord walls), which is expected for island habitats. This is consistent (albeit weakly) with the findings of Meyer et al. (2016) for Arctic dropstone communities, in which dispersal-limitation caused by increasing distance from a large, hard-substrate larval source (i.e. a 'mainland') explained most of the variability in the communities (Meyer et al. 2016). Dropstones within WAP fjords likely have a residence time of years because the sedimentation rate in the fjords is $\sim 0.5 - 1 \text{ cm yr}^{-1}$, while dropstones on the outer shelf likely remain exposed for decades because the sedimentation rate is 2 orders of magnitude lower ($\sim 0.02 \text{ cm yr}^{-1}$; Grange and Smith, 2013). Increasing exposure time increases the probability that a dropstone will be

colonized, at a given rate of colonization. Because occupancy rates of dropstones in the fjords and on the shelf appear comparable for a given size class of dropstone, colonization rates are likely substantially lower on the open shelf. Future colonization studies are needed to constrain the rates of colonization and other processes on dropstones, including post-settlement dynamics, such as competition and mortality, as well as the residence time (time to burial) of dropstone substrates.

In addition to island biogeography theory, models explicitly relating sample area, or oceanic island size, to species richness have been developed (e.g. McGuinness 1984, Durrett and Levin 1996, He and Legendre 1996, Scheiner 2003, Tjørve 2003, Smith 2010). The power model, $S = cA^z$, is most commonly applied (He and Legendre 1996, Scheiner 2003). In this equation, c and z are constants and island communities tend to yield an exponent, z , of approximately 0.2–0.3 (Durrett and Levin 1996, Rosenzweig 2003). Our dropstone data set can be modeled with an exponent of 0.208–0.311, consistent with power models fitted to island habitats and other species–area studies worldwide.

Drivers of small-scale community structure patterns

Patterns of dropstone community similarity varied at scales ranging from the individual dropstone to 100s of kilometers along the WAP. In contrast to the soft-sediment megafauna (Grange and Smith 2013), the dropstone community composition did not cluster tightly by fjord, with nMDS clusters for Barilari Bay and the open shelf stations substantially overlapping. The dropstone community appears to be more similar across fjord and shelf habitats than the soft-sediment megafauna. The relatively strong clustering of Andvord Bay dropstone samples may be driven by the extremely high abundances of a single morphotype, Bryozoan sp. 5, which was far less abundant at the other sampling locations. The presence of uncolonized dropstones may simply reflect more recent deposition and not a lack of substrate utilization since it can be advantageous for suspension-feeding fauna to settle higher in the benthic boundary layer where the flux of suspended particles is higher (Vogel 1981, Mullineaux 1988, Schulz et al. 2010). At the within-fjord scale, diversity did not decrease with decreasing distance to the glacial front as expected from comparison with northern hemisphere high-latitude fjords; this finding is consistent with

soft-sediment-community patterns in the WAP (Grange and Smith 2013), in which megabenthic diversity remained high within a few kilometers of glacial termini. It was postulated that relatively low disturbance from meltwater and sediment plumes in WAP fjords allows the maintenance of such high abundance and diversity within soft-sediment megafaunal assemblages (Grange and Smith 2013). This hypothesis also appears viable for dropstone megafauna, i.e. fjord sedimentation rates are low enough to allow colonization of dropstones even in the inner basins of the fjords where strong burial disturbance is expected. The megafaunal communities studied here are below the depth of iceberg scour and appear to be free of anchor-ice formation; they thus may experience lower rates of other types of physical disturbance than at shallow depths along the Antarctic shelf (Barnes and Conlan 2007, Smale and Barnes 2008).

Drivers of large-scale community structure patterns

At larger scales of 100s of kilometers, bottom-water temperature (a proxy for water mass identity and potential larval sources) became an important factor in differentiating communities among our study sites. Bottom water temperatures between Andvord Bay and Flandres Bay, for example, differ by $>1^{\circ}\text{C}$ even though they are neighboring fjords, and Flandres Bay more closely resembled open shelf waters along the southern WAP that are influenced by warm, upper circumpolar deep water (UCDW) (Hofmann et al. 1996, Smith et al. 1999, Savidge and Amft 2009, Piñones et al. 2011, Cook et al. 2016). Recent studies provide little evidence of modified UCDW inside Andvord Bay (Ø. Lundesgaard and P. Winsor pers. comm.), while this water mass does occur in Flandres Bay southward along the WAP (Cook et al. 2016), suggesting that the adjacent fjords, Andvord and Flandres Bays (Fig. 2.1) may have different water mass sources and experience less exchange than might be expected based on their proximity. In general, circulation in Andvord Bay is weak, decoupled from processes on the open shelf (Ø. Lundesgaard and P. Winsor pers. comm.). This could contribute to poor connectivity between fjords as well as between fjord and shelf sites, leading to community differences on scales of 10–100 km. Similar results were observed

in the Arctic as well, where variability in functional traits of dropstone fauna was best correlated with bottom-water temperature (Meyer et al. 2015).

In addition to bottom-water temperature, the mean dropstone size, sediment cover, and annual overlying primary production were best correlated with benthic megafaunal community composition. Overlying production constrains the flux of organic carbon to the seafloor, especially along the WAP where export ratios can be high (Smith et al. 2008, Buesseler et al. 2010). Interestingly, annual production estimated via nitrate uptake was more weakly correlated with benthic community composition than production estimated from silicic acid uptake, which represents only the production due to diatoms. These results suggest that mobile, predatory/scavenging megafauna may be more abundant in areas where episodic delivery of phytodetritus from large diatom blooms is prevalent. This response is likely indirect as predators may respond to an aggregation or enhanced activity of surface deposit-feeding megafauna that respond quickly to phytodetrital inputs (Sumida et al. 2008, 2014). The correlation of large poriferan (suspension-feeders) abundance with diatom production may reflect their ability to cope with variable and highly seasonal food availability by utilizing different food sources, especially when productivity is episodic (e.g. Thurber 2007). The smaller tunicate and bryozoan morphotypes were correlated with production estimated by nitrate drawdown and oppositely correlated with dropstone sediment cover. This suggests the need for dropstones and a reliance on a consistent food source. These organisms are likely more successful in areas of high and less variable total production (i.e. fewer large diatom blooms) and low dropstone sediment cover.

Ecosystem function of dropstones

Glacial dropstones on the WAP contribute disproportionately on an area basis to the overall gamma diversity of the WAP fjord-shelf system at 400–700 m by providing ~1% of the seafloor habitat space but contributing 20% of the regional soft and hard substrate species pool. Comparison with a soft-sediment megafaunal survey of this region (Grange and Smith 2013) revealed 44 overlapping morphotypes and an additional 29 morphotypes that were previously not recorded, 22 of which were hard-substrate obligates.

While dropstones support colonization by obligate hard-substrate fauna, they also support ecological functions for mobile megafauna. In particular, a demersal fish (*Chaenodraco wilsoni*) was observed numerous times guarding egg masses attached to the tops of dropstones (Kock et al. 2008), and a benthic medusa (*Ptychogastria polaris*) was also seen adhered to dropstones (Fig. 2.8). While *C. wilsoni* deposits eggs on dropstones, other benthic notothenoids, such as *Chaenocephalus aceratus*, have been observed guarding gravel nests in the northern Antarctic Peninsula region (Detrich et al. 2005, Reid et al. 2007).

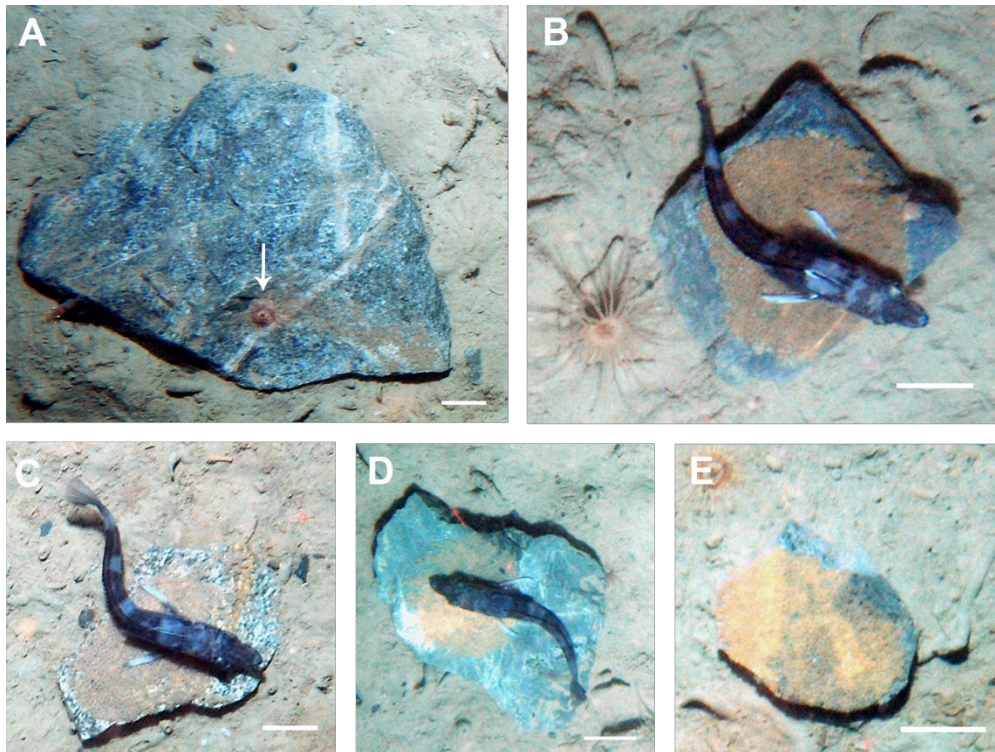


Figure 2.8 Examples of (A) *Ptychogastria polaris* (arrow), (B, C, D) *Chaenodraco wilsoni* guarding egg masses on dropstones, and (E) *C. wilsoni* egg mass on dropstone. All scale bars = 5 cm.

Enhanced burial of this substrate, by increased sedimentation due to climate warming and glacial melt or other mechanisms, could reduce the extent of nursery grounds of these benthic fishes as well as the habitat space for obligate fauna. Although increased melting could also lead to higher rates of calving,

iceberg production and, therefore, dropstone deposition rate, there is no evidence to suggest the total amount of hard substrate would increase. Given the importance of dropstones as a habitat for obligate hard substrate fauna and even mobile fauna in these fjord and shelf ecosystems, the ecological role of dropstones merits study in other parts of the Southern Ocean and in polar regions generally.

Conclusions

Glacial dropstones in high-latitude fjord and shelf ecosystems provide heterogeneity and enhance WAP regional species richness at 400–700 m depths by 20%. Dropstones appear to function as island habitats in these ecosystems by adhering to principles of island biogeography theory. Dropstone megafaunal abundance and diversity in Andvord, Barilari, and Flandres Bays were most highly correlated with mean dropstone size, bottom-water temperature, overlying annual primary production, and dropstone sediment cover. The 3 feeding modes of megafauna observed in this study were correlated differently with environmental parameters, but this could not explain large proportions of variability in the community composition. Rather, it appears a combination of island-like assembly processes and influences from the abiotic environment have shaped these benthic communities. Dropstone community structure in both the Antarctic and Arctic ecosystems appear to be mainly influenced by dispersal and recruitment limitation. The use of dropstones as egg-brooding sites by the benthic fish *Chaenodraco wilsoni* indicates that both sessile (hard-substrate obligate) and mobile components of fjord megabenthos may be negatively impacted if warming increases fjord sedimentation rates and dropstone burial in the future.

Acknowledgements

This work was conducted in collaboration with Drs. Craig R. Smith, Kyle Edwards and Maria Vernet. Funding was provided by National Science Foundation grants for the LARISSA (OPP 0732711), FOODBANCS2 (OPP 0636806), and FjordEco (OPP 1443680) projects to Craig R. Smith. We thank the captains and crews of the AVIB ‘Nathaniel B. Palmer’ and ASRV ‘Laurence M. Gould’ as well as the

1231 numerous USAP personnel and scientists who assisted in the field. We also thank Dr. Thomas Desvignes
1232 (Oregon State University) for fish identifications and Dr. Laura Grange and Christian Clark for their help in
1233 the field and processing of the original benthic imagery.

1234

1235 *References*

1236 Amon DJ, Ziegler AF, Dahlgren TG, Glover AG and others (2016) Insights into the abundance and
1237 diversity of abyssal megafauna in a polymetallic-nodule region in the eastern Clarion-Clipperton
1238 Zone. *Sci Rep* 6: 30492

1239 Barnes DK, Conlan KE (2007) Disturbance, colonization and development of Antarctic benthic
1240 communities. *Philos Trans R Soc Lond B Biol Sci* 362: 11–38

1241 Bates D, Mächler M, Bolker B, Walker S (2015) Fitting linear mixed-effects models using lme4. *J Stat*
1242 *Softw* 67: 1–46

1243 Bennett MR, Doyle P, Mather AE (1996) Dropstones: their origin and significance. *Palaeogeogr*
1244 *Palaeoclimatol Palaeo ecol* 121: 331–339

1245 Boldt KV, Nittrouer CA, Hallet B, Koppes MN, Forrest BK, Wellner JS, Anderson JB (2013) Modern rates
1246 of glacial sediment accumulation along a 15° S-N transect in fjords from the Antarctic Peninsula
1247 to southern Chile. *J Geophys Res Earth Surf* 118: 2072–2088

1248 Brueggeman P (1998) Underwater field guide to Ross Island & McMurdo Sound, Antarctica.
1249 www.peterbrueggeman.com/nsf/fguide/

1250 Buesseler KO, McDonnell AMP, Schofield OME, Steinberg DK, Ducklow HW (2010) High particle export
1251 over the continental shelf of the west Antarctic Peninsula. *Geophys Res Lett* 37: L22606

1252 Cook AJ, Fox AJ, Vaughan DG, Ferrigno JG (2005) Retreating glacier fronts on the Antarctic Peninsula
1253 over the past half-century. *Science* 308: 541–544

- 1254 Cook AJ, Holland PR, Meredith MP, Murray T, Luckman A, Vaughan DG (2016) Ocean forcing of glacier
1255 retreat in the western Antarctic Peninsula. *Science* 353: 283–286
- 1256 Cummings V, Thrush S, Norkko A, Andrew A, Hewitt J, Funnell G, Schwarz AM (2006) Accounting for
1257 local scale variability in benthos: implications for future assessments of latitudinal trends in the
1258 coastal Ross Sea. *Antarct Sci* 18: 633–644
- 1259 Detrich HW III, Jones CD, Kim S, North AW, Thurber A, Vacchi M (2005) Nesting behavior of the icefish
1260 *Chaenocephalus aceratus* at Bouvetøya Island, Southern Ocean. *Polar Biol* 28: 828–832
- 1261 Domack EW, Ishman S (1993) Oceanographic and physiographic controls on modern sedimentation
1262 within Antarctic fjords. *Geol Soc Am Bull* 105: 1175–1189
- 1263 Domack EW, McClennen CE (1996) Accumulation of glacial marine sediments in fjords of the Antarctic
1264 Peninsula and their use as late Holocene paleoenvironmental indicators. *Antarct Res Ser* 70:
1265 135–154
- 1266 Durrett R, Levin S (1996) Spatial models for species area curves. *J Theor Biol* 179: 119–127
- 1267 Elverhoi A, Seland R (1983) Glaciomarine sedimentation in a modern fjord environment, Spitsbergen.
1268 *Polar Res* 1: 127–149
- 1269 Grange LJ, Smith CR (2013) Megafaunal communities in rapidly warming fjords along the West Antarctic
1270 Peninsula: hotspots of abundance and beta diversity. *PLOS ONE* 8: e77917
- 1271 Gutt J (2001) On the direct impact of ice on marine benthic communities, a review. *Polar Biol* 24:
1272 553–564
- 1273 Gutt J, Piepenburg D (2003) Scale-dependent impact on diversity of Antarctic benthos caused by
1274 grounding of icebergs. *Mar Ecol Prog Ser* 253: 77–83
- 1275 He F, Legendre P (1996) On species-area relations. *Am Nat* 148: 719–737

- 1276 Hofmann EE, Klinck JM, Lascara CM, Smith DA (1996) Water mass distribution and circulation west of
1277 the Antarctic Peninsula and including Bransfield Strait. In: Ross RM, Hofmann EE, Quetin LB
1278 (eds) Foundations for ecological research west of the Antarctic Peninsula. American Geophysical
1279 Union, Washington, DC, p 61–80
- 1280 Huston M (1979) A general hypothesis of species diversity. *Am Nat* 113: 81–101
- 1281 Kock KH, Pshenichnov L, Jones CD, Gröger J, Riehl R (2008) The biology of the spiny icefish
1282 *Chaenodraco wilsoni* Regan, 1914. *Polar Biol* 31: 381–393
- 1283 Lacharité M, Metaxas A (2017) Hard substrate in the deep ocean: how sediment features influence
1284 epibenthic megafauna on the eastern Canadian margin. *Deep Sea Res I* 126: 50–61
- 1285 MacArthur RH, Wilson EO (1967) The theory of island biogeography. Princeton University Press,
1286 Princeton, NJ
- 1287 Magurran AE (2004) Measuring biological diversity. Blackwell Publishing, Oxford
- 1288 McClintock JB, Amsler CD, Baker BJ, van Soest RWM (2005) Ecology of Antarctic marine sponges: an
1289 overview. *Integr Comp Biol* 45: 359–368 *13 Mar Ecol Prog Ser* 583: 1–14, 2017
- 1290 McGuinness KA (1984) Species–area curves. *Biol Rev Camb Philos Soc* 59: 423–440
- 1291 Meredith MP (2005) Rapid climate change in the ocean west of the Antarctic Peninsula during the second
1292 half of the 20th century. *Geophys Res Lett* 32: L19604
- 1293 Meyer KS, Sweetman AK, Young CM, Renaud PE (2015) Environmental factors structuring Arctic
1294 megabenthos — a case study from a shelf and two fjords. *Front Mar Sci* 2:22
- 1295 Meyer KS, Young CM, Sweetman AK, Taylor J, Soltwedel T, Bergmann M (2016) Rocky islands in a sea
1296 of mud: biotic and abiotic factors structuring deep-sea dropstone communities. *Mar Ecol Prog Ser*
1297 556: 45–57

- 1298 Mullineaux LS (1988) The role of settlement in structuring a hard-substratum community in the deep sea.
1299 J Exp Mar Biol Ecol 120: 247–261
- 1300 Oksanen J, Blanchet FG, Friendly M, Kindt R and others (2017) vegan: community ecology package.
1301 <https://cran.r-project.org/package=vegan>
- 1302 Oschmann W (1990) Dropstones — rocky mini-islands in high-latitude pelagic soft substrate
1303 environments. Senckenb Marit 21: 55–75
- 1304 Piñones A, Hofmann EE, Dinniman MS, Klinck JM (2011) Lagrangian simulation of transport pathways
1305 and residence times along the western Antarctic Peninsula. DeepSea Res II 58: 1524–1539
- 1306 Post AL, Lavoie C, Domack EW, Leventer A, Shevenell A, Fraser AD, NBP 14-02 Science Team (2017)
1307 Environmental drivers of benthic communities and habitat heterogeneity on an East Antarctic
1308 shelf. Antarct Sci 29: 17–32
- 1309 Pritchard HD, Vaughan DG (2007) Widespread acceleration of tidewater glaciers on the Antarctic
1310 Peninsula. J Geophys Res 112(F3): F03S29
- 1311 Reid WDK, Clarke S, Collins MA, Belchier M (2007) Distribution and ecology of *Chaenocephalus aceratus*
1312 (*Channichthyidae*) around South Georgia and Shag Rocks (Southern Ocean). Polar Biol 30:
1313 1523–1533
- 1314 Rosenzweig ML (1995) Species diversity in space and time. Cambridge University Press, Cambridge
- 1315 Rosenzweig ML (2003) Reconciliation ecology and the future of species diversity. Oryx 37: 194–205
- 1316 Savidge DK, Amft JA (2009) Circulation on the West Antarctic Peninsula derived from 6 years of
1317 shipboard ADCP transects. Deep Sea Res I 56: 1633–1655
- 1318 Scheiner SM (2003) Six types of species-area curves. Glob Ecol Biogeogr 12: 441–447
- 1319 Schönberg CHL, Fromont J (2012) Sponge gardens of Ningaloo Reef (Carnarvon Shelf, Western
1320 Australia) are biodiversity hotspots. Hydrobiologia 687: 143–161

- 1321 Schulz M, Bergmann M, von Juterzenka K, Soltwedel T (2010) Colonisation of hard substrata along a
1322 channel system in the deep Greenland Sea. *Polar Biol* 33: 1359–1369
- 1323 Simberloff DS (1974) Equilibrium theory of island biogeography and ecology. *Annu Rev Ecol Evol Syst* 5:
1324 161–182
- 1325 Smale DA, Barnes DKA (2008) Likely responses of the Antarctic benthos to climate-related changes in
1326 physical disturbance during the 21st century, based primarily on evidence from the West Antarctic
1327 Peninsula region. *Ecography* 31: 289–305
- 1328 Smith AB (2010) Caution with curves: caveats for using the species–area relationship in conservation.
1329 *Biol Conserv* 143: 555–564
- 1330 Smith CR, Mincks S, DeMaster DJ (2006) A synthesis of benthic–pelagic coupling on the Antarctic shelf:
1331 food banks, ecosystem inertia and global climate change. *Deep Sea Res II* 53: 875–894
- 1332 Smith CR, Mincks S, DeMaster DJ (2008) The FOODBANCS project: introduction and sinking fluxes of
1333 organic carbon, chlorophyll-a and phytodetritus on the western Antarctic Peninsula continental
1334 shelf. *Deep Sea Res II* 55: 2404–2414
- 1335 Smith CR, DeMaster DJ, Thomas CJ, Sršen P, Grange L, Evrard V, DeLeo F (2012) Pelagic–benthic
1336 coupling, food banks, and climate change on the West Antarctic Peninsula shelf. *Oceanography*
1337 25: 188–201
- 1338 Smith DA, Hofmann EE, Klinck JM, Lascara CM (1999) Hydrography and circulation of the West Antarctic
1339 Peninsula Continental Shelf. *Deep Sea Res I* 46: 925–949
- 1340 Starmans A, Gutt J, Arntz WE (1999) Mega-epibenthic communities in Arctic and Antarctic shelf areas.
1341 *Mar Biol* 135: 269–280
- 1342 Sumida PYG, Bernardino AF, Stedall VP, Glover AG, Smith CR (2008) Temporal changes in benthic
1343 megafaunal abundance and composition across the West Antarctic Peninsula shelf: results from
1344 video surveys. *Deep Sea Res II* 55: 2465–2477

1345 Sumida PYG, Smith CR, Bernardino AF, Polito PS, Vieira DR (2014) Seasonal dynamics of epibenthic
 1346 megafauna on the deep West Antarctic Peninsula in response to variable phytodetrital influx. R
 1347 Soc Open Sci 1: 140294

1348 Sutherland DA, Roth GE, Hamilton GS, Mernild SH, Stearns LA, Straneo F (2014) Quantifying flow
 1349 regimes in a Greenland glacial fjord using iceberg drifters. Geophys Res Lett 41:8411–8420

1350 Syvitski JPM, Andrews JT, Dowdeswell JA (1996) Sediment deposition in an iceberg-dominated
 1351 glacimarine environment, East Greenland: basin fill implications. Global Planet Change 12:
 1352 251–270

1353 Thrush SF, Hewitt JE, Cummings VJ, Norkko A, Chiantore M (2010) Beta-diversity and species
 1354 accumulation in Antarctic coastal benthos: influence of habitat, distance and productivity on
 1355 ecological connectivity. PLOS ONE 5: e11899

1356 Thurber AR (2007) Diets of Antarctic sponges: links between the pelagic microbial loop and benthic
 1357 metazoan food web. Mar Ecol Prog Ser 351: 77–89

1358 Tjørve E (2003) Shapes and functions of species area curves: a review of possible models. J Biogeogr
 1359 30: 827–835

1360 Vaughan DG, Marshall GJ, Connolley WM, King JC, Mulvaney R (2001) Devil in the detail. Science 293:
 1361 1777–1779

1362 Vogel S (1981) Life in moving fluids: the physical biology of flow. Princeton University Press, Princeton,
 1363 NJ

1364 Wentworth CK (1922) A scale of grade and class terms for clastic sediments. J Geol 30:377–392

1365 Włodarska-Kowalczyk M, Pearson TH, Kendall MA (2005) Benthic response to chronic natural physical
 1366 disturbance by glacial sedimentation in an Arctic fjord. Mar Ecol Prog Ser 303: 31–4 1

Chapter III Dispersal of Antarctic Fjord Benthic Fauna: A Modeling Study

Abstract

Larval dispersal is one of the most important community assembly and population maintenance processes, yet it is extremely difficult to measure at ecologically relevant spatio-temporal scales. This study utilizes a high-resolution hydrodynamic model and particle tracking model to explore the dispersal of simulated larvae in a topographically complex region of the West Antarctic Peninsula. The larvae modeled represent two end members of dispersal potential observed in Antarctic benthos, high and low, characterized by a long development period and no behavior vs a very short development period and downward swimming behavior. In simulations of the low dispersal potential scenario, the 10,000 larvae simulated failed to disperse to and settle within a neighboring fjord (< 50 km away) within the pre-competency and settlement period, suggesting that self-recruitment is very important for fjord populations with low dispersal. For highly dispersing organisms, connectivity between fjords only occurred when larvae were in the water column for at least 35 days prior to settlement, but even a much longer time in the plankton (up to 150 days) yielded little dispersal between neighboring fjords. This suggests that these fjords harbor ecologically distinct populations in which self-recruitment may be important for maintaining population sizes and that connectivity between fjords is likely achieved through stepping-stone dispersal. Investigation of the surface currents and winds of this region suggest that for passive larvae that are mixed into surface (< 100 m) layers, episodic katabatic wind events may aid substantially in dispersal to regions > 100 km away from the natal population. This work highlights the utility of bio-physical models and provides insights into the dispersal dynamics of benthic communities which has not previously been assessed in this region.

Introduction

The biogeography of Antarctic benthic organisms is governed by a suite of evolutionary and ecological processes, including larval dispersal (Arntz et al. 1994; Clarke 2008b; Clarke et al. 2009; Thatje 2012). Much of the epibenthic megafaunal community is sessile so the potential for long-distance dispersal

occurs during the larval stage. Long-distance dispersal can be advantageous because it may increase genetic variation and provide opportunities for exploitation of new habitats which may have more suitable living conditions (Hill, 1991; Krug 2001; Palmer and Strathmann 1981; Pechenik 1999; Strathmann 1985; Strathmann 1974). Life history strategies of Antarctic benthic fauna vary widely; larvae may be released into the water column (planktonic) or remain at or near the seafloor for development (demersal/benthic). During this developmental period, larvae may actively feed (planktotrophy) or utilize nutritional stores (lecithotrophy) (Jablonski and Lutz 1983; Mileikovsky 1971b; Stanwell-Smith et al. 1999). Some organisms, especially echinoderms, brood their offspring or exhibit direct development in which the first “larval” stage is simply a small version of the adult form (Poulin and F  ral 1996). Antarctic benthic species are K-selected meaning they grow and develop slowly, reach maturity much later in life than congeners at lower latitudes, are long-lived, and may allocate energy toward fewer, more developed offspring (Bosch 1989; Clarke 1979; Emlet and Hoegh-Guldberg 1997; Pearse et al. 1991; Strathmann et al. 2006). It was previously hypothesized that the timing of reproduction for Antarctic macrobenthos with planktotrophic larvae would be tightly coupled to the timing of spring phytoplankton blooms because of the strong seasonality in food availability, and this phenomenon is observed in some species (Pearse, McClintock, and Bosch 1991; Damon Stanwell-Smith et al. 1999; Damon Stanwell-Smith and Peck 1998; Starr, Himmelman, and Therriault 1990). Seasonal cycles of sea ice cover cause surface salinity fluctuations that create a particularly harsh environment, which was predicted to select for non-planktonic larvae resulting in a dominance by fauna that brood or have direct development (Peck, Convey, and Barnes 2006; Thorson 1950b). However, there are now many well-known exceptions to these hypotheses demonstrating that planktotrophy is actually a common strategy among Antarctic benthic fauna (Bosch and Pearse 1990; Clarke 1992; Mileikovsky 1971b; Pearse, 1994; Pearse et al. 1991; Poulin and F  ral 1996; Smith et al. 2006).

Dispersal potential, or the distance an organism may travel away from its spawning grounds to its settlement location, may increase as a function of the time spent in the water column, known as the pelagic larval duration (PLD) (Cowen and Sponaugle 2009; Palumbi 2003b; Shanks 2009; Shanks et al.

2003; Siegel et al. 2003). The PLD is generally longer for planktotrophic larvae compared to lecithotrophic larvae, generating the notion that planktotrophic larvae disperse farther. Though the positive relationship between dispersal distance and PLD is documented for several species, the strength of this correlation varies dramatically across taxa (Selkoe and Toonen 2011), suggesting that this “rule” is more of a trend. One limitation to this assumption is the PLD itself. The PLD is interpreted as the *maximum* amount of time a larval form spends in the water column prior to settlement and assuming so will produce a maximum estimate of dispersal distance (Young et al. 2012). After the PLD has been reached, it is assumed that all larvae that have not yet settled perish. However, based on laboratory culturing methods and observation, literature reports of PLD often actually represent the *minimum* time larvae spend in the water column before they are competent of settlement known as the pre-competency period. It is important to have accurate PLD and pre-competency period data to make accurate estimates of dispersal distance. Several studies now report surprising degrees of isolation and population genetic structure observed in populations of organisms with otherwise high dispersal potential (Almany et al. 2017; Cunningham et al. 2009; Damerau et al. 2014; Hoffman et al. 2011; Ledoux et al. 2012; Paris et al. 2007; Riesgo et al. 2015; Siegel et al. 2008; Sköld et al. 2003; Swearer et al. 2002). The importance of considering larval behaviors (Bingham and Young 1991; North et al. 2008; Palumbi 1994; Paris et al. 2007; Woodson and McManus 2007), and ocean circulation features such as fronts or eddies (Mullineaux and Mills 1997; Palumbi 2003; Thornhill et al. 2008; Xu et al. 2018) when inferring the dispersal distance is now widely recognized. For example, in highly retentive systems (e.g. enclosed bays and fjords), circulation can produce population- or even species-level differentiation over short distances for organisms with otherwise high dispersal inferred from their planktonic larvae and long PLDs (Bilton et al. 2002; Cunningham et al. 2009; Wright 1943).

Larval dispersal influences both local and distant population dynamics by limiting the exchange of individuals between populations (i.e. connectivity). Such processes are considered in metacommunity dynamics, where a metacommunity is a network of subpopulations connected via immigration or dispersal such that the dynamics of local populations affect the dynamics at a regional scale. Individual populations

may be larval sources (a population which exports larvae) or sinks (a population which relies on imported larvae or self-recruitment) (Leibold et al. 2004; Pulliam 1988). Identification of source and sink populations is particularly useful for conservation and management applications at a variety of spatial scales (Gaines et al. 2010; Palumbi 2004; Shanks et al. 2003). Marine population connectivity is most commonly assessed using genetic techniques including mitochondrial DNA sequences, microsatellite markers, or nucleotide polymorphisms to determine population divergence and compare genetic population structure via F-statistics such as F_{ST} (Bryan-Brown et al. 2017; Hedrick and Miller 1992; Holsinger and Weir 2009; Selkoe and Toonen 2006; Sunnucks 2000; Vignal et al. 2002). These genetic metrics measure processes occurring over evolutionary time scales that may not be ecologically informative and in fact fail to detect population structure when exchange between populations is ≤ 100 migrants per generation (Crandall et al. 2018; Slatkin 1995). Ecologically relevant connectivity (i.e. sufficient exchange between populations to affect population dynamics) occurs on much shorter temporal scales than genetic techniques can detect and is, therefore, much more difficult to measure (Cowen and Sponaugle 2009; McCartney-Melstad et al. 2018). Settlement and survival of only a few individuals per generation may be sufficient to maintain genetically homogeneous populations when the populations are, in reality, ecologically distinct (Slatkin 1993; Wright 1950). Genetic techniques are also unable to capture recent changes in gene flow which may be informative for ecosystem management (McCartney-Melstad et al. 2018; Riginos et al. 2016) though recent technical advances are promising (Crandall et al. 2018). To study ecological connectivity, it is useful to approach larval dispersal from a metacommunity perspective (Leibold et al. 2004; Levin 1974, 1976; Marquet et al. 1993; Mouquet et al. 2006; Mouquet and Loreau 2003; Wilson 1992) and in regions experiencing pronounced climatic changes or other environmental stressors, understanding source-sink population dynamics is crucial to prediction of future community composition.

Estimates of larval dispersal in the ocean requires modeling both the physical and biological processes that control larval movement that vary in space and time across several orders of magnitude (Pineda and Reynolds 2018). Computational advances now enable ecologists to couple high-resolution regional

hydrodynamic models to larval behavior models to track large numbers of simulated larvae, and thus predict more realistic dispersal patterns. One such model, of many (Bidegain et al. 2013; Doos et al. 2013; Paris et al. 2013; van Sebille et al. 2018), is the Lagrangian TRANSport model or LTRANS (North 2008; North et al. 2006; North et al. 2011). This type of model can be used to determine the dispersal potential of a wide range of fauna and explore biophysical relationships such as dispersal directionality and barriers in habitats ranging from the intertidal to the deep sea (Hilario et al. 2015; Kettle and Haines 2006; North et al. 2011; Piñones et al. 2013; Watson et al. 2011; Young et al. 2012). Most dispersal-related studies from the Antarctic utilize genetic markers to assess connectivity and focus on the connection across the Antarctic Circumpolar Current (Damerau et al. 2012; Hunter and Halanych 2008; Riesgo et al. 2015; Thornhill et al. 2008; Wilson et al. 2007; Wilson et al. 2009). Few attempts have been made to use Lagrangian models or a combination of techniques (Brasier et al. 2017; Matschiner et al. 2009; Piñones et al. 2013). Considerable effort has been made to model dispersal of Antarctic krill as this is considered a keystone species of Antarctic food webs and there are substantial fisheries for krill in the Southern Ocean. The coastal West Antarctic Peninsula (WAP) contains an extensive network of fjords of variable geometry, each containing multiple deep, sedimented basins separated by sills often > 200 m deep (Munoz and Wellner 2018). Fjords have been shown to create barriers to dispersal over short distances because larvae must be entrained within upper ocean layers to cross the shallow sills and penetrate fjords (Bouchet and Taviani 1992; Buhl-Mortensen and Hoisaeter 1993). The topography and hydrography of the WAP region generates complicated circulation patterns (Lundesgaard et al., in revision). Currents in the Gerlache and Bismarck Straits routinely reach $\sim 40 \text{ cm s}^{-1}$, but inside fjords and especially within the deep (> 400 m) basins, the systems are quiescent (Lundesgaard et al., in revision). The northern portion of the WAP is dominated by Bransfield Strait Water (BSW: $< 0^\circ\text{C}$, 34.45-34.6 PSU, Hofmann et al. 1996) while southern portions are heavily influenced by Circumpolar Deep Water (CDW: $> 1^\circ\text{C}$, up to 34.73 PSU, Hofmann et al. 1996). Periodic intrusions of CDW onto southern portions of the WAP shelf are linked to warming of coastal waters and basal melting of glaciers (Cook et al. 2016). The confluence of CDW-dominated southern waters and BSW-dominated northern water masses occurs in the vicinity of Flandres and Andvord Bays, two glaciomarine fjords located near Anvers Island (Cook et al. 2016). Comparison of benthic communities in these fjords found surprising dissimilarity between sites <

50 km apart (Grange and Smith 2013). High retention in these fjords and limited exchange with the outer shelf (Hofmann et al. 1996) could be driving some of the observed spatial differences in benthic community composition over relatively small scales. However, abundances of benthic fauna are up to 38 times greater in these fjords and individuals are significantly larger compared to the adjacent shelf (Grange and Smith 2013). Fecundity scales with body size (Strathmann and Strathmann 1982), so benthic populations in WAP fjords may be producing large numbers of larvae that, depending on circulation patterns, could be sources of larvae to more distant locations on the WAP shelf.

This study aimed to assess the dispersal of benthic megafauna from within two glaciomarine fjords, Andvord and Flandres Bays, by coupling a high-resolution hydrodynamic model (ROMS) with a particle-tracking model (LTRANS). We aim to answer the following questions: (1) Can larvae released from within Andvord Bay settle in Flandres Bay (and vice versa) during the summer season (Dec. - Apr.) given reasonable pre-competency periods and pelagic larval durations? (2) How do environmental conditions (i.e. winds, currents, day of release) affect settlement patterns? (3) How do settlement patterns differ across reproductive strategies (i.e. for larvae with low versus high dispersal potential)?

Methods

Hydrodynamic and Particle-Tracking Models

We model particle distributions within a domain encompassing two glaciomarine fjords of the WAP; Andvord Bay and Flandres Bay, as well as the surrounding Gerlache and Bismarck Straits (Figure 3.1). Fjord basin names will be referred to by acronyms as provided in Figure 3.1. The offline Lagrangian TRANSPORT model, LTRANS, (E. W. North et al. 2006) was utilized to assess the dispersal patterns of simulated larvae (Figure 3.1). LTRANS uses predictions from the Regional Ocean Modeling System (ROMS) as input to force the hydrodynamics experienced by particles (Haidvogel et al. 2008; Shchepetkin and McWilliams 2009). We utilized 3-hourly advection and diffusion predictions from ROMS

which were generated over 25 depth layers with a 350-m horizontal resolution (Hahn-Woernle et al., in revision) that accurately resolved mesoscale circulation features. Topography for the model domain was produced from multiple products including Global Multiresolution Topography Synthesis (Ryan et al. 2009), General Bathymetric Chart of the Oceans, and high-resolution multibeam data available from the Marine Geoscience Data System (MGDS; <http://www.marine-geo.org>). Tides were provided by the TPXO8 global model (Egbert and Bennett 1994; Egbert and Erofeeva 2002). The atmospheric forcing was based on the Regional Atmospheric Climate MOdel (Reijmer, van Meijgaard, and van den Broeke 2005; Van Wessem et al. 2014) and output at 3-hour resolution was further calibrated to observations from Automated Weather Stations (AWS) to correct underestimates in air temperature and humidity as well as overestimates in short-wave radiation due to a shading effect by the surrounding steep topography. Water properties at boundaries were constrained by observations of temperature and salinity from CTD profiles from 1999-2017 (Lundesgaard et al., in press). The model parameterization and results are fully described in Hahn-Woernle et al. (in revision). The hydrodynamic model begins November 1, 2015 with a 30-day spin-up period and characterizes the circulation for the summer months December - April. The particle tracking model results are, therefore, applicable to larvae produced and released in summer and dispersal patterns for organisms spawning during the winter are not addressed here. We track particles for up to 150 days through the month of April and although there is evidence that sea-ice dynamics by late April can affect circulation, the hydrodynamic model used did not have a sea-ice component.

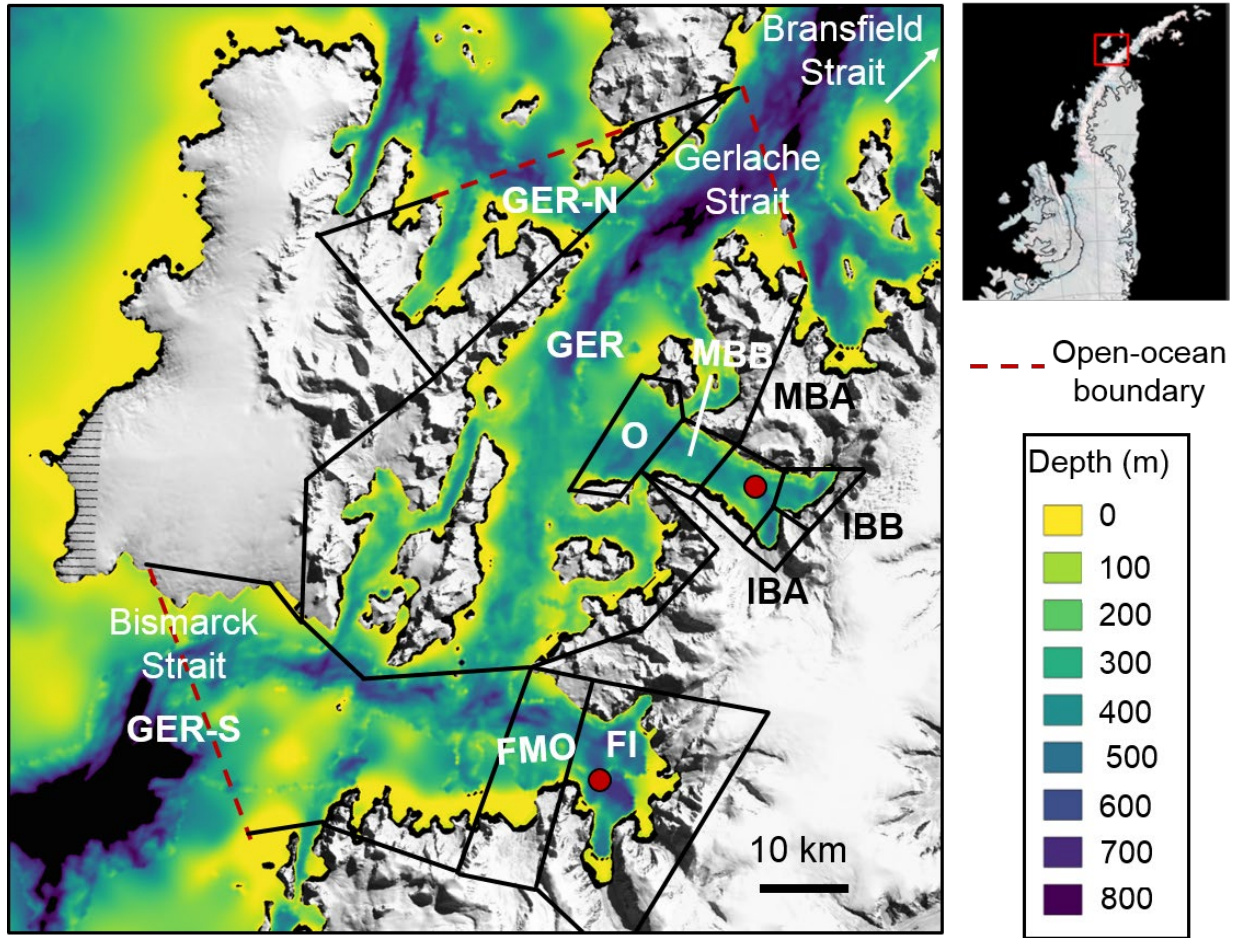


Figure 3.1. The model domain encompassing Andvord and Flandres Bays as well as the surrounding Gerlache, Bransfield, and Bismarck Straits. Bathymetry (depth in meters) is shown in color. Polygons in black were used to tabulate particle settlement locations and are referred to as: Inner Basin A (IBA), Inner Basin B (IBB), Middle Basin A (MBA), Middle Basin B (MBB), Outer Basin (O) in Andvord Bay, Gerlache Strait (GER), Northern Gerlache Strait (GER-N), Southern Gerlache Strait (GER-S), and Mouth (FMO) and Inner Basin (FI) in Flandres Bay. Particle release locations in MBA and FI are labeled with solid red dots. Red dashed lines represent the three open-ocean boundaries defining the model domain.

The movement of particles was forced by 3-hourly predictions of advection and diffusion from ROMS. To track particles at sub-grid cell temporal and spatial scales, LTRANS employs an interpolation scheme and prescribes additional random motion to particles (North et al. 2006). In all model runs, particles were

tracked at 60-second intervals and three-dimensional positions reported every 3 hours for up to 150 days to represent the pre-competency periods, PLDs and behaviors of Antarctic benthic invertebrates reported in the literature (Table 3.1). In general, invertebrates with high dispersal potential were characterized by planktotrophic larvae with long pre-competency periods and PLDs and high fecundity while invertebrates with low dispersal potential had lecithotrophic larvae, short pre-competency periods and PLDs, demersal swimming behavior and lower fecundity. Using these values, we constructed four dispersal scenarios: AndHigh, FlaHigh, AndLow and FlaLow (Table 3.2). AndLow and FlaLow modeled larvae with low dispersal potential, after the tunicate larvae of *Cnemidocarpa verrucosa* that is found in Andvord Bay and the surrounding WAP. Larvae of this tunicate have a pre-competency period of 8 days followed by downward swimming behavior (1 mm s^{-1}) for an additional 15 for a total PLD of 23 days (Sahade et al. 2004; Strathmann et al. 2006). Model simulations released particles from MBA in Andvord Bay (AndLow) and FI in Flandres Bay (FlaLow) on December 1 and simulations ran for a total of 23 days. AndHigh and FlaHigh simulations modeled larvae with high dispersal potential represented by Echinoderm larvae with pre-competency periods of 35-120 days, no directed swimming behavior (i.e. passive particles) and a PLD of 150 days (Bosch and Pearse 1990; Bosch 1989; Bosch et al. 1987; Galley et al. 2008; Galley et al. 2005; Grange 2005; McClintock and Pearse 1987; Pearse and McClintock 1990). Again, particles were released from MBA in Andvord Bay (AndHigh) and FI in Flandres Bay (FlaHigh). We assessed the effect of release date on dispersal and settlement patterns by repeating model runs every day for the first 15 days of December, resulting in a total of 15 simulations each for AndHigh and FlaHigh scenarios. In all simulations and scenarios, 10,000 particles were released approximately 50 mab to avoid model boundary layer effects. During all simulations of all four dispersal scenarios, settlement was deemed “successful” if a particle contacted the seafloor after the appropriate pre-competency period was reached, and after this time these particles stopped moving. We are confident that 10,000 particles reasonably captured the variability of dispersal pathways as the variance of displacement distances changed little when particle number was doubled from 5,000 to 10,000. To investigate the role of WAP fjords as larval sources to the broader WAP shelf, the number of larvae exported from our model domain was tabulated in each simulation by defining the three open-ocean boundaries in our model domain as non-reflective boundaries (Figure 3.1). This means that particles predicted to have a trajectory crossing these

boundaries would be stopped at the boundary for the remainder of the simulation. This represents larvae that would be exported out of the model domain. Results from our model simulations represent the dispersal of larvae from an individual during a single austral summer spawning event in the absence of mortality. We consider the influences of population-level fecundity, dispersal patterns and mortality on overall connectivity in our study region in the Discussion.

Table 3.1. Life history traits of Antarctic organisms with high and low dispersal potential from the literature. Larval mode indicates whether the organism produces planktotrophic (feeding) or lecithotrophic (non-feeding) larvae. Larval release time is the time of spawning as reported in the literature. Pre-competency period represents the minimum time required for larvae to develop in the water column. The pelagic larval duration (PLD) is the maximum time larvae spend in the water column to develop and settle, after which point 100% mortality is assumed. Fecundity is the number of eggs (larvae) produced per female per spawning event.

Organism	Larval Mode	Larval Release Time	Pre-Competency Period	Pelagic Larval Duration	Fecundity	References
Low Dispersal Potential						
Tunicata *						
<i>Cnemidocarpa verrucosa</i> *	lecithotrophic	June - July / Oct. - Nov.	8-16 days	~ 8 days	unreported	12, 13
Porifera *	lecithotrophic	unreported	Hours	12 hrs - 2 weeks	unreported	14, 15, 16
High Dispersal Potential						
Brachiopoda *						
<i>Liothyrella uva</i>	lecithotrophic	Jan.	Brooded	31 - 45 days	100-4,000	7, 8, 9
Echinodermata: Crinoidea *						
<i>Promachorcinus kergulensis</i>	lecithotrophic	Oct. - Nov.	60 - 90 days	unreported	29,000	5
Echinodermata: Echinoidea *						
<i>Sterechinus neumayeri</i> *	planktotrophic	Nov. - Dec.	115 days	unreported	12,700	1, 3, 19, 20
Echinodermata: Asteroidea *						
<i>Porania antarctica</i> *	planktotrophic	Nov. - Jan.	65 - 78 days	unreported	35,000	2, 6, 17
Asteroidea sp.	planktotrophic / lecithotrophic	unreported	150 - 180 / 60 - 90 days	unreported	unreported	11
<i>Lophaster gaini</i> *	lecithotrophic	Feb. - Mar.	unreported	unreported	3,000 - 5,000	11
<i>Psilaster charcoti</i> *	lecithotrophic	Nov. - Dec.	unreported	unreported	10,000	17, 20
<i>Odontaster</i> spp.*	planktotrophic	Sept. - Nov.	167 days	unreported	unreported	10, 11, 18
<i>Acodontaster</i> spp.	lecithotrophic	Nov. - May	91 - 100 days	unreported	unreported	5, 13, 17
Echinodermata: Holothuroidea *						
<i>Protelpidia murrayi</i> / <i>Peniagone vignoni</i>	lecithotrophic	unreported	60-90 days	unreported	1498-9986	4

Statistical Analyses

Particle distributions at the end of each 23-day (AndLow and FlaLow) or 150-day (AndHigh and FlaHigh) simulations were tabulated to determine the percentage of particles settled in different regions of the model domain including those that crossed the open-ocean boundaries via Gerlache or Bismarck Straits (Figure 3.1). A $0.005^\circ \times 0.01^\circ$ grid was applied to the resulting particle distributions using the mapplot package in R (Gerritsen 2018) to generate heatmaps of settled particle distributions (Figures 3.2, 3.3 and 3.4). For AndHigh and FlaHigh scenarios, these heatmaps each represent pooled distributions from all 15 simulations.

The mean dispersal distance of larvae for each simulation was calculated as the mean cumulative distance particles had traveled by the end of the simulation. This value represents an overestimate of the linear distance a particle traveled (from release point to settlement location) but provides a measure of overall movement for comparison. For AndHigh and FlaHigh scenarios, the mean dispersal distance was calculated for each pre-competency period. We also investigated the influence of physical forcing from surface wind speed and current velocity. Wind speeds were measured from an AWS atop Useful Island in the Gerlache Strait during December 2015 - April 2016 and were rotated 60° such that positive wind speeds correspond to winds directed into Andvord Bay and negative wind speeds correspond to the down-fjord direction out of Andvord Bay (Lundesgaard et al. 2019). Wind-speed data was originally collected at 10-minute intervals so these data were down-sampled using the decimate function in R to generate a 3-hourly time series (Ligges et al. 2015). Current velocity was determined from 3-hourly output of ROMS predicted u - and v - velocity components within the surface or bottom depth layer of the model domain. To investigate the effect of surface winds and current velocities on settlement distributions resulting from AndHigh and FlaHigh simulations, time-series of these environmental data were correlated with the timing of the maximum distance each particle traveled in a single 3-hour period during each simulation using Spearman correlation. To investigate the periodicity of these time series, spectral analysis was conducted via the pspectrum function in R (Barbour et al. 2019) which determined the

dominant frequencies of variability in current velocity, wind speed and particle transport throughout the time series.

Table 3.2. Modeling scenario details. Pre-competency period and pelagic larval durations (PLD) are given in days.

Scenario	Release location	Release depth (m)	Particles released	Pre-competency period	Pelagic Larval Duration (PLD)	Start date	End date
AndLow	Andvord (MBA) -64.85946, -62.57267	456	10,000	8	23	12/1/2015	12/23/2016
FlaLow	Flandres (FI) -65.07292, -63.16805	546	10,000	8	23	12/1/2015	12/23/2016
AndHigh	Andvord (MBA) -64.85946, -62.57267	456	10,000	35, 60, 90, 120	150	12/1/2015 - 12/15/2015	4/28/2016
FlaHigh	Flandres (FI) -65.07292, -63.16805	546	10,000	35, 60, 90, 120	150	12/1/2015 - 12/15/2015	4/28/2016

Results

Low-dispersal-potential simulations: AndLow and FlaLow

After 8 days of passive transport, the simulated larvae of low-dispersal potential were competent to settle and began swimming toward the seafloor. In scenario AndLow, particles rapidly settled requiring < 1 day on average to settle after pre-competency was reached indicating many particles remained near the seafloor during dispersal. However, some particles were found as shallow as 118 m which corresponds to a 338 m vertical displacement in Andvord Bay. The mean dispersal distance of these simulated larvae was 23.88 ± 5.41 km; however, no particles exited the model domain. In fact, only 0.22% of particles

1643 exited Andvord Bay and settled within the Gerlache Strait (GER) leaving more than 99% of particles
1644 settled within Andvord Bay and in basins < 8km from the original release location.

1645

1646 In scenario FlaLow, particles remained closer to the seafloor with a maximum displacement of 256 m and
1647 were retained within the fjord. During the 23-day simulation, no particles exited Flandres Bay and the
1648 mean dispersal distance was nearly half that of AndLow at only 10.64 ± 2.04 km. In fact, only 1.02% of
1649 particles even left the inner basin (FI) from which they were released to settled in the fjord mouth region
1650 (FMO). For a comparison of similar lateral displacement, 10.3% of particles in the AndLow simulation
1651 settled in MBB which is a similar distance from MBA as FMO is from FI indicating that the inner basins of
1652 Flandres Bay retained particles more than in Andvord Bay. Retentive features could be seen in the
1653 particle distributions in the inner basins of Flandres Bay throughout the simulation. More than 98 % of
1654 particles remained in FI from which they were released or settled in the adjacent basin (FMO) a maximum
1655 of 6 km away. Particles released from neither Andvord Bay nor Flandres Bay settled within the
1656 neighboring fjord during the simulations of larvae with low dispersal potential (Figure 3.2).

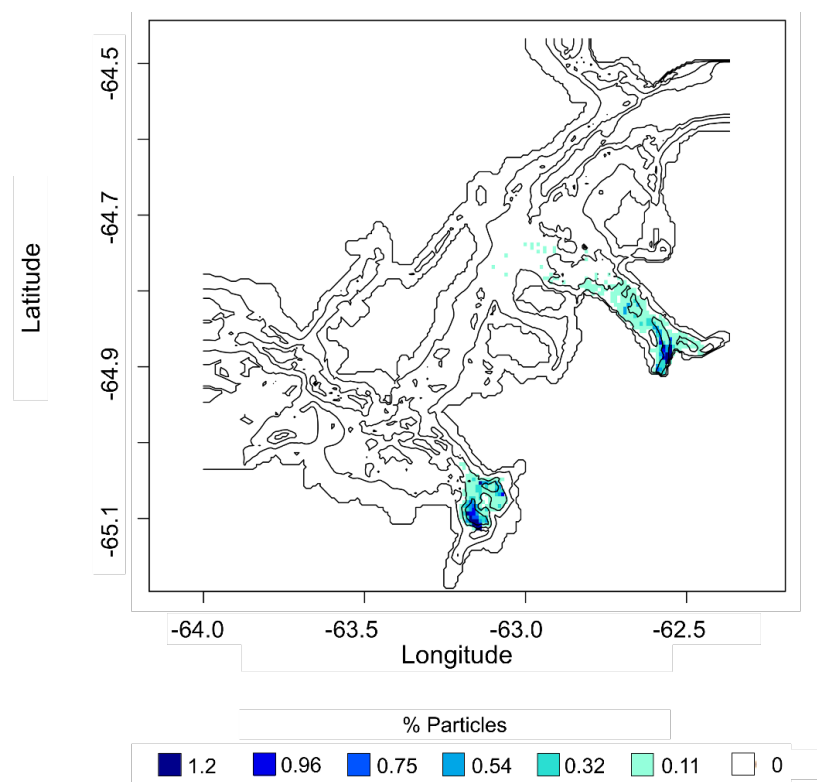


Figure 3.2 Settled particle distributions after 23-day (scenarios AndLow and FlaLow) simulations of 10,000 larvae; one simulated larval release from Andvord Bay (AndLow) and one from Flandres Bay (FlaLow). Colors correspond to settled particle percentage per grid cell. Bathymetric contours represent 0, 200, 400, 600 and 800 m isobaths.

High-dispersal-potential simulations: AndHigh and FlaHigh

In all 15 simulations of scenario AndHigh, particles were transported laterally into the inner basins of Andvord Bay and out of the fjord toward the Gerlache Strait. A retentive feature was observed in MBB which recirculated particles toward MBA increasing the retention time of particles within the fjord. Similar circulation features were observed in other regions of the model domain including within the inner basins of Flandres Bay (Figure 3.3). Particles first exited the Andvord Bay via the southwest edge of the fjord mouth and followed the shallowing bathymetry into Gerlache Strait at a depth of approximately 240 m (236.16 - 240.97 m) about 8.6 days (± 2 days) after initial release. It took 33.5 days (± 6 days) for the first particle from Andvord Bay to reach the inner basins of Flandres Bay (FI). After the minimum pre-competency period of 35 days, particles were capable of settlement. After only 1 day of settlement > 24% of particles had settled, predominantly within Andvord Bay (21.31%), indicating that many particles had remained close to the seafloor during passive transport. By day 60, almost 75% of particles had settled within Andvord Bay with an additional 16.8% in the Gerlache Strait; however, no particles had settled within Flandres Bay though there were particles present in the fjord by this time. By day 90, nearly all particles had settled (> 98%) and no additional particles reached Flandres Bay. By the end of the 150-day simulations, all particles (except those which exited the model domain via open-ocean boundaries) had settled, and 0.03% of particles settled in Flandres Bay, on average for a pre-competency period of 35 days. Patterns of initial movements were similar for simulations of 60, 90 and 120-day pre-competency periods, however the total number of particles settling in each fjord as well as those exiting the domain differed and these patterns will be discussed further.

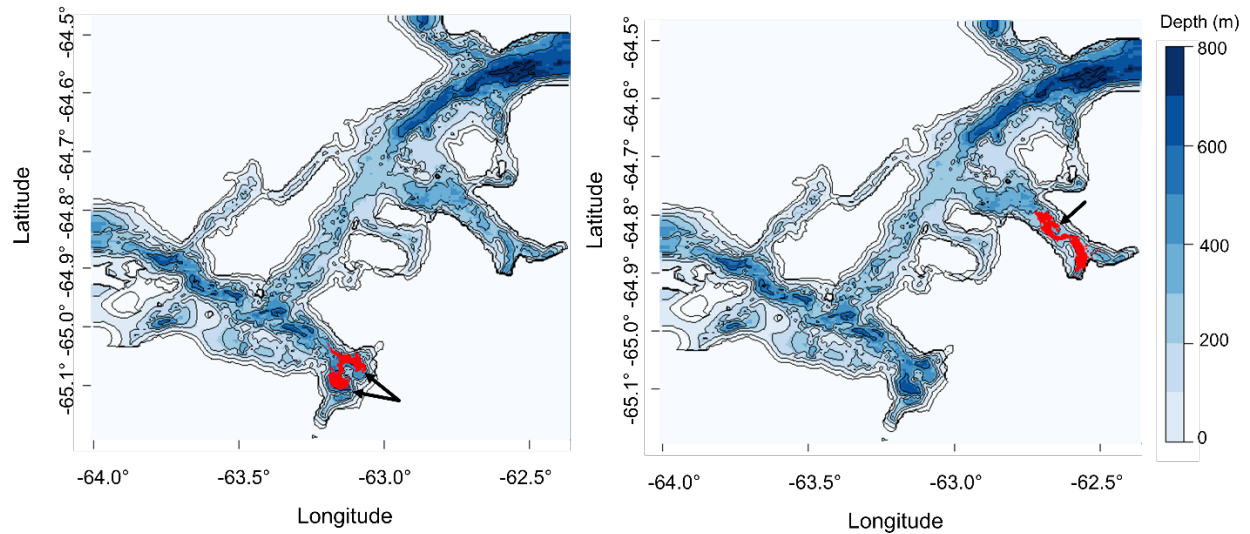


Figure 3.3 Recirculation features (black arrows) visible in the particle distributions (red points) of high dispersal potential simulations of particles released from Andvord Bay (right) and from Flandres Bay (left) each 6.5 days after initial release. Colors and contours correspond to the bathymetry (m).

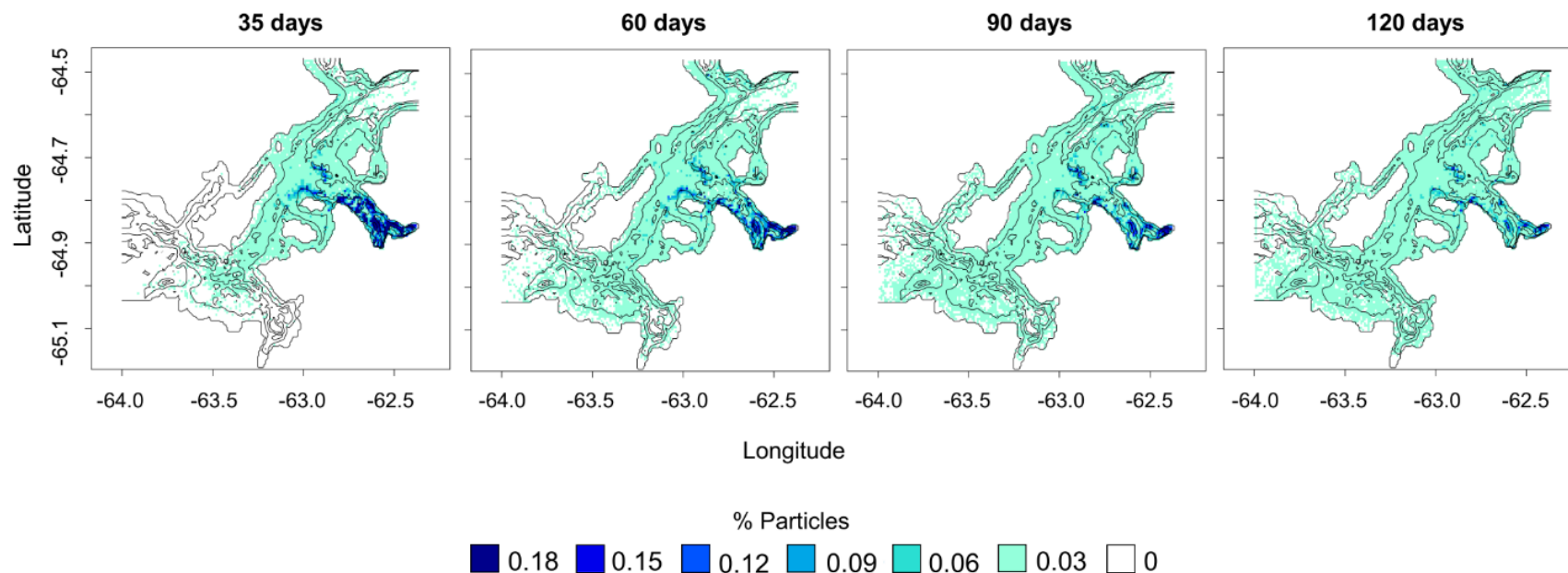
Particles first exited the domain via the Gerlache Strait boundary (GER) after 35.5 days (± 2.88 days), the northern Gerlache Strait boundary (GER-N) after 36.2 days (± 2.4 days) and via the southern Gerlache Strait boundary (GER-S) after 51.2 days (± 8.9 days). Overall, 19.49 - 39.18% of all particles exited the model domain over the course of the simulations depending on the pre-competency period. There was no obvious pattern in settlement or exit times across the different release days, but the earliest arriving particles into Gerlache Strait (GER) occurred after only 6.125-6.875 days from particle releases on Dec. 5, 8-9, and 11th. Overall, the percentage of particles from Andvord Bay that settled within Flandres Bay increased with increasing pre-competency period as expected; however, this percentage was $< 1.59\%$ for any release date and across all pre-competency periods (Figure 3.4).

In simulations of scenario FlaHigh, particles remained entrained in retentive circulation features within the inner basins of Flandres Bay after initial release (Figure 3.3, left) and eventually moved into the mouth of Flandres Bay (FMO) where they became more dispersed. Particles entered the bordering Gerlache Strait

(GER-S) within 12.25 days (± 2.5 days). Approximately 22 days later (± 3.7 days), the first particles entered Andvord Bay and the first particles entered the inner basins within 42.65 days (± 6 days). During the simulations, particles exited the model domain via the southern Gerlache Strait boundary first after 34.65 days (± 4.9 days) and it took 48.875 (± 4.7 days) and 55.6 days (± 6.7 days) for particles to exit the domain via the northern Gerlache Strait boundaries (GER and GER-N, respectively). These transport times are comparable to simulations of particles released from Andvord Bay (AndHigh). Settlement in Andvord Bay was low regardless of pre-competency period; on average, 0.17%, 0.82%, 1.18% and 2.33% of particles from Flandres Bay settled within Andvord Bay for pre-competency periods of 35, 60, 90 and 120 days, respectively (Figure 3.5). The variability of particles settled in Andvord Bay was high across different release dates with percentages ranging from 0.02% - 0.46%, 0.31% - 3.1%, 0.71% - 2.48%, and 1.82% - 3.38% for pre-competency periods of 35, 60, 90, and 120 days, respectively. For particles with a pre-competency period of 35 days, only 5 of the 15 simulations experienced successful transport into IBA from FI. For this connection to be present in all 15 simulations, a pre-competency period of > 90 days was required.

The effect of release day was also evident in patterns of transport. For all pre-competency periods investigated, particles released on December 8th entered the Gerlache Strait fastest (in 9 days), and the percentage of successfully settled particles within Andvord Bay was highest for this simulation. A greater proportion of particles successfully settled in the neighboring fjord when released from within Flandres Bay than from Andvord Bay for all pre-competency periods (Figure 3.6). However, a greater proportion of particles settled within the basin from which they were released for FlaHigh simulations compared to AndHigh. Even particles with a long pre-competency period of 120 days, more than four times as many particles settled in FI during FlaHigh simulations compared to those settling in MBA during AndHigh simulations (22% vs 4.82%). For intermediate pre-competency periods (e.g. 60 - 90 days), the patterns of settlement in neighboring fjords was similar between release locations.

1725



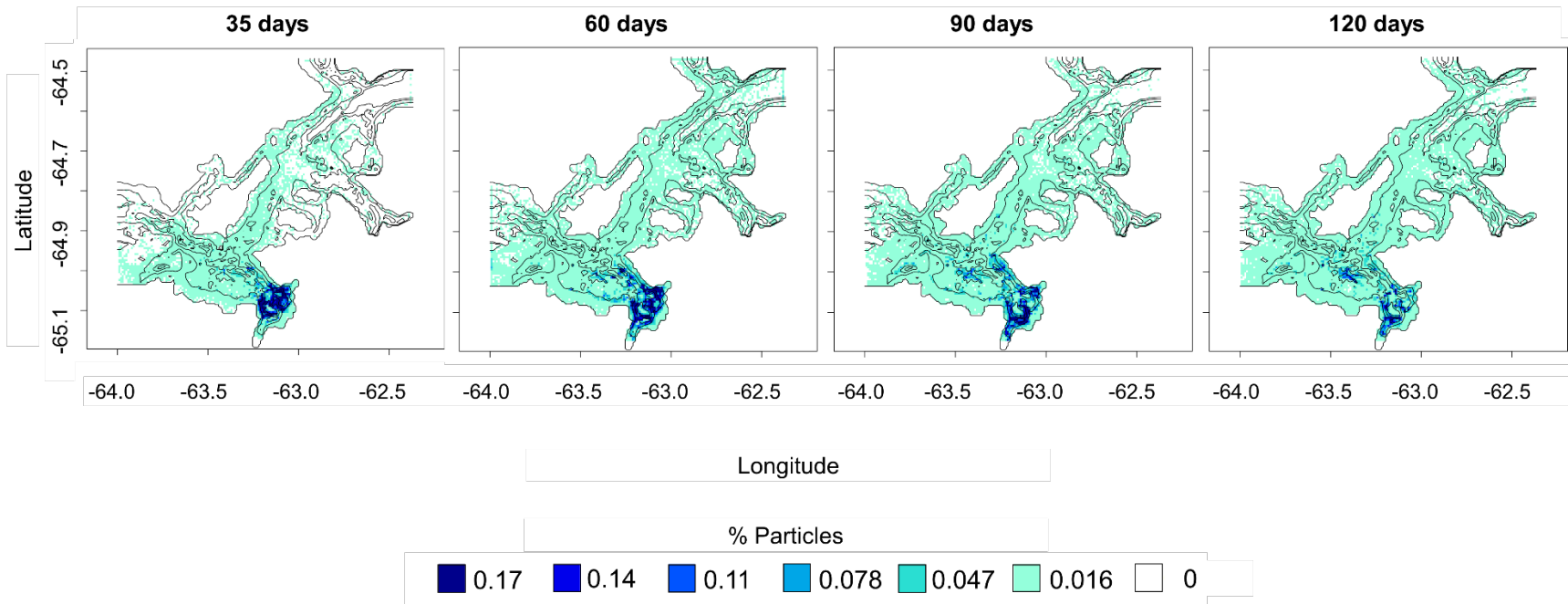
1726

1727 **Figure 3.4** Settled particle distributions at the end of April for all 15 simulations of 10,000 "highly dispersing larvae" each released from Andvord
 1728 Bay (AndHigh) with pre-competency periods of 35, 60, 90, and 120 days. Colors represent the percentage of particles per grid cell. Bathymetric
 1729 contours represent 0, 200, 400, 600 and 800 m isobaths.

1730

1731

1732



1733

1734 **Figure 3.5** Settled particle distributions at the end of April for 15 simulations of 10,000 "highly dispersing larvae" each released from Flandres Bay
 1735 (FlaHigh) with pre-competency periods of 35, 60, 90, and 120 days. Colors represent the percentage of settled particles per grid cell. Bathymetric
 1736 contours represent 0, 200, 400, 600 and 800 m isobaths.

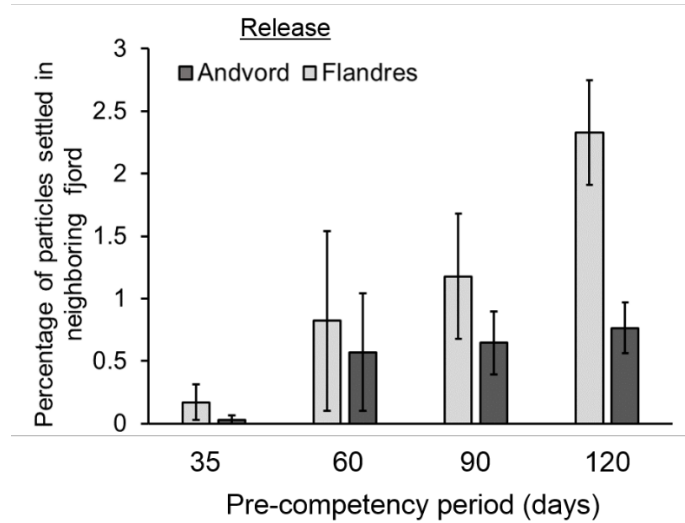


Figure 3.6 The percentage of particles (\pm S.D.) settled within the neighboring fjord when released from Andvord Bay (dark bars, AndHigh) and Flandres Bay (light bars, FlaHigh) for 35, 60, 90 and 120-day pre-competency periods.

Overall, the mean dispersal distance for high dispersing larvae increased with increasing pre-competency period (112.2 ± 16 km to 507.2 ± 13 km) but the dispersal distances of particles in FlaHigh simulations were lower than those in AndHigh simulations for all pre-competency periods (64.95 ± 10.8 km to 411.1 ± 21.6 km) (Figure 3.7). These dispersal distances represent the total track length traveled by larvae. For reference, the furthest direct distance between settlement locations or open-ocean boundaries was approximately 100 km. In AndHigh and FlaHigh simulations, the number of particles exiting the model domain via open-ocean boundaries increased with increasing pre-competency period. For larvae with a pre-competency period of 120 days, 30% of particles exited the domain via the northern Gerlache Strait boundary in AndHigh simulations and 13% of particles in FlaHigh simulations exited the domain via the southern boundary at the Bismarck Strait across all pre-competency periods. In total, 20-39% of larvae exited the domain across all boundaries for high dispersal simulations with a pre-competency period of 120 days.

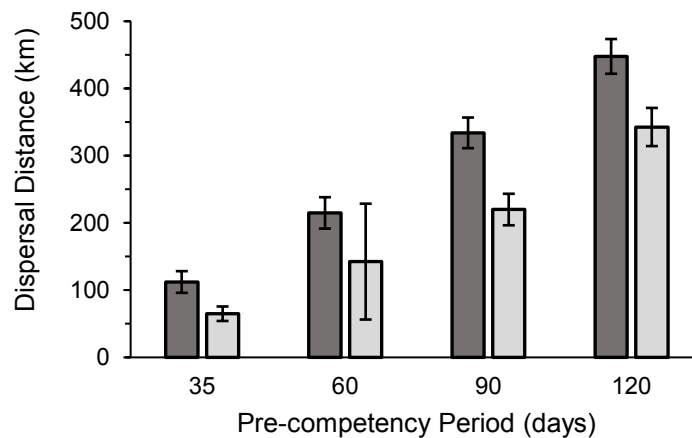


Figure 3.7. Mean dispersal distance (km) for particles from all 15 simulations AndHigh (dark bars) and FlaHigh (light bars) scenarios across different pre-competency periods. Error bars report the standard deviation (days).

Surface Winds and Current Velocities

The date of maximum horizontal and vertical transport of each particle during a single 3-hour period in the 15 simulations of scenarios AndHigh and FlaHigh was determined and used to generate histograms of the distributions. The distribution for particles from simulations in the AndHigh scenario was multi-modal with slight periodic signals and modes at approximately 68, 130 and 150 days (Figure 3.8, grey bars). A similar distribution of transport times for particles in the FlaHigh scenario that had modes at 127, 132 and 149 days (Figure 3.9, grey bars). For AndHigh simulations, correlation analyses between this distribution, surface current velocities and surface wind speed revealed a weak positive correlation with surface current velocities and a stronger negative correlation with down-fjord wind speed ($\rho = 0.154$ and -0.275 , respectively). Spectral analysis revealed that the dominant periodicities of the horizontal transport distribution matched those of the O_1 and K_1 tidal constituents with frequencies of approximately 24 hours which were also identified as the dominant tidal frequencies measured from oceanographic moorings in

the Gerlache Strait (Lundesgaard et al. 2019) and 15-20-day periodicities of surface wind speeds (Appendix, Figure 3.1). Similar periodicities of 24 hours and 15-20 days were also present in the distribution of particle exit times through open-ocean boundaries in the Gerlache Strait. Particles released around December 5-11th, 2015 were exported from the fjords more rapidly in both scenarios AndHigh and FlaHigh. Although AWS wind speed data is not available prior to December 15th, 2015, shipboard measurements in Andvord Bay revealed a very strong down-fjord wind event with wind speeds $> 25 \text{ m s}^{-1}$ and capable of exporting the surface 35 m of fjord waters (Lundesgaard, Powell, et al. 2019). The average surface current velocity around December 8th, 2015 in Andvord Bay (MBA) was 3.7 cm s^{-1} , more than twice the full time series average. Therefore, it is likely that this wind event transported particles released in Andvord Bay that had reached the upper $\sim 35 \text{ m}$ of the water column by this time. Direct comparison of particle transport times and wind speeds oriented along-fjord for Flandres Bay was not possible during this study. However, prominent times of horizontal particle transport also matched the dominant tidal frequencies (~ 12 and 24 hours) and surface current velocities in FI (Figure 3.9). The highest surface current velocity in Flandres Bay occurred on day 128 of the model reaching $> 9 \text{ cm s}^{-1}$, and remained above 3 cm s^{-1} for a 24-hr period. This matches one of the maximum frequencies of the horizontal transport distribution within Flandres Bay. Overall, there was a stronger correlation between maximum horizontal transport times and surface current velocities for particles released from Flandres Bay (FlaHigh) compared to those released from Andvord Bay (AndHigh, $\rho = 0.20$ and 0.14 , respectively). Surface wind speeds and current velocities were very weakly correlated with the times of maximum vertical transport of particles for both AndHigh and FlaHigh (Appendix, Figures 3.2 and 3.3). Furthermore, times of maximum particle advection (both horizontally and vertically) roughly match times of particle export through open-ocean boundaries (Appendix, Figure 3.4).

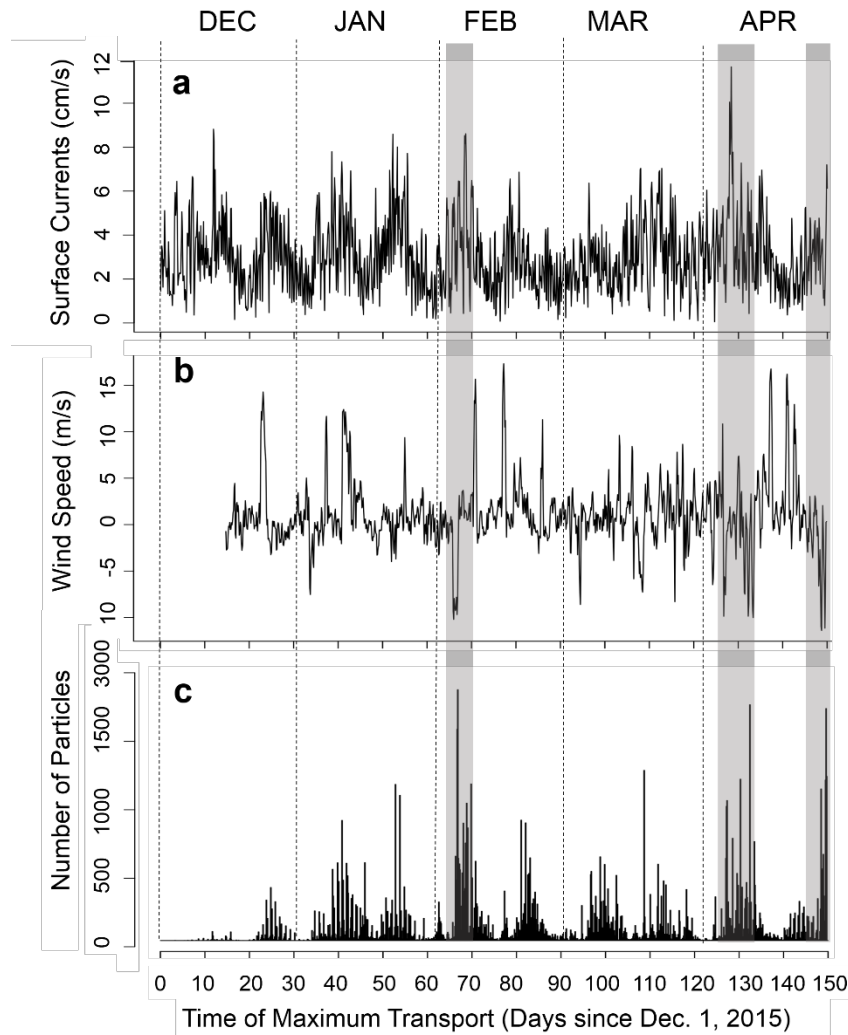


Figure 3.8 Environmental conditions and time of maximum horizontal transport for 15 high-dispersal potential simulations released from Andvord Bay (AndHigh). Time is days since Dec. 1st, 2015 and all data were sampled every 3 hours. Dotted lines delineate calendar months that are labeled at the top. (a) Surface current velocity (cm/s) measured at MBA, (b) Surface wind speeds (m/s) measured at an Automated Weather Station in Gerlache Strait. Positive values are up-fjord winds while negative values are down-fjord winds. (c) Time of maximum transport of each particle during the 15 simulations Dec. 1 - Apr. 28. There are 3 main peaks in the distribution highlighted by the grey bars.

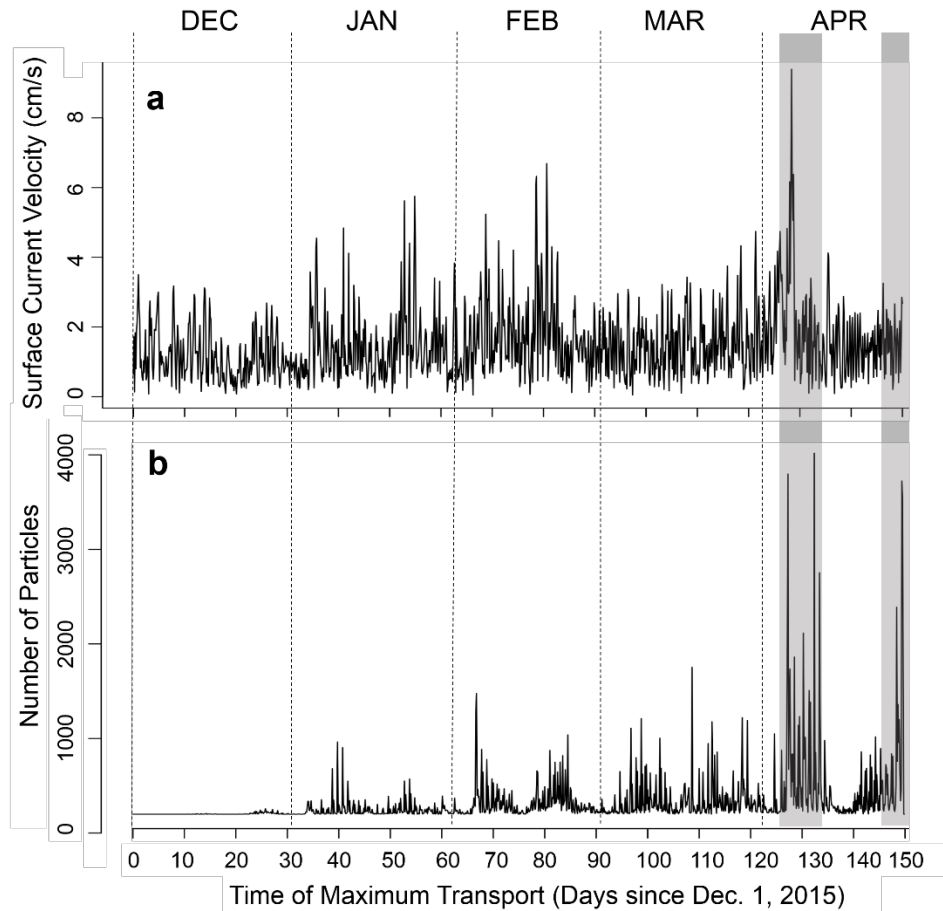


Figure 3.9 Environmental conditions and time of maximum transport for 15 high-dispersal potential simulations released from Flandres Bay (FlaHigh). Elapsed time is days since Dec. 1st, 2015 and all data were sampled every 3 hours. Dotted lines delineate calendar months that are labeled at the top (a) Surface current velocity (cm/s) measured at the release point, FI. (b) Time of maximum transport of each particle during the 15 simulations Dec. 1 - Apr. 28. There are 2 main peaks in the transport distribution highlighted by the grey bars.

Discussion

In this study, we simulated the dispersal of benthic megafaunal larvae across a spectrum of dispersal potential released in austral summer from within two glaciomarine fjords along the West Antarctic

Peninsula. Low dispersing larvae were characterized by a short pre-competency period (8 days), short pelagic larval duration (23 days) and downward swimming behavior (1 mm s^{-1}). Common Antarctic organisms that have low dispersal capabilities include tunicates (e.g. *C. verrucosa* which our simulations best emulated) and sponges (reviewed in Table 3.1). Most tunicate species reproduce via swimming lecithotrophic larvae with extremely short pelagic stages (e.g. as short as 1 hour) particularly in shallow water (Ben-Shlomo et al. 2010; Lambert 2005; Sahade et al. 2004; Strathmann et al. 2006). Similarly, sponge larvae typically settle < 2 weeks after initial release and in as little as 12-24 hours (Leys and Ereskovsky 2006) while swimming at $0.1\text{-}1 \text{ cms}^{-1}$ (Maldonado 2006). Simulations of low dispersing larvae revealed no connectivity between neighboring fjords during a single spawning event in austral summer. The realized dispersal distance of simulated larvae was low when released from either fjord (mean of 10.64 - 23.88 km). It is possible that larval releases in less retentive locations such as the Gerlache and Bransfield Straits would generate larger dispersal distances of low dispersal potential organisms than measured in this study. The proportion of self-recruitment (i.e. settled in the same fjord basin from which they were released) was high for larvae released in both Andvord and Flandres Bays, reaching up to 22%. In addition, no low dispersing larvae released from either Andvord or Flandres Bays were able to settle in the neighboring fjord during the 23-day pelagic larval duration (Figure 3.10). We conclude that self-recruitment is likely to maintain fjord populations of low dispersing organisms such as tunicates and sponges, especially within the middle and inner basins (MBA, IBA, IBB, FI). Photographic surveys have found adult populations of several tunicate species in both Andvord and Flandres Bays as well as on the adjacent shelf (Grange and Smith 2013; Ziegler et al. 2017) with abundances and dominant species differing between fjords. Tunicate species turnover between fjords is unlikely to be caused by resource competition alone and is likely aided by dispersal-limitation of these low dispersing species. While beyond the scope of this study, our results suggest the potential for differences in population genetic structure of low dispersing organisms (e.g. tunicates) between Andvord and Flandres Bays. Other studies have found genetic structure in tunicate populations along the Chilean coast over very small (< 10 km) spatial scales (Giles et al. 2017). Population genetic studies of tunicates in the Antarctic are limited and focus on connectivity across the Antarctic Circumpolar Current and Polar Front (e.g. Demarchi *et al.*, 2010).

Although this study simulated larval releases during austral summer (December), some tunicates, including *C. verrucosa*, have been observed releasing larvae during the winter (Sahade et al. 2004). It is unlikely that dispersal distances would be greater for this species during winter, especially for deep populations, because water flow is less coupled to atmospheric forcing in winter due to the presence of sea ice (Lundesgaard et al., in press). Therefore, we expect increased retention of low dispersing larvae released during winter resulting in an even shorter dispersal distance which could increase the source of larvae to local populations and self-recruitment (Swearer et al. 2002). Though self-recruitment maintains isolated populations with few or no additional larval sources (Hastings and Botsford 2006), these populations are then particularly sensitive to changes in local conditions and stochastic events which could rapidly remove a substantial proportion of the population. In glaciomarine fjords, stochastic events impacting the benthos may be large turbidity events or ice scour in shallower regions (<200 m). This study simulated larvae originating from only two locations; however, larval sources from stepping-stone populations outside of the fjords likely exist as there are deep sedimented basins and dropstones present throughout the Gerlache Strait which provide suitable habitat for these organisms (Grange and Smith 2013; Ziegler et al. 2017). Exploration of fjord walls is also necessary to determine if additional fjord populations of hard-substrate organisms exist that could act as local larval sources. Future work should assess the connectivity of these populations accounting for the supply of larvae from stepping-stone populations nearby. Based on our results, we conclude that Andvord and Flandres Bays are not significant sources of low dispersing larvae (e.g. Tunicates, sponges) to neighboring fjords within our study region nor to the greater West Antarctic Peninsula shelf.

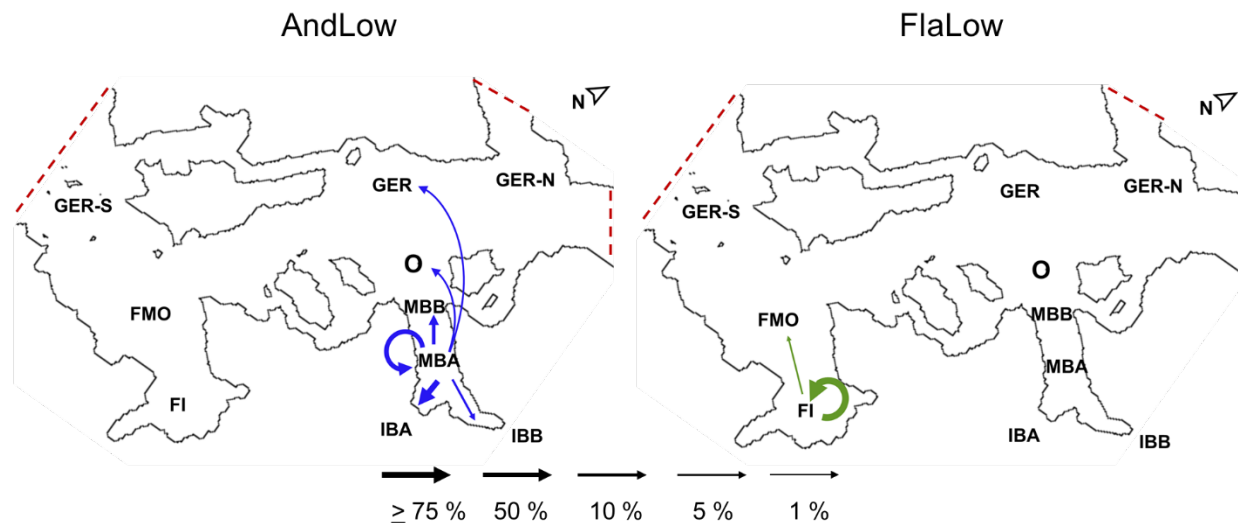
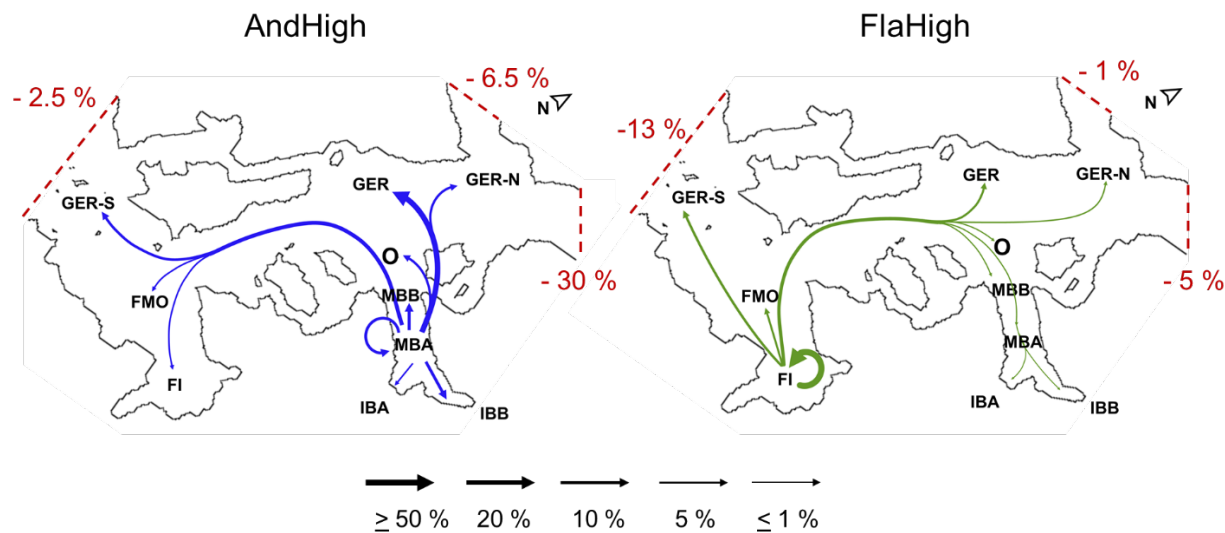


Figure 3.10 Conceptual connectivity diagrams illustrating settlement between regions (see Figure 3.1) for low dispersal simulations (AndLow and FlaLow). Lines connect release points (MBA and FI) to regions in which particles settled successfully and are weighted by the percentage of settled particles. Blue lines correspond to particle releases from MBA while green lines represent particle releases from FI. Regions with no lines reaching them did not experience settlement during the simulations. Red dashed lines represent open-ocean boundaries.

We also simulated the dispersal of highly dispersing larvae with pre-competency periods ranging from 35 to 120 days, and a total pelagic larval duration of 150 days, following release from within Andvord and Flandres Bays over a 15-day period in December. Long pre-competency periods and pelagic larval durations both increased the potential for long-distance dispersal and the influence of oceanographic conditions on larval settlement distributions. We found that a pre-competency period of at least 35 days was required for transport to and settlement within the neighboring fjord for releases both from Andvord and Flandres Bays. The percentage of larvae successfully settling in the neighboring fjord increased with increasing pre-competency period. While connectivity between Andvord and Flandres Bays occurred during all 150-day simulations, < 3% of all particles settled within neighboring fjords from either release

location suggesting that populations within these fjords are ecologically isolated. This lends support to the hypothesis that some components of the benthic community are recruitment-limited (e.g. dropstone fauna, Ziegler et al. 2017) and that dispersal contributes to the species turnover observed between fjords (Grange and Smith 2013). We investigated the effects of specific oceanographic conditions on larval transport and settlement by comparing time series of surface winds and currents to modeled larval distributions. We found that episodic down-fjord winds (i.e. Katabatic winds) increased lateral as well as vertical transport of larvae during our simulations and increased the percentage of larvae exported to the broader WAP shelf. In fact, up to 30% of particles released from Andvord Bay exited the model domain via the open-ocean boundary in the northern Gerlache Strait while 13% of larvae released from Flandres Bay exited the southern boundary via the Bismarck Strait (Figure 3.11). The generally northeasterly flow of both the Gerlache Strait and Antarctic Circumpolar Current west of Anvers Island likely carry these exported larvae toward the northern reaches of the WAP. Episodic down-fjord winds may be an important mechanism providing connections between the WAP fjord populations we investigated and the northern WAP shelf. Our results were consistent with the observation that there is a weakly layered system within Andvord Bay in which water is generally flowing into the fjord at depths > 300m and out of the fjord at the surface, < 300 m (Lundesgaard et al., in press). Processes transporting larvae into the surface layers of the fjord can have a great impact on the overall dispersal distance and likelihood of larval export from our model domain. It will be important to consider changes in the stratification and buoyancy forcing within WAP fjords as atmospheric and ocean temperatures continue to rise as these mechanisms could increase surface water outflow from the fjord exporting larvae that are entrained into surface layers. It is possible that this effect is currently greatest during the late summer period when solar radiation has warmed the ocean and ice melt is at a maximum, therefore, if spawning occurs during the earlier summer or during winter months there is likely less vertical advection and less larval export. Modeling of hydrodynamic processes in winter months is required to accurately assess this hypothesis. For high dispersing larvae (e.g. asteroids and other echinoderms), we conclude that Andvord and Flandres Bays do not exchange significant amounts of larvae during an austral summer spawning but may be significant sources of larvae to the broader WAP shelf, especially to northern WAP regions.

1905



1906

1907

Figure 3.11 Conceptual connectivity diagrams illustrating settlement between regions (see Figure 3.1) for high dispersal simulations (AndHigh and FlaHigh). Lines connect release points (MBA and FI) to regions in which particles settled successfully and are weighted by the percentage of settled particles. Blue lines correspond to particle releases from MBA while green lines represent particle releases from FI. Regions with no lines reaching them did not experience settlement during the simulations. Percentages of particles exiting the domain across each open-ocean boundary are provided in red.

1913

1914

All dispersal models are limited by the parameterization of biological processes and information available regarding organism fecundity, larval behavior, development, and mortality. Model results are sensitive to fecundity as this dictates the number of larvae simulated, and larger numbers better capture the variability of larval trajectories. In this study, we assumed a fecundity of 10000 for an individual during a single spawning event based on fecundity reported in the literature (reviewed in Table 3.1). Alternatively, our model results can also represent the dispersal of larvae from an individual that releases 10000 larvae every day for a 15-day period, or a total fecundity of up to 150000. While this is an appropriate fecundity for organisms with high dispersing planktotrophic larvae, organisms producing lecithotrophic (non-

1920

1921

feeding) larvae typically have lower individual fecundity due to energetic tradeoffs. Therefore, the number of low dispersing larvae per individual settling outside of the fjords we investigated is likely to be lower than we observed. Dispersal model results may also be sensitive to the incorporation of larval mortality, which is typically assumed to be 100% after the completion of the PLD and assumed to occur at a fixed level for the duration of the development and settlement periods. Mortality during pelagic larval stages is highly variable, and estimated from 3-20% of larvae per day (Connolly and Baird 2010; Cowen et al. 2000; Doherty et al. 2004; Rumrill 1990). Post-settlement processes (e.g. competition and predation) can also cause high mortality rates, e.g. as high as 96% (Doherty et al. 2004). We chose not to prescribe any larval mortality during our simulations, so our results are over-estimates of larval settlement. Our model results represent the probability that larvae successfully settle in a location given a release from either Andvord or Flandres Bay. Therefore, we can use published estimates of larval mortality and our model results to estimate the level of migration between fjords. The larval migration can be described by the equation $L * P * \exp(-m * PLD)$ where L is the larval supply at our origin location, P is the proportion of larvae settling at the desired end location, m is the daily rate of mortality and PLD is the transport time measured in our model. For example, 1.58% of larvae released from Andvord Bay with a pre-competency period of 120 days settle successfully within Flandres Bay. On average, these larvae spend 123.7 days in the water column before settling. With an estimated larval mortality rate of 0.5% per day, only 0.85% of the original larval pool are expected to successfully settle in Flandres Bay. If we increase the mortality rate to 5% per day, the expected number of successfully settling larvae is reduced to only 0.003% of the original larval pool which is approximately 5 individuals per generation. At a mortality rate of 20% per day, no larvae successfully settle in Flandres Bay (4.3×10^{-8}). To maintain a migration rate of 100 individuals per generation with the fecundity and PLD from our model results, the larval mortality rate could not exceed approximately 13% per day. To maintain 100 migrations per generation with a 20% per day larval mortality rate, the total larval supply must be on the order of 1×10^{13} larvae. Assuming an individual fecundity of 10000, this represents a population of 1×10^9 individuals which is three orders of magnitude larger than the estimated population of the most abundant ophiuroid (*Ophionotus victoriae*) in MBA and four orders of magnitude larger than the least abundant asteroids (Grange and Smith, 2013). Therefore,

1949 to maintain substantial connectivity between Andvord and Flandres Bays, organisms must have a high
1950 fecundity or experience low mortality during the dispersal process.

1951

1952 Conclusions

1953 In summary, this study simulated the dispersal of benthic megafaunal larvae released from within two
1954 glaciomarine fjords of the West Antarctic Peninsula using coupled high-resolution hydrodynamic and
1955 particle-tracking models. We investigated the role of ocean/atmospheric conditions on the dispersal and
1956 settlement of larvae representing two end members of dispersal potential. Our simulations revealed that
1957 ecologically relevant connectivity is lacking between neighboring fjords separated by < 50 km for
1958 organisms assumed to have low dispersal potential (e.g. tunicates and sponges) and was limited for high-
1959 dispersal potential organisms (e.g. Asteroids and other echinoderms). Episodic down-fjord wind events
1960 increased the transport and export of high dispersing larvae from coastal fjords to the northern West
1961 Antarctic Peninsula and may increase connectivity between these regions. Future ocean conditions within
1962 these glaciomarine fjords may become increasingly important in controlling the vertical movement of
1963 larvae as larval export from the fjords and to the broader shelf occurred within surface (< 300 m) layers.

1964

1965 *References*

- 1966 Almany, G. R. et al. (2017) 'Larval fish dispersal in a coral-reef seascape', *Nature Ecology and Evolution*,
1967 1(6), pp. 1–7. doi: 10.1038/s41559-017-0148.
- 1968 Arntz, W. E., Brey, T. and Gallardo, V. A. (1994) 'Arctic Zoobenthos', *Oceanography and Marine Biology:*
1969 *An Annual Review*, 32, pp. 241–304.
- 1970 Barbour, J. A., Parker, R. L. and Kennel, J. (2019) 'Package "psd", pp. 1–52.
- 1971 Ben-Shlomo, R. et al. (2010) 'Population genetics of the invasive ascidian *Botryllus schlosseri* from South
1972 American coasts', *Marine Ecology Progress Series*, 412, pp. 85–92. doi: 10.3354/meps08688.

- 1973 Bidegain, G. et al. (2013) 'LARVAHS: Predicting clam larval dispersal and recruitment using habitat
1974 suitability-based particle tracking model', *Ecological Modelling*, 268, pp. 78–92. doi:
1975 10.1016/j.ecolmodel.2013.07.020.
- 1976 Bilton, D. T., Paula, J. and Bishop, J. D. D. (2002) 'Dispersal, genetic differentiation and speciation in
1977 estuarine organisms', *Estuarine, Coastal and Shelf Science*, 55(6), pp. 937–952. doi:
1978 10.1006/ecss.2002.1037.
- 1979 Bingham, B. L. and Young, C. M. (1991) 'Larval behavior of the ascidian *Ecteinascidia turbinata*
1980 Herdman; an in situ experimental study of the effects of swimming on dispersal', *Journal of*
1981 *Experimental Marine Biology and Ecology*, 145(2), pp. 189–204. doi: 10.1016/0022-
1982 0981(91)90175-V.
- 1983 Bosch, Isidro, Katherine A. Beauchamp, M. Elizabeth Steele, and John S. Pearse. (1987). "Development ,
1984 Metamorphosis , and Seasonal Abundance of Embryos and Larvae of the Antarctic Sea Urchin
1985 *Sterechinus neumayeri*." *Biological Bulletin* 173 (1): 126–35.
- 1986 Bosch, I. (1989) 'Contrasting Modes of Reproduction in Two Antarctic Asteroids of the Genus *Porania*,
1987 With a Description of Unusual Feeding and Non-feeding Larval Types', *Biological Bulletin*, 177(1),
1988 pp. 77–82. doi: 10.2307/1541836.
- 1989 Bosch, I. and Pearse, J. S. (1990) 'Developmental types of shallow-water asteroids of McMurdo Sound,
1990 Antarctica', *Marine Biology*, 104(1), pp. 41–46. doi: 10.1007/BF01313155.
- 1991 Bouchet, P. and Taviani, M. (1992) 'The Mediterranean deep-sea fauna: pseudopopulations of Atlantic
1992 species?', *Deep Sea Research Part A, Oceanographic Research Papers*, 39(2), pp. 169–184.
1993 doi: 10.1016/0198-0149(92)90103-Z.
- 1994 Brasier, M. J. et al. (2017) 'Distributional Patterns of Polychaetes Across the West Antarctic Based on
1995 DNA Barcoding and Particle Tracking Analyses', *Frontiers in Marine Science*, 4, 356. doi:
1996 10.3389/fmars.2017.00356.

- 1997 Bryan-Brown, D. N. et al. (2017) 'Patterns and trends in marine population connectivity research', *Marine*
1998 *Ecology Progress Series*, 585, pp. 243–256.
- 1999 Buhl-Mortensen, L. and Hoisaeter, T. (1993) 'Mollusc fauna along an offshore -fjord gradient', *Marine*
2000 *Ecology Progress Series*, 97, pp. 209–224.
- 2001 Clarke, A. (1979) 'On Living in Cold Water: K-Strategies in Antarctic Benthos', *Marine Biology*, 55, pp.
2002 111–119.
- 2003 Clarke, A. (1992) 'Reproduction in the cold: Thorson revisited', *Invertebrate Reproduction &*
2004 *Development*. Taylor & Francis Group, 22(1–3), pp. 175–183. doi:
2005 10.1080/07924259.1992.9672270.
- 2006 Clarke, A. (2008) 'Antarctic marine benthic diversity: patterns and processes', *Journal of Experimental*
2007 *Marine Biology and Ecology*, 366(1–2), pp. 48–55. doi: 10.1016/j.jembe.2008.07.008.
- 2008 Clarke, A., Griffiths, H. J., Barnes, D. K. A., Meredith, M. P., & Grant, S. M. (2009). Spatial variation in
2009 seabed temperatures in the Southern Ocean: Implications for benthic ecology and biogeography.
2010 *Journal of Geophysical Research: Biogeosciences*, 114(3), 1–11.
2011 <https://doi.org/10.1029/2008JG000886>
- 2012 Connolly, S. R. and Baird, A. H. (2010) 'Estimating dispersal potential for marine larvae: dynamic models
2013 applied to scleractinian corals.', *Ecology*, 91(12), pp. 3572–83. Available at:
2014 <http://www.ncbi.nlm.nih.gov/pubmed/21302829>.
- 2015 Cook, A. J. et al. (2016) 'Ocean forcing of glacier retreat in the western Antarctic Peninsula', *Science*,
2016 353(6296), pp. 283–286. doi: 10.1126/science.aae0017.
- 2017 Cowen, R. K. et al. (2000) 'Connectivity of marine populations: Open or closed?', *Science*, 287(5454), pp.
2018 857–859. doi: 10.1126/science.287.5454.857.

- 2019 Cowen, R. K. and Sponaugle, S. (2009) 'Larval Dispersal and Marine Population Connectivity', *Annual*
 2020 *Review of Marine Science*, 1(1), pp. 443–466. doi: 10.1146/annurev.marine.010908.163757.
- 2021 Crandall, E. D., Toonen, R. J. and Selkoe, K. A. (2018) 'A coalescent sampler successfully detects
 2022 biologically meaningful population structure overlooked by F-statistics', *Evolutionary Applications*,
 2023 12(2), pp. 255–265. doi: 10.1111/eva.12712.
- 2024 Cunningham, K. M. et al. (2009) 'Genetic isolation by distance and localized fjord population structure in
 2025 Pacific cod (*Gadus macrocephalus*): limited effective dispersal in the northeastern Pacific Ocean',
 2026 *Canadian Journal of Fisheries and Aquatic Sciences*, 66(1), pp. 153–166. doi: 10.1139/F08-199.
- 2027 Damerau, M. et al. (2012) 'Comparative population genetics of seven notothenioid fish species reveals
 2028 high levels of gene flow along ocean currents in the southern Scotia Arc, Antarctica', *Polar*
 2029 *Biology*, 35(7), pp. 1073–1086. doi: 10.1007/s00300-012-1155-x.
- 2030 Damerau, M. et al. (2014) 'Population divergences despite long pelagic larval stages: Lessons from
 2031 crocodile icefishes (Channichthyidae)', *Molecular Ecology*, 23(2), pp. 284–299. doi:
 2032 10.1111/mec.12612.
- 2033 Demarchi, M. et al. (2010) 'Population genetic structure of the Antarctic ascidian *Aplidium falklandicum*
 2034 from Scotia Arc and South Shetland Islands', *Polar Biology*, 33(11), pp. 1567–1576. doi:
 2035 10.1007/s00300-010-0848-2.
- 2036 Doherty, P. J. et al. (2004) 'High Mortality During Settlement Is a Population Bottleneck for a Tropical
 2037 Surgeonfish', *Ecology*, 85(9), pp. 2422–2428. doi: 10.1890/04-0366.
- 2038 Döös, K., Kjellsson, J. and Jonsson, B. (2013) 'TRACMASS - A lagrangian trajectory model', in
 2039 Preventive Methods for Coastal Protection: Towards the Use of Ocean Dynamics for Pollution
 2040 Control, pp. 225–249. doi: 10.1007/978-3-319-00440-2.
- 2041 Egbert, G. D. and Bennett, A. F. (1994) 'TOPEX / Poseidon tides estimated using a global inverse model',
 2042 *Journal of Geophysical Research*, 99(C12), pp. 24821–24852. doi: 10.1029/94JC01894.

2043 Egbert, G. D. and Erofeeva, S. Y. (2002) 'Efficient inverse modeling of barotropic ocean tides', *Journal of*
2044 *Atmospheric and Oceanic Technology*, 19(2), pp. 183–204. doi: 10.1175/1520-
2045 0426(2002)019<0183:EIMOBO>2.0.CO;2.

2046 Emlet, R. B. and Hoegh-Guldberg, O. (1997) 'Effects of Egg Size on Postlarval Performance:
2047 Experimental Evidence from a Sea Urchin', *Evolution*, 51(1), p. 141. doi: 10.2307/2410967.

2048 Gaines, S. D. et al. (2010) 'Designing marine reserve networks for both conservation and fisheries
2049 management', *Proceedings of the National Academy of Sciences*, 107(43), pp. 18286–18293.
2050 doi: 10.1073/pnas.0906473107.

2051 Galley, E. A. et al. (2005) 'Reproductive biology and biochemical composition of the brooding echinoid
2052 *Amphipneustes lorioli* on the Antarctic continental shelf', *Marine Biology*, 148(1), pp. 59–71. doi:
2053 10.1007/s00227-005-0069-3.

2054 Galley, E. A. et al. (2008) 'Reproductive biology of two species of holothurian from the deep-sea order
2055 Elaspoda, on the Antarctic continental shelf', *Deep-Sea Research Part II: Topical Studies in*
2056 *Oceanography*, 55(22–23), pp. 2515–2526. doi: 10.1016/j.dsr2.2008.07.002.

2057 Gerritsen, H. (2018) 'Package "mapplots"', pp. 1–30.

2058 Giles, E. C. et al. (2017) 'Novel microsatellite markers for *Pyura chilensis* reveal fine-scale genetic
2059 structure along the southern coast of Chile', *Marine Biodiversity*, 48(4), pp. 1777–1786. doi:
2060 10.1007/s12526-017-0672-9.

2061 Grange, L. J. (2005) Reproductive Success in Antarctic Marine Invertebrates.

2062 Grange, L. J. and Smith, C. R. (2013) 'Megafaunal communities in rapidly warming fjords along the West
2063 Antarctic Peninsula: Hotspots of abundance and beta diversity', *PLoS one*, 8(12). doi:
2064 10.1371/journal.pone.0077917.

2065 Haidvogel, D. B. et al. (2008) 'Ocean forecasting in terrain-following coordinates: Formulation and skill
 2066 assessment of the Regional Ocean Modeling System', *Journal of Computational Physics*, 227(7),
 2067 pp. 3595–3624. doi: 10.1016/j.jcp.2007.06.016.

2068 Hastings, A., & Botsford, L. W. (2006). Persistence of spatial populations depends on returning home.
 2069 *Proceedings of the National Academy of Sciences*, 103(15), 6067–6072.
 2070 <https://doi.org/10.1073/pnas.0506651103>.

2071 Hedrick, P. w. and Miller, P. S. (1992) 'Conservation Genetics: Techniques and Fundamentals',
 2072 *Ecological Applications*, 2(1), pp. 30–46.

2073 Hill, A. E. (1991). Advection-diffusion-mortality solutions for investigating pelagic larval dispersal. *Marine*
 2074 *Ecology Progress Series*, 70(2), 117–128. <https://doi.org/10.3354/meps070117>

2075 Hilario, A. et al. (2015) 'Estimating dispersal distance in the deep sea: challenges and applications to
 2076 marine reserves', *Frontiers in Marine Science*, 2, pp. 1–14. doi: 10.3389/fmars.2015.00006.

2077 Hoffman, J. I. et al. (2011) 'Strong population genetic structure in a broadcast-spawning Antarctic marine
 2078 invertebrate', *Journal of Heredity*, 102(1), pp. 55–66. doi: 10.1093/jhered/esq094.

2079 Hofmann, E. E. et al. (1996) 'Water mass distribution and circulation west of the Antarctic Peninsula',
 2080 *Antarctic Research Series*, 70, pp. 61–80.

2081 Holsinger, K. E. and Weir, B. S. (2009) 'Genetics in geographically structured populations: Defining,
 2082 estimating and interpreting FST', *Nature Reviews Genetics*, 10(9), pp. 639–650. doi:
 2083 10.1038/nrg2611.

2084 Hunter, R. L. and Halanych, K. M. (2008) 'Evaluating connectivity in the brooding brittle star *Astrothoma*
 2085 *agassizii* across the drake passage in the Southern Ocean', *Journal of Heredity*, 99(2), pp. 137–
 2086 148. doi: 10.1093/jhered/esm119.

2087 Jablonski, D. and Lutz, R. A. (1983) 'Larval ecology of marine benthic invertebrates: paleobiological
2088 implications.', *Biological Reviews*, 58(1), pp. 21–89. doi: 10.1111/j.1469-185X.1983.tb00380.x.

2089 Kettle, A. J. and Haines, K. (2006) 'How does the European eel (*Anguilla anguilla*) retain its population
2090 structure during its larval migration across the North Atlantic Ocean?', *Canadian Journal of*
2091 *Fisheries and Aquatic Sciences*, 63(1), pp. 90–106. doi: 10.1139/f05-198.

2092 Krug, P. J. (2001). Bet-hedging dispersal strategy of a specialist marine herbivore: A settlement
2093 dimorphism among sibling larvae of *Alderia modesta*. *Marine Ecology Progress Series*, 213, 177–
2094 192. <https://doi.org/10.3354/meps213177>.

2095 Lambert, G. (2005) 'Ecology and natural history of the protochordates', *Canadian Journal of Zoology*, 83,
2096 pp. 34–50. doi: 10.1139/Z04-156.

2097 Ledoux, J. B. et al. (2012) 'Fine-scale spatial genetic structure in the brooding sea urchin *Abatus cordatus*
2098 suggests vulnerability of the Southern Ocean marine invertebrates facing global change', *Polar*
2099 *Biology*, 35(4), pp. 611–623. doi: 10.1007/s00300-011-1106-y.

2100 Leibold, M. A. et al. (2004) 'The metacommunity concept: A framework for multi-scale community
2101 ecology', *Ecology Letters*, 7(7), pp. 601–613. doi: 10.1111/j.1461-0248.2004.00608.x.

2102 Levin, S. A. (1974) 'Dispersion and Population Interactions', *The American Naturalist*, 108(960), pp. 207–
2103 228.

2104 Levin, S. A. (1976) 'Population Dynamic Models in Heterogeneous Environments', *Annual Review of*
2105 *Ecology and Systematics*, 7, pp. 287–310.

2106 Leys, S. P. and Ereskovsky, A. V (2006) 'Embryogenesis and larval differentiation in sponges', *Canadian*
2107 *Journal of Zoology*, 84(2), pp. 262–287. doi: 10.1139/z05-170.

2108 Ligges, U. et al. (2015) 'Package "signal"', pp. 1–68.

2109 Lundesgaard, Ø., Winsor, P., Truffer, M., Merrifield, M., Powell, B., Statscewich, H., ... & Smith, C. R.
 2110 (2019). Hydrography and energetics of a cold subpolar fjord: Andvord Bay, western Antarctic
 2111 Peninsula. *Progress in Oceanography*, 102224.

2112 Lundesgaard, Ø., Powell, B., et al. (2019) 'Response of an Antarctic Peninsula fjord to summer katabatic
 2113 wind events', *Journal of Physical Oceanography*, 49(6), pp. 1485–1502. doi: 10.1175/jpo-d-18-
 2114 0119.1.

2115 Maldonado, M. (2006) 'The ecology of the sponge larva', *Canadian Journal of Zoology*, 84(2), pp. 175–
 2116 194. doi: 10.1139/z05-177.

2117 Marquet, P. et al. (1993) 'Ecological and evolutionary consequences of patchiness: a marine-terrestrial
 2118 perspective. In: Levin SA, Powell TM, Steele JH (eds) Patch Dynamics, 96, pp. 277–304.

2119 Matschiner, M., Hanel, R. and Salzburger, W. (2009) 'Gene flow by larval dispersal in the Antarctic
 2120 notothenioid fish *Gobionotothen gibberifrons*', *Molecular Ecology*, 18(12), pp. 2574–2587. doi:
 2121 10.1111/j.1365-294X.2009.04220.x.

2122 McCartney-Melstad, E., Vu, J. K. and Shaffer, H. B. (2018) 'Genomic data recover previously
 2123 undetectable fragmentation effects in an endangered amphibian', *Molecular Ecology*, 27(22), pp.
 2124 4430–4443. doi: 10.1111/mec.14892.

2125 McClintock, J. B. et al. (2005) 'Ecology of Antarctic Marine Sponges: An Overview', *Integrative and*
 2126 *Comparative Biology*, 45(2), pp. 359–368.

2127 McClintock, J. B. and Pearse, J. S. (1987) 'Reproductive biology of the common Antarctic crinoid
 2128 *Promachocrinus kerguelensis* (Echinodermata: Crinoidea)', *Marine Biology*, 96(3), pp. 375–383.
 2129 doi: 10.1007/BF00412521.

2130 Meidlinger, K., Tyler, P. A. and Peck, L. S. (1998) 'Reproductive patterns in the Antarctic brachiopod
 2131 *Liothyrella uva*', *Marine Biology*, 132(1), pp. 153–162. doi: 10.1007/s002270050381.

2132 Mileikovsky, S. A. (1971) 'Types of larval development in marine bottom invertebrates, their distribution
2133 and ecological significance: a re-evaluation', *Marine Biology*, 10, pp. 193–213.

2134 Mouquet, N. et al. (2006) 'Consequences of varying regional heterogeneity in source-sink
2135 metacommunities', *Oikos*, 113(3), pp. 481–488. doi: 10.1111/j.2006.0030-1299.14582.x.

2136 Mouquet, N. and Loreau, M. (2003) 'Community Patterns in Source-Sink Metacommunities', *The
2137 American Naturalist*, 162(5), pp. 544–557. doi: 10.1007/s11172-006-0459-9.

2138 Mullineaux, L. S. and Mills, S. W. (1997) 'A test of the larval retention hypothesis in seamount-generated
2139 flows.', *Deep-Sea Research I*, 44(5), pp. 745–770.

2140 Munoz, Y. P. and Wellner, J. S. (2018) 'Seafloor geomorphology of western Antarctic Peninsula bays: A
2141 signature of ice flow behaviour', *Cryosphere*, 12(1), pp. 205–225. doi: 10.5194/tc-12-205-2018.

2142 North, E. (2008) 'LTRANS Model Description', *Continental Shelf Research*, (April), pp. 1–6.

2143 North, E. W. et al. (2006) 'Using a random displacement model to simulate turbulent particle motion in a
2144 baroclinic frontal zone: A new implementation scheme and model performance tests', *Journal of
2145 Marine Systems*, 60(3–4), pp. 365–380. doi: 10.1016/j.jmarsys.2005.08.003.

2146 North, E. W. et al. (2008) 'Vertical swimming behavior influences the dispersal of simulated oyster larvae
2147 in a coupled particle-tracking and hydrodynamic model of Chesapeake Bay', *Marine Ecology
2148 Progress Series*, 359(Leis 2007), pp. 99–115. doi: 10.3354/meps07317.

2149 North, E. W. et al. (2011) 'Simulating Oil Droplet Dispersal From the Deepwater Horizon Spill With a
2150 Lagrangian Approach', *Geophysical Monograph Series*, 195, pp. 217–226. doi:
2151 10.1029/2011GM001102.

2152 Palmer, A. R., & Strathmann, R. R. (1981). Scale of dispersal in varying environments and its implications
2153 for life histories of marine invertebrates. *Oecologia*, 48(3), 308–318.
2154 <https://doi.org/10.1007/BF00346487>

2155 Palumbi, S. R. (1994) 'Genetic divergence, reproductive isolation, and marine speciation', *Annual Review*
 2156 *of Ecology and Systematics*, 25, pp. 547–572. doi: 10.1146/annurev.es.25.110194.002555.

2157 Palumbi, Stephen R (2003a) 'Ecological subsidies alter the structure of marine communities',
 2158 *Proceedings of the National Academy of Sciences*, 100(21), pp. 11927–11928.

2159 Palumbi, Stephen R. (2003b) 'Population Genetics, Demographic Connectivity, and the Design of Marine
 2160 Reserves', *Ecological Applications*, 13(1 Supplement), pp. S146–S158. doi: 10.1890/1051-
 2161 0761(2003)013[0146:PGDCAT]2.0.CO;2.

2162 Palumbi, S. R. (2004) 'Marine Reserves and Ocean Neighborhoods: The Spatial Scale of Marine
 2163 Populations and Their Management', *Annual Review of Environment and Resources*, 29(1), pp.
 2164 31–68. doi: 10.1146/annurev.energy.29.062403.102254.

2165 Paris, C. B., Chérubin, L. M., & Cowen, R. K. (2007). Surfing, spinning, or diving from reef to reef: Effects
 2166 on population connectivity. *Marine Ecology Progress Series*, 347, 285–300.
 2167 <https://doi.org/10.3354/meps06985>

2168 Paris, C. B., Helgers, J., van Sebille, E., & Srinivasan, A. (2013). Connectivity Modeling System: A
 2169 probabilistic modeling tool for the multi-scale tracking of biotic and abiotic variability in the ocean.
 2170 *Environmental Modelling and Software*, 42(April), 47–54.
 2171 <https://doi.org/10.1016/j.envsoft.2012.12.006>

2172 Pearse, J. S. (1994) 'Cold-water echinoderms break "Thorson's Rule"', in *Reproduction, Larval Biology,*
 2173 *and Recruitment of the Deep-sea Benthos*, pp. 26–43.

2174 Pearse, J. S. and B., M. J. (1990) 'A comparison of reproduction by the brooding spatangoid echinoids
 2175 *Abatus shackletoni* and *A. nimrodi* in McMurdo Sound, Antarctica', *Invertebrate Reproduction &*
 2176 *Development*. Taylor & Francis Group, 17(3), pp. 181–191. doi:
 2177 10.1080/07924259.1990.9672110.

2178 Pearse, J. S. and Bosch, I. (1986) 'Are the feeding larvae of the commonest Antarctic Asteroid really
2179 demersal?', *Bulletin of Marine Science*, 39(2), pp. 477–484.

2180 Pearse, J. S., McClintock, J. B. and Bosch, I. (1991) 'Reproduction of Antarctic benthic marine
2181 invertebrates: Tempos, modes, and timing', *American Zoologist*, 31(1), pp. 65–80. doi:
2182 10.1093/icb/31.1.65.

2183 Pechenik, J. A. (1999). On the advantages and disadvantages of larval stages in benthic marine
2184 invertebrate life cycles. *Marine Ecology Progress Series*, 177, 269–297.
2185 <https://doi.org/10.3354/meps177269>

2186 Peck, L. S., Brockington, S., & Brey, T. (1997). Growth and metabolism in the Antarctic brachiopod
2187 *Liothyrella uva*. *Philosophical Transactions of the Royal Society of London. Series B: Biological*
2188 *Sciences*, 352(1355), 851–858. doi: 10.1098/rstb.1997.0065.

2189 Peck, L. S., Convey, P. and Barnes, D. K. A. (2006) 'Environmental constraints on life histories in
2190 Antarctic ecosystems: Tempos, timings and predictability', *Biological Reviews of the Cambridge*
2191 *Philosophical Society*, 81(1), pp. 75–109. doi: 10.1017/S1464793105006871.

2192 Peck, L. S. and Robinson, K. (1994) 'Pelagic larval development in the brooding Antarctic brachiopod
2193 *Liothyrella uva*', *Marine Biology*, 120(2), pp. 279–286. doi: 10.1007/BF00349689.

2194 Pineda, J. and Reynolds, N. (2018) 'Larval Transport in the Coastal Zone: Biological and Physical
2195 Processes', pp. 141–159. doi: 10.1093/oso/9780198786962.003.0011.

2196 Piñones, A. et al. (2013) 'Modeling the remote and local connectivity of Antarctic krill populations along
2197 the western Antarctic Peninsula', *Marine Ecology Progress Series*, 481, pp. 69–92. doi:
2198 10.3354/meps10256.

2199 Poulin, É. and Féral, J.-P. (1996) 'Why are there so many species of brooding Antarctic echinoids?',
2200 *Evolution*, 50(2), pp. 820–830. doi: 10.1111/j.1540-6237.2012.00858.x.

- 2201 Pulliam, H. R. (1988) 'Sources, Sinks, and Population Regulation', *The American Naturalist*, 132(5), pp.
2202 652–661. doi: 10.1086/284880.
- 2203 Reijmer, C. H., van Meijgaard, E. and van den Broeke, M. R. (2005) 'Evaluation of temperature and wind
2204 over Antarctica in a Regional Atmospheric Climate Model using 1 year of automatic weather
2205 station data and upper air observations', *Journal of Geophysical Research D: Atmospheres*,
2206 110(4), pp. 1–12. doi: 10.1029/2004JD005234.
- 2207 Riesgo, A., Taboada, S. and Avila, C. (2015) 'Evolutionary patterns in Antarctic marine invertebrates: An
2208 update on molecular studies', *Marine Genomics*, 23, pp. 1–13. doi:
2209 10.1016/j.margen.2015.07.005.
- 2210 Riginos, C. et al. (2016) 'Navigating the currents of seascape genomics: How spatial analyses can
2211 augment population genomic studies', *Current Zoology*, 62(6), pp. 581–601. doi:
2212 10.1093/cz/zow067.
- 2213 Rumrill, S. S. (1990) 'Natural mortality of marine invertebrate larvae', *Ophelia*, 32(1–2), pp. 163–198.
- 2214 Ryan, W. B. F. et al. (2009) 'Global multi-resolution topography synthesis', *Geochemistry, Geophysics*,
2215 *Geosystems*, 10(3). doi: 10.1029/2008GC002332.
- 2216 Sahade, R., Tatián, M. and Esnal, G. B. (2004) 'Reproductive ecology of the ascidian *Cnemidocarpa*
2217 *verrucosa* at Potter Cover South Shetland Islands, Antarctica', *Marine Ecology Progress Series*,
2218 272, pp. 131–140. doi: 10.3354/meps272131.
- 2219 van Sebille, E. et al. (2018) 'Lagrangian ocean analysis: Fundamentals and practices', *Ocean Modelling*,
2220 121(July 2016), pp. 49–75. doi: 10.1016/j.ocemod.2017.11.008.
- 2221 Selkoe, K. A. and Toonen, R. J. (2006) 'Microsatellites for ecologists: A practical guide to using and
2222 evaluating microsatellite markers', *Ecology Letters*, 9(5), pp. 615–629. doi: 10.1111/j.1461-
2223 0248.2006.00889.x.

- 2224 Selkoe, K. A. and Toonen, R. J. (2011) 'Marine connectivity: A new look at pelagic larval duration and
2225 genetic metrics of dispersal', *Marine Ecology Progress Series*, 436, pp. 291–305. doi:
2226 10.3354/meps09238.
- 2227 Shanks, A. L. (2009) 'Pelagic larval duration and dispersal distance revisited', *The Biological Bulletin*,
2228 216(June), pp. 373–385. doi: 10.2307/25548167.
- 2229 Shanks, A. L., Grantham, B. A. and Carr, M. H. (2003) 'Propagule dispersal distance and the size and
2230 spacing of marine reserves', *Ecological Applications*, 13(1), pp. 159–169.
- 2231 Shchepetkin, A. F. and McWilliams, J. C. (2009) 'Correction and commentary for "Ocean forecasting in
2232 terrain-following coordinates: Formulation and skill assessment of the regional ocean modeling
2233 system" by Haidvogel et al., J. Comp. Phys. 227, pp. 3595–3624', *Journal of Computational
2234 Physics*, 228(24), pp. 8985–9000. doi: 10.1016/j.jcp.2009.09.002.
- 2235 Siegel, D. A. et al. (2003) 'Lagrangian descriptions of marine larval dispersion', *Marine Ecology Progress
2236 Series*, 260, pp. 83–96. doi: 10.3354/meps260083.
- 2237 Siegel, D. A. et al. (2008) 'The stochastic nature of larval connectivity among nearshore marine
2238 populations', *Proceedings of the National Academy of Sciences*, 105(26), pp. 8974–8979. doi:
2239 10.1073/pnas.0802544105.
- 2240 Sköld, M., Wing, S. R. and Mladenov, P. V. (2003) 'Genetic subdivision of a sea star with high dispersal
2241 capability in relation to physical barriers in a fjordic seascape', *Marine Ecology Progress Series*,
2242 250(Palumbi 1994), pp. 163–174. doi: 10.3354/meps250163.
- 2243 Slatkin, M. (1993) 'Isolation by Distance in Equilibrium and Non-Equilibrium Populations', *Evolution*, 47(1),
2244 pp. 264–279.
- 2245 Slatkin, M. (1995) 'A measure of population subdivision based on microsatellite allele frequencies',
2246 *Genetics*, 139(1), pp. 457–462.

- 2247 Smith, C. R., Mincks, S., & DeMaster, D. J. (2006). A synthesis of benthic-pelagic coupling on the
2248 Antarctic shelf: Food banks, ecosystem inertia and global climate change. *Deep-Sea Research Part*
2249 *II: Topical Studies in Oceanography*, 53(8–10), 875–894. <https://doi.org/10.1016/j.dsr2.2006.02.001>
- 2250 Stanwell-Smith, D. et al. (1999) 'The distribution, abundance and seasonality of pelagic marine
2251 invertebrate larvae in the maritime Antarctic', *Philosophical Transactions of the Royal Society B:*
2252 *Biological Sciences*, 354(1382), pp. 471–484. doi: 10.1098/rstb.1999.0398.
- 2253 Stanwell-Smith, D. and Clarke, A. (1998) 'Seasonality of reproduction in the cushion star *Odontaster*
2254 *validus* at Signy Island, Antarctica', *Marine Biology*, 131(3), pp. 479–487. doi:
2255 10.1007/s002270050339.
- 2256 Stanwell-Smith, D. and Peck, L. S. (1998) 'Temperature and embryonic development in relation to
2257 spawning and field occurrence of larvae of three Antarctic echinoderms', *Biological Bulletin*,
2258 194(1), pp. 44–52. doi: 10.2307/1542512.
- 2259 Starr, M., Himmelman, J. H. and Theriault, J.-C. (1990) 'Direct Coupling of Marine Invertebrate Spawning
2260 with Phytoplankton Blooms', *Science*, 247(4946), pp. 1071–1074.
- 2261 Strathmann, Richard R. (1974). The Spread of Sibling Larvae of Sedentary Marine Invertebrates. *The*
2262 *American Naturalist*, 108(959), 29–44.
- 2263 Strathmann, R. R. (1985). Feeding and nonfeeding larval development and life-history evolution in marine
2264 invertebrates. *Annual Review of Ecology and Systematics*. Vol. 16, (November 1985), 339–361.
2265 <https://doi.org/10.1146/annurev.es.16.110185.002011>
- 2266 Strathmann, R.R., & Strathmann, M. F. (1982). The Relationship Between Adult Size and Brooding in
2267 Marine Invertebrates. *The American Naturalist*, 119(1), 91–101.
- 2268 Strathmann, R. R., Kendall, L. R. and Marsh, A. G. (2006) 'Embryonic and larval development of a cold
2269 adapted Antarctic ascidian', *Polar Biology*, 29(6), pp. 495–501. doi: 10.1007/s00300-005-0080-7.

- 2270 Sunnucks, P. (2000) 'Efficient genetic markers for population biology', *Trends in Ecology and Evolution*,
2271 15(5), pp. 199–203.
- 2272 Swearer, S. E. et al. (2002) 'Evidence of self-recruitment in demersal marine populations', *Bulletin of*
2273 *Marine Science*, 70(1), pp. 251–271. doi: 10.1111/j.1365-2621.2005.00959x.
- 2274 Thatje, S. (2012) 'Effects of capability for dispersal on the evolution of diversity in Antarctic benthos',
2275 *Integrative and Comparative Biology*, 52(4), pp. 470–482. doi: 10.1093/icb/ics105.
- 2276 Thornhill, D. J. et al. (2008) 'Open-ocean barriers to dispersal: A test case with the Antarctic Polar Front
2277 and the ribbon worm *Parborlasia corrugatus* (Nemertea: Lineidae)', *Molecular Ecology*, 17(23),
2278 pp. 5104–5117. doi: 10.1111/j.1365-294X.2008.03970x.
- 2279 Thorson, G. (1950) 'Reproductive and larval ecology of marine bottom invertebrates', *Biological Reviews*,
2280 25, pp. 1–45. doi: <https://doi.org/10.1111/j.1469-185X.1950.tb00585.x>.
- 2281 Van Sebille, E., Griffies, S. M., Abernathey, R., Adams, T. P., Berloff, P., Biastoch, A., ... Zika, J. D.
2282 (2018). Lagrangian ocean analysis: Fundamentals and practices. *Ocean Modelling*, 121, 49–75.
2283 <https://doi.org/10.1016/j.ocemod.2017.11.008>
- 2284 Van Wessem, J. M. et al. (2014) 'Improved representation of East Antarctic surface mass balance in a
2285 regional atmospheric climate model', *Journal of Glaciology*, 60(222), pp. 761–770. doi:
2286 10.3189/2014JoG14J051
- 2287 Vignal, A. et al. (2002) 'A review on SNPs and other types of molecular markers and their use in animal
2288 genetics', *Genetics, Selection and Evolution*, 34, pp. 275–305.
- 2289 Watson, J. R. et al. (2011) 'Currents connecting communities: nearshore community similarity and ocean
2290 circulation', *Ecology*, 92(6), pp. 1193–1200.
- 2291 Wilson, D. S. (1992) 'Complex Interactions in Metacommunities, with Implications for Biodiversity and
2292 Higher Levels of Selection', *Ecology*, 73(6), pp. 1984–2000.

- 2293 Wilson, N. G. et al. (2007) 'Multiple lineages and absence of panmixia in the "circumpolar" crinoid
2294 *Promachocrinus kerguelensis* from the Atlantic sector of Antarctica', *Marine Biology*, 152(4), pp.
2295 895–904. doi: 10.1007/s00227-007-0742-9.
- 2296 Wilson, N. G., SchrodL, M. and Halanych, K. M. (2009) 'Ocean barriers and glaciation: Evidence for
2297 explosive radiation of mitochondrial lineages in the Antarctic sea slug *Doris kerguelensis*
2298 (Mollusca, Nudibranchia)', *Molecular Ecology*, pp. 965–984. doi: 10.1111/j.1365-
2299 294X.2008.04071x.
- 2300 Woodson, C. B. and McManus, M. A. (2007) 'Foraging behavior can influence dispersal of marine
2301 organisms', *Limnology and Oceanography*, 52(6), pp. 2701–2709. doi:
2302 10.4319/lo.2007.52.6.2701.
- 2303 Wright, S. (1943) 'Isolation by Distance', *Genetics*, 28(2), pp. 114–138.
- 2304 Wright, S. (1950) 'The Genetical Structure of Populations', *Nature*, 166, pp. 247–249.
- 2305 Xu, G., McGillicuddy Jr., D. J., Mills, S. W., & Mullineaux, L. S. (2018). Dispersal of Hydrothermal Vent
2306 Larvae at East Pacific Rise 9 – 10 ° N Segment. *Journal of Geophysical Research: Oceans*, 123,
2307 7877–7895. <https://doi.org/10.1029/2018JC014290>
- 2308 Young, C. M. et al. (2012) 'Dispersal of deep-sea larvae from the intra-American seas: Simulations of
2309 trajectories using ocean models', *Integrative and Comparative Biology*, 52(4), pp. 483–496. doi:
2310 10.1093/icb/ics090.
- 2311 Ziegler, A. F., Smith, C.R., Edwards, K.F., and Vernet, M. (2017) 'Glacial dropstones: Islands enhancing
2312 seafloor species richness of benthic megafauna in West Antarctic Peninsula fjords', *Marine*
2313 *Ecology Progress Series*, 583, pp. 1–14. doi: 10.3354/meps12363.

**Chapter IV Intense deposition and rapid processing of seafloor phytodetritus in a
glaciomarine fjord, Andvord Bay (Antarctica)**

Abstract

The west Antarctic Peninsula (WAP) region encompasses numerous fjords known to be hotspots of benthic biodiversity and biomass. These diverse ecosystems are undergoing rapid climate warming and oceanographic change; consequent glacial melt and retreat may dramatically alter benthic communities and ecosystem functions in WAP fjords. In addition to climate warming, there is extreme variability in seasonal productivity and phytodetrital food input to the deep shelf benthos of the WAP. Here we document the flux and utilization of phytodetritus at 530 m depth in Andvord Bay, a WAP glaciomarine fjord, using seafloor time-lapse images spanning a 10-month period, from December 2015 to September 2016. To explore the relationship between sea-surface conditions and detrital export, we developed a color-based method to quantify seafloor phytodetritus cover in time-lapse images, and then correlated phytodetritus cover with environmental parameters including sea-ice cover and surface wind speed. During the most rapid period of phytodetritus accumulation in early January 2016, approximately 3 cm of phytodetritus was deposited on the fjord floor over six days, representing a large input of organic carbon to the benthos. The timing of this rapid export event was not related to overlying wind conditions and occurred in summer when the fjord was ice-free. To assess the response of the megafaunal community, we measured fecal pellet production by the dominant surface deposit-feeder, the ampharetid polychaete *Amythas membranifera*. The deposit-feeding rate of *A. membranifera* increased substantially during high seafloor phytodetritus cover and returned to background levels for the rest of the autumn and winter. Ampharetids and mobile megafauna were observed to deposit feed throughout the entire time-series, including beneath winter sea ice, suggesting that the delivery of phytodetritus from surface phytoplankton blooms in spring/summer sustains these abundant populations year-round in the form of a sediment food bank. *A. membranifera* can reach densities of $>37 \text{ m}^{-2}$ and, as a population, processes a volume equivalent to the top 1.05 cm of sediment annually. The maximum individual feeding rates measured are

comparable to those of some temperate intertidal deposit feeders. Nonetheless, phytodetritus on 31-73 % of the seafloor was consumed by macrofauna or microbial populations not visible in time-lapse photographs, suggesting that recently deposited phytodetritus is processed primarily by these smaller size classes. This study demonstrates the seasonal coupling and subsequent decoupling of detritivore activity in response to a massive detrital deposition event in a deep WAP fjord. This work indicates that both megafaunal deposit feeders and smaller size classes play important roles in processing labile organic matter in WAP fjord ecosystems.

Introduction

Primary production along the west Antarctic Peninsula (WAP) is extremely variable, both in space and time, and is driven by seasonal cycles of light availability (Ducklow et al. 2007) and sea-ice cover (Ducklow et al. 2007; Karl et al. 1991; Smith et al. 2006b). During spring, light penetration increases in the upper water column as sea ice retreats and is combined with high nutrient concentrations from deep winter mixing to yield phytoplankton blooms (Ducklow et al. 2007). Phytoplankton productivity and biomass peak during spring-summer months (December – February) until light or nutrients become limiting (Holm-Hansen et al. 1989; Schofield et al. 2017; Vernet et al. 2008). Primary productivity then declines and remains extremely low throughout the late fall and winter months after sea ice returns and light becomes limited (June-October). As a result of this annual cycle, organic matter flux is also highly variable along the coastal WAP both in timing and intensity (Buesseler et al. 2010; Ducklow et al. 2007, 2008; Wefer et al. 1988). Episodic pulses of labile organic matter (i.e. phytodetritus) sinking to the seafloor provide food for benthic organisms, especially deposit-feeders (e.g. Sumida et al. 2014). Studies of monthly organic matter flux on the WAP have found variability by orders of magnitude over a single season with > 70% of the annual flux arriving in a single month (Wefer et al. 1988). Seafloor photography and sediment coring have indicated accumulations of phytodetritus as thick as 2 cm on the Antarctic shelf during periods of high productivity and export, suggesting that phytodetritus accumulations are a common and widespread phenomenon (Smith et al. 2008; Sumida et al. 2014).

2366

2367 Continental margins, such as along the WAP, represent 15% of the global seafloor and are important
2368 sites for carbon burial, nutrient cycling, and pelagic-benthic coupling (Levin and Dayton 2009).
2369 Continental shelves are responsible for 50-90% of organic carbon recycling (Bauer et al. 2013), and
2370 carbon burial within fjords alone is estimated to constitute 11 % of annual marine carbon burial globally
2371 (Bernier 1982; R. W. Smith et al. 2015). In Andvord Bay, organic carbon accumulation rates have been
2372 measured at 17-24 g C m⁻² y⁻¹ (Eidam *et al.*, in press) which is higher than other high-productivity regions
2373 like the northern Bransfield Strait and the Ross Sea (Isla et al. 2002). This represents approximately 2 - 6
2374 % of overlying primary production buried in coastal sediments annually, making this region a sedimentary
2375 organic carbon sink (Isla et al. 2002). The delivery of phytodetritus to the seafloor from surface
2376 phytoplankton blooms is one example of a link between pelagic and benthic ecosystems and has been
2377 observed broadly across ocean basins (Beaulieu 2002).

2378

2379 While pelagic and benthic habitats can be vertically separated by hundreds to thousands of meters, tight
2380 coupling of processes can occur. For example, the feeding behavior, timing of reproduction, and growth
2381 of megafauna can be tightly coupled to organic-matter flux events in abyssal habitats (e.g. Lampitt 1985;
2382 R. S. Lampitt et al. 2001; Rice et al. 1986; Ruhl 2007). Food availability affects individual metabolic
2383 processes which can influence population and community dynamics. The megafauna may respond
2384 rapidly to food inputs and can be responsible for processing the majority of phytodetritus flux (Bett et al.
2385 2001; Billett et al. 2001; Lampitt et al. 2001; Lauerman and Kaufmann 1998; Miller et al. 2000; Smith et al.
2386 1996; K. L. Smith et al. 1993; P. Sumida et al. 2014). On the open WAP shelf, large mobile holothurians
2387 are an abundant component of the megafaunal deposit-feeding community and are capable of processing
2388 the upper 1 mm of sediment annually (Sumida et al. 2014). However, year-round recruitment and feeding
2389 by deposit-feeders suggests these deep benthic communities can be surprisingly decoupled from upper-
2390 ocean seasonality and are sustained by a food bank of organic carbon deposited in spring and summer
2391 months (Mincks and Smith 2007; Mincks et al. 2005; Sumida et al. 2014). While holothurians are a

conspicuous component of the Antarctic epibenthos (Arntz et al. 1994; Gutt and Starman 1998; Starman et al. 1999), they do not dominate benthic communities in many WAP habitats. In coastal fjords, for example, ophiuroids and asteroids, as well as other deposit-feeders, such as ampharetid polychaetes, can be much more abundant (Grange and Smith 2013). In addition to harboring distinct benthic communities, fjords along the WAP also contain a higher abundance and diversity of megafauna, and can sustain even higher rates of primary production than the already productive open shelf (Vernet *et al.*, 2008; Nowacek *et al.*, 2011; Pan *et al.*, submitted). While these contrasts suggest that pelagic-benthic coupling and the megafaunal response to detrital food inputs in WAP fjords differs from the open shelf, this relationship remains unexplored. Changes in productivity, in the efficiency of the biological pump and ultimately in the strength of pelagic-benthic coupling, especially at high-latitudes, may be influenced by large-scale changes in atmospheric CO₂ (J. T. Turner 2015) and global climate variability (Kim *et al.* 2016), emphasizing the importance of understanding these processes under current climate conditions to facilitate future projections.

Pelagic-benthic coupling is traditionally studied through a combination of organic-matter flux and productivity measurements, as well as assays of benthic biotic abundance, diversity, and rates (e.g. feeding rates, fecundity) from benthic photography or sample collections (Bett *et al.* 2001; Billett *et al.* 2001; Lampitt *et al.* 2001; Miller *et al.* 2000; Mincks and Smith 2007; Mincks *et al.* 2005; Smith *et al.* 1996; Smith *et al.* 1993; Sumida *et al.* 2014). Organic-matter flux is typically assessed via moored sediment traps; however, long-term sediment trap deployments can be challenging under sea ice and in very high flux environments. Therefore, additional methodologies for the measurement of phytodetritus at the seafloor are potentially valuable. For example, benthic time-lapse cameras provided the initial robust evidence that phytodetritus is seasonally supplied to the deep seafloor (Billett *et al.* 2001; Lampitt 1985; Lampitt *et al.* 2001). In these early works, abyssal seafloor phytodetritus was quantified by the reciprocal of the light intensity and ranked in comparison to other reference times (Lampitt 1985). Later work produced similar semi-quantitative ranking systems for comparing phytodetrital cover in benthic

2418 photographs in regions of the WAP shelf (Smith et al. 2006a, 2008; Sumida et al. 2014). More complex
2419 quantifications of seafloor phytodetritus using color have now been developed for the abyssal North
2420 Atlantic (Morris *et al.*, 2016) and the Weddell Sea (Cape et al., submitted).

2421

2422 This study aimed to (1) develop and implement an automated color-based method to quantify seafloor
2423 phytodetritus cover from benthic time-lapse photographs, (2) assess the deposit-feeding response to the
2424 input of phytodetritus, and (3) explore correlations between phytodetrital flux and surface-ocean
2425 conditions such as wind events and sea-ice cover in a WAP fjord. We found a pulsed delivery of
2426 phytodetritus which blanketed the fjord floor with approximately 3 cm of phytodetritus, followed by a rapid
2427 increase in deposit-feeding rate during our 16-month photographic time series.

2428

2429 *Methods*

2430

2431 Study Site

2432 The FjordEco Project conducted a 16-month field program between November 2015 and March 2017
2433 focused on Andvord Bay, a glaciomarine fjord on the WAP centered at 64° 50.67" S, 62° 36.60" W. The
2434 fjord consists of several deep (> 400 m) basins (Figure 4.1) and is surrounded by glaciers flowing into the
2435 fjord at rates of up to 7 m d⁻¹ (Lundesgaard et al., in press). The rate of change in glacial area within
2436 Andvord Bay has been relatively low over the last few decades, indicating that most of the glaciers in
2437 Andvord Bay are not currently in a state of rapid retreat (Cook et al. 2016). For detailed hydrography of
2438 the region, see Lundesgaard et al. (in press).

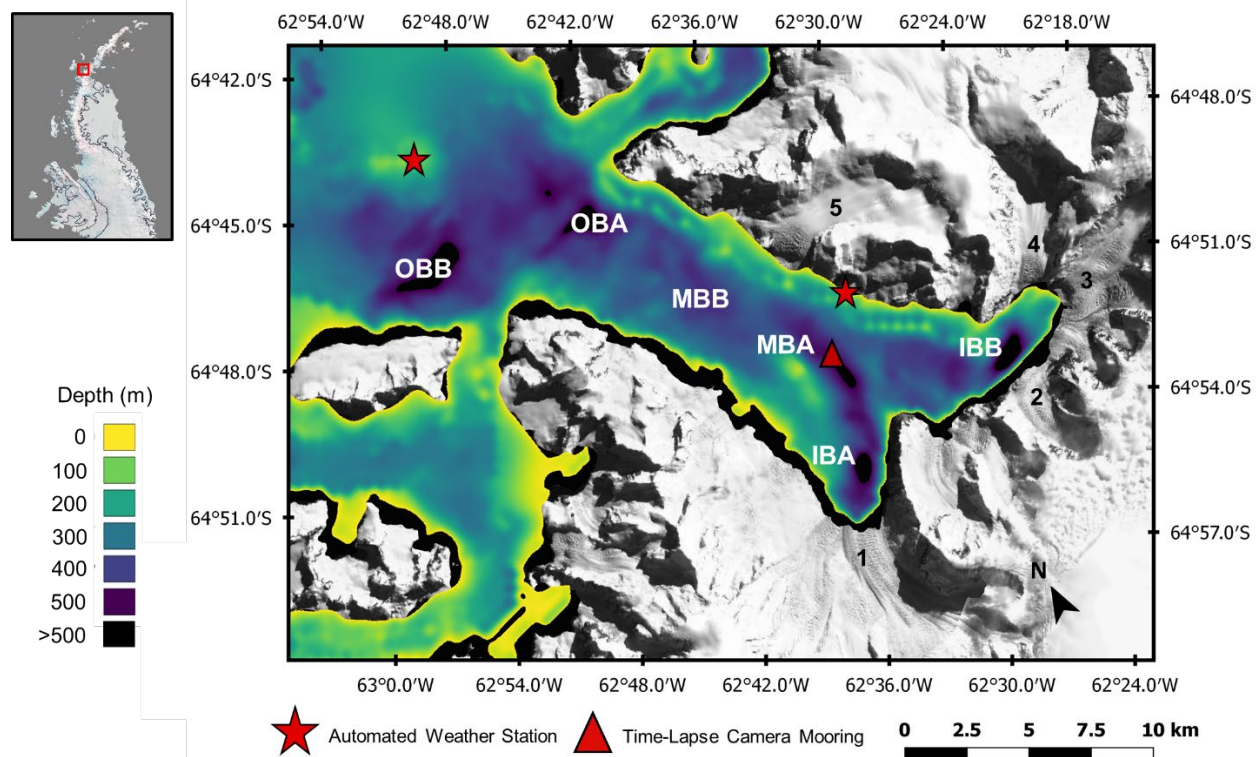
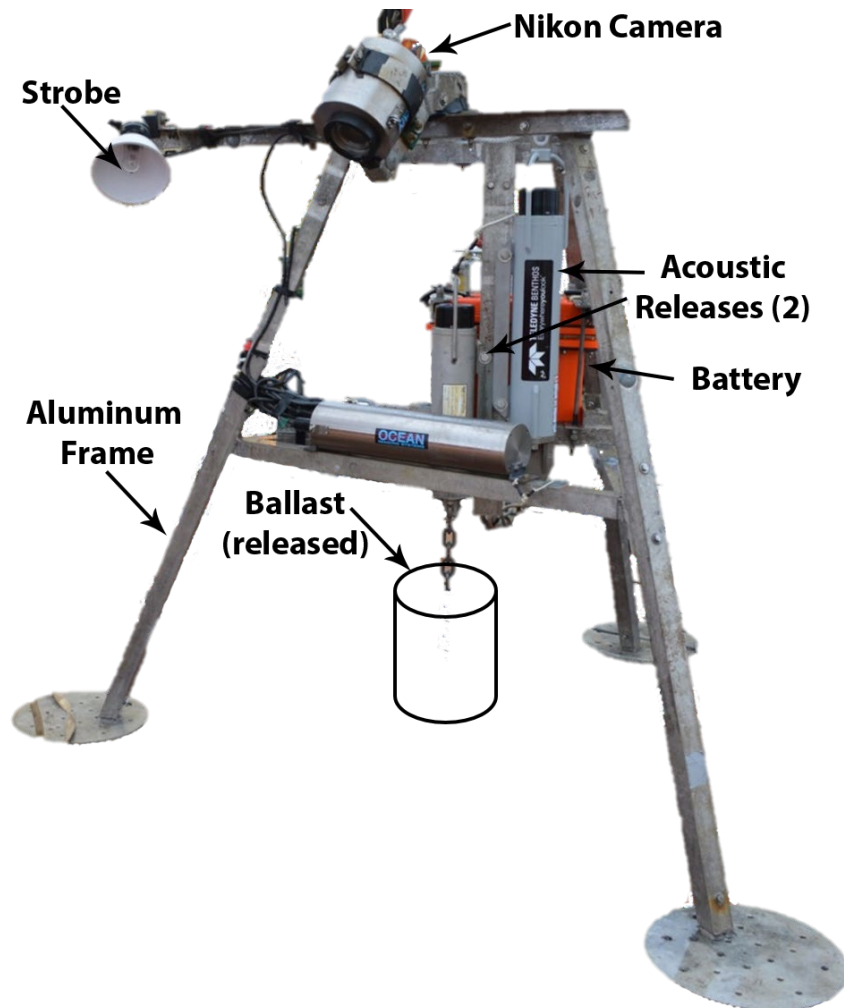


Figure 4.1 Map of the West Antarctic Peninsula and Andvord Bay with bathymetry (Ryan et al. 2009) and satellite imagery (Bindschadler et al. 2008) showing the location of tidewater glaciers. Glaciers: (1) Bagshawe, (2) Rudolph, (3) Moser, (4) Arago, and (5) Ceville Glaciers. The location of two Automated Weather Stations (AWS) atop Useful island at the mouth of the Andvord Bay and at Neko Harbor within Andvord Bay are shown by red stars. Fjord basin location names are as follows: Inner Basin A (IBA), Inner Basin B (IBB), Middle Basin A (MBA), Outer Basin A (OBA), Outer Basin B (OBB). The location of the time-lapse camera mooring in MBA is shown by the red triangle.

Benthic Time-Lapse Imagery

A moored benthic time-lapse camera system was deployed in December 2015 in MBA (64° 51.47" S, 62° 33.87" W) on the seafloor at 532 m depth (Figure 4.1). This system was recovered, recharged and re-deployed in April 2016, and finally recovered in March 2017. The benthic time-lapse camera system

(Figure 4.2) consisted of an Ocean Instruments DSC 10000 Camera System including a Nikon D80 camera with a 20 mm f/2.8 lens, and a 3831 200 W-S Strobe system, both in titanium housings, powered by a 24-volt Deep-Sea Power and Light Sea Battery. The camera was mounted ~161 cm above the seafloor at a 45° angle, with the strobe mounted 83 cm from the camera at an angle of approximately 45°. All components were mounted on an aluminum tripod frame which was equipped with dual Benthos acoustic releases, lead weight for ballast, and positive buoyancy provided by 7 x 17" Benthos glass flotation spheres (not shown). The camera system generated images of approximately 6 m² of the seafloor, with the well-illuminated portion covering approximately 4 m² (Figure 4.3). Photographs were captured every 6 hours for the deployment period of December 8, 2015-April 6, 2016 and every 12 hours from April 23, 2016 - September 14, 2016. This produced 769 benthic photographs over the course of the successful 10-month deployment. All photographs were color-corrected in Photoshop to reduce blue color bias and spatial variation of brightness using the auto color, tone and contrast features in Photoshop as well as exposure -0.3 and +0.45 Gamma corrections. Due to the oblique angle of the camera, photographs were adjusted to simulate a vertical, downward view enabling linear measurements. We first overlaid a calibrated Canadian perspective grid (Figure 4.3) (Wakefield and Genin 1987), then used Photoshop's lens correction for vertical perspective and finally stretched the image horizontally to obtain the correct aspect ratio. Images with poor illumination or other obstructions (e.g., large pelagic animals) were removed prior to further analyses (54 images, 7 % of total). Sample images from throughout the time-series are provided in Figure 4.4.



2472

2473 **Figure 4.2** The time-lapse camera tripod with main components labeled. For scale, the vertical distance
 2474 from the base to the camera lens is 161 cm.

2475

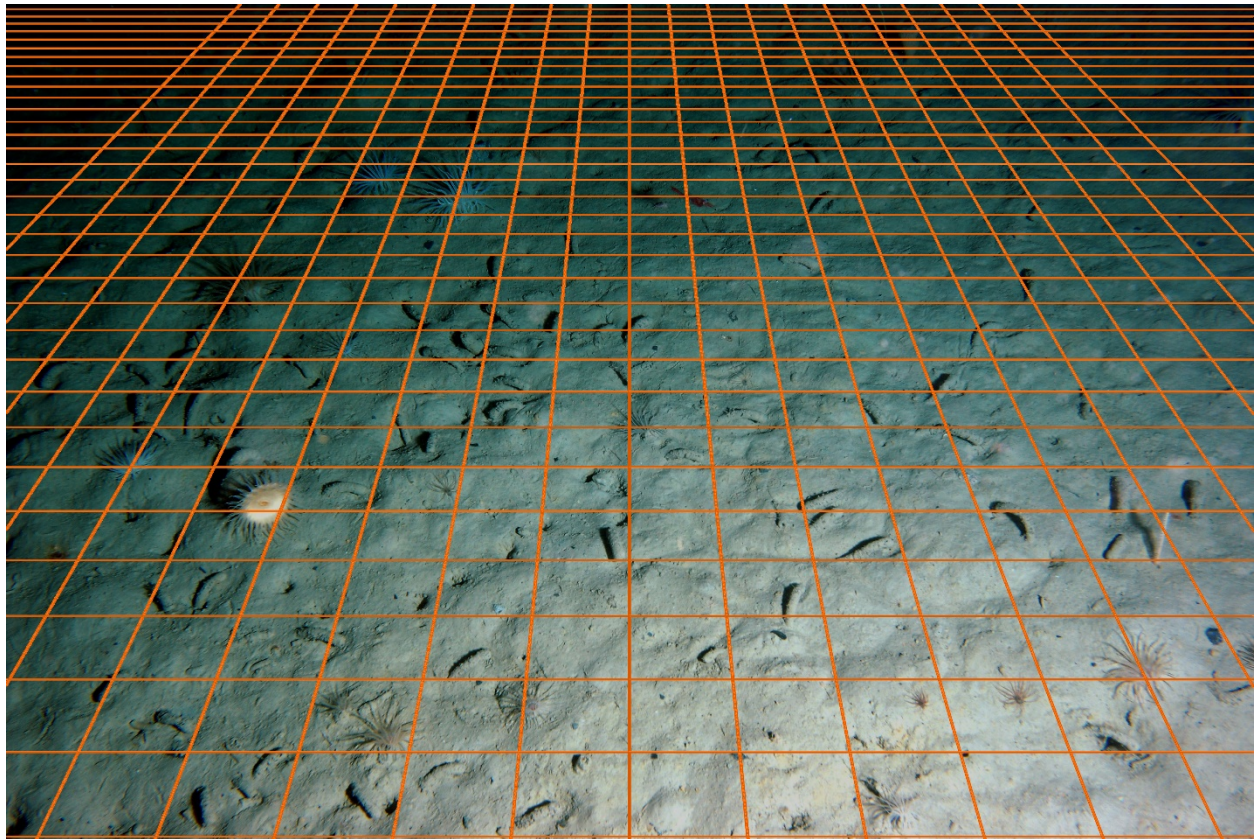


Figure 4.3 An image from the time-lapse camera with Canadian perspective grid overlaid. Each grid square is 20 x 20 cm.

Quantification of Seafloor Phytodetritus Cover

The color of seafloor features in our images is highly sensitive to illumination intensity and water absorption of different wavelengths of light. Therefore, we used the camera tripod geometry to determine regions of the seafloor located at similar path lengths of light from the strobe and thus experiencing similar attenuation and color shifts. Based on the distribution of megafaunal deposit-feeding polychaetes (*Amythas membranifera*) and the spatial consistency in color parameters, we selected a 60-cm band of seafloor for analysis (yellow arcs, Figure 4.5). Within this band, feeding regions of ampharetids (white and red circles) and smaller, non-overlapping control regions of sediment (black circles) were demarcated

2488 (Figure 4.5). Ampharetid feeding zones were defined as circles, centered on the opening of each tube,
2489 with a radius equal to the longest distance (16 cm) at which fecal pellets or cleared sediment was
2490 observed in the time-lapse record adjacent to each worm tube. Control regions were devoid of
2491 ampharetids and other visible epifauna. Individual control regions were 25% of the size of *A.*
2492 *membranifera* feeding regions and were distributed to maximize coverage within the band while
2493 eliminating overlap with ampharetid feeding regions or other sessile fauna (e.g. anemones). Ampharetid
2494 density differed between the two time-lapse camera deployments; thus, the feeding rate of six
2495 ampharetids could be measured during the first deployment period, while the rates of only three could be
2496 measured during the second deployment (Figure 4.5). *A. membranifera* feeding impacted 69 % and 27 %
2497 of the seafloor measured in the first and second deployments, respectively.

2498

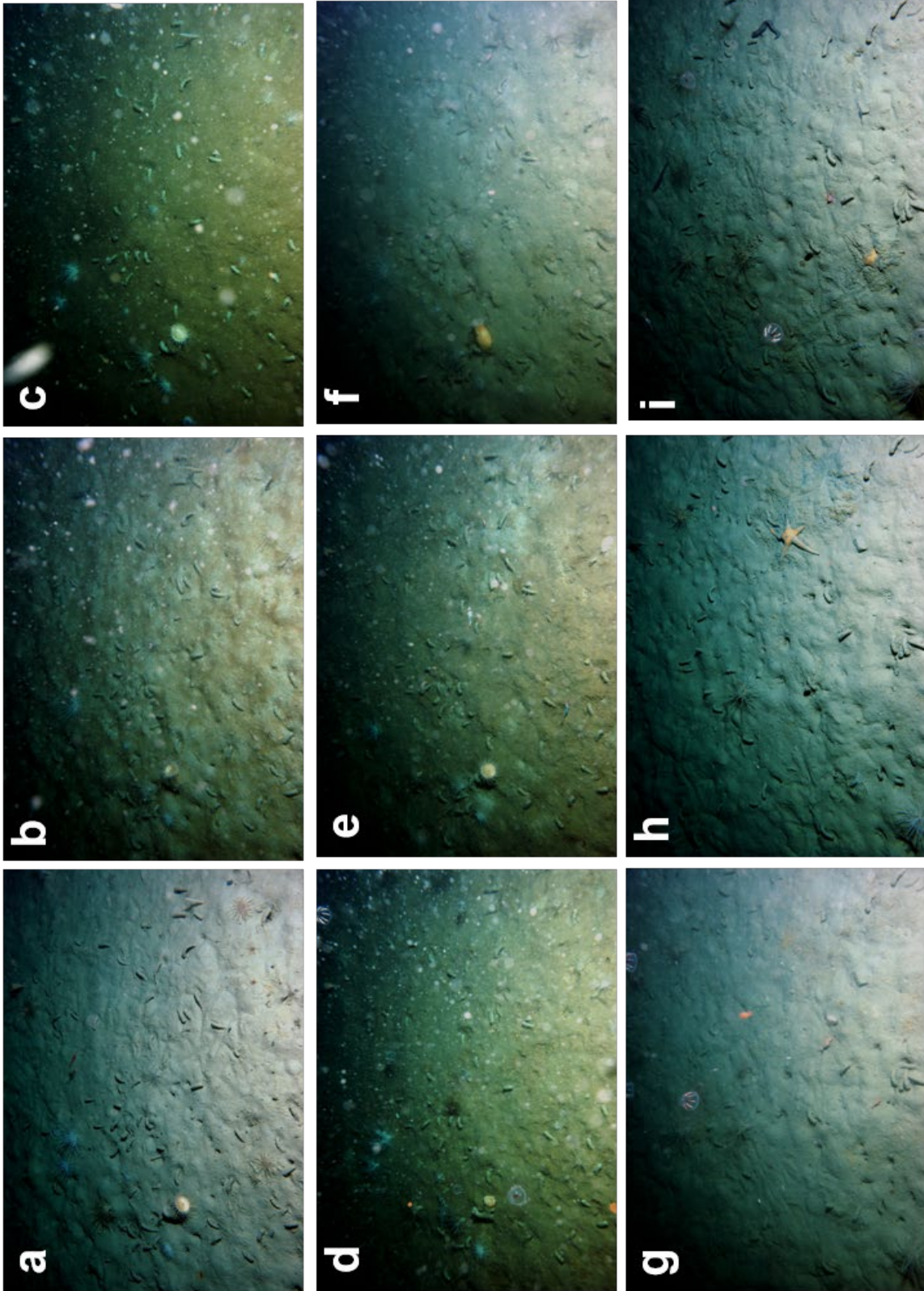


Figure 4.4 Example of time-lapse camera images across the full time series. Images (a) - (f) are from the first deployment while (g) - (i) are from the second. (a) 12/8/2015 little to no phytodetritus visible, (b) 1/5/2015 thin phytodetritus accumulating in seafloor depressions, (c) 1/11/2016 3 cm of phytodetritus blanketing seafloor, (d) 1/15/2016 *A. membranifera* feeding depressions forming, (e) 1/23/2016 small areas of seafloor cleared of phytodetritus by *A. membranifera*, (f) 3/17/2016 thin phytodetritus cover, (g) 5/2/2016 no seafloor phytodetritus cover is visible (h) 7/28/2016 no seafloor phytodetritus cover is visible , and (i) 9/14/2016, no seafloor phytodetritus cover is visible.

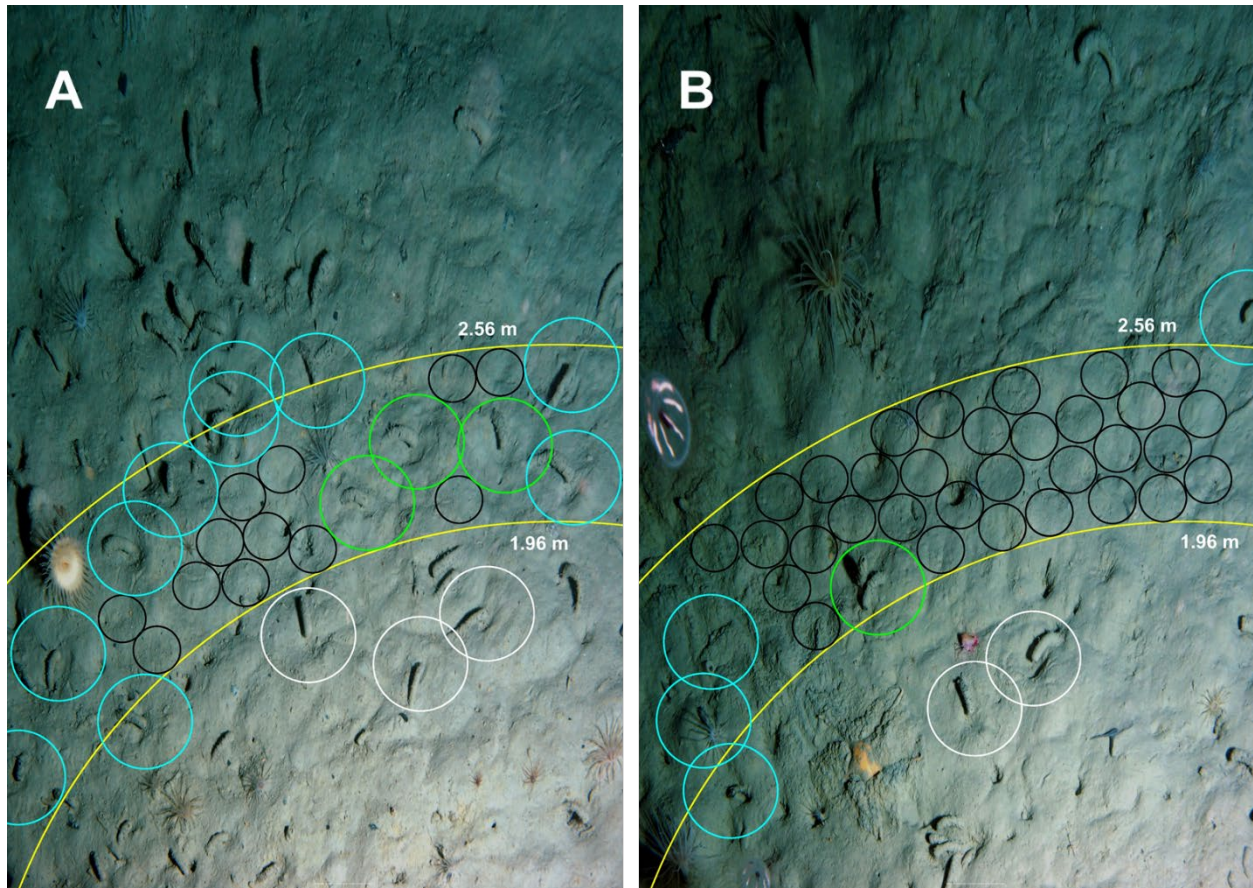


Figure 4.5 Replicate seafloor regions extracted for quantification of phytodetritus cover and fecal pellet production. Yellow lines represent constant path length from strobe to seafloor at 1.96 m and 2.56 m during both deployment periods (A = Dec - Apr., B = Apr. - Sept.). Green circles show the locations of

Amythas membranifera feeding regions from which both phytodetritus cover and fecal-pellet production were measured. White circles show the locations of additional ampharetid feeding region replicates outside of the band of uniform light path length used only for fecal-pellet production measurements. Blue circles indicate ampharetid feeding regions which were used to arrange control regions (black circles) so as not to interact with ampharetids and were not analyzed further. Small black circles are control regions of sediment free of *A. membranifera* feeding and other sessile fauna.

Time-lapse images containing obvious patches or a layer of phytodetritus were used to sample values of hue (H), saturation (S), and value (V) using Photoshop to define a range of values characteristic of phytodetritus in HSV color space. This was conducted at several times throughout the time series to ensure quantification captured all stages of phytodetritus deposition, accumulation, and degradation. Phytodetritus was defined in HSV-space as in Table 1. Because there was no phytodetritus accumulation after the camera was redeployed in April 2016, the same phytodetritus color definition was used for both deployments. Observations of seafloor phytodetritus color have previously been described as varying from “white” to “green” (Thiel et al. 1989); however, during this time series, color was less variable, ranging from pale yellow-green to dark green. We produced an image time series for each ampharetid feeding area and control region shown in Figure 4.5. Once imported into R (R Core Team, 2013) these images were converted from RGB to HSV-color space using the Imager package (Barthelme et al. 2019); images with poor lighting, or with the seafloor obscured were removed from further analysis. Phytodetritus cover was defined as the percentage of pixels (out of a total of 275260 or 68836 pixels for ampharetid and control regions, respectively) in which H, S, and V values fell within. The final time series utilized phytodetritus cover data from 715 images. Visual inspection of the resulting pixel selections aided in assessing quality of the color-recognition method with sources of error presented in the results and the Appendix.

2537

Phytodetritus definition in HSV color space	
Hue	80 - 160
Saturation	0.2 - 0.6
Value	0.2 - 0.55

2538

2539 **Table 4.1** Numeric ranges of Hue (H), Saturation (S) and Value (V) for obvious phytodetritus in time-lapse
2540 images. These ranges were used to define phytodetritus in HSV color space and determine percent cover
2541 of phytodetritus.

2542

2543 Ampharetid Fecal-Pellet Production

2544 *Amythas membranifera* (Ampharetidae) is a tube-dwelling polychaete abundant and conspicuous in
2545 Andvord Bay (Figure 4.6). Ampharetids are selective particle feeders that consume detritus using palps
2546 that extend from the end of their sediment tube (Jumars, Dorgan, and Lindsay 2015). Under conditions of
2547 low organic matter flux, ampharetids can form feeding pits in front of their tubes that concentrate sinking
2548 material within the feeding zone (Jumars and Wheatcroft 1989). There was no evidence of substantial
2549 lateral movement of phytodetritus, therefore, we assumed that phytodetritus was consumed where it was
2550 deposited. Ampharetid fecal material is packaged into cylindrical feces (i.e. fecal pellets) and defecated in
2551 front of the tube (Nowell et al. 1984) allowing for measurement of fecal-pellet production over time (Figure
2552 4.6). Fecal-pellet production rate is proportional to volumetric feeding rate for deposit-feeders because
2553 most of the material ingested is undigestible sediment (Lopez and Levinton 1987). Therefore, we used
2554 the volumetric fecal pellet production rate as an index of ampharetid volumetric feeding rate. In
2555 successive photographs, the number, length and diameter of fecal pellets produced by each ampharetid
2556 (white circles in Figure 4.5) was measured using ImageJ, with volume calculated assuming a cylindrical
2557 pellet shape. The mean *A. membranifera* fecal pellet production rate ($\text{cm}^3 \text{d}^{-1}$) was calculated for six

individuals from December - April, and for three individuals during April - September. The annual volumetric equivalent of sediment processed for the population of *A. membranifera* within MBA was calculated by multiplying the mean fecal pellet production rate by a population density of 37 m⁻² (Grange and Smith 2013). To determine a weight-specific feeding rate, 24 individuals of *A. membranifera* collected during from MBA in December 2015/April 2016 were weighed. Mean sediment density of the top 2 cm of sediment in MBA was provided by Eidam et al. (in press). Weight-specific feeding rate (mass of sediment per mass of worm per time) is equal to the mean fecal pellet production rate * sediment density / mean weight of *A. membranifera*.

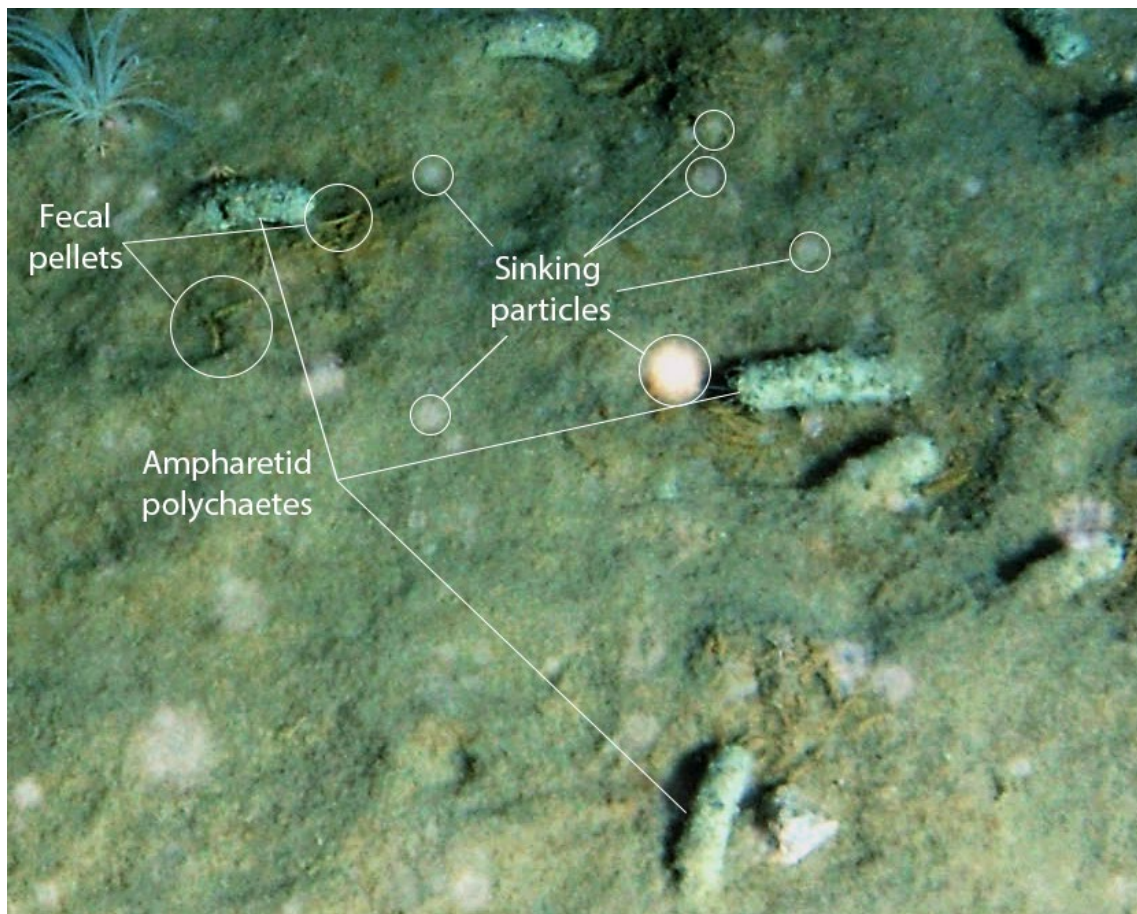


Figure 4.6 Ampharetid polychaete (*Amythas membranifera*) tubes with cylindrical fecal pellets and sinking particles labeled. Sinking particles are recognized by their diffuse (out-of-focus) borders and appearance.

2570

2571 Sinking Particle Abundance

2572 Particles sinking through the water column (e.g., phytodetritus) appeared as white, poorly focused spots in
2573 time-lapse images and were particularly abundant during rapid phytodetritus accumulation on the seafloor
2574 (Figure 4.7). The relative abundance of sinking particles was determined throughout the camera
2575 deployment period by counting bright white and poorly focused particles visible in the upper right corner
2576 of time-lapse images where light penetration through the water column best illuminated particles (Figure
2577 4.7, yellow box). The resulting abundance is semi-quantitative as it is biased by the higher visibility of
2578 large particles and those closer to the light source and camera. The particle abundance time series was
2579 used to explore trends in timing and magnitude of sinking particle flux compared to the accumulation of
2580 material on the seafloor.

2581

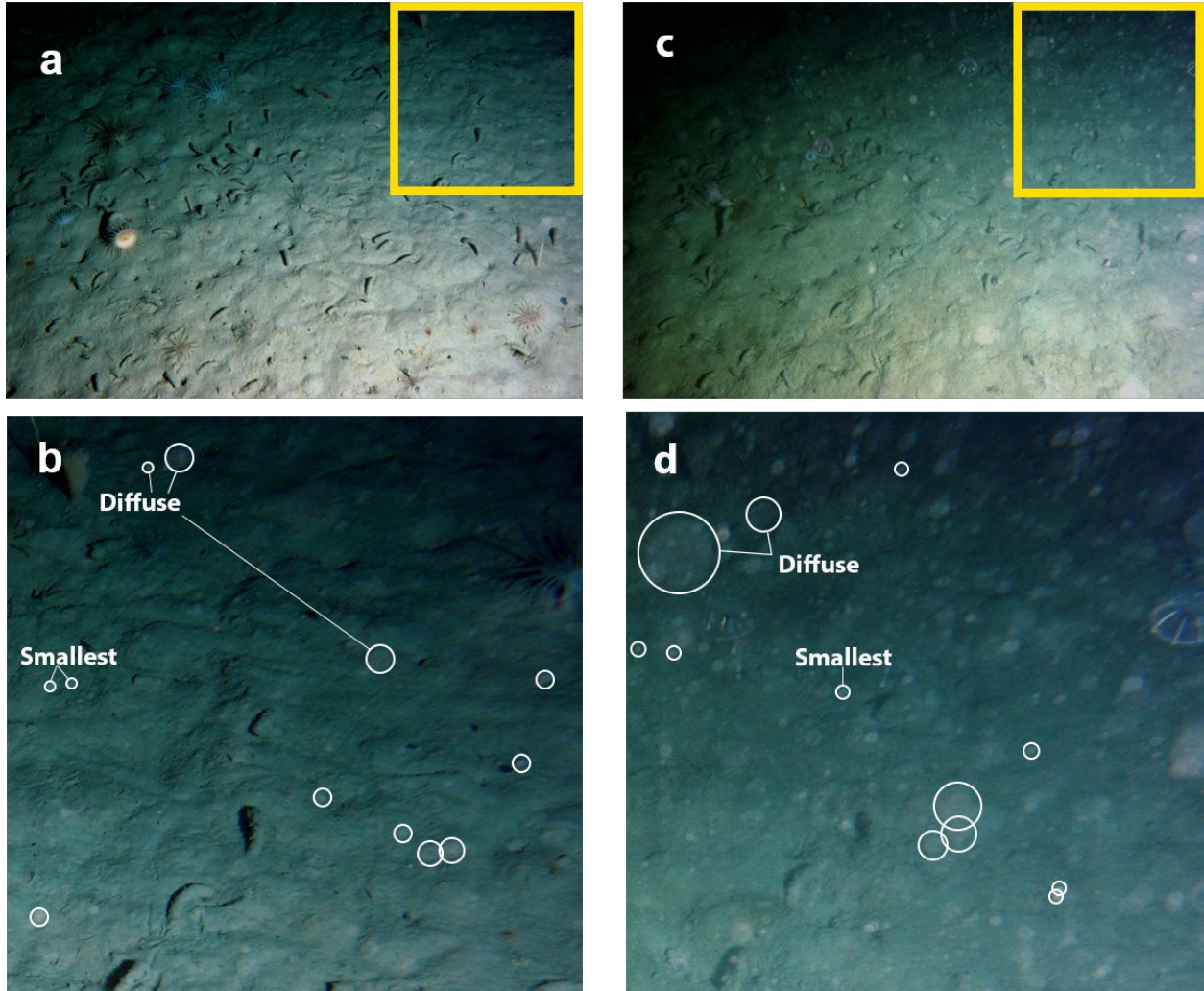


Figure 4.7 Comparison of sinking particle abundances during very low abundance (a, b) on day 0 (Dec. 8, 2015) of the time series and very high abundance (c, d) after 112 days (March 29, 2016). Particle abundances are 20 and 162 per image for b and d, respectively. Particles were counted from the upper right corner of oblique images (bordered by yellow in a and c) which are shown below in b and d. Particles indicated by white circles provide examples of the diffuse appearance of some particles and the smallest particle counted in each of the images.

Winds

2591 Surface wind speeds were recorded every 10 minutes at an Automated Weather Station (AWS) atop
2592 Useful Island in the Gerlache Strait from December 15, 2015 – March 5, 2017 (Figure 4.1). Data are
2593 archived by University of Wisconsin-Madison (Lazzara et al. 2012) and available at the Antarctic
2594 Meteorological Research Center website (amrc.ssec.wisc.edu/aws). Note that this AWS was located at an
2595 elevation of approximately 60 m above sea level and may overestimate wind speeds at the water surface.
2596 Daily files were combined and interpolated onto an even 10-minute grid and a low-pass daily average
2597 filter was applied to reduce noise. Wind components were rotated by 60° such that positive values for the
2598 v-component aligned approximately “down-fjord”. Strong winds in this direction were characterized by
2599 anomalously low relative humidity, consistent with katabatic air flowing down the glaciated plateau
2600 (Lundesgaard et al., in press). To align with camera data, daily average wind speeds were calculated for
2601 the 24-hour period preceding benthic photographs (Figure 4.8 B).

2602

2603 Sea ice

2604 A semi-quantitative measure of sea-ice cover was determined from a time-lapse camera mounted atop an
2605 AWS at Neko Harbor in Andvord Bay (Figure 4.1). The camera captured hourly images of sea ice in MBA
2606 and in IBA in front of Bagshawe Glacier. Sea-ice conditions were assessed visually in unobstructed
2607 images during the same period as the benthic time-lapse camera record (Figure 4.8C). Sea-ice cover was
2608 categorized as a fraction (0, 1/3, 2/3, or 1), converted to a percentage and used to calculate weekly
2609 running averages (Lundesgaard et al., in revision). Sea ice cover was also qualitatively assessed from
2610 cloud-free imagery of Andvord Bay for the period prior to the camera deployment (Aug. - Dec. 2015) to
2611 estimate the date of sea-ice retreat and seasonal opening of the fjord (Appendix 4.9).

2612

2613 Correlations and regressions

2614 The correlation of particle abundance, sea-ice cover, surface winds, fecal pellet production and
2615 phytodetritus cover of control sediments were explored via Spearman rank correlation with Hochberg
2616 adjustments to account for non-normality using the “cor” function in R (Table 3.2). Correlations with sea-
2617 ice cover were conducted only with data when sea-ice cover was > 0. Exponential regressions of
2618 phytodetritus cover were conducted for the 90-day period following peak phytodetritus cover for both
2619 ampharetid feeding zones and control sediment regions to compare rates of phytodetritus disappearance.
2620 Regressions were calculated in R using the lm() function to relate the log(phytodetritus cover) to elapsed
2621 time throughout the time series.

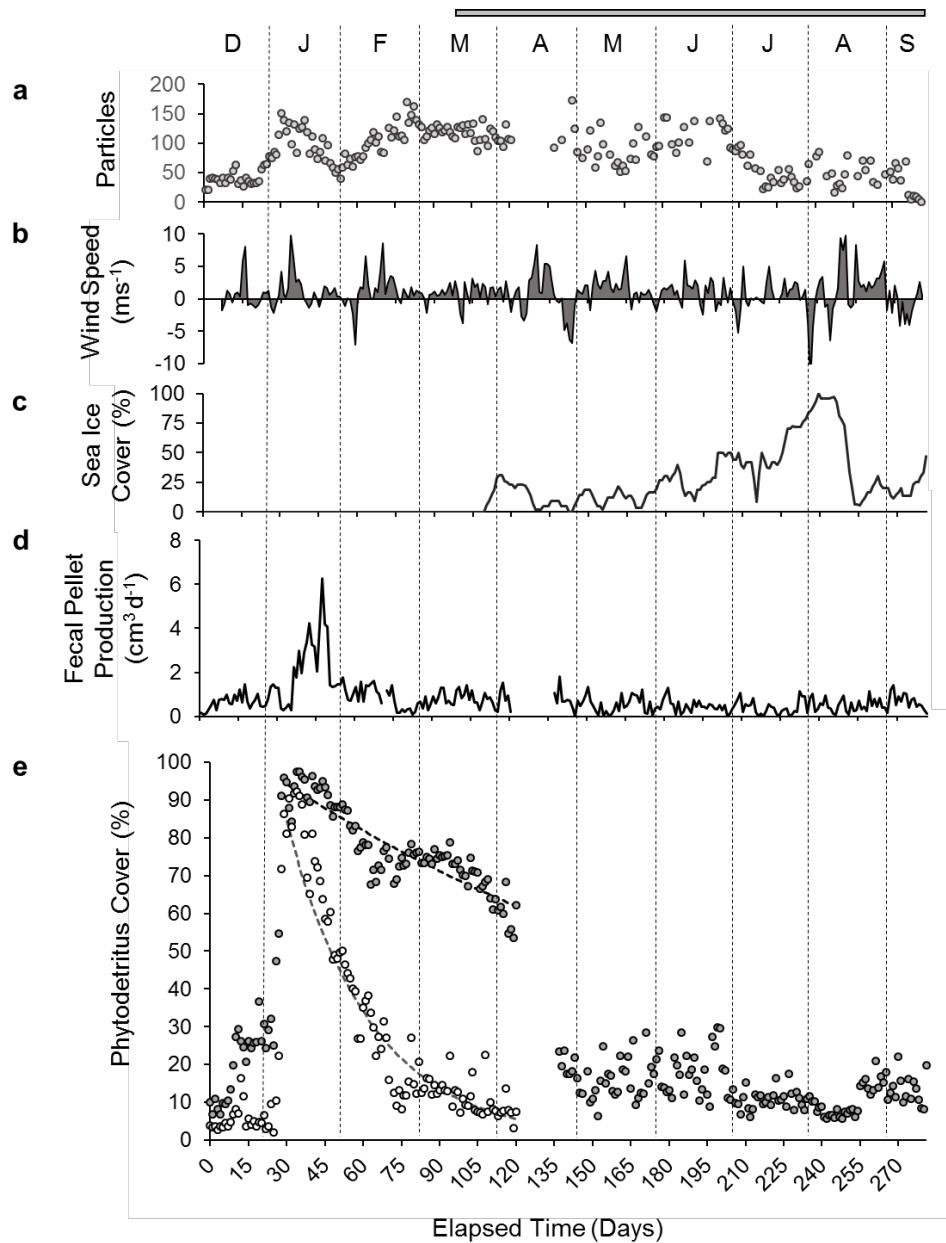


Figure 4.8 Time-series of (a) mean daily sinking particle abundance, (b) daily-averaged wind speeds (m s⁻¹) recorded from the Useful Island AWS with a low-pass filter applied. (c) Running weekly average of percent sea-ice cover measured from a time-lapse camera mounted on the Neko Harbor AWS. (d) Mean daily ampharetid fecal pellet production rate (cm³ d⁻¹). (e) Mean daily phytodetritus cover (%) of control regions (dark grey points) and *A. membranifera* feeding regions (white points). Exponential regressions

for control ($y = 295.9 e^{-0.032 x}$) and ampharetid feeding regions ($y = 124 e^{-0.008 x}$) during the 90-day period immediately following peak phytodetritus cover are provided by dark grey and light grey dashed lines, respectively. Dotted vertical lines separate months labeled by single letters above plot (a). The grey bar at the top of the figure represents days experiencing < 12 hours of daylight.

Results

By assessing phytodetritus cover within seafloor regions of constant light intensity, we reduced error from differences in light attenuation and color absorption and could optimize color-recognition for differing light fields within the same photograph. Phytodetritus cover may be underestimated during periods of high turbidity because the particles reduce visibility of the seafloor and substantially modify the scattering of light through the water column changing the appearance of colors. Omission of poor-quality images during periods of high turbidity removed substantial outliers from our dataset and did not significantly obscure the pattern of seafloor phytodetritus cover over the 10-month period (Figure 4.8 E). Phytodetritus cover may have been overestimated after redeployment of the camera in April since there was no visible phytodetritus with which to calibrate our selection criteria. However, phytodetritus cover was visibly low during this time, and we are confident that the method proved useful for assessing relative changes in phytodetritus cover. Unlike previous color-based assessments of seafloor phytodetritus, our study utilized oblique-angle imagery. The camera and light angle created shadows in the lee of seafloor features such as ampharetid tubes. We investigated the effect of polychaete tube shadows on quantification of phytodetritus cover within the feeding regions of the ampharetids and found little difference in measurements when shaded regions were excluded (Appendix 4.2). Each ampharetid feeding area had a similar bias from shadows because the ampharetid tubes were very similar in size. We are confident that the phytodetritus cover measurements made by our method were not significantly affected by inclusion of the ampharetid tubes themselves or their shadows within the measurement areas and produced a robust record of phytodetritus cover on the seafloor.

Color-based quantification of seafloor phytodetritus cover indicated rapid arrival, accumulation and subsequent consumption of seafloor phytodetritus in Andvord Bay (Figure 4.8). At the beginning of the time series in December, the water column contained few sinking particles and almost no phytodetritus was visible on the seafloor (≤ 10 % cover, Figure 4.4a). Particle abundance began to increase, and phytodetritus visibly accumulated in depressions on the seafloor by late December (Figure 4.3 b). There was a short and intense deposition event in early January 2016 in which approximately 3 cm of phytodetritus was deposited over the seafloor over a period of approximately 6 days (January 5 - 11, 2016). Deposition thickness was estimated by the burial height of *A. membranifera* tubes projecting above the seafloor during the 6 days. (Appendix 4.3). Seafloor phytodetritus cover reached its maximum during this period, with thickening of the phytodetrital carpet indicated by a darkening of the green color (Appendix 4.7 B). The abundance of large particles in the water column also increased dramatically, with phytodetritus cover and sinking particle abundance well correlated ($\rho = 0.49$), indicating that phytodetritus was sinking from the euphotic zone. Phytodetritus cover decreased from its peak in January until early April when the time-lapse camera mooring was recovered and re-deployed. From mid-April until mid-September, phytodetritus cover was low (< 30 % cover) and particle abundance in the water column was highly variable, with a marked decrease in July (Figure 4.3 g-i and Figure 4.8 A).

Sea ice was absent during the high flux event in early January and the fjord remained ice-free until mid-late March. Sea-ice cover did not reach > 50 % in MBA until July (Figure 4.8 C) and reached 100 % cover in August synchronously with low seafloor phytodetritus cover and particle abundance in the water column. Sea-ice cover was the negatively correlated with phytodetritus cover (-0.44 , Table 4.2) and the maximum correlation occurred with an 18-day lag. Satellite imagery indicates that sea-ice cover was nearly 100% in August 2015 and sea ice was advected in and out of Andvord Bay throughout October. By November, sea-ice cover was low and nearly 0% by early December.

Average down-fjord wind speeds were low throughout the time series with short periods (~ 1 day) in which mean daily wind speeds exceeded 10 ms⁻¹ (Lundesgaard et al., in press) (Figure 4.8 B). Daily averaged wind speeds not correlated with phytodetritus cover (rho = 0.07), sea-ice cover (rho = -0.10), and sinking particle abundance (rho = 0.03) (Table 4.2).

	Sea Ice	Winds	Particles	Fecal Pellets
Phytodetritus	-0.44	0.07	0.49	0.43
Sea Ice		-0.10	-0.33	-0.14
Winds			0.03	-0.03
Particles				0.10
Fecal Pellets				

Table 4.2 Correlation table for environmental data and fecal-pellet production measurements.

Environmental data include sea-ice cover (Sea Ice), low-pass filtered daily wind speed (ms⁻¹) (Winds) and sinking particle abundance (Particles). Mean daily fecal pellet production rate (Fecal Pellets) is also provided. Correlations in bold are discussed further.

During the time series, the fecal pellet production rate of *A. membranifera* increased with an increase phytodetritus cover, as illustrated by corresponding peaks, and a positive correlation (rho = 0.43) in phytodetritus cover versus fecal pellet production rate (Figures 4.8 D and E). During the 90 days immediately following the peak of phytodetritus cover, the disappearance of phytodetritus occurred faster in ampharetid feeding regions than in control regions (Figure 4.8 E). After the bulk of the newly deposited phytodetritus was consumed or degraded, fecal pellet production rates returned to levels comparable to those of early December. Fecal pellets were produced throughout the time-series including in winter (September) when visible phytodetritus cover and sinking particle abundance were very low (Figure 4.4 G-I).

2698

2699 *Discussion*

2700 Carbon input to the benthos

2701 In this study, we observed a strong seasonal cycle of sea-ice cover which was strongly negatively
2702 correlated with seafloor phytodetritus cover. This relationship supports the concept that seasonal sea ice
2703 cover alters light availability and stratification in the surface ocean to control phytoplankton growth and
2704 that this seasonal production pattern is propagated to the seafloor. Extensive work investigating the
2705 phenology of phytoplankton blooms and subsequent organic-matter flux along the WAP have also
2706 observed this relationship (Ducklow et al. 2008; Vernet et al. 2008). However, in other regions, such as
2707 the Ross Sea, organic matter export can lag up to two weeks behind the initial disappearance of sea ice
2708 (Dunbar et al. 1998) or even reach a maximum after sea ice substantially reforms at the end of summer
2709 (Smith et al. 2006b). Wind stress has also been suggested to enhance phytodetritus deposition via
2710 turbulent particle coagulation promoting faster sinking rates and, therefore, more efficient export (Ducklow
2711 et al. 2008; Dunbar et al. 1998; Isla et al. 2009; Jackson 1990; Jackson and Lochmann 1992; Karl et
2712 al. 1991; Kiorboe et al. 1994; Vernet et al. 2017; Wefer et al. 1988). In this study, we found neither
2713 evidence of enhanced phytodetritus deposition during katabatic wind events in Andvord Bay nor any
2714 correlation of winds with any benthic parameters investigated (Table 2). Recent modeling of Andvord Bay
2715 found that episodic katabatic winds can export the upper 35 m of fjord waters, removing phytoplankton
2716 biomass from within the fjord rather than promoting aggregation and particle sinking within the fjord
2717 (Lundesgaard, Powell, et al. 2019).

2718

2719 In Andvord Bay, observations of the phytoplankton community composition differed slightly from the
2720 typical succession of phytoplankton along the WAP (Ducklow et al. 2008; Garibotti et al. 2003; Mascioni
2721 et al. 2019; Schofield et al. 2017). We did not observe an early December diatom bloom in 2015. Instead,
2722 flagellates (mainly cryptomonads) dominated the community in December, and these were succeeded by

large diatoms by early January and then replaced by assorted flagellates (e.g. dinoflagellates) in February to April when small diatoms then appeared (Pan *et al.*, submitted; Mascioni *et al.*, 2019). Natural senescence, nutrient-limitation (e.g. nitrate, phosphate, silica or iron), or zooplankton grazing can initiate or enhance the sedimentation of phytoplankton cells (Krause et al. 2019; Smetacek 1985; Waite et al. 1992). The rapid sedimentation observed during our time-lapse record may have been caused by micronutrient-limitation which favored a transition from large centric diatoms to nanoplankton; these diatoms were not captured by our field sampling in late December (Pan *et al.*, submitted).

Carbon consumption in the benthos

Phytodetritus accumulated later within ampharetid feeding areas and the removal of phytodetritus cover in feeding areas was nearly 3 times faster than within control areas (Figure 4.8 E). Nevertheless, phytodetritus carpeted the seafloor in both types of areas in early January 2016. This suggests that consumption of phytodetritus by *A. membranifera* balanced phytodetritus flux until early January, when the flux dramatically increased and overwhelmed the deposit feeders. This allowed the accumulation of ~3 cm of phytodetritus across the seafloor. The feeding rate of *A. membranifera* then increased > 3-fold, presumably in response to this dramatic increase in food availability. Increases in deposit-feeding rate with increasing food availability or quality has been observed for many deposit-feeders including holothurians on the WAP shelf (Sumida et al. 2014) and the abyss (Billett et al. 2001; Smith et al. 1994; Thiel et al. 1989), megafauna within submarine canyons (Amaro et al. 2015; Vetter and Dayton 1999), deposit-feeding amphipods (Cammen 1989), and polychaetes within enriched coastal environments (Dade et al. 1990; Linton and Taghon 2000b, 2000a; Taghon and Jumars 1984). Our observations indicate that *A. membranifera* increased its feeding rate during a period of high food concentration and quality to increase energy absorption, adhering to the predictions of optimal foraging and digestion theory for complex food materials (Dade et al. 1990; Jumars 2000; Jumars and Wheatcroft 1989; Linton and Taghon 2000b; Penry and Jumars 1986, 1990; Taghon and Jumars 1984). During the period of rapid feeding, *A. membranifera* was not limited by food and quality was presumably high, therefore, the costs

2749 associated with rapid feeding could be offset by a reduced assimilation efficiency. *A. membranifera*
2750 continued to feed throughout the winter (July - Sept.) despite low sinking particle abundance and no
2751 visible accumulation of seafloor phytodetritus. During the winter, food availability was apparently low and
2752 limiting and a reduced feeding rate may have been driven by lower food quality and longer digestion
2753 times when a greater proportion of the material ingested may have been sediment rather than
2754 phytodetritus. This feeding in winter is presumably facilitated by the period in early January when detrital
2755 flux overwhelmed deposit-feeding rates, potentially producing a sediment food bank which could then
2756 sustain deposit feeders throughout the winter. Such seafloor food banks have previously been observed
2757 in other high-latitude areas such as the WAP (Mincks et al. 2005; Purinton et al. 2008), the Ross Sea
2758 (Norkko et al. 2007) and the Arctic (Berge et al. 2015; Kedra et al. 2012; Mazurkiewicz et al. 2019;
2759 Włodarska-Kowalczyk et al. 2016).

2760

2761 On average, each ampharetid we measured could consume approximately 285 ml of sediment annually
2762 which is comparable to the intertidal deposit-feeding polychaetes *Clymenella torquata* (274 ml y⁻¹, Rhoads
2763 1967) and *Pectinaria gouldii* (400 ml y⁻¹, Gordon Jr. 1966) from temperate regions (Table 3.3). *A.*
2764 *membranifera* in Andvord Bay were on average 7cm in length and 2.45 g (\pm 0.72 g) resulting in a low
2765 weight-specific feeding rate (Table 3.3). However, when feeding at maximal rates directly following rapid
2766 seafloor phytodetritus accumulation, the *A. membranifera* feeding rate was comparable to many other
2767 larger bodied, temperate deposit feeders. *A. membranifera* in Andvord Bay live at dramatically lower
2768 temperatures (< 1°C) and at much greater water depths (> 400 m) than the intertidal polychaetes. *A.*
2769 *membranifera* is one of the most abundant deposit feeders in Andvord Bay, reaching densities of > 37 m⁻²
2770 (Grange and Smith 2013) and as a population, *A. membranifera* can process the equivalent of the top ~
2771 1 cm of sediment annually. Sedimentation in the middle basin of Andvord Bay is approximately 0.6 cm y⁻¹
2772 (Eidam et al., in press) suggesting that on average, each sediment particle passes through the gut of *A.*
2773 *membranifera* nearly twice before final burial in the sediments. In this way, *A. membranifera* may exert a
2774 strong influence on organic carbon burial and diagenesis within deep basins of Andvord Bay.

2775

2776 **Table 4.3** Deposit-feeding rates (mg sediment mg⁻¹ body weight d⁻¹ and cm³ ind⁻¹ d⁻¹) from the literature

2777 for comparison. For this study, the mean feeding rate is reported, and maximum is in parentheses.

Species	Weight-Specific Feeding Rate (mg sed mg ⁻¹ body wt d ⁻¹)	Volumetric Feeding Rate (cm ³ ind ⁻¹ d ⁻¹)	Reference
Gastropoda			
<i>Ilyanassa obsoleta</i>	0.4		Connor & Edgar 1982 ^a
<i>Hydrobia neglecta</i>	2.9		Hylleberg 1975 ^a
<i>Hydrobia ventrosa</i>	4.3		Hylleberg 1975 ^a
<i>Potamopyrgus jenkinsi</i>	5.9		Heywood & Edwards 1962 ^a
<i>Amphibola crenata</i>	25		Juniper 1981 ^a
Bivalvia			
<i>Macoma nasuta</i>	1 - 2		Hylleberg & Gallucci 1975 ^a
<i>Macoma balthica</i>	9		Kofoed unpub. ^a
<i>Yolida limatula</i>	10 - 20		Bender & Davis 1984 ^a
<i>Nacula annulata</i>	2 - 5		Cheng 1983 ^a
Annelida			
<i>Tubifex tubifex</i>	1.6		Ivlev 1939 ^a
<i>Capitella capitata</i>	8 - 10		Forbes 1984 ^a
<i>Nereis succinea</i>	3.5		Cammen 1980 ^a
<i>Scoloplus</i> sp.	45 - 120		Rice unpub. ^a
<i>Axiiothella rubrocincta</i>	10 - 30		Kudenov 1982 ^a
<i>Arenicola marina</i>	5.1		Jacobsen 1967 ^a
<i>Arenicola clapedi</i>	25		Hobson 1967 ^a
<i>Pectinaria gouldii</i>	21		Gordon 1966 ^a
<i>Clymenella torquata</i>		0.75	Rhoads 1967
<i>Pseudopolydora kempj japonica</i>		18.65 - 29.82	Taghon and Jumars 1984
<i>Amphicteis scaphobranchiata</i>		20.62 - 35.48	Taghon and Jumars 1984

<i>Amythas membranifera</i>	0.2 (1.6)	0.78 (6.25)	This study
Arthropoda			
<i>Hyalella axteca</i>	1.3		Hargrave 1972 ^a
<i>Ilyoplax pusilla</i>	5.7		Ono 1965 ^a
<i>Scopimera globosa</i>	0.8		Ono 1965 ^a
Vertebrata			
<i>Liza dumerili</i>	0.6		Marais 1980 ^a
Holothuroidea			
<i>Stichopus japonicus</i>	0.72 - 1.104		Tanaka 1958 ^b
<i>Holothuria scabra</i>	5.856 - 7.44		Wiedemeyer 1993 ^b
<i>Holothuria atra</i>	10.848 - 10.944		Wiedemeyer 1993 ^b
<i>Holothuria tubulosa</i>	1.176 - 11.736		Coulon & Jangoux 1993 ^b
<i>Holothuria forskali</i>	0.144 - 2.448		Manship 1995 ^b
<i>Leptosynapta inhaerens</i>	0.432 - 14.232		Manship 1995 ^b
<i>Protelpidia murrayi</i>		9 - 19	Sumida et al. 2014
Echinoidea			
<i>Sterechinus neumayeri</i>	6x10 ⁻⁶		Brockington et al. 2001

^a References from Lopez and Levinton, 1987

^b References from Roberts et al. 2000

2778

2779 Conclusion

2780 This study utilized a color-based analysis of benthic time-lapse imagery to quantify the deposition and
2781 processing of phytodetritus at the seafloor within a productive, glaciomarine fjord of the WAP. Our results
2782 showed that deposition of phytodetritus can be rapid and provide an important supply of food to the
2783 benthos, especially detritivores. The timing of phytodetritus deposition was not correlated with katabatic
2784 wind events but was related to the seasonal cycle of overlying sea ice. Abundant deposit feeding
2785 polychaetes, *Amythas membranifera*, consumed this detritus rapidly and did not cease feeding in winter
2786 when sinking detritus was limited, suggesting that phytodetritus deposition led to the formation of a
2787 sediment food bank. This reservoir of labile organic carbon is important for sustaining high abundances of

2788 detritivores within the fjord even during the low-productivity winter. As a population, *A. membranifera*
2789 process the surface 1 cm of sediment annually, making them important components of the organic carbon
2790 cycling processes within Andvord Bay.

2791

2792 Acknowledgements:

2793 This work was conducted in collaboration with Drs. Øyvind Lundesgaard, Mattias Cape and Craig Smith
2794 and financially supported by National Science Foundation funding for the FjordEco Project (Grant OPP
2795 1443680 to Dr. Craig Smith). We thank USAP personnel and the Captains and crews of the RVIB
2796 *Nathaniel B. Palmer* and ASRV *Laurence M. Gould* for outstanding support during our field program. We
2797 also thank all principal investigators, students, and other participants of the FjordEco cruises (LMG15-10,
2798 NBP 16-03 and LMG 17-02) as well as additional collaborators including Dr. Andrew Sweetman, Dr.
2799 Charles Nittrouer, Dr. Emily Eidam and Dr. Andrew Thurber.

2800

2801 *References*

- 2802 Amaro, T., de Stigter, H., Lavaleye, M., & Duineveld, G. (2015). Organic matter enrichment in the
2803 Whittard Channel; its origin and possible effects on benthic megafauna. *Deep-Sea Research Part I: Oceanographic Research Papers*, 102(May), 90–100. <https://doi.org/10.1016/j.dsr.2015.04.014>
2804
- 2805 Arendt, K. E., Dutz, J., Jónasdóttir, S. H., Jung-Madsen, S., Mortensen, J., Møller, E. F., & Nielsen, T. G.
2806 (2011). Effects of suspended sediments on copepods feeding in a glacial influenced sub-Arctic fjord.
2807 *Journal of Plankton Research*, 33(10), 1526–1537. <https://doi.org/10.1093/plankt/fbr054>
- 2808 Arntz, W. E., Brey, T., & Gallardo, V. A. (1994). Antarctic Zoobenthos. *Oceanography and Marine Biology: An Annual Review*, 32, 241–304.
2809
- 2810 Atkinson, A., Schmidt, K., Fielding, S., Kawaguchi, S., & Geissler, P. A. (2012). Variable food absorption
2811 by Antarctic krill: Relationships between diet, egestion rate and the composition and sinking rates of

2812 their fecal pellets. *Deep-Sea Research Part II: Topical Studies in Oceanography*, 59–60, 147–158.
 2813 <https://doi.org/10.1016/j.dsr2.2011.06.008>

2814 Atkinson, Angus, Siegel, V., Pakhomov, E., & Rothery, P. (2004). Long-term decline in krill stock and
 2815 increase in salps within the Southern Ocean. *Nature*, 432, 100–103.
 2816 <https://doi.org/10.1038/nature02950.1>.

2817 Barthelme, S., Tschumperle, D., Wijffels, J., & Assemlal, H. E. (2019). Package “imager.” Retrieved from
 2818 <http://dahtah.github.io/imager>, <https://cran.r-project.org/web/packages/imager/imager.pdf>

2819 Bauer, J. E., Cai, W. J., Raymond, P. A., Bianchi, T. S., Hopkinson, C. S., & Regnier, P. A. G. (2013). The
 2820 changing carbon cycle of the coastal ocean. *Nature*, 504(7478), 61–70.
 2821 <https://doi.org/10.1038/nature12857>

2822 Beaulieu, S. E. (2002). Accumulation and fate of phytodetritus on the sea floor. *Oceanography and*
 2823 *Marine Biology: An Annual Review*, 40, 171–232. <https://doi.org/10.1201/9780203180594.ch4>

2824 Belcher, A., Manno, G. A. T. C., & Ward, A. A. P. (2017). The potential role of Antarctic krill faecal pellets
 2825 in efficient carbon export at the marginal ice zone of the South Orkney Islands in spring. *Polar*
 2826 *Biology*, 40, 2001–2013. <https://doi.org/10.1007/s00300-017-2118-z>

2827 Berge, J., Daase, M., Renaud, P. E., Ambrose, W. G., Darnis, G., Last, K. S., ... Callesen, T. A. (2015).
 2828 Unexpected levels of biological activity during the polar night offer new perspectives on a warming
 2829 arctic. *Current Biology*, 25(19), 2555–2561. <https://doi.org/10.1016/j.cub.2015.08.024>

2830 Berner, R. A. (1982). Burial of organic carbon and pyrite sulfur in the modern ocean: its geochemical and
 2831 environmental significance. *American Journal of Science*, 282, 451–473.
 2832 <https://doi.org/10.2475/ajs.282.4.451>

2833 Bett, B. J., Malzone, M. G., Narayanaswamy, B. E., & Wigham, B. D. (2001). Temporal variability in
 2834 phytodetritus and megabenthic activity at the seabed in the deep northeast Atlantic. *Progress in*
 2835 *Oceanography*, 50(1–4), 349–368. [https://doi.org/10.1016/S0079-6611\(01\)00066-0](https://doi.org/10.1016/S0079-6611(01)00066-0)

2836 Billett, D. S. M., Bett, B. J., Rice, A. L., Thurston, M. H., Galéron, J., Sibuet, M., & Wolff, G. A. (2001).

2837 Long-term change in the megabenthos of the Porcupine Abyssal Plain (NE Atlantic). *Progress in*
2838 *Oceanography*, 50(1–4), 325–348. [https://doi.org/10.1016/S0079-6611\(01\)00060-X](https://doi.org/10.1016/S0079-6611(01)00060-X)

2839 Bindschadler, R., Vornberger, P., Fleming, A., Fox, A., Mullins, J., Binnie, D., ... Gorodetzky, D. (2008).
2840 The Landsat Image Mosaic of Antarctica. *Remote Sensing of Environment*, 112(12), 4214–4226.
2841 <https://doi.org/10.1016/j.rse.2008.07.006>

2842 Buesseler, K. O., Lamborg, C. H., Boyd, P. W., Lam, P. J., Trull, T. W., Bidigare, R. R., ... Wilson, S.
2843 (2007). Revisiting carbon flux through the Ocean's twilight zone. *Science*, 316(April), 567–570.
2844 <https://doi.org/10.1126/science.1137959>

2845 Buesseler, K. O., McDonnell, A. M. P., Schofield, O. M. E., Steinberg, D. K., & Ducklow, H. W. (2010).
2846 High particle export over the continental shelf of the west Antarctic Peninsula. *Geophysical*
2847 *Research Letters*, 37(22), 1–5. <https://doi.org/10.1029/2010GL045448>

2848 Cammen, L. M. (1989). The relationship between ingestion rate of deposit feeders and sediment
2849 nutritional value. In G. Lopez, G. Taghon, & J. Levinton (Eds.), *Ecology of Marine Deposit Feeders*
2850 (pp. 201–222). New York: Springer-Verlag.

2851 Dade, W. B., Jumars, P. A., & Penry, D. L. (1990). Supply-side optimization: maximizing absorptive rates.
2852 *Behavioural Mechanisms of Food Selection*, 20, 531–556.

2853 Damerau, M., M. Matschiner, W. Salzburger, and R. Hanel. 2014. "Population Divergences despite Long
2854 Pelagic Larval Stages: Lessons from Crocodile Icefishes (Channichthyidae)." *Molecular Ecology* 23
2855 (2): 284–99. <https://doi.org/10.1111/mec.12612>.

2856 Damerau, Malte, Michael Matschiner, Walter Salzburger, and Reinhold Hanel. 2012. "Comparative
2857 Population Genetics of Seven Notothenioid Fish Species Reveals High Levels of Gene Flow along
2858 Ocean Currents in the Southern Scotia Arc, Antarctica." *Polar Biology* 35 (7): 1073–86.
2859 <https://doi.org/10.1007/s00300-012-1155-x>.

2860 Dayton, P. K., Jarrell, S. C., Kim, S., Parnell, P. . E., Thrush, S. F., Hammerstrom, K., & Leichter, J. J.
2861 (2019). Benthic responses to an Antarctic regime shift : food particle size and recruitment biology.

2862 *Ecological Applications*, 29(1), 1–20. <https://doi.org/10.1002/eap.1823>

2863 Dierssen, H. M., Smith, R. C., & Vernet, M. (2002). Glacial meltwater dynamics in coastal waters west of
 2864 the Antarctic peninsula, 99(4).

2865 Ducklow, H., Clarke, A., Dickhut, R., Doney, S. C., Geisz, H., Huang, K., ... Fraser, W. (2012). The
 2866 Marine System of the Western Antarctic Peninsula. *Antarctic Ecosystems: An Extreme Environment*
 2867 *in a Changing World*, 121–159. <https://doi.org/10.1002/9781444347241.ch5>

2868 Ducklow, H. W., Baker, K., Martinson, D. G., Quetin, L. B., Ross, R. M., Smith, R. C., ... Fraser, W.
 2869 (2007). Marine pelagic ecosystems: The West Antarctic Peninsula. *Philosophical Transactions of*
 2870 *the Royal Society B: Biological Sciences*, 362(1477), 67–94. <https://doi.org/10.1098/rstb.2006.1955>

2871 Ducklow, H. W., Erickson, M., Kelly, J., Montes-Hugo, M., Ribic, C. A., Smith, R. C., ... Karl, D. M. (2008).
 2872 Particle export from the upper ocean over the continental shelf of the west Antarctic Peninsula: A
 2873 long-term record, 1992–2007. *Deep-Sea Research Part II: Topical Studies in Oceanography*, 55(18–
 2874 19), 2118–2131. <https://doi.org/10.1016/j.dsr2.2008.04.028>

2875 Dunbar, R. B., Leventer, A. R., & Mucciarone, D. A. (1998). Water column sediment fluxes in the Ross
 2876 Sea, Antarctica: Atmospheric and sea ice forcing. *Journal of Geophysical Research*, 103(C13),
 2877 30741–30759. <https://doi.org/10.1029/1998JC900001>

2878 Eidam, E. F., Nittrouer, C. A., Homolka, K. K., & Smith, C. R. (2019). Variability of sediment accumulation
 2879 rates in an Antarctic fjord, 1–15.

2880 Garibotti, I. A., Vernet, M., Kozlowski, W. A., & Ferrario, M. E. (2003). Composition and biomass of
 2881 phytoplankton assemblages in coastal Antarctic waters: A comparison of chemotaxonomic and
 2882 microscopic analyses. *Marine Ecology Progress Series*, 247, 27–42.
 2883 <https://doi.org/10.3354/meps247027>

2884 Gleiber, M. R., Steinberg, D. K., & Ducklow, H. W. (2012). Time series of vertical flux of zooplankton fecal
 2885 pellets on the continental shelf of the western Antarctic Peninsula. *Marine Ecology Progress Series*,
 2886 471, 23–36. <https://doi.org/10.3354/meps10021>

2887 Gordon Jr., D. C. (1966). The Effects of the Deposit Feeding Polychaete *Pectinaria gouldii* on the
 2888 Intertidal Sediments of Barnstable Harbor. *Limnology and Oceanography*, 11(3), 327–332.

2889 Górska, B., & Włodarska-Kowalczyk, M. (2017). Food and disturbance effects on Arctic benthic biomass
 2890 and production size spectra. *Progress in Oceanography*, 152, 50–61.
 2891 <https://doi.org/10.1016/j.pocean.2017.02.005>

2892 Grange, L. J., & Smith, C. R. (2013). Megafaunal communities in rapidly warming fjords along the West
 2893 Antarctic Peninsula: Hotspots of abundance and beta diversity. *PLoS ONE*, 8(12).
 2894 <https://doi.org/10.1371/journal.pone.0077917>

2895 Grebmeier, J. M., Overland, J. E., Moore, S. E., Farley, E. V., Carmack, E. C., Cooper, L. W., ... McNutt,
 2896 S. L. (2006). A major ecosystem shift in the northern Bering sea. *Science*, 311(5766), 1461–1464.
 2897 <https://doi.org/10.1126/science.1121365>

2898 Griffiths, Huw J., Andrew J.S. Meijers, and Thomas J. Bracegirdle. 2017. “More Losers than Winners in a
 2899 Century of Future Southern Ocean Seafloor Warming.” *Nature Climate Change*, 7 (10): 749–54.
 2900 <https://doi.org/10.1038/nclimate3377>.

2901

2902 Gutt, J., & Starmans, A. (1998). Structure and biodiversity of megabenthos in the Weddell and Lazarev
 2903 Seas (Antarctica): Ecological role of physical parameters and biological interactions. *Polar Biology*,
 2904 20(4), 229–247. <https://doi.org/10.1007/s0030000050300>

2905 Haberman, K. L., Ross, R. M., & Quetin, L. B. (2003). Diet of the Antarctic krill (*Euphausia superba*): II .
 2906 Selective grazing in mixed phytoplankton assemblages, 283, 97–113.

2907 Holm-Hansen, O., Mitchell, B. G., Hewes, C. D., & Karl, D. M. (1989). Phytoplankton blooms in the vicinity
 2908 of Palmer Station, Antarctica. *Polar Biology*, 10, 49–57. <https://doi.org/10.1007/BF00238290>

2909 Isla, E., Gerdes, D., Palanques, A., Gili, J. M., Arntz, W. E., & König-Langlo, G. (2009). Downward particle
 2910 fluxes, wind and a phytoplankton bloom over a polar continental shelf: A stormy impulse for the
 2911 biological pump. *Marine Geology*, 259(1–4), 59–72. <https://doi.org/10.1016/j.margeo.2008.12.011>

2912 Isla, E., Masqué, P., Palanques, A., Sanchez-Cabeza, J. A., Bruach, J. M., Guillén, J., & Puig, P. (2002).
 2913 Sediment accumulation rates and carbon burial in the bottom sediment in a high-productivity area:
 2914 Gerlache Strait (Antarctica). *Deep-Sea Research Part II: Topical Studies in Oceanography*, 49(16),
 2915 3275–3287. [https://doi.org/10.1016/S0967-0645\(02\)00083-8](https://doi.org/10.1016/S0967-0645(02)00083-8)

2916 Jackson, G. A. (1990). A model of the formation of marine algal flocs by physical coagulation processes.
 2917 *Deep Sea Research Part A. Oceanographic Research*, 37(8), 1197–1211.

2918 Jackson, G. A., & Lochmann, S. E. (1992). Effect of coagulation on nutrient and light limitation of an algal
 2919 bloom. *Limnology and Oceanography*, 37(1), 77–89.

2920 Jumars, P. A. (2000). Animal guts as ideal chemical reactors: Maximizing absorption rates. *American*
 2921 *Naturalist*, 155(4), 527–543. <https://doi.org/10.1086/303333>

2922 Jumars, P. A., Dorgan, K. M., & Lindsay, S. M. (2015). Diet of Worms Emended: An Update of Polychaete
 2923 Feeding Guilds. *Annual Review of Marine Science*, 7(1), 497–520. [https://doi.org/10.1146/annurev-](https://doi.org/10.1146/annurev-marine-010814-020007)
 2924 [marine-010814-020007](https://doi.org/10.1146/annurev-marine-010814-020007)

2925 Jumars, P. A., & Wheatcroft, R. A. (1989). Responses of benthos to changing food quality and quantity ,
 2926 with a focus on deposit feeding and bioturbation. In *Productivity of the Ocean: Present and Past* (pp.
 2927 235–253).

2928 Karl, D. M., Tilbrook, B. D., & Tien, G. (1991). Seasonal coupling of organic matter production and particle
 2929 flux in the western Bransfield Strait, Antarctica. *Deep Sea Research*, 38(89), 1097–1126.

2930 Kedra, M., Kuliński, K., Walkusz, W., & Legeżyńska, J. (2012). The shallow benthic food web structure in
 2931 the high Arctic does not follow seasonal changes in the surrounding environment. *Estuarine,*
 2932 *Coastal and Shelf Science*, 114, 183–191. <https://doi.org/10.1016/j.ecss.2012.08.015>

2933 Kim, H., Martinson, D. G., Ducklow, H. W., Doney, S. C., Iannuzzi, R. A., & Meredith, M. P. (2016).
 2934 Climate forcing for dynamics of dissolved inorganic nutrients at Palmer Station, Antarctica: An
 2935 interdecadal (1993–2013) analysis. *Journal of Geophysical Research: Biogeosciences*, 121(9),
 2936 2369–2389. <https://doi.org/10.1002/2015JG003311>

2937 Kiorboe, T., Lundsgaard, C., Olesen, M., & Hansen, J. L. S. (1994). Aggregation and sedimentation
 2938 processes during a spring phytoplankton bloom: A field experiment to test coagulation theory.
 2939 *J.Mar.Res.*, 52(2), 297–323. <https://doi.org/10.1357/0022240943077145>

2940 Kohlbach, D., Graeve, M., Lange, B. A., David, C., Schaafsma, F. L., van Franeker, J. A., ... Flores, H.
 2941 (2018). Dependency of Antarctic zooplankton species on ice algae-produced carbon suggests a sea
 2942 ice-driven pelagic ecosystem during winter. *Global Change Biology*, 24(10), 4667–4681.
 2943 <https://doi.org/10.1111/gcb.14392>

2944 Krause, J. W., Schulz, I. K., Rowe, K. A., Dobbins, W., Winding, M. H. S., Sejr, M. K., ... Agustí, S.
 2945 (2019). Silicic acid limitation drives bloom termination and potential carbon sequestration in an Arctic
 2946 bloom. *Scientific Reports*, 9(1), 1–11. <https://doi.org/10.1038/s41598-019-44587-4>

2947 Lampitt, R. S. (1985). Evidence for the seasonal deposition of detritus to the deep-sea floor and its
 2948 subsequent resuspension. *Deep-Sea Research*, 32(8), 885–897.

2949 Lampitt, R. S., Bett, B. J., Kiriakoulakis, K., Popova, E. E., Ragueneau, O., Vangriesheim, A., & Wolff, G.
 2950 A. (2001). Material supply to the abyssal seafloor in the northeast Atlantic. *Progress in*
 2951 *Oceanography*, 50(1–4), 27–63. [https://doi.org/10.1016/S0079-6611\(01\)00047-7](https://doi.org/10.1016/S0079-6611(01)00047-7)

2952 Lauerman, L. M. L., & Kaufmann, R. S. (1998). Deep-sea epibenthic echinoderms and a temporally
 2953 varying food supply: Results from a one year time series in the N.E. Pacific. *Deep-Sea Research*
 2954 *Part II: Topical Studies in Oceanography*, 45(4–5), 817–842. [https://doi.org/10.1016/S0967-](https://doi.org/10.1016/S0967-0645(98)00004-6)
 2955 [0645\(98\)00004-6](https://doi.org/10.1016/S0967-0645(98)00004-6)

2956 Lazzara, M. A., Weidner, G. A., Keller, L. M., Thom, J. E., & Cassano, J. J. (2012). Antarctic automatic
 2957 weather station program: 30 years of polar observations. *Bulletin of the American Meteorological*
 2958 *Society*, 93(10), 1519–1537. <https://doi.org/10.1175/BAMS-D-11-00015.1>

2959 Levin, L. A., Boesch, D. F., Covich, A., Dahm, C., Erséus, C., Ewel, K. C., ... Weslawski, J. M. (2001).
 2960 The function of marine critical transition zones and the importance of sediment biodiversity.
 2961 *Ecosystems*, 4(5), 430–451. <https://doi.org/10.1007/s10021-001-0021-4>

2962 Levin, L. A., & Dayton, P. K. (2009). Ecological theory and continental margins: where shallow meets
 2963 deep. *Trends in Ecology and Evolution*, 24(11), 606–617. <https://doi.org/10.1016/j.tree.2009.04.012>

2964 Linton, D. L., & Taghon, G. L. (2000a). Feeding, growth, and fecundity of *Abarenicola pacifica* in relation
 2965 to sediment organic concentration. *Journal of Experimental Marine Biology and Ecology*, 254, 85–
 2966 107.

2967 Linton, D. L., & Taghon, G. L. (2000b). Feeding, growth, and fecundity of *Capitella* sp. I in relation to
 2968 sediment organic concentration. *Marine Ecology Progress Series*, 205, 229–240.
 2969 <https://doi.org/10.3354/meps205229>

2970 Loeb, V., Siegel, V., Holm-Hansen, O., Hewitt, R., Fraser, W., Trivelpiece, W., & Trivelpiece, S. (1997).
 2971 Effects of sea-ice extent and krill or salp dominance on the Antarctic food web. *Nature*, 387(6636),
 2972 897–900. <https://doi.org/10.1038/43174>

2973 Lundesgaard, Ø., Powell, B., Merrifield, M., Hahn-Woernle, L., & Winsor, P. (2019). Response of an
 2974 Antarctic Peninsula fjord to summer katabatic wind events. *Journal of Physical Oceanography*,
 2975 49(6), 1485–1502. <https://doi.org/10.1175/jpo-d-18-0119.1>

2976 Lundesgaard, Ø., Winsor, P., Truffer, M., Merrifield, M., Powell, B., Statscewich, H., ... & Smith, C. R.
 2977 (2019). Hydrography and energetics of a cold subpolar fjord: Andvord Bay, western Antarctic
 2978 Peninsula. *Progress in Oceanography*, 102224.

2979 Mascioni, M., Almandoz, G. ., Cefarelli, A. O., Cusick, A., & Vernet, M. (2019). Phytoplankton composition
 2980 and bloom formation in unexplored nearshore waters of the western Antarctic Peninsula. *Polar*
 2981 *Biology*.

2982 Mazurkiewicz, M., Górská, B., Renaud, P. E., Legeżyńska, J., Berge, J., & Włodarska-Kowalczyk, M.
 2983 (2019). Seasonal constancy (summer vs. winter) of benthic size spectra in an Arctic fjord. *Polar*
 2984 *Biology*, 42(7), 1255–1270. <https://doi.org/10.1007/s00300-019-02515-2>

2985 McMahon, K. W., Ambrose, W. G., Johnson, B. J., Sun, M. Y., Lopez, G. R., Clough, L. M., & Carroll, M.
 2986 L. (2006). Benthic community response to ice algae and phytoplankton in Ny Ålesund, Svalbard.

- 2987 *Marine Ecology Progress Series*, 310(Hsiao 1992), 1–14. <https://doi.org/10.3354/meps310001>
- 2988 Mendes, C. R. B., Tavano, V. M., Dotto, T. S., Kerr, R., Silva de Souza, M., Garcia, C. A. E., & Secchi, E.
 2989 R. (2018). New insights on the dominance of cryptophytes in Antarctic coastal waters: A case study
 2990 in Gerlache Strait. *Deep-Sea Research Part II*, 149, 161–170.
 2991 <https://doi.org/10.1016/j.dsr2.2017.02.010>
- 2992 Miller, R. J., Smith, C. R., DeMaster, D. J., & Fornes, W. L. (2000). Feeding selectivity and rapid particle
 2993 processing by deep-sea megafaunal deposit feeders: A ²³⁴Th tracer approach. *Journal of Marine*
 2994 *Research*, 58(4), 653–673. <https://doi.org/10.1357/002224000321511061>
- 2995 Mincks, S. L., & Smith, C. R. (2007). Recruitment patterns in Antarctic Peninsula shelf sediments:
 2996 Evidence of decoupling from seasonal phytodetritus pulses. *Polar Biology*, 30(5), 587–600.
 2997 <https://doi.org/10.1007/s00300-006-0216-4>
- 2998 Mincks, S. L., Smith, C. R., & DeMaster, D. J. (2005). Persistence of labile organic matter and microbial
 2999 biomass in Antarctic shelf sediments: Evidence of a sediment “food bank.” *Marine Ecology Progress*
 3000 *Series*, 300, 3–19. <https://doi.org/10.3354/meps300003>
- 3001 Moon, H. W., Wan Hussin, W. M. R., Kim, H. C., & Ahn, I. Y. (2015). The impacts of climate change on
 3002 Antarctic nearshore mega-epifaunal benthic assemblages in a glacial fjord on King George Island:
 3003 Responses and implications. *Ecological Indicators*, 57, 280–292.
 3004 <https://doi.org/10.1016/j.ecolind.2015.04.031>
- 3005 Moore, J. C., Berlow, E. L., Coleman, D. C., De Suiter, P. C., Dong, Q., Hastings, A., ... Wall, D. H.
 3006 (2004). Detritus, trophic dynamics and biodiversity. *Ecology Letters*, 7(7), 584–600.
 3007 <https://doi.org/10.1111/j.1461-0248.2004.00606.x>
- 3008 Morata, N., Michaud, E., & Włodarska-Kowalczyk, M. (2013). Impact of early food input on the Arctic
 3009 benthos activities during the polar night. *Polar Biology*, 38(1), 99–114.
 3010 <https://doi.org/10.1007/s00300-013-1414-5>
- 3011 Norling, K., Rosenberg, R., Hulth, S., Gremare, A., & Bonsdorff, E. (2007). Importance of functional

3012 biodiversity and species-specific traits of benthic fauna for ecosystem functions in marine sediment.
 3013 *Marine Ecology Progress Series*, 332, 11–23. <https://doi.org/10.3354/meps332011>
 3014 Nowacek, D. P., Friedlaender, A. S., Halpin, P. N., Hazen, E. L., Johnston, D. W., Read, A. J., ... Zhu, Y.
 3015 (2011). Super-aggregations of krill and humpback whales in Wilhelmina Bay, Antarctic Peninsula.
 3016 *PloS One*, 6(4), e19173. <https://doi.org/10.1371/journal.pone.0019173>
 3017 Nowell, A. R. M., Jumars, P. A., & Fauchald, K. (1984). The foraging strategy of a subtidal and deep-sea
 3018 deposit feeder I. *Limnology and Oceanography*, 29(3), 645–649.
 3019 Pakhomov, E. A., Froneman, P. W., & Perissinotto, R. (2002). Salp/krill interactions in the Southern
 3020 Ocean: Spatial segregation and implications for the carbon flux. *Deep-Sea Research Part II: Topical*
 3021 *Studies in Oceanography*, 49(9–10), 1881–1907. [https://doi.org/10.1016/S0967-0645\(02\)00017-6](https://doi.org/10.1016/S0967-0645(02)00017-6)
 3022 Pan, B. J., Vernet, M., Reynolds, R. A., & Greg Mitchell, B. (2019). The optical and biological properties of
 3023 glacial meltwater in an Antarctic fjord. *PLoS ONE*, 14(2), 1–30.
 3024 <https://doi.org/10.1371/journal.pone.0211107>
 3025 Pan, B., Vernet, V., Manck, L., Forsch, K., Ekern, L., Mascioni, M., ... Orona, A. J. (2019). Environmental
 3026 drivers on phytoplankton taxonomic composition in an Antarctic fjord. *Progress in Oceanography*.
 3027 Parrish, C. C. (2013). Lipids in Marine Ecosystems. *ISRN Oceanography*, 2013, 1–16.
 3028 <https://doi.org/10.5402/2013/604045>
 3029 Penry, D. L., & Jumars, P. A. (1986). Chemical Reactor Analysis and Optimal Digestion. *BioScience*,
 3030 36(5), 310–315.
 3031 Penry, D. L., & Jumars, P. A. (1990). Gut architecture, digestive constraints and feeding ecology of
 3032 deposit-feeding and carnivorous polychaetes. *Oecologia*, 82(1), 1–11.
 3033 <https://doi.org/10.1007/BF00318526>
 3034 Pfannkuche, O. (1993). Benthic response to the sedimentation of particulate organic matter at the
 3035 BIOTRANS station, 47N, 20W. *Deep-Sea Research II*, 40(1/2), 135–149.
 3036 Pimm, S. L. (1982). *Food Webs*. (M. . Usher & M. . Rosenzweig, Eds.). Chapman and Hall.

3037 Purinton, B. L., DeMaster, D. J., Thomas, C. J., & Smith, C. R. (2008). ^{14}C as a tracer of labile organic
 3038 matter in Antarctic benthic food webs. *Deep-Sea Research Part II: Topical Studies in*
 3039 *Oceanography*, 55(22–23), 2438–2450. <https://doi.org/10.1016/j.dsr2.2008.06.004>
 3040 Queirós, A. M., Stephens, N., Cook, R., Ravaglioli, C., Nunes, J., Dashfield, S., ... Widdicombe, S.
 3041 (2015). Can benthic community structure be used to predict the process of bioturbation in real
 3042 ecosystems? *Progress in Oceanography*, 137, 559–569.
 3043 <https://doi.org/10.1016/j.pocean.2015.04.027>
 3044 Renaud, P. E., Riedel, A., Michel, C., Morata, N., Gosselin, M., Juul-Pedersen, T., & Chiuchiolo, A.
 3045 (2007). Seasonal variation in benthic community oxygen demand: A response to an ice algal bloom
 3046 in the Beaufort Sea, Canadian Arctic? *Journal of Marine Systems*, 67(1–2), 1–12.
 3047 <https://doi.org/10.1016/j.jmarsys.2006.07.006>
 3048 Renaud, P. E., Sejr, M. K., Bluhm, B. A., Sirenko, B., & Ellingsen, I. H. (2015). The future of Arctic
 3049 benthos: Expansion, invasion, and biodiversity. *Progress in Oceanography*, 139, 244–257.
 3050 <https://doi.org/10.1016/j.pocean.2015.07.007>
 3051 Rhoads, D. C. (1967). Biogenic Reworking of Intertidal and Subtidal Sediments in Barnstable Harbor and
 3052 Buzzards Bay, Massachusetts. *The Journal of Geology*, 75(4), 461–476.
 3053 Rice, A. . L., Billett, D. S. M. D. S. M., Fry, J., John, A. W. G., Lampitt, R. S. R. S., Mantoura, R. F. C., &
 3054 Morris, R. J. (1986). Seasonal deposition of phytodetritus to the deep-sea floor. *Proceedings of the*
 3055 *Royal Society of Edinburgh*, 88B, 265–279.
 3056 Ross, R. M., Quetin, L. B., Baker, K. S., Vernet, M., & Smith, R. C. (2000). Growth limitation in young
 3057 *Euphausia superba* under field conditions. *Limnology and Oceanography*, 45(1), 31–43.
 3058 <https://doi.org/10.4319/lo.2000.45.1.0031>
 3059 Ruhl, H. A. (2007). Abundance and size distribution dynamics of abyssal epibenthic megafauna in the
 3060 Northeast Pacific. *Ecology*, 88(5), 1250–1262. <https://doi.org/10.1890/06-0890>
 3061 Ryan, W. B. F., Carbotte, S. M., Coplan, J. O., O'Hara, S., Melkonian, A., Arko, R., ... Zemsky, R. (2009).

3062 Global multi-resolution topography synthesis. *Geochemistry, Geophysics, Geosystems*, 10(3).
 3063 <https://doi.org/10.1029/2008GC002332>

3064 Sahade, R., Lager, C., Torre, L., Momo, F., Monien, P., Schloss, I., ... Abele, D. (2015). Climate change
 3065 and glacier retreat drive shifts in an Antarctic benthic ecosystem. *Science Advances*, 1(10).
 3066 <https://doi.org/10.1126/sciadv.1500050>

3067 Schofield, O., Saba, G., Coleman, K., Carvalho, F., Couto, N., Ducklow, H., ... Waite, N. (2017). Decadal
 3068 variability in coastal phytoplankton community composition in a changing West Antarctic Peninsula.
 3069 *Deep-Sea Research Part I: Oceanographic Research Papers*, 124(March), 42–54.
 3070 <https://doi.org/10.1016/j.dsr.2017.04.014>

3071 Smetacek, V. (1985). Role of sinking in diatom life-history cycles: ecological, evolutionary and geological
 3072 significance. *Marine Biology*, 84, 239–251. <https://doi.org/10.1007/BF00392493>

3073 Smith, C., DeMaster, D., Thomas, C., Srsen, P., Grange, L., Evrard, V., & DeLeo, F. (2012). Pelagic-
 3074 Benthic Coupling, Food Banks, and Climate Change on the West Antarctic Peninsula Shelf.
 3075 *Oceanography*, 25(3), 188–201. <https://doi.org/10.5670/oceanog.2012.94>

3076 Smith, C. R., De Leo, F. C., Bernardino, A. F., Sweetman, A. K., & Arbizu, P. M. (2008). Abyssal food
 3077 limitation, ecosystem structure and climate change. *Trends in Ecology and Evolution*, 23(9), 518–
 3078 528. <https://doi.org/10.1016/j.tree.2008.05.002>

3079 Smith, C. R., Hoover, D. J., Doan, S. E., Pope, R. H., Demaster, D. J., Dobbs, F. C., & Altabet, M. A.
 3080 (1996). Phytodetritus at the abyssal sea floor across 10° of latitude in the central equatorial Pacific.
 3081 *Deep-Sea Research Part II: Topical Studies in Oceanography*, 43(4–6), 1309–1338.
 3082 [https://doi.org/10.1016/0967-0645\(96\)00015-X](https://doi.org/10.1016/0967-0645(96)00015-X)

3083 Smith, C. R., Mincks, S., & DeMaster, D. J. (2006a). A synthesis of benthic-pelagic coupling on the
 3084 Antarctic shelf: Food banks, ecosystem inertia and global climate change. *Deep-Sea Research Part*
 3085 *II: Topical Studies in Oceanography*, 53(8–10), 875–894. <https://doi.org/10.1016/j.dsr2.2006.02.001>

3086 Smith, C. R., Mincks, S., & DeMaster, D. J. (2006b). A synthesis of benthic-pelagic coupling on the

3087 Antarctic shelf: Food banks, ecosystem inertia and global climate change. *Deep-Sea Research Part*
3088 *II: Topical Studies in Oceanography*, 53(8–10), 875–894. <https://doi.org/10.1016/j.dsr2.2006.02.001>

3089 Smith, C. R., Mincks, S., & DeMaster, D. J. (2008). The FOODBANCS project: Introduction and sinking
3090 fluxes of organic carbon, chlorophyll-a and phytodetritus on the western Antarctic Peninsula
3091 continental shelf. *Deep-Sea Research Part II: Topical Studies in Oceanography*, 55(22–23), 2404–
3092 2414. <https://doi.org/10.1016/j.dsr2.2008.06.001>

3093 Smith, C. R., Sweetman, A. K., Nunnally, C. C., Lewis, M., Vernet, M., Ekern, L., & Ziegler, A. (2018).
3094 Benthic Ecosystem Studies in a Rapidly Warming Antarctic Fjord Reveal High Export Flux and
3095 Benthic Abundance Very Near Tidewater Glaciers , Indicating High Sensitivity to Climate Warming.
3096 In *AGU Ocean Sciences Meeting Abstracts*.

3097 Smith, K. L., Kaufmann, R. S., & Baldwin, R. J. (1994). Coupling of near-bottom pelagic and benthic
3098 processes at abyssal depths in the eastern North Pacific Ocean. *Limnology and Oceanography*,
3099 39(5), 1101–1118. <https://doi.org/10.4319/lo.1994.39.5.1101>

3100 Smith, K. L., Kaufmann, R. S., & Wakefield, W. W. (1993). Mobile megafaunal activity monitored with a
3101 time-lapse camera in the abyssal North Pacific. *Deep-Sea Research Part I*, 40(11–12), 2307–2324.
3102 [https://doi.org/10.1016/0967-0637\(93\)90106-D](https://doi.org/10.1016/0967-0637(93)90106-D)

3103 Smith, R. W., Bianchi, T. S., Allison, M., Savage, C., & Galy, V. (2015). High rates of organic carbon
3104 burial in fjord sediments globally. *Nature Geoscience*, 8(6), 450–453.
3105 <https://doi.org/10.1038/NGEO2421>

3106 Starman, a, Gutt, J., & Arntz, W. E. (1999). Mega-epibenthic communities in Arctic and Antarctic shelf
3107 areas. *Marine Biology*, 135(January), 269–280.

3108 Stead, R. A., Richoux, N. B., Pereda, S. V., & Thompson, R. J. (2013). Influence of an intermittent food
3109 supply on energy storage by the subpolar deposit feeder *Yoldia hyperborea* (Bivalvia: Nuculanidae).
3110 *Polar Biology*, 36(9), 1333–1345. <https://doi.org/10.1007/s00300-013-1353-1>

3111 Steinberg, D.K., Martinson, D. G., & Costa, D. P. (2012). Two decades of pelagic ecology of the Western

3112 Antarctic Peninsula. *Oceanography*, 25(3), 56–67. <https://doi.org/10.5670/oceanog.2011.65>

3113 Steinberg, Deborah K, & Landry, M. R. (2017). Zooplankton and the Ocean Carbon Cycle. *Annual Review*
 3114 *of Marine Science*, 9, 413–444. <https://doi.org/10.1146/annurev-marine-010814-015924>

3115 Steinberg, Deborah K, Lomas, M. W., & Cope, J. S. (2012). Long-term increase in mesozooplankton
 3116 biomass in the Sargasso Sea : Linkage to climate and implications for food web dynamics and
 3117 biogeochemical cycling. *Global Biogeochemical Cycles*, 26, 1–16.
 3118 <https://doi.org/10.1029/2010GB004026>

3119 Sumida, P., Smith, C., Bernardino, a, Polito, P., & Vieira, D. (2014). Seasonal dynamics of epibenthic
 3120 megafauna on the deep West Antarctic Peninsula in response to variable phytodetrital influx. *Royal*
 3121 *Society*, 1, 1–13. <https://doi.org/10.1098/rsos.140294>

3122 Sumida, P. Y. G., Smith, C. R., Bernardino, A. F., Polito, P. S., & Vieira, D. R. (2014). Seasonal dynamics
 3123 of megafauna on the deep West Antarctic Peninsula shelf in response to variable phytodetrital
 3124 influx. *Royal Society Open Science*, 1(3). <https://doi.org/10.1098/rsos.140294>

3125 Taghon, G. L., & Jumars, P. A. (1984). Variable ingestion rate and its role in optimal foraging behavior of
 3126 marine deposit feeders. *Ecology*, 65(2), 549–558. <https://doi.org/10.2307/1941417>

3127 Team, R. C. (2013). R: A language and environment for statistical computing. *R Foundation for Statistical*
 3128 *Computing*. <https://doi.org/10.1108/eb003648>

3129 Tenore, K. R. (1988). Nitrogen in benthic food chain. *Nitrogen Cycling in Coastal Marine Environment*,
 3130 191–206. <https://doi.org/10.5651/jaas.9.123>

3131 Thiel, H., Pfannkuche, O., Schriever, G., Lochte, K., Gooday, A. J., Hemleben, C., ... Riemann, F. (1989).
 3132 Phytodetritus on the deep-sea floor in a central oceanic region of the northeast Atlantic. *Biological*
 3133 *Oceanography*, 6(2), 203–239. <https://doi.org/10.1080/01965581.1988.10749527>

3134 Thomas, D. N., & Dieckmann, G. S. (2002). Antarctic Sea Ice—a Habitat for Extremophiles. *Science*,
 3135 295(January), 641–644. Retrieved from
 3136 http://webmail.img.usap.gov/?_task=mail&_framed=1&_action=get&_mbox=INBOX&_uid=118&_par

3137 t=2&_frame=1%0Apapers3://publication/uuid/139C9382-4FDC-40EE-8B0C-830415E0C3C3

3138 Torre, L., Servetto, N., Eöry, M. L., Momo, F., Tatián, M., Abele, D., & Sahade, R. (2012). Respiratory
 3139 responses of three Antarctic ascidians and a sea pen to increased sediment concentrations. *Polar*
 3140 *Biology*, 35(11), 1743–1748. <https://doi.org/10.1007/s00300-012-1208-1>

3141 Torstensson, A., Hedblom, M., Andersson, J., Andersson, M. X., & Wulff, A. (2013). Synergism between
 3142 elevated pCO₂ and temperature on the Antarctic sea ice diatom *Nitzschia lecontei*. *Biogeosciences*,
 3143 10(10), 6391–6401. <https://doi.org/10.5194/bg-10-6391-2013>

3144 Trivelpiece, W. Z., Hinke, J. T., Miller, A. K., Reiss, C. S., Trivelpiece, S. G., & Watters, G. M. (2011).
 3145 Variability in krill biomass links harvesting and climate warming to penguin population changes in
 3146 Antarctica. *Proceedings of the National Academy of Sciences*, 108(18), 7625–7628.
 3147 <https://doi.org/10.1073/pnas.1016560108>

3148 Turner, J. T. (2015). Zooplankton fecal pellets, marine snow, phytodetritus and the ocean's biological
 3149 pump. *Progress in Oceanography*, 130, 205–248. <https://doi.org/10.1016/j.pocean.2014.08.005>

3150 Vargas, C., Escribano, R., & Poulet, S. (2006). Phytoplankton food quality determines time-windows for
 3151 successful zooplankton reproductive pulses. *Ecology*, 87(12), 2992–2999.

3152 Veit-Köhler, G., Guilini, K., Peeken, I., Sachs, O., Sauter, E. J., & Würzberg, L. (2011). Antarctic deep-sea
 3153 meiofauna and bacteria react to the deposition of particulate organic matter after a phytoplankton
 3154 bloom. *Deep-Sea Research Part II: Topical Studies in Oceanography*, 58(19–20), 1983–1995.
 3155 <https://doi.org/10.1016/j.dsr2.2011.05.008>

3156 Vernet, M., Martinson, D., Iannuzzi, R., Stammerjohn, S., Kozlowski, W., Sines, K., ... Garibotti, I. (2008).
 3157 Primary production within the sea-ice zone west of the Antarctic Peninsula: I-Sea ice, summer
 3158 mixed layer, and irradiance. *Deep-Sea Research Part II: Topical Studies in Oceanography*, 55(18–
 3159 19), 2068–2085. <https://doi.org/10.1016/j.dsr2.2008.05.021>

3160 Vernet, M., Richardson, T. L., Metfies, K., Eva-Maria Nöthig, & Peeken, I. (2017). Models of plankton
 3161 community changes during a warm water anomaly in Arctic waters show altered trophic pathways

3162 with minimal changes in carbon export. *Frontiers in Marine Science*, 4(MAY), 1–19.
 3163 <https://doi.org/10.3389/fmars.2017.00160>

3164 Vetter, E. W., & Dayton, P. K. (1999). Organic enrichment by macrophyte detritus, and abundance
 3165 patterns of megafaunal populations in submarine canyons. *Marine Ecology Progress Series*, 186,
 3166 137–148. <https://doi.org/10.3354/meps186137>

3167 Waite, A., Bienfang, P. K., & Harrison, P. J. (1992). Spring bloom sedimentation in a subarctic ecosystem
 3168 - I. Nutrient sensitivity. *Marine Biology*, 114(1), 119–129. <https://doi.org/10.1007/BF00350861>

3169 Wakefield, W. W., & Genin, A. (1987). The use of a Canadian (perspective) grid in deep-sea
 3170 photography. *Deep Sea Research Part A, Oceanographic Research Papers*, 34(3), 469–478.
 3171 [https://doi.org/10.1016/0198-0149\(87\)90148-8](https://doi.org/10.1016/0198-0149(87)90148-8)

3172 Wefer, G., Fischer, G., Fuetterer, D., & Gersonde, R. (1988). Seasonal particle flux in the Bransfield
 3173 Strait, Antarctica. *Deep Sea Research*, 35(6), 891–898.

3174 Wing, S. R., Leichter, J. J., Wing, L. C., Stokes, D., Genovese, S. J., McMullin, R. M., & Shatova, O. A.
 3175 (2018). Contribution of sea ice microbial production to Antarctic benthic communities is driven by
 3176 sea ice dynamics and composition of functional guilds. *Global Change Biology*, 24(April), 3642–
 3177 3653. <https://doi.org/10.1111/gcb.14291>

3178 Włodarska-Kowalczyk, M., Górka, B., Deja, K., & Morata, N. (2016). Do benthic meiofaunal and
 3179 macrofaunal communities respond to seasonality in pelagial processes in an Arctic fjord
 3180 (Kongsfjorden, Spitsbergen)? *Polar Biology*, 39(11), 2115–2129. [https://doi.org/10.1007/s00300-](https://doi.org/10.1007/s00300-016-1982-2)
 3181 016-1982-2

3182 Włodarska-kowalczyk, M., Pearson, T. H., & Kendall, M. A. (2005). Benthic response to chronic natural
 3183 physical disturbance by glacial sedimentation in an Arctic fjord. *Marine Ecology Progress Series*,
 3184 303, 31–41.

3185 Zajaczkowski, M. (2008). Sediment supply and fluxes in glacial and outwash fjords, Kongsfjorden and
 3186 Adventfjorden, Svalbard. *Polish Polar Research*, 29(1), 59–72.

3187 Zhang, Q., Warwick, R. M., McNeill, C. L., Widdicombe, C. E., Sheehan, A., & Widdicombe, S. (2015). An
 3188 unusually large phytoplankton spring bloom drives rapid changes in benthic diversity and ecosystem
 3189 function. *Progress in Oceanography*, 137, 533–545. <https://doi.org/10.1016/j.pocean.2015.04.029>

3190 Zhu, Z. Y., Wu, Y., Liu, S. M., Wenger, F., Hu, J., Zhang, J., & Zhang, R. F. (2016). Organic carbon flux
 3191 and particulate organic matter composition in Arctic valley glaciers: Examples from the Bayelva
 3192 River and adjacent Kongsfjorden. *Biogeosciences*, 13(4), 975–987. [https://doi.org/10.5194/bg-13-](https://doi.org/10.5194/bg-13-975-2016)
 3193 975-2016

3194

Chapter V Conclusion: Community Structure and Function of West Antarctic Peninsula

Benthos

This dissertation research explored the influence of three environmental processes on benthic community structure and function within glaciomarine fjords of the West Antarctic Peninsula (WAP). As the glaciers within this ecosystem calve and melt, they produce buoyant, low-salinity water that can alter the circulation within the fjord and the exchange of water with the outer shelf. This meltwater also transports sediments across the continental shelf and affects phytoplankton growth. **Chapter II** tested the effect of habitat heterogeneity provided by glacial dropstones on community structure and diversity. Overall, dropstones contributed disproportionately to the regional WAP megafaunal species richness contributing an additional 20% of morphotypes while constituting < 1% of the total seafloor area surveyed. Many of the morphotypes associated with dropstones were hard substrate obligates (e.g. stalked tunicates, bryozoans) that require the dropstones for attachment and were predominantly suspension-feeders that benefit from settling higher in the water column to overcome flow limitations within the benthic boundary layer. These sessile organisms create three-dimensional habitat structure which further increases species richness by creating refugia for associated fauna (Lene Buhl-Mortensen et al. 2010; Cordes et al. 2010). This effect was observed repeatedly, for example, by the association of amphipods and stalked tunicates. The dropstones also provided important brooding habitat for the demersal fish *Chaenodraco wilsoni* which is a key predator of Antarctic benthic invertebrates. Though utilized by a variety of fauna, many of the dropstones observed in this study were partially or entirely devoid of fauna indicating that dropstone fauna were not space-limited, and that fjord circulation and water exchange between the fjord and open shelf is important in constraining dropstone colonization. The results of **Chapter II** not only support the habitat heterogeneity hypothesis as an important factor structuring WAP benthic communities but also disprove the assumption that WAP fjord communities represent a subset of the regional WAP species pool, emphasizing the importance of dropstones as a previously overlooked ecological component of the polar benthos providing a mechanism constraining dropstone colonization in this ecosystem.

If the glaciers within WAP fjords increase melting or retreating, it is likely that sedimentation rate of both fine-grained sediments and abundance of dropstones will increase. Research in Arctic glaciomarine fjords has shown that high sedimentation rates result in reduced benthic abundance, diversity and biomass (Włodarska-Kowalczyk et al. 2005, 2012). When WAP fjord sedimentation rates increase, the soft-sediment communities are likely to become more like Arctic glaciomarine fjord communities. Glacial retreat can also increase calving which produces icebergs which can transport dropstones across the continental shelf. Therefore, the abundance of dropstones may increase both in WAP fjords and on the open shelf. There is no evidence, however, that increased dropstone abundance would increase the abundance of dropstone organisms because they are not space limited. In addition, the burial rate of dropstones is likely to increase with an increase in sedimentation rate and, therefore, reduce the lifetime of a dropstone community. If dropstones are exposed on the seafloor for a shorter time, fewer larvae have the chance to settle on the dropstones and the communities will be kept in an earlier state of succession with reduced diversity.

Abundances of benthic megafauna have been observed to be 3-38 times greater inside WAP fjords compared to the outer shelf and body sizes of some taxa are substantially larger (Grange and Smith 2013). Thus, fjord populations are likely to contribute a substantial proportion of larvae to the regional larval pool. Though these fjords may be sources of larvae, previous comparisons of community structure between fjords found that each fjord harbored some unique fauna absent or in low abundances in other neighboring fjords suggesting limited connectivity between them. The goals of **Chapter III** were to test the hypothesis that WAP fjords are ecologically distinct with limited connectivity of benthic epifaunal larvae with a range of reproductive strategies, and to assess the role of fjords as sources of larvae both to neighboring fjords as well as the broader WAP shelf. The modeling efforts in **Chapter III** indicate that the fjords investigated (Andvord and Flandres Bays) are not significant sources of low dispersing larvae to neither neighboring fjords nor to the broader WAP shelf. In fact, no connectivity existed between these two fjords that were < 50 km apart, and no simulated larvae were transported out of the coastal region. The greatest proportion of larval settlement occurred within the same basin from which simulated larvae

3249 were released suggesting that self-recruitment is an important process maintaining fjord populations of
3250 fauna with low dispersal potential, especially within the inner basins of Andvord and Flandres Bays.
3251 These organisms include sessile fauna such as tunicates and sponges like those observed colonizing
3252 dropstones. The connectivity between individual dropstones warrants more in-depth research as these
3253 islands could function stepping-stones to connect distant populations of hard-substrate fauna and explain
3254 the ubiquity of hard-substrate fauna in habitats containing little dropstone area. Additionally, the fjord
3255 walls and sills are likely to be colonized by this fauna such that there is much more contiguous hard-
3256 substrate habitat than soft-sediment inside of fjords.

3257 Although settlement between fjords increased with increasing pre-competency period, even under
3258 conditions that maximized the chances of connectivity, < 3% of simulated larvae successfully settled in
3259 the neighboring fjord suggesting that Andvord and Flandres Bays are not significant larval sources for
3260 each other. Previous work has shown that Andvord Bay is quiescent and low energy with little freshwater
3261 input and weak estuarine circulation (Lundesgaard et al., in press). The greatest mixing and exchange
3262 between fjord waters and the outer Gerlache Strait occurred during a Katabatic wind event observed in
3263 December. Katabatic winds increased the export of larvae from the fjords (mainly Andvord Bay) and
3264 increased the proportion of larvae exported from the model domain reaching up to 30%. While little
3265 connectivity existed between fjords, Katabatic wind events may be disproportionately important for
3266 generating conditions that favor rarer long-range dispersal providing infrequent events necessary for
3267 maintaining connectivity even over large spatial scales.

3268 Ocean temperatures on the WAP shelf are predicted to increase by up to 2°C by 2099 (Griffiths et al.
3269 2017) and warmer ocean temperatures have been shown to accelerate glacial melt and retreat in this
3270 region (Cook et al. 2016). Glacial meltwater increases the buoyant layer of water in the fjord that can
3271 increase the vertical mixing of water as it rises to the surface and increase the exchange of surface
3272 waters due to estuarine circulation. Vertical mixing transports benthic larvae into surface layers that are
3273 more likely to be exported from the fjord by episodic Katabatic wind events and along the outer WAP shelf
3274 which is more energetic year-round. The findings of **Chapter III** confirm the hypothesis that WAP fjord

3275 benthic communities are limited by dispersal processes including the oceanographic and meteorological
3276 conditions that causes ecologically distinct populations over small spatial scales (< 100 km).

3277

3278 While Chapters II and III investigated environmental processes occurring at local and regional spatial
3279 scales, **Chapter IV** explored the response of the megafaunal community to *temporal* changes in food
3280 availability within a single fjord basin. Food availability constrains benthic faunal growth, reproduction,
3281 abundance, biomass, and a variety of ecosystem functions including the rates of bioturbation and carbon
3282 burial. The specific goals of **Chapter IV** were to quantify the food availability arriving on the seafloor of
3283 Andvord Bay and the processing of this organic matter by benthic fauna using time-lapse imagery. The
3284 time-lapse record revealed a very rapid deposition of phytodetritus in which a layer of organic matter
3285 approximately 3 cm thick accumulated on the seafloor in only 6 days. A predominant hypothesis
3286 regarding the rapid deposition of phytodetritus is particle aggregation facilitated by winds and this work
3287 tested whether the arrival of phytodetritus on the seafloor was correlated to overlying conditions including
3288 surface wind speed and sea ice concentration. The hypothesis that high winds enhanced particle
3289 aggregation and flux was not supported by the analyses in **Chapter IV**. The methodology developed in
3290 **Chapter IV** represents an extension of previous image analysis methods that has been adapted for use
3291 on oblique-angle, time-lapse imagery to quantify the arrival and consumption of seafloor phytodetritus.
3292 The method allowed for a detailed statistical comparison of small-scale seafloor areas revealing that
3293 sessile deposit-feeding polychaetes, *Amythas membranifera* (Ampharetidae), increased their feeding rate
3294 nearly 3-fold in response to the input of phytodetritus and consumed phytodetritus approximately three
3295 times faster than the infaunal community. Feeding by *A. membranifera* continued throughout the winter
3296 when the flux of organic matter was low and there was no visible phytodetritus on the seafloor indicating
3297 that the massive deposition of phytodetritus in the spring (January) produced a sediment food bank that
3298 supported the detritivores throughout the low-productive winter. These results suggest that the
3299 development of a sediment food bank is paramount to the maintenance of the abundant detritivore
3300 communities established within Andvord Bay and likely within other WAP fjords. This work provided

3301 robust data documenting how phytodetritus is utilized on the seafloor by the benthic community which is
3302 necessary if we are to forecast the effects of future climate change on these communities.

3303

3304 Climate change is predicted to generate conditions along the WAP favoring nanoplankton via either
3305 bottom-up effects in the physical environment (e.g. stratification, turbidity) or top-down effects from
3306 changes in food-web structure (Ducklow et al. 2012; Smith et al. 2012). Rising ocean and air
3307 temperatures increase meltwater input from glaciers, icebergs and sea ice which increases the
3308 stratification in the euphotic zone (Dierssen et al. 2002). Enhanced stratification can act to increase or
3309 decrease phytoplankton productivity; high stratification retains phytoplankton in favorable light conditions
3310 promoting growth but mixing across the pycnocline, and hence upward nutrient flux, is simultaneously
3311 reduced. Nano- and pico-plankton (e.g. cryptophytes) are favored under highly stratified conditions
3312 because they have a greater surface area:volume ratio, maintaining the uptake of nutrients when
3313 concentrations are low. Although increased meltwater input can also increase turbidity from glacial
3314 sediments and reduce light availability in the euphotic zone (Pan et al. 2019), cryptophytes are capable of
3315 maintaining high productivity in a suboptimal light fields, further promoting their dominance in areas of
3316 high meltwater input (e.g. glaciomarine fjords) (Mendes et al. 2018).

3317 Phytoplankton community composition directly impacts the grazing rate of zooplankton and their
3318 production of fecal pellets, which can provide efficient export of organic carbon to depth (Atkinson et al.
3319 2012; Belcher et al. 2017; Buesseler et al. 2007, 2010; Gleiber et al. 2012; Haberman et al. 2003; Ross et
3320 al. 2000; Steinberg et al. 2012; Steinberg and Landry 2017; Steinberg et al. 2012). Increased abundances
3321 of cryptophytes and other nanoplankton expected in the future will reduce the availability of diatoms, the
3322 preferred food of Antarctic krill, which produce fast-sinking fecal pellets (Haberman et al. 2003; Ross et al.
3323 2000). Mesozooplankton such as copepods, or less-selective feeders such as salps, are better adapted
3324 to exploit nano- and pico-plankton and could outcompete krill if diatom biomass is reduced (Atkinson et al.
3325 2004; Loeb et al. 1997; Pakhomov et al. 2002). The addition of microzooplankton as an intermediate
3326 trophic step between phytoplankton and krill lengthens the typically short Antarctic pelagic food web and

3327 reduces the efficiency of carbon transport to the seafloor and to higher trophic levels dependent on krill
 3328 (Trivelpiece et al. 2011).

3329 Reduced export efficiency of organic matter from the euphotic zone would directly limit the magnitude of
 3330 organic matter reaching the seafloor. As observed in this study, the flux of organic matter must be higher
 3331 than benthic consumption over days to weeks for a sediment food bank to develop. If the phenology of
 3332 phytoplankton blooms on the WAP changes such that pulsed accumulation events are replaced by a
 3333 steady rain of organic matter throughout the production season, food banks may no longer develop. The
 3334 timescale over which a food bank forms is much shorter than the time over which it supports benthic
 3335 detritivores. For example, the rapid sedimentation event in this study lasted approximately 6 days, yet we
 3336 observed elevated sediment chlorophyll concentrations (an indicator of labile organic matter) and
 3337 elevated sediment community respiration rates within Andvord Bay months after the phytodetrital pulse to
 3338 the seafloor (Smith et al. 2018). Because of this time lag, food banks are buffered from perturbations in
 3339 overlying phytoplankton productivity and, like other detritus-based food webs, deposit-feeder
 3340 assemblages in Andvord Bay may be stabilized by sustained detrital food availability (Moore et al. 2004).
 3341 In addition, detritus-based communities typically have high redundancy of functional groups (e.g. deposit-
 3342 feeders) and short food webs which further increase resilience and stability (Levin et al. 2001; Pimm
 3343 1982). If climate warming reduces the formation of a food bank, detritivore populations may become less
 3344 stable and more food-limited during winter months, yielding decreased growth, abundance, biomass and
 3345 reproductive output (Górska and Włodarska-Kowalczyk 2017; Linton and Taghon 2000b, 2000a;
 3346 Mazurkiewicz et al. 2019; Smith et al. 2008; Włodarska-Kowalczyk et al. 2016) as well as reducing
 3347 sediment community respiration rates (Amaro et al. 2015; Pfannkuche 1993; Renaud et al. 2007; Smith et
 3348 al. 2008; Smith et al. 1994; Sumida et al. 2014; Veit-Köhler et al. 2011; Vetter and Dayton 1999).
 3349 Ultimately, the structure and activity of the infaunal community controls the rates of important ecosystem
 3350 functions such as bioturbation and organic matter remineralization (Norling et al. 2007; Queirós et al.
 3351 2015; Smith et al. 2008; Zhang et al. 2015).

3352 In our study, phytodetritus was consumed where it landed on the seafloor as there was little evidence of
 3353 lateral movement post-settlement. *Amythas membranifera* occupied 27-69 % of the seafloor area, and

3354 therefore, we estimate 31-73 % of the seafloor phytodetritus entered the benthic food web through the
3355 activities macro-, meio-fauna and microbes not visible in our photographs within the control regions of
3356 sediment. This is a substantial proportion of the benthic food supply which supports a high abundance
3357 and diversity of detritivores which may decline if future conditions alter the formation of a sediment food
3358 bank in this region.

3359

3360 Predicted warming-driven shifts in phytoplankton and zooplankton community structure have the potential
3361 to alter the nutrient content of organic matter arriving at the seafloor along the WAP. Antarctic krill have
3362 been shown to preferentially absorb more nitrogen from phytoplankton than other zooplankton which
3363 increases the C:N ratio of their fecal pellets (Atkinson et al. 2012). Future lengthening of the pelagic food
3364 web (as explained above) would further increase the C:N ratio of organic matter reaching the seafloor
3365 (Tenore 1988). Reduced availability of high-quality organic compounds, such as essential fatty acids
3366 (EFA), could be detrimental to benthic consumers. In the Arctic, some deposit feeders preferentially
3367 consume ice algae (i.e. diatom) detritus, likely due to higher EFA content relative to other phytoplankton
3368 (McMahon et al. 2006; Stead et al. 2013). In zooplankton, a diet enriched in polyunsaturated fatty acids
3369 (PUFAs) can increase reproductive success (Kohlbach et al. 2018; Vargas et al. 2006). The early delivery
3370 of ice algae to Arctic benthos represents a high-quality food source providing energy required for growth
3371 and reproduction which may not be met if the composition of phytodetritus input changes (McMahon et al.
3372 2006; Morata, Michaud, and Włodarska-Kowalczyk 2013). Deposit feeders in the Antarctic are likely to
3373 respond similarly to reduced diatom detritus as these organisms also require a dietary source of essential
3374 fatty acids for growth and reproduction (Parrish 2013) and enhanced PUFA content has been
3375 documented in Antarctic diatoms (Thomas and Dieckmann 2002; Torstensson et al. 2013).

3376 Sessile deposit-feeders currently dominate the megabenthos in Andvord Bay (Grange and Smith 2013)
3377 but suspension feeders may become more successful if sinking organic matter becomes dominated by
3378 small detrital particles. In the Arctic, changing bloom phenology has considerably reduced benthic
3379 macrofaunal biomass and affected higher trophic levels (Grebmeier et al. 2006; Renaud et al. 2015).
3380 Sessile fauna, especially suspension feeders, are particularly sensitive to changes in turbidity. The

delivery of fine grained sediments via glacial meltwater can disturb benthic communities by burial and clogging of suspension feeding structures (Wlodarska-kowalczyk et al. 2005). In Potter Cove (King George Island), ascidian feeding and respiration rates declined over time in response to increased turbidity from glacial melt and retreat, leading to a shift in the community with decreasing dominance by suspension-feeding ascidians (Moon et al. 2015; Sahade et al. 2015; Torre et al. 2012). In McMurdo Sound, suspension feeder recruitment and growth dramatically increased as a result of unusually abundant pico- and bacterio-plankton during a prolonged iceberg jam (Dayton et al. 2019). In McMurdo Sound, 39-71 % of the sediment community biomass is supported by organic matter from the sea-ice microbial community alone (Wing et al. 2018). At present, meltwater input and turbidity are low in the inner and middle basins Andvord Bay ($< 10 \text{ mg L}^{-1}$) relative to other high-latitude fjords (Arendt et al. 2011; Pan et al. 2019; Zajaczkowski 2008; Zhu et al. 2016, Lundesgaard et al., in press). In the future, glacial sedimentation will further dilute the rain of organic matter to the Andvord Bay benthos and when coupled with the selectivity of deposit-feeders for small particles and potentially depleted nutrient content of sinking organic matter, this could reduce nutrient absorption efficiency and the energy gained per unit feeding effort (i.e. deposit feeders will expend more energy to obtain organic matter at a comparable rate to the present) (Purinton et al. 2008). This could have long-term effects on the size structure of the benthic community supporting smaller deposit-feeders that selectively feed on smaller particles and suspension feeders that are more successful at exploiting small particles, and potentially reduce benthic biomass.

This dissertation research produced significant contributions to the understanding of how the structure and function of glaciomarine fjord benthic communities are shaped by environmental drivers including habitat heterogeneity, dispersal and food availability. Each of the studies presented would benefit from additional data collection. In **Chapter II** additional photographic surveys within the Gerlache Strait could aid in identifying stepping-stone populations hypothesized to exist, and characterize community structure patterns along the WAP shelf (i.e. rather than onshore-offshore comparison) that could be used to generate substrate maps for habitat suitability of different benthic taxa. Studies, such as **Chapter II**, rely

on generalized feeding guild assignments (or functional group) which are not well defined for most Antarctic species. Additional diet and behavior information (e.g. from stable isotopes) would help to constrain the feeding guilds assigned to fauna *a priori*. As many benthic consumers are generalists, assignment to a single feeding guild such as “detritivore” may not resolve their true ecological role. The modeling efforts presented in **Chapter III** would greatly benefit from more detailed assessments of larval parameters for benthic invertebrates including fecundity, larval development times and larval durations. Data that exist do not cover a wide diversity of organisms because some taxonomic groups are more conducive to lab-based husbandry than others, especially under realistic Antarctic conditions over developmental timescales of several months. With better constrained parameterization of the biological components of dispersal, model results will continue to become more advanced, realistic and ecologically informative. To better predict dispersal changes under future climate conditions would require continued efforts to collect high-resolution hydrographic and meteorological data along the WAP or other areas of interest within the Antarctic. A major gap of knowledge, for example, is the circulation along glacial fronts which could be important sites of buoyancy-driven mixing from subglacial discharge of meltwater. This process could greatly affect fjord circulation in future if the input of freshwater increases, particularly within inner basins which experienced the lowest dispersal in model simulations. Finer temporal resolution would also be beneficial as this work demonstrated the great impact that short-duration events, such as Katabatic winds, can have on both the surface ocean circulation and cascading effects to other components of the ecosystem. It would be interesting to combine the efforts of **Chapters II** and **III** to understand the dispersal, colonization and maintenance of glaciomarine fjord hard-substrate communities, specifically. To do so, deployment and monitoring of artificial dropstones or other hard settlement substrates could provide time series information of colonization and post-settlement processes. Photographic surveys of the sills and exploration of fjord wall communities could provide information about other potential larval sources which have been unaccounted for in the study presented here. Finally, the analyses in **Chapter IV** would benefit greatly from concurrent measurements of organic carbon flux via sediment traps. The methodology developed in chapter IV provides a robust relative measure of phytodetritus cover but a more quantitative measure of the organic carbon mass flux would allow more accurate quantification of carbon processing or calibration of the method. The camera

mooring utilized could also have been outfitted with additional turbidity, T, S, O₂, ADCP sensors which would have provided additional context to the conditions of the seafloor throughout the entire time series. Synthesis of the data presented here with respiration incubation data (A. Sweetman, unpub. data) would provide further insights into the contributions of the infauna vs epifauna to organic carbon and nutrient recycling. The use of linear inverse modeling (LIM) with these combined data sets could generate an overall carbon flow model for the fjord (van Oevelen et al. 2006) which would be useful to compare under predicted future climate conditions as well as to carbon flow models of other high-latitude fjord ecosystems. Ultimately, these improvements would help to resolve the relationships explored in this dissertation and better quantify the role of glaciomarine fjords of the West Antarctic Peninsula in the broader Antarctic marine ecosystem.

References

Amaro, Teresa, Henko de Stigter, Marc Lavaleye, and Gerard Duineveld. 2015. "Organic Matter Enrichment in the Whittard Channel; Its Origin and Possible Effects on Benthic Megafauna." *Deep-Sea Research Part I: Oceanographic Research Papers* 102 (May): 90–100.
<https://doi.org/10.1016/j.dsr.2015.04.014>.

Arendt, Kristine Engel, Jörg Dutz, Sigrún Huld Jónasdóttir, Signe Jung-Madsen, John Mortensen, Eva Friis Møller, and Torkel Gissel Nielsen. 2011. "Effects of Suspended Sediments on Copepods Feeding in a Glacial Influenced Sub-Arctic Fjord." *Journal of Plankton Research* 33 (10): 1526–37.
<https://doi.org/10.1093/plankt/fbr054>.

Atkinson, A., K. Schmidt, S. Fielding, S. Kawaguchi, and P. A. Geissler. 2012. "Variable Food Absorption by Antarctic Krill: Relationships between Diet, Egestion Rate and the Composition and Sinking Rates of Their Fecal Pellets." *Deep-Sea Research Part II: Topical Studies in Oceanography* 59–60: 147–58. <https://doi.org/10.1016/j.dsr2.2011.06.008>.

Atkinson, Angus, Volker Siegel, Evgeny Pakhomov, and Peter Rothery. 2004. "Long-Term Decline in Krill Stock and Increase in Salps within the Southern Ocean." *Nature* 432: 100–103.

3462 <https://doi.org/10.1038/nature02950.1>.

3463 Belcher, A, G A Tarling C Manno, and A Atkinson P Ward. 2017. "The Potential Role of Antarctic Krill
3464 Faecal Pellets in Efficient Carbon Export at the Marginal Ice Zone of the South Orkney Islands in
3465 Spring." *Polar Biology* 40: 2001–13. <https://doi.org/10.1007/s00300-017-2118-z>.

3466 Buesseler, Ken O., Andrew M.P. McDonnell, Oscar M.E. Schofield, Deborah K. Steinberg, and Hugh W.
3467 Ducklow. 2010. "High Particle Export over the Continental Shelf of the West Antarctic Peninsula."
3468 *Geophysical Research Letters* 37 (22): 1–5. <https://doi.org/10.1029/2010GL045448>.

3469 Buesseler, Ken O, Carl H Lamborg, Philip W Boyd, Phoebe J Lam, Thomas W Trull, Robert R Bidigare,
3470 James K B Bishop, et al. 2007. "Revisiting Carbon Flux through the Ocean's Twilight Zone." *Science*
3471 316 (April): 567–70. <https://doi.org/10.1126/science.1137959>.

3472 Buhl-Mortensen, Lene, Ann Vanreusel, Andrew J. Gooday, Lisa A. Levin, Imants G. Priede, Pål Buhl-
3473 Mortensen, Hendrik Gheerardyn, Nicola J. King, and Maarten Raes. 2010. "Biological Structures as
3474 a Source of Habitat Heterogeneity and Biodiversity on the Deep Ocean Margins." *Marine Ecology* 31
3475 (1): 21–50. <https://doi.org/10.1111/j.1439-0485.2010.00359.x>.

3476 Cordes, Erik E., Marina R. Cunha, Joëlle Galéron, Camilo Mora, Karine Olu-Le Roy, Myriam Sibuet,
3477 Saskia Van Gaever, Ann Vanreusel, and Lisa A. Levin. 2010. "The Influence of Geological,
3478 Geochemical, and Biogenic Habitat Heterogeneity on Seep Biodiversity." *Marine Ecology* 31 (1):
3479 51–65. <https://doi.org/10.1111/j.1439-0485.2009.00334.x>.

3480 Dayton, Paul K., Shannon C. Jarrell, Stacy Kim, P. Ed Parnell, Simon F. Thrush, Kamille Hammerstrom,
3481 and James J. Leichter. 2019. "Benthic Responses to an Antarctic Regime Shift : Food Particle Size
3482 and Recruitment Biology." *Ecological Applications* 29 (1): 1–20. <https://doi.org/10.1002/eap.1823>.

3483 Dierssen, Heidi M, Raymond C Smith, and Maria Vernet. 2002. "Glacial Meltwater Dynamics in Coastal
3484 Waters West of the Antarctic Peninsula" 99 (4).

3485 Ducklow, Hugh, Andrew Clarke, Rebecca Dickhut, Scott C. Doney, Heidi Geisz, Kuan Huang, Douglas G.
3486 Martinson, et al. 2012. "The Marine System of the Western Antarctic Peninsula." *Antarctic*

3487 *Ecosystems: An Extreme Environment in a Changing World*, 121–59.

3488 <https://doi.org/10.1002/9781444347241.ch5>.

3489 Gleiber, Miram R., Deborah K. Steinberg, and Hugh W. Ducklow. 2012. “Time Series of Vertical Flux of

3490 Zooplankton Fecal Pellets on the Continental Shelf of the Western Antarctic Peninsula.” *Marine*

3491 *Ecology Progress Series* 471: 23–36. <https://doi.org/10.3354/meps10021>.

3492 Górská, Barbara, and Maria Włodarska-Kowalczyk. 2017. “Food and Disturbance Effects on Arctic

3493 Benthic Biomass and Production Size Spectra.” *Progress in Oceanography* 152: 50–61.

3494 <https://doi.org/10.1016/j.pocean.2017.02.005>.

3495 Grange, Laura J., and Craig R. Smith. 2013. “Megafaunal Communities in Rapidly Warming Fjords along

3496 the West Antarctic Peninsula: Hotspots of Abundance and Beta Diversity.” *PLoS ONE* 8 (12).

3497 <https://doi.org/10.1371/journal.pone.0077917>.

3498 Grebmeier, Jacqueline M., James E. Overland, Sue E. Moore, Ed V. Farley, Eddy C. Carmack, Lee W.

3499 Cooper, Karen E. Frey, John H. Helle, Fiona A. McLaughlin, and S. Lyn McNutt. 2006. “A Major

3500 Ecosystem Shift in the Northern Bering Sea.” *Science* 311 (5766): 1461–64.

3501 <https://doi.org/10.1126/science.1121365>.

3502 Haberman, Karen L, Robin M Ross, and Langdon B Quetin. 2003. “Diet of the Antarctic Krill (*Euphausia*

3503 *Superba Dana*): II . Selective Grazing in Mixed Phytoplankton Assemblages” 283: 97–113.

3504 Kohlbach, Doreen, Martin Graeve, Benjamin A. Lange, Carmen David, Fokje L. Schaafsma, Jan Andries

3505 van Franeker, Martina Vorkamp, Angelika Brandt, and Hauke Flores. 2018. “Dependency of

3506 Antarctic Zooplankton Species on Ice Algae-Produced Carbon Suggests a Sea Ice-Driven Pelagic

3507 Ecosystem during Winter.” *Global Change Biology* 24 (10): 4667–81.

3508 <https://doi.org/10.1111/gcb.14392>.

3509 Levin, Lisa A., Donald F. Boesch, Alan Covich, Cliff Dahm, Christer Erséus, Katherine C. Ewel, Ronald T.

3510 Kneib, et al. 2001. “The Function of Marine Critical Transition Zones and the Importance of

3511 Sediment Biodiversity.” *Ecosystems* 4 (5): 430–51. <https://doi.org/10.1007/s10021-001-0021-4>.

- 3512 Linton, Debra L., and Gary L. Taghon. 2000a. "Feeding, Growth, and Fecundity of *Abarenicola Pacifica* in
3513 Relation to Sediment Organic Concentration." *Journal of Experimental Marine Biology and Ecology*
3514 254: 85–107.
- 3515 Linton, Debra L., and Gary L. Taghon. 2000b. "Feeding, Growth, and Fecundity of *Capitella* Sp. I in
3516 Relation to Sediment Organic Concentration." *Marine Ecology Progress Series* 205: 229–40.
3517 <https://doi.org/10.3354/meps205229>.
- 3518 Loeb, V., V. Siegel, O. Holm-Hansen, R. Hewitt, W. Fraser, W. Trivelpiece, and S. Trivelpiece. 1997.
3519 "Effects of Sea-Ice Extent and Krill or Salp Dominance on the Antarctic Food Web." *Nature* 387
3520 (6636): 897–900. <https://doi.org/10.1038/43174>.
- 3521 Mazurkiewicz, Mikołaj, Barbara Górska, Paul E. Renaud, Joanna Legeżyńska, Jørgen Berge, and Maria
3522 Włodarska-Kowalczyk. 2019. "Seasonal Constancy (Summer vs. Winter) of Benthic Size Spectra in
3523 an Arctic Fjord." *Polar Biology* 42 (7): 1255–70. <https://doi.org/10.1007/s00300-019-02515-2>.
- 3524 McMahon, Kelton W., William G. Ambrose, Beverly J. Johnson, Ming Yi Sun, Glenn R. Lopez, Lisa M.
3525 Clough, and Michael L. Carroll. 2006. "Benthic Community Response to Ice Algae and
3526 Phytoplankton in Ny Ålesund, Svalbard." *Marine Ecology Progress Series* 310 (Hsiao 1992): 1–14.
3527 <https://doi.org/10.3354/meps310001>.
- 3528 Mendes, Carlos Rafael Borges, Virginia Maria Tavano, Tiago Segabinazzi Dotto, Rodrigo Kerr, Marcio
3529 Silva de Souza, Carlos Alberto Eiras Garcia, and Eduardo Resende Secchi. 2018. "New Insights on
3530 the Dominance of Cryptophytes in Antarctic Coastal Waters: A Case Study in Gerlache Strait."
3531 *Deep-Sea Research Part II* 149: 161–70. <https://doi.org/10.1016/j.dsr2.2017.02.010>.
- 3532 Moon, Hye Won, Wan Mohd Rauhan Wan Hussin, Hyun Cheol Kim, and In Young Ahn. 2015. "The
3533 Impacts of Climate Change on Antarctic Nearshore Mega-Epifaunal Benthic Assemblages in a
3534 Glacial Fjord on King George Island: Responses and Implications." *Ecological Indicators* 57: 280–
3535 92. <https://doi.org/10.1016/j.ecolind.2015.04.031>.
- 3536 Moore, John C., Eric L. Berlow, David C. Coleman, Peter C. De Suiter, Quan Dong, Alan Hastings, Nancy
3537 Collins Johnson, et al. 2004. "Detritus, Trophic Dynamics and Biodiversity." *Ecology Letters* 7 (7):

3538 584–600. <https://doi.org/10.1111/j.1461-0248.2004.00606.x>.

3539 Morata, Nathalie, Emma Michaud, and Maria Włodarska-Kowalczyk. 2013. “Impact of Early Food Input on
3540 the Arctic Benthos Activities during the Polar Night.” *Polar Biology* 38 (1): 99–114.
3541 <https://doi.org/10.1007/s00300-013-1414-5>.

3542 Norling, K., R. Rosenberg, S. Hulth, A. Gremare, and E. Bonsdorff. 2007. “Importance of Functional
3543 Biodiversity and Species-Specific Traits of Benthic Fauna for Ecosystem Functions in Marine
3544 Sediment.” *Marine Ecology Progress Series* 332: 11–23. <https://doi.org/10.3354/meps332011>.

3545 Oevelen, Dick van, Karline Soetaert, Jack J. Middelburg, Peter M. J. Herman, Leon Moodley, Ilse
3546 Hamels, Tom Moens, and Carlo H. R. Heip. 2006. “Carbon Flows through a Benthic Food Web:
3547 Integrating Biomass, Isotope and Tracer Data.” *Journal of Marine Research* 64 (3): 453–82.
3548 <https://doi.org/10.1357/002224006778189581>.

3549 Pakhomov, E. A., P. W. Froneman, and R. Perissinotto. 2002. “Salp/Krill Interactions in the Southern
3550 Ocean: Spatial Segregation and Implications for the Carbon Flux.” *Deep-Sea Research Part II:
3551 Topical Studies in Oceanography* 49 (9–10): 1881–1907. [https://doi.org/10.1016/S0967-](https://doi.org/10.1016/S0967-0645(02)00017-6)
3552 [0645\(02\)00017-6](https://doi.org/10.1016/S0967-0645(02)00017-6).

3553 Pan, B. Jack, Maria Vernet, Rick A. Reynolds, and B. Greg Mitchell. 2019. “The Optical and Biological
3554 Properties of Glacial Meltwater in an Antarctic Fjord.” *PLoS ONE* 14 (2): 1–30.
3555 <https://doi.org/10.1371/journal.pone.0211107>.

3556 Parrish, Christopher C. 2013. “Lipids in Marine Ecosystems.” *ISRN Oceanography* 2013: 1–16.
3557 <https://doi.org/10.5402/2013/604045>.

3558 Pfannkuche, O. 1993. “Benthic Response to the Sedimentation of Particulate Organic Matter at the
3559 BIOTRANS Station, 47N, 20W.” *Deep-Sea Research II* 40 (1/2): 135–49.

3560 Pimm, Stuart L. 1982. *Food Webs*. Edited by M.B Usher and M.L Rosenzweig. Chapman and Hall.

3561 Purinton, Brett L., David J. DeMaster, Carrie J. Thomas, and Craig R. Smith. 2008. “¹⁴C as a Tracer of
3562 Labile Organic Matter in Antarctic Benthic Food Webs.” *Deep-Sea Research Part II: Topical Studies*

3563 *in Oceanography* 55 (22–23): 2438–50. <https://doi.org/10.1016/j.dsr2.2008.06.004>.

3564 Queirós, Ana M., Nicholas Stephens, Richard Cook, Chiara Ravaglioli, Joana Nunes, Sarah Dashfield,
3565 Carolyn Harris, et al. 2015. “Can Benthic Community Structure Be Used to Predict the Process of
3566 Bioturbation in Real Ecosystems?” *Progress in Oceanography* 137: 559–69.
3567 <https://doi.org/10.1016/j.pocean.2015.04.027>.

3568 Renaud, Paul E., Andrea Riedel, Christine Michel, Nathalie Morata, Michel Gosselin, Thomas Juul-
3569 Pedersen, and Amy Chiuchiolo. 2007. “Seasonal Variation in Benthic Community Oxygen Demand:
3570 A Response to an Ice Algal Bloom in the Beaufort Sea, Canadian Arctic?” *Journal of Marine*
3571 *Systems* 67 (1–2): 1–12. <https://doi.org/10.1016/j.jmarsys.2006.07.006>.

3572 Renaud, Paul E., Mikael K. Sejr, Bodil A. Bluhm, Boris Sirenko, and Ingrid H. Ellingsen. 2015. “The
3573 Future of Arctic Benthos: Expansion, Invasion, and Biodiversity.” *Progress in Oceanography* 139:
3574 244–57. <https://doi.org/10.1016/j.pocean.2015.07.007>.

3575 Ross, Robin M., Langdon B. Quetin, Karen S. Baker, Maria Vernet, and Raymond C. Smith. 2000.
3576 “Growth Limitation in Young Euphausia Superba under Field Conditions.” *Limnology and*
3577 *Oceanography* 45 (1): 31–43. <https://doi.org/10.4319/lo.2000.45.1.0031>.

3578 Sahade, Ricardo, Cristian Lager, Luciana Torre, Fernando Momo, Patrick Monien, Irene Schloss, David
3579 K.A. Barnes, et al. 2015. “Climate Change and Glacier Retreat Drive Shifts in an Antarctic Benthic
3580 Ecosystem.” *Science Advances* 1 (10). <https://doi.org/10.1126/sciadv.1500050>.

3581 Smith, Craig, David DeMaster, Carrie Thomas, Pavica Srsen, Laura Grange, Victor Evrard, and Fabio
3582 DeLeo. 2012. “Pelagic-Benthic Coupling, Food Banks, and Climate Change on the West Antarctic
3583 Peninsula Shelf.” *Oceanography* 25 (3): 188–201. <https://doi.org/10.5670/oceanog.2012.94>.

3584 Smith, Craig R., Fabio C. De Leo, Angelo F. Bernardino, Andrew K. Sweetman, and Pedro Martinez
3585 Arbizu. 2008. “Abyssal Food Limitation, Ecosystem Structure and Climate Change.” *Trends in*
3586 *Ecology and Evolution* 23 (9): 518–28. <https://doi.org/10.1016/j.tree.2008.05.002>.

3587 Smith, Craig R., Andrew K. Sweetman, Clifton Charles Nunnally, McKenna Lewis, Maria Vernet, Lindsey

3588 Ekern, and Amanda Ziegler. 2018. "Benthic Ecosystem Studies in a Rapidly Warming Antarctic
3589 Fjord Reveal High Export Flux and Benthic Abundance Very Near Tidewater Glaciers , Indicating
3590 High Sensitivity to Climate Warming." In *AGU Ocean Sciences Meeting Abstracts*.

3591 Smith, K.L., R.S. Kaufmann, and R.J. Baldwin. 1994. "Coupling of Near-bottom Pelagic and Benthic
3592 Processes at Abyssal Depths in the Eastern North Pacific Ocean." *Limnology and Oceanography* 39
3593 (5): 1101–18. <https://doi.org/10.4319/lo.1994.39.5.1101>.

3594 Stead, R. A., N. B. Richoux, S. V. Pereda, and R. J. Thompson. 2013. "Influence of an Intermittent Food
3595 Supply on Energy Storage by the Subpolar Deposit Feeder *Yoldia Hyperborea* (Bivalvia:
3596 Nuculanidae)." *Polar Biology* 36 (9): 1333–45. <https://doi.org/10.1007/s00300-013-1353-1>.

3597 Steinberg, D.K., D.G. Martinson, and D.P. Costa. 2012. "Two Decades of Pelagic Ecology of the Western
3598 Antarctic Peninsula." *Oceanography* 25 (3): 56–67. <https://doi.org/10.5670/oceanog.2011.65>.

3599 Steinberg, Deborah K, and Michael R Landry. 2017. "Zooplankton and the Ocean Carbon Cycle." *Annual*
3600 *Review of Marine Science* 9: 413–44. <https://doi.org/10.1146/annurev-marine-010814-015924>.

3601 Steinberg, Deborah K, Michael W Lomas, and Joseph S Cope. 2012. "Long-Term Increase in
3602 Mesozooplankton Biomass in the Sargasso Sea : Linkage to Climate and Implications for Food Web
3603 Dynamics and Biogeochemical Cycling." *Global Biogeochemical Cycles* 26: 1–16.
3604 <https://doi.org/10.1029/2010GB004026>.

3605 Sumida, P. Y.G., C. R. Smith, A. F. Bernardino, P. S. Polito, and D. R. Vieira. 2014. "Seasonal Dynamics
3606 of Megafauna on the Deep West Antarctic Peninsula Shelf in Response to Variable Phytodetrital
3607 Influx." *Royal Society Open Science* 1 (3). <https://doi.org/10.1098/rsos.140294>.

3608 Tenore, Kenneth R. 1988. "Nitrogen in Benthic Food Chain." *Nitrogen Cycling in Coastal Marine*
3609 *Environment*, 191–206. <https://doi.org/10.5651/jaas.9.123>.

3610 Thomas, D N, and G S Dieckmann. 2002. "Antarctic Sea Ice—a Habitat for Extremophiles." *Science* 295
3611 (January): 641–44.
3612 http://webmail.img.usap.gov/?_task=mail&_framed=1&_action=get&_mbox=INBOX&_uid=118&_par

3613 t=2&_frame=1%0Apapers3://publication/uuid/139C9382-4FDC-40EE-8B0C-830415E0C3C3.

3614 Torre, Luciana, Natalia Servetto, Matias Leonel Eöry, Fernando Momo, Marcos Tatián, Doris Abele, and
3615 Ricardo Sahade. 2012. "Respiratory Responses of Three Antarctic Ascidians and a Sea Pen to
3616 Increased Sediment Concentrations." *Polar Biology* 35 (11): 1743–48.
3617 <https://doi.org/10.1007/s00300-012-1208-1>.

3618 Torstensson, A., M. Hedblom, J. Andersson, M. X. Andersson, and A. Wulff. 2013. "Synergism between
3619 Elevated PCO₂ and Temperature on the Antarctic Sea Ice Diatom *Nitzschia Lecointei*."
3620 *Biogeosciences* 10 (10): 6391–6401. <https://doi.org/10.5194/bg-10-6391-2013>.

3621 Trivelpiece, W. Z., J. T. Hinke, A. K. Miller, C. S. Reiss, S. G. Trivelpiece, and G. M. Watters. 2011.
3622 "Variability in Krill Biomass Links Harvesting and Climate Warming to Penguin Population Changes
3623 in Antarctica." *Proceedings of the National Academy of Sciences* 108 (18): 7625–28.
3624 <https://doi.org/10.1073/pnas.1016560108>.

3625 Vargas, Christian, Ruben Escribano, and Serge Poulet. 2006. "Phytoplankton Food Quality Determines
3626 Time-Windows for Successful Zooplankton Reproductive Pulses." *Ecology* 87 (12): 2992–99.

3627 Veit-Köhler, Gritta, Katja Guilini, Ilka Peeken, Oliver Sachs, Eberhard J. Sauter, and Laura Würzberg.
3628 2011. "Antarctic Deep-Sea Meiofauna and Bacteria React to the Deposition of Particulate Organic
3629 Matter after a Phytoplankton Bloom." *Deep-Sea Research Part II: Topical Studies in Oceanography*
3630 58 (19–20): 1983–95. <https://doi.org/10.1016/j.dsr2.2011.05.008>.

3631 Vetter, E. W., and P. K. Dayton. 1999. "Organic Enrichment by Macrophyte Detritus, and Abundance
3632 Patterns of Megafaunal Populations in Submarine Canyons." *Marine Ecology Progress Series* 186:
3633 137–48. <https://doi.org/10.3354/meps186137>.

3634 Wing, Stephen R, James J Leichter, Lucy C Wing, Dale Stokes, Sal J Genovese, Rebecca M McMullin,
3635 and Olya A Shatova. 2018. "Contribution of Sea Ice Microbial Production to Antarctic Benthic
3636 Communities Is Driven by Sea Ice Dynamics and Composition of Functional Guilds." *Global Change
3637 Biology* 24 (April): 3642–53. <https://doi.org/10.1111/gcb.14291>.

3638 Włodarska-Kowalczyk, Maria, Barbara Górka, Kajetan Deja, and Nathalie Morata. 2016. "Do Benthic
 3639 Meiofaunal and Macrofaunal Communities Respond to Seasonality in Pelagic Processes in an
 3640 Arctic Fjord (Kongsfjorden, Spitsbergen)?" *Polar Biology* 39 (11): 2115–29.
 3641 <https://doi.org/10.1007/s00300-016-1982-2>.

3642 Włodarska-kowalczyk, Maria, Thomas H Pearson, and Michael A Kendall. 2005. "Benthic Response to
 3643 Chronic Natural Physical Disturbance by Glacial Sedimentation in an Arctic Fjord." *Marine Ecology
 3644 Progress Series* 303: 31–41.

3645 Zajackowski, Marek. 2008. "Sediment Supply and Fluxes in Glacial and Outwash Fjords, Kongsfjorden
 3646 and Adventfjorden, Svalbard." *Polish Polar Research* 29 (1): 59–72.

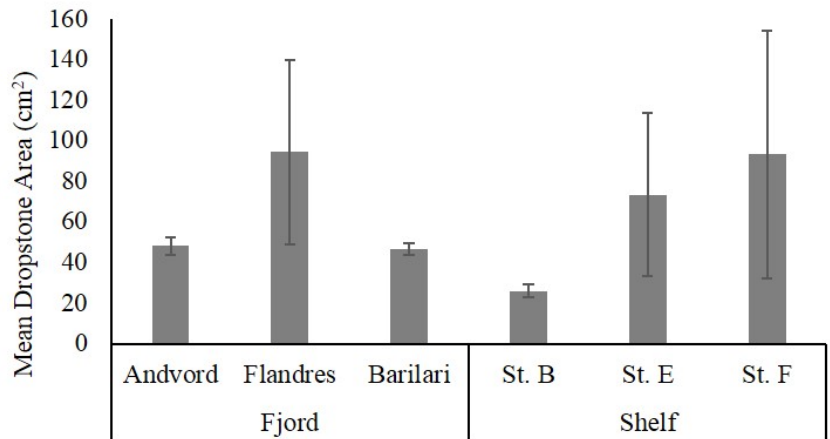
3647 Zhang, Qingtian, Richard M. Warwick, Caroline L. McNeill, Claire E. Widdicombe, Aaron Sheehan, and
 3648 Stephen Widdicombe. 2015. "An Unusually Large Phytoplankton Spring Bloom Drives Rapid
 3649 Changes in Benthic Diversity and Ecosystem Function." *Progress in Oceanography* 137: 533–45.
 3650 <https://doi.org/10.1016/j.pocean.2015.04.029>.

3651 Zhu, Zhuo Yi, Ying Wu, Su Mei Liu, Fred Wenger, Jun Hu, Jing Zhang, and Rui Feng Zhang. 2016.
 3652 "Organic Carbon Flux and Particulate Organic Matter Composition in Arctic Valley Glaciers: Examples
 3653 from the Bayelva River and Adjacent Kongsfjorden." *Biogeosciences* 13 (4): 975–87.
 3654 <https://doi.org/10.5194/bg-13-975-2016>.

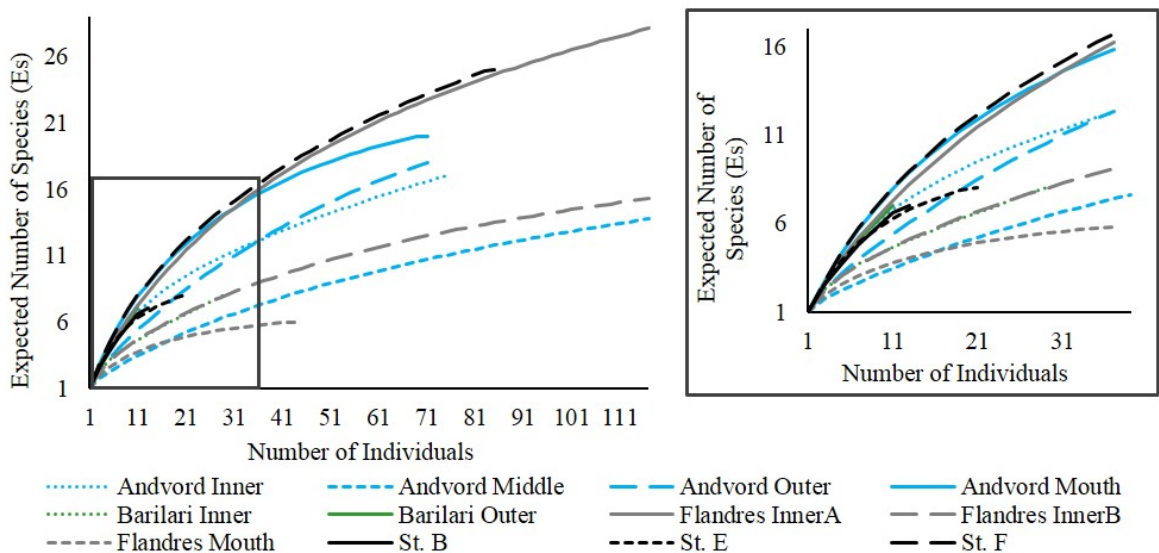
3655
 3656
 3657

Appendix: Supplementary Material

Supplementary material for Chapter II:



Supplementary Figure 2.1 Mean dropstone area (cm²) by sampling site. Error bars provide 95 % confidence intervals.



Supplementary Figure 2.2 Rarefaction curves for each sampling site showing the expected number of species across sampled individuals. Note that shelf stations B, E and F as well as Barilari Inner basin have < 30 individuals. The enlarged area (right) shows the trajectories of each curve when sampling < 30 individuals.

3673 **Supplementary Table 2.1** Sampling site positions (decimal degrees) and average bottom depths (m).

Site	Latitude (°S)	Longitude (°W)	Depth (m)
Andvord Bay	64.838	62.630	671
Inner	64.860	62.562	525
Middle	64.820	62.655	437
Outer	64.780	62.737	543
Mouth	64.781	62.877	531
Flandres Bay	65.046	63.260	493
InnerA	65.054	63.105	679
InnerB	65.105	63.146	678
Outer	65.003	63.316	724
Barilari Bay	65.920	64.716	620
Inner	65.944	64.637	610
Outer	65.773	64.855	630
St. B	64.857	65.345	578
St. E	65.973	67.293	597
St. F	66.984	69.713	590

3685 .

3686 **Supplementary Table 2.2** Summary of the environmental data utilized for the Canonical Analysis of Principal Coordinates. Temperature data
 3687 represents bottom temperatures > 350 m collected via CTD. Primary production rates represent annual estimates based on uptake rates of silicic
 3688 acid during incubations onboard at the time benthic images were collected.

	Transect	Area (cm ²)	Sediment (%)	Percent Hard (%)	Density (m ⁻²)	Temp. (°C)	PP_Si (mgCm ⁻² y ⁻¹)	PP_N (mgCm ⁻² y ⁻¹)	Distance (km)
Andvord Inner	1285	40.3	60.6	0.374	5.61	-0.034	366.47	528.68	6.2
Andvord Inner	1286	56.5	62.9	0.296	3.80	-0.035	511.55	609.83	6.2
Andvord Middle	1337	49.3	68.7	0.690	10.10	0.048	333.95	273.35	11.1
Andvord Middle	1338	43.9	67.1	0.533	8.18	0.010	419.09	317.17	11.1
Andvord Mouth	1289	70.1	61.2	0.212	1.60	0.013	308.27	247.39	20.8
Andvord Mouth	1290	66.0	65.9	0.417	2.65	0.000	417.85	-	20.8
Andvord Outer	1283	46.3	65.7	0.245	3.59	0.017	354.27	566.43	16.4
Andvord Outer	1284	48.4	68.9	0.265	4.91	0.042	419.04	675.51	16.4
Barilari Inner	1295	50.2	76.4	0.128	2.92	0.952	405.05	543.79	8.71
Barilari Inner	1297	37.6	80.6	0.056	2.15	0.932	-	-	8.71
Barilari Outer	1300	50.0	74.3	0.088	2.14	0.919	533.38	526.97	27.7
Flandres Inner A	1279	92.8	62.1	0.320	2.83	0.827	364.86	420.72	6.3
Flandres Inner A	1280	126.8	65.2	0.300	3.28	0.757	566.64	505.05	6.3
Flandres Inner B	1276	118.4	56.5	0.871	8.38	0.754	328.69	430.74	7.8
Flandres Inner B	1278	67.5	54.8	1.000	13.2	0.753	356.82	444.86	7.8
Flandres Outer	1281	163	45.5	0.561	1.24	0.926	508.62	442.45	16.4
Flandres Outer	1282	136.6	44.0	0.475	2.09	0.971	654.27	610.73	16.4

3689

3690

3691 **Supplementary Table 2.3** List of megafaunal morphotypes (or putative species) identified in this study. Morphotypes unique to this study
 3692 compared to those identified in Grange and Smith (2013) for the same study sites are denoted with *.

3693	Annelida	3714	Bryozoa	3735	Cnidaria
3694	<i>Amythas membranifera</i>	3715	Bryozoan sp. 1 (<i>Cellarinella</i> sp.) *	3736	Anemone sp. 2
3695	<i>Chaetopterus</i> sp. 1 *	3716	Bryozoan sp. 2 (<i>Camptoplites</i> sp.)	3737	Anemone sp. 3
3696	<i>Prionosyllis kerguelensis</i>	3717	Bryozoan sp. 3 (<i>Cellaria</i> sp.) *	3738	Anemone sp. 7
3697	Sabellid sp. 1	3718	Bryozoan sp. 4 *	3739	Anemone sp. 14 *
3698	Polynoid sp. 2	3719	Bryozoan sp. 5 *	3740	Hormathiid anemone sp. 1
3699	Serpulida sp. 1 *	3720	Bryozoan sp. 6 *	3741	Primnoid sp. 1
3700	Arthropoda - Crustacea	3721	<i>Reteporella</i> sp. *	3742	Coral sp. 1 *
3701	Ampeliscid amphipod	3722	Chordata - Tunicata	3743	Hydroid sp. 1
3702	Amphipod sp. 1 - Eusirid	3723	<i>Cnemidocarpa verrucosa</i>	3744	Hydroid sp. 5 (<i>Ophiodes arboreus</i> ?) *
3703	Amphipod sp. 3 - <i>Anthomastus commensal</i>	3724	<i>Pyura bouvetensis</i>	3745	<i>Ptychogastria Polaris</i>
3704	<i>Ceratoserolis meridionalis</i>	3725	Tunicate sp. 2	3746	Echinodermata - Asteroidea
3705	Krill sp. 1 *	3726	Tunicate sp. 4	3747	Asteroid sp. 1
3706	<i>Notocrangon antarcticus</i>	3727	Tunicate sp. 5	3748	Asteroid sp. 3 (<i>Diplasterias brucei</i>)
3707	Scallopiformes sp. 1 *	3728	Tunicate sp. 11 *	3749	Asteroid sp. 9 (<i>Lophaster gaini</i>) *
3708	Arthropoda - Pycnogonida	3729	Tunicate sp. 12 *	3750	<i>Cuenotaster involutus</i>
3709	Pycnogonida sp. 1	3730	Chordata - Pisces	3751	Echinodermata - Crinoidea
3710	Pycnogonida sp. 4 *	3731	<i>Chaenodraco wilsonii</i>	3752	Crinoid sp. 4 *
3711	Brachiopoda	3732	Fish sp. 1	3753	Echinodermata - Echinoidea
3712	Brachiopoda sp. 1	3733	Fish sp. 5 (<i>Channichthyidae</i> sp.)	3754	Echinoid sp. 1 (<i>Sterechinus neumayeri</i> ?)
3713		3734	<i>Pleuragramma antarcticum</i>	3755	

3756	Echinodermata - Holothuroidea	3766	Nemertea	3776	Porifera sp. 7 *
3757	<i>Rhipidothuria racowitzai</i>	3767	<i>Parborlasia corrugatus</i>	3777	Porifera sp. 8 *
3758	Echinodermata - Ophiuroidea	3768	Porifera	3778	<i>Stylocordyla borealis</i>
3759	<i>Ophionotus victoriae</i>	3769	Porifera sp. 1 *	3779	<i>Cinachyra antarctica</i>
3760	<i>Ophiosparte gigas</i>	3770	Porifera sp. 2 *	3780	Demospongiae sp. 1
3761	Ophiuroid sp. 1 *	3771	Porifera sp. 3 *	3781	Demospongiae sp. 2
3762	Mollusca	3772	Porifera sp. 4 (<i>Leucetta leptoraphis?</i>) *	3782	Demospongiae sp. 4
3763	Bivalve sp. 2	3773	Porifera sp. 5 (<i>Suberites</i> sp.?) *	3783	Demospongiae sp. 6 (<i>Kirkpatrickia variolosa</i>)
3764	<i>Marseniopsis</i> sp. 1 (<i>Marseniopsis mollis?</i>)	3774	Porifera sp. 6 (<i>Homaxinella</i> sp.?) *	3784	Demospongiae sp. 7
3765		3775		3785	Hexactinellid sp. 1
3786					
3787					
3788					
3789					
3790					
3791					
3792					
3793					
3794					

3795 **Supplementary Table 2.4** Rank abundance of top five morphotypes across all sites.

FJORD		
Andvord Bay	Flandres Bay	Barilari Bay
Bryozoan sp. 5	<i>Diplasterias brucei</i>	Tunicate sp. 5
Serpulida sp. 1	Brachiopod sp. 1	Bryozoan sp. 5
<i>Notocrangon antarcticus</i>	<i>Prionosyllis kerguelensis</i>	Bryozoan sp. 2
<i>Amythas membranifera</i>	Porifera sp. 7	Ophiuroid sp. 1
Anemone sp. 2	Porifera sp. 8	<i>Prionosyllis kerguelensis</i>
SHELF		
St. B	St. E	St. F
Hydroid sp. 4	Tunicate sp. 2	Porifera sp. 3
Bryozoan sp. 5	Demospongiae sp. 7	Hydroid sp. 4
<i>Diplasterias brucei</i>	Ophiuroid sp. 1	Porifera sp. 8
Scalpelliformes sp. 1	Hormathiid sp. 1	Brachiopod sp. 1
Tunicate sp. 5	<i>Chaetopterus</i> sp. 1	Bryozoan sp. 5

3796

3797

3798

3799

3800

3801

3802

3803

3804

3805

Supplementary Table 2.5 Fixed and random effect estimates for richness and abundance GLMMs. Area = dropstone plan area (cm²), Sediment = percentage of dropstone plan area covered in sediment, PercentHard = percentage of seafloor in an image to consist of exposed hard substrate, Density = dropstone density (m⁻²), and Habitat = distinction whether the dropstone occurred in the fjord or on the open shelf. Estimates represent the proportion of variance explained by that effect. Note that significant p-values are denoted with *.

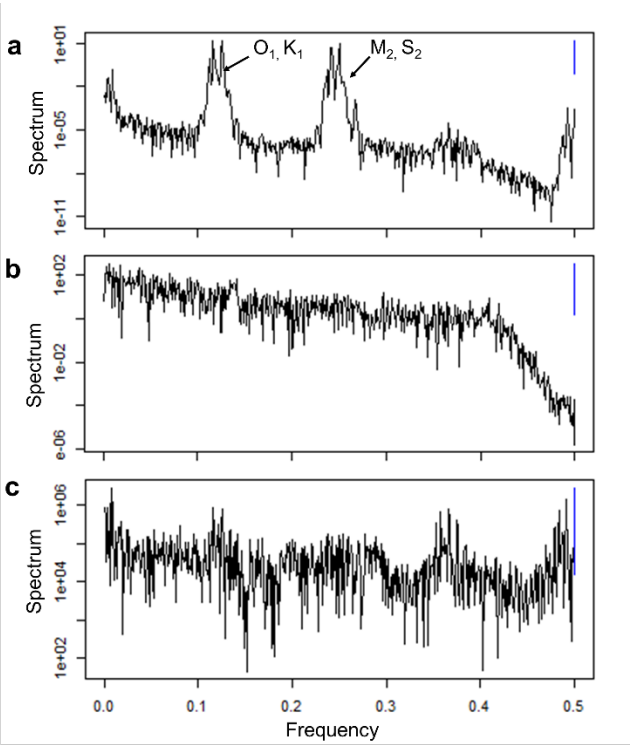
GLMM Fixed and Random Effect Estimates				
	Richness Model		Abundance Model	
Fixed Effects	Estimate	p-value	Estimate	p-value
log(Area)	0.311	< 2e ⁻¹⁶ *	0.512	< 2e ⁻¹⁶ *
Sediment	0.020	0.64	-0.029	0.55
Percent Hard	0.008	0.86	-0.003	0.96
Density	0.037	0.34	0.039	0.49
Habitat	0.296	0.08	0.148	0.53
Random Effects	Estimate	p-value	Estimate	p-value
Stone	-	-	0.407	-
Transect	-	-	0.127	-
Site	0.012	-	-	-

Supplementary Table 2.6 Summary of results from Canonical Analysis of Principle Coordinates (CAP). R² and p-values were determined using the “adonis” function in R for each environmental parameter; Area = Dropstone plan area, Sediment = Plan area of sediment cover, Density = dropstone density (m⁻²), PercentHard = percentage of exposed hard substrate, Temp = bottom temperature >350 m, Distance = distance from nearest glacial terminus (km), PP_Si = annual primary production (mgCm⁻²d⁻¹) based on average of two silicic acid uptake incubations.

	Area	Sediment	PercentHard	Density	Temp	Distance	PP_Si	PP_N
R ²	0.148	0.116	0.111	0.124	0.198	0.072	0.169	0.053
p-value	0.075	0.179	0.042*	0.0003*	0.065	0.150	0.003*	0.583

Supplementary materials for Chapter III:

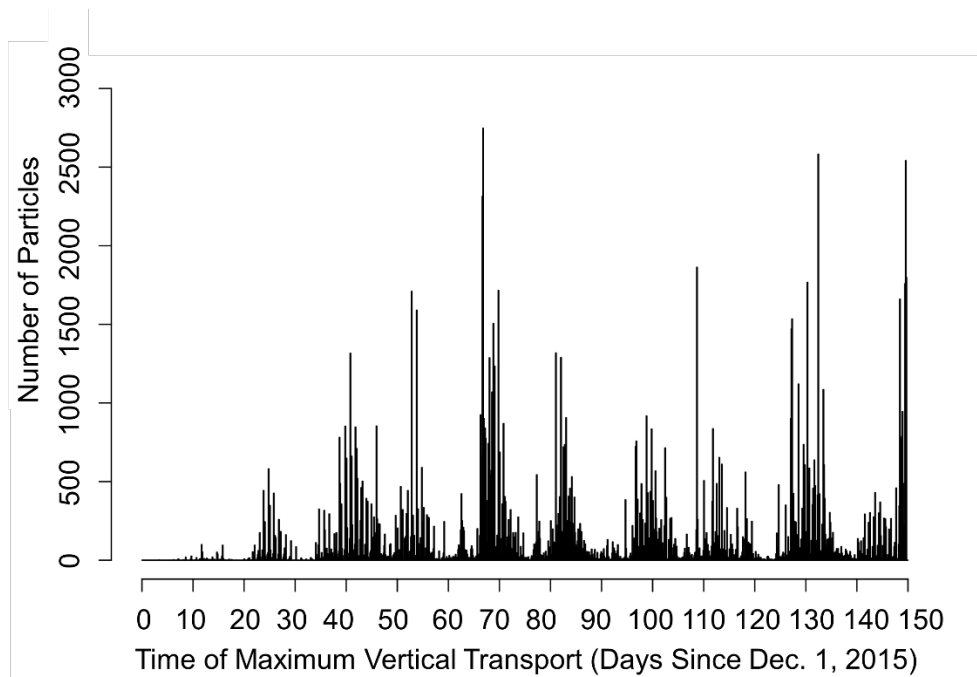
Spectral analyses were conducted in R using the package ‘psd’ (Barbour et al. 2019) which identified the dominant periodicities in data for sea-surface height (a proxy for tidal currents), wind speed and the time of maximum horizontal transport experienced by particles. We find similar dominant periodicities for each dataset present in the transport distribution (Figure 3.1).



Supplementary Figure 3.1 Periodograms resulting from spectral analysis of (a) Sea-surface height (m) (b) Wind speed (m/s) and (c) Time of maximum horizontal transport of particles from AndHigh simulations. Note the tidal component frequencies labeled in (a).

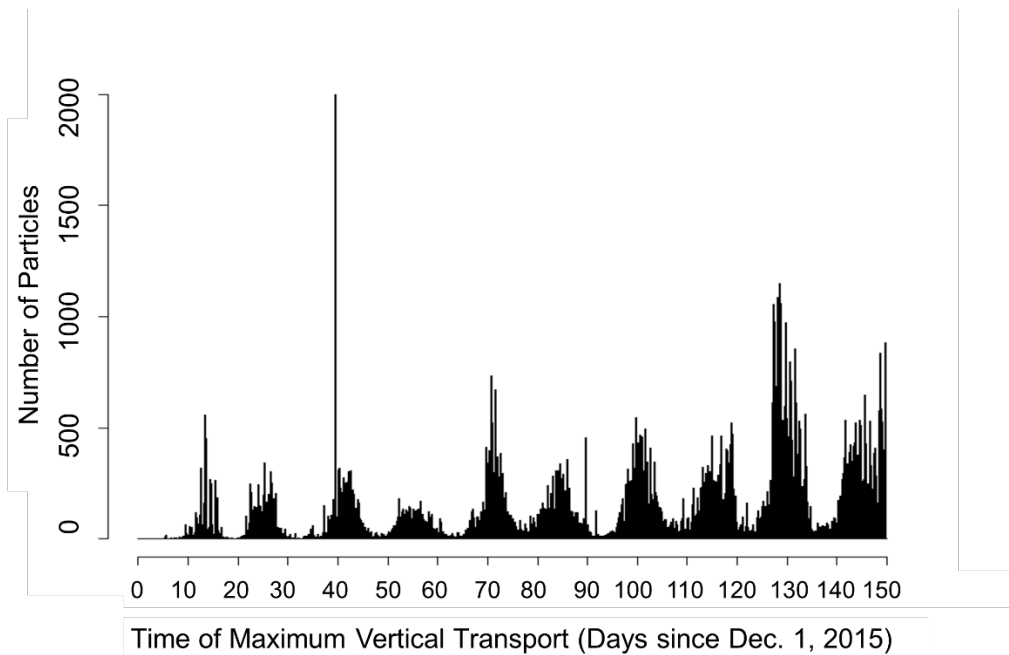
Times of maximum vertical transport of particles were also weakly correlated with overlying conditions including surface wind speed and surface current velocities. For AndHigh simulations, correlations

between the timing of maximum vertical transport and wind were weak ($\rho=0.035$) but stronger for current velocity (0.157). Similarly, for FlaHigh simulations correlation between the timing of maximum vertical transport and surface winds was weaker than for current velocity ($\rho=0.04$ and $\rho=0.172$, respectively). Peak times of maximum vertical transport for particles in both AndHigh and FlaHigh simulations were similar to the timing of maximum horizontal transport (e.g. approximately 68, 130 and 150 days).



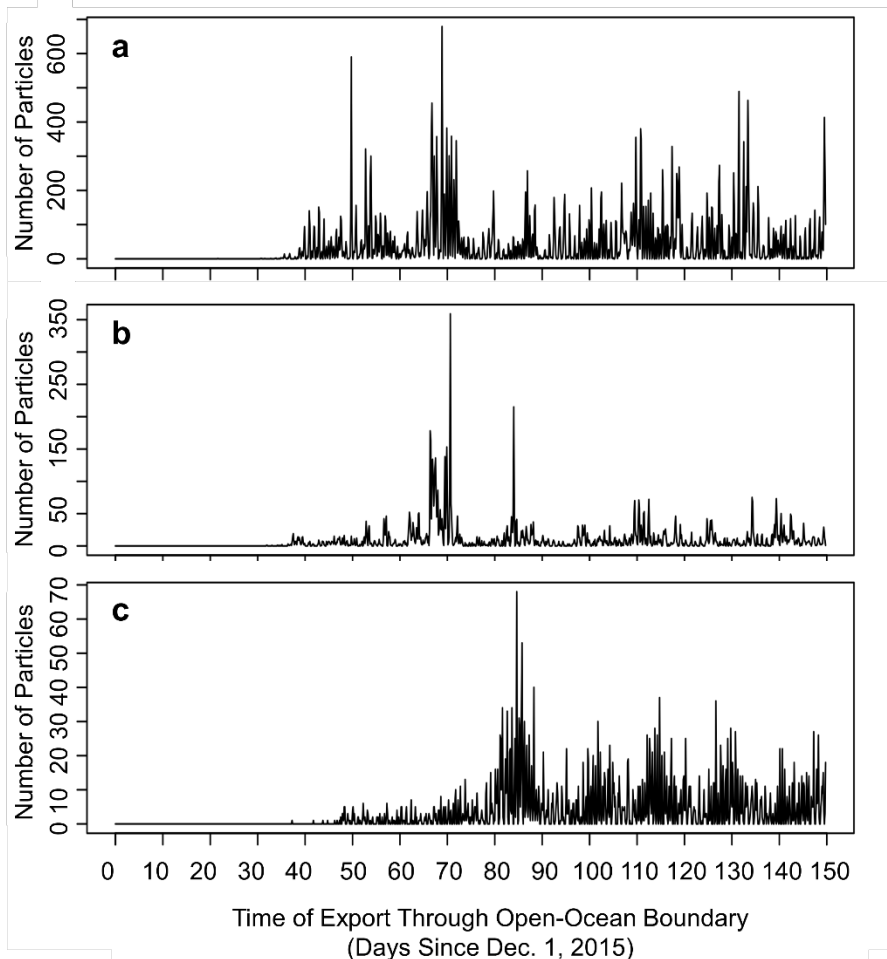
Supplementary Figure 3.2 Histogram reporting the number of particles experiencing their maximum vertical transport during the 150-day simulations (AndHigh). Note that the modes match those of the maximum horizontal transport as well as the times of export from the model domain (see Supplementary Figure 3.3).

Times of maximum vertical transport during FlaHigh simulations were slightly different from those in AndHigh simulations, with a large peak at day 40 and smaller peaks around day 130 and 150.



3848

3849 **Figure 3.3** Histogram reporting the number of particles experiencing their maximum vertical transport
 3850 during the 150-day simulations (FlaHigh). Note that the modes roughly match those of the maximum
 3851 horizontal transport as well as the times of export from the model domain (see Supplementary Figure
 3852 3.4).



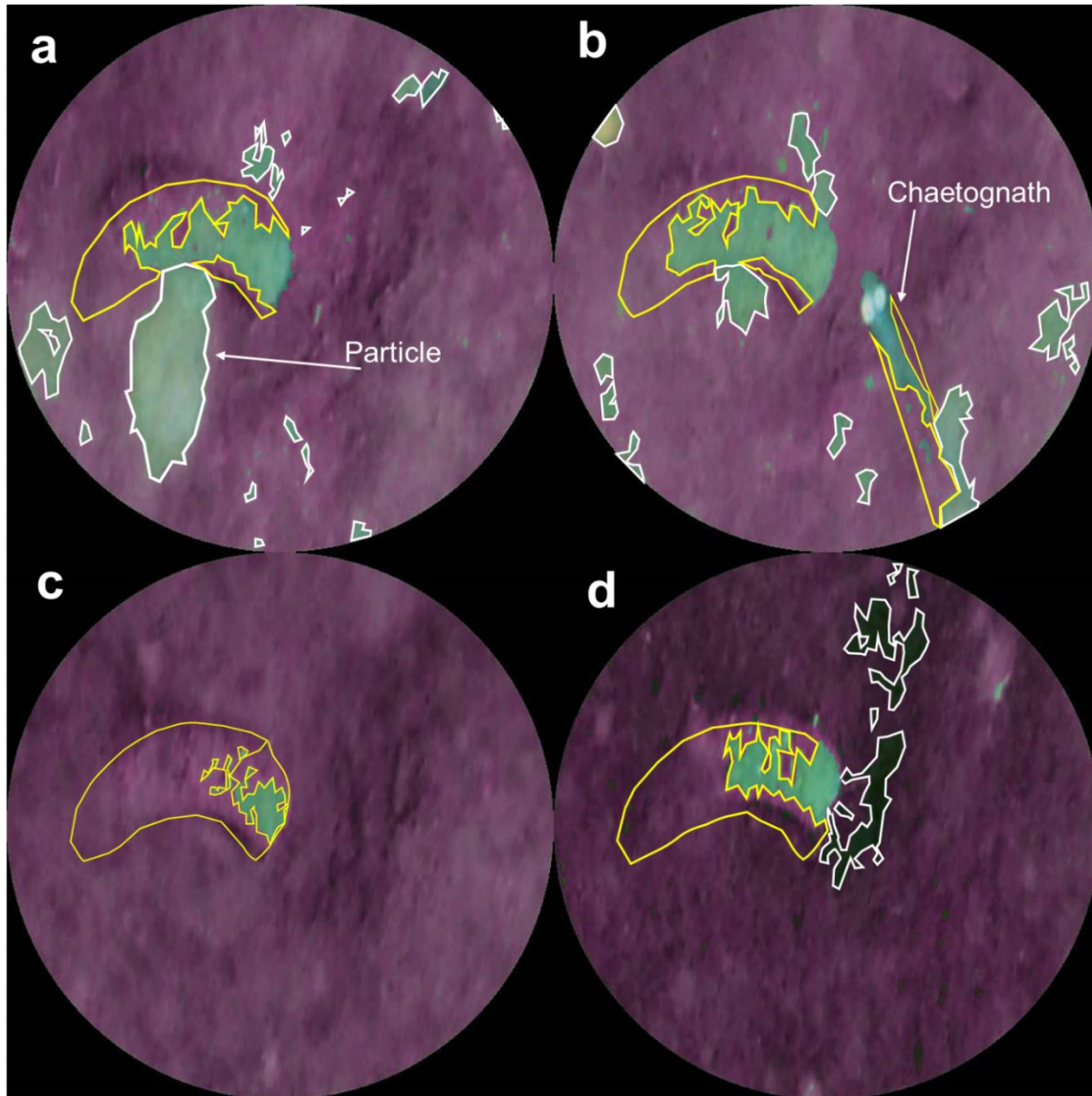
Supplementary Figure 3.4 Histograms of particle export through open-ocean boundaries of the main Gerlache Strait (a), northern Gerlache Strait (b) and the Bismarck Strait (c).

Supplementary materials for Chapter IV:

Assessing the success of the color-recognition procedure

The quantification of phytodetritus cover in this study relied upon visual identification of phytodetritus to first generate the definition of phytodetritus in HSV color-space. Therefore, assessment of the success of the resulting color-recognition procedure also relies upon visual comparison. Supplementary Figure 3.1 shows 4 images used to quantify seafloor phytodetritus cover in which pixels selected as phytodetritus have been colored pink. Visual inspection of these images revealed some places where the algorithm

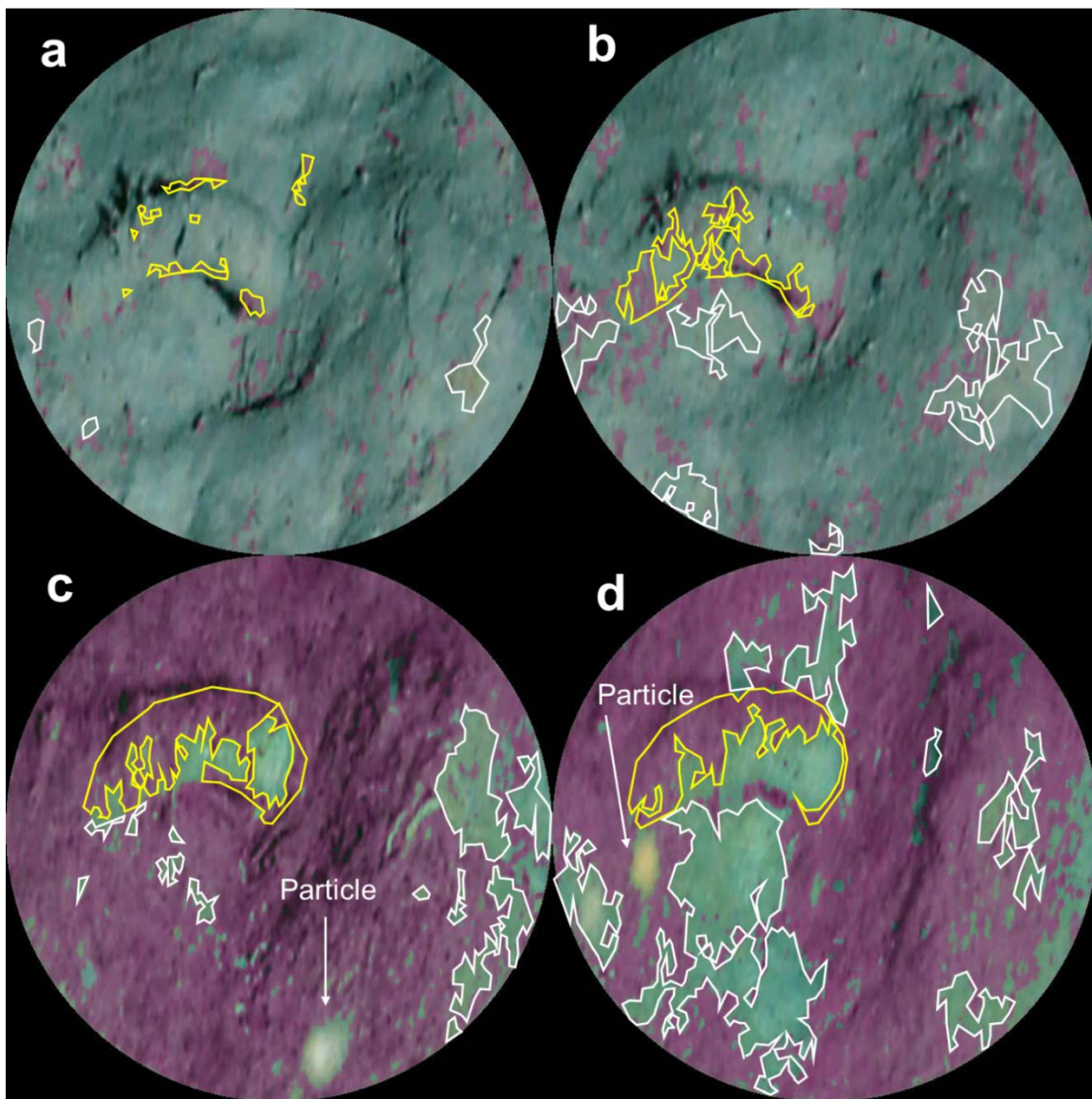
failed to select pixels that appear to be phytodetritus (white outlined regions) and other places where the algorithm misidentified phytodetritus (yellow outlined regions). Both occurred at times in the same image (Supplementary Figure 4.1, a-b, d) and often underestimates were caused by particles or transparent organisms (e.g. chaetognaths) altering the color of the seafloor behind them (Supplementary Figure 4.1, a-b). Overestimated phytodetritus was mostly caused by selection of phytodetritus on top of the *A. membranifera* tubes but also selection of fecal casts as phytodetritus.



Supplementary Figure 4.1. Examples of *A. membranifera* feeding regions in which phytodetritus has been selected by the color-recognition procedure (pink pixels) during the peak phytodetritus accumulation

period in January 2016. White outlined regions indicate where the algorithm failed to identify phytodetritus that is present, and yellow outlined regions indicate where the algorithm misidentified sediments or *A. membranifera* tube as phytodetritus. Phytodetritus cover for each is (a) 77.8%, (b) 85.4%, (c) 91.8%, and (d) 87.2%. The images were taken on: (a) 1/5/16, (b) 1/6/16, (c) 1/7/16 and (d) 1/9/16. The arrows indicate locations of (a) a particle and (b) a chaetognath obscuring the seafloor behind them.

Phytodetritus cover is most obvious to the naked eye between January 4 - February 16, 2016 when phytodetritus deposition rapidly increased and prior to a turbidity event when visibility dramatically decreased. Although the pixel selection algorithm may have been measuring phytodetritus cover accurately prior to January 4th, 2016, visual assessment of success is difficult as the algorithm can determine cover at the pixel scale, but a human can only see larger aggregations of phytodetritus. Therefore, in photographs captured before January 4th, 2016 it is difficult to assess the success of the algorithm. It isn't until phytodetritus accumulates more broadly along the seafloor (after January 4th, 2016) that it is distinct enough to delineate in photographs visually (Supplementary Figure 4.2, c-d). It is possible that because the range of HSV values used to define phytodetritus were determined primarily from photographs after January 4th, 2016 that the algorithm is poorly calibrated for the previous period. Similarly, the same definitions were used for the second deployment of the camera (April 23 - September 14, 2016) during which time phytodetritus quantification may be less accurate. Because we are most interested in the period of most rapid accumulation and consumption of phytodetritus (January 4th - April 6, 2016), we are confident that it is this period for which the algorithm performs best. Therefore, though there are many possible sources of error, we are confident that by measuring many replicate seafloor regions (see Chapter III Figure 4.5) and generating a daily averaged phytodetritus cover time series that we accounted for this variability and that the conclusions based on our photographic analyses are valid.

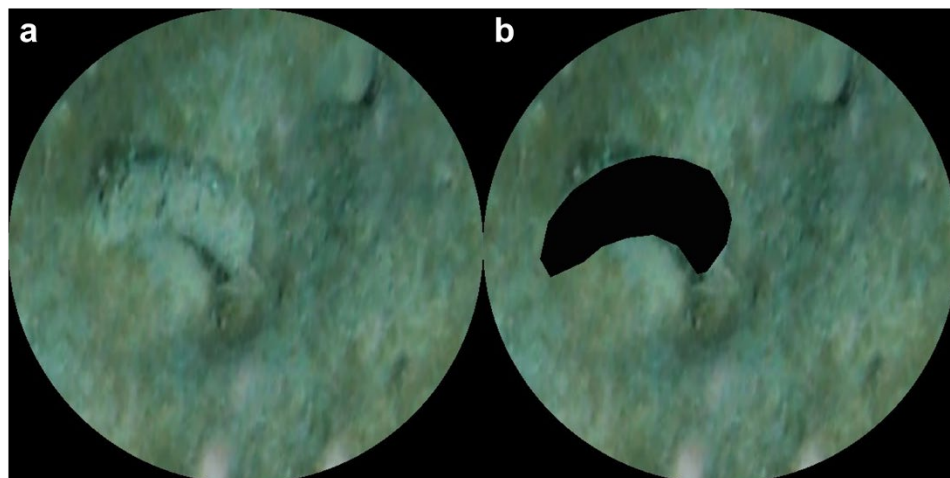


Supplementary Figure 4.2. Examples of *A. membranifera* feeding regions in which phytodetritus has been selected by the color-recognition procedure (pink pixels) prior to the deposition event (a-b) and after the event (c-d). White outlines regions indicate where the algorithm failed to identify phytodetritus that is visibly present, and yellow outlined regions indicate where the algorithm misidentified sediments or *A. membranifera* tubes as phytodetritus. Phytodetritus cover for each is (a) 3.7%, (b) 10.8%, (c) 59.4%, and (d) 37.9 %. The dates the images were taken are: (a) 12/8/15, (b) 12/29/15, (c) 1/29/16, and (d) 2/6/16. Note that in images (c-d) the phytodetritus is visually distinct from the background sediment compared to images (a-b).

3904

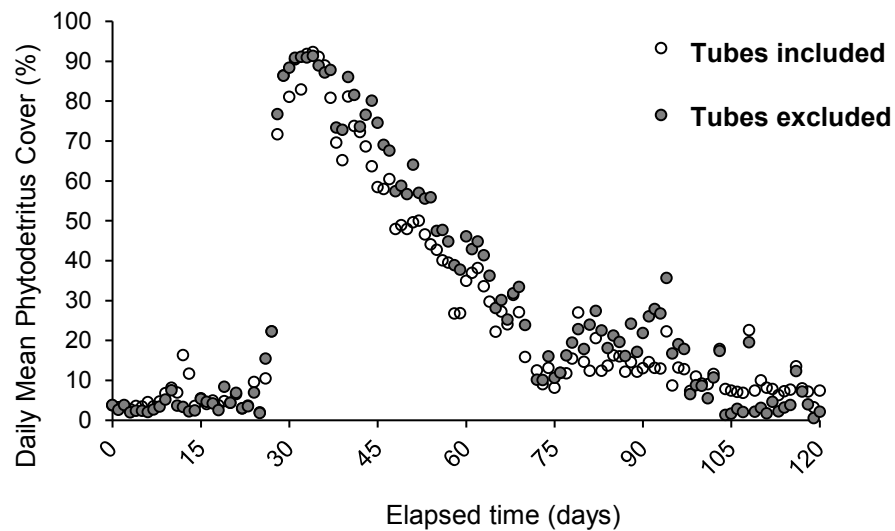
3905 The effect of *A.membranifera* tubes on seafloor phytodetritus quantification

3906 *Amythas membranifera* tubes shade or block a portion of the seafloor in the images used to quantify
3907 seafloor phytodetritus due to the oblique angle of the camera and strobe. To assess the effect of *A.*
3908 *membranifera* tubes on quantification of seafloor phytodetritus cover, we compared time series generated
3909 with and without inclusion of the tubes for the first 120 days of the time series when phytodetritus was
3910 present. The time series without ampharetid tubes was generated by masking *A. membranifera* tubes in
3911 each image prior to running the pixel selection algorithm in R (Supplementary Figure 4.3). The percent
3912 cover of phytodetritus was then calculated using the total area of seafloor minus the masked area of the
3913 tube. The pattern of seafloor phytodetritus cover was very similar regardless of inclusion or exclusion of
3914 *A. membranifera* tubes (Supplementary Figure 4.4). On average, seafloor phytodetritus cover was 5 %
3915 higher when *A. membranifera* tubes were included (Supplementary Figure 4.5) and a maximum
3916 difference of 13 % occurred when phytodetritus had accumulated and covered part of base of the
3917 otherwise excluded tube (Supplementary Figure 4.6). The excluded area ranged from approximately 48 -
3918 67 cm² which represented 5.9 - 8.3 % of the total image area. Though phytodetritus could accumulate
3919 atop the tubes, they were never 100 % covered by phytodetritus because *A. membranifera* actively lifted
3920 the tube opening to remain above at the surface of the phytodetritus layer. From these results, we
3921 concluded that phytodetritus cover was not significantly affected by the inclusion of *A. membranifera*
3922 tubes and the resulting time series of phytodetritus cover was a robust and conservative estimate.

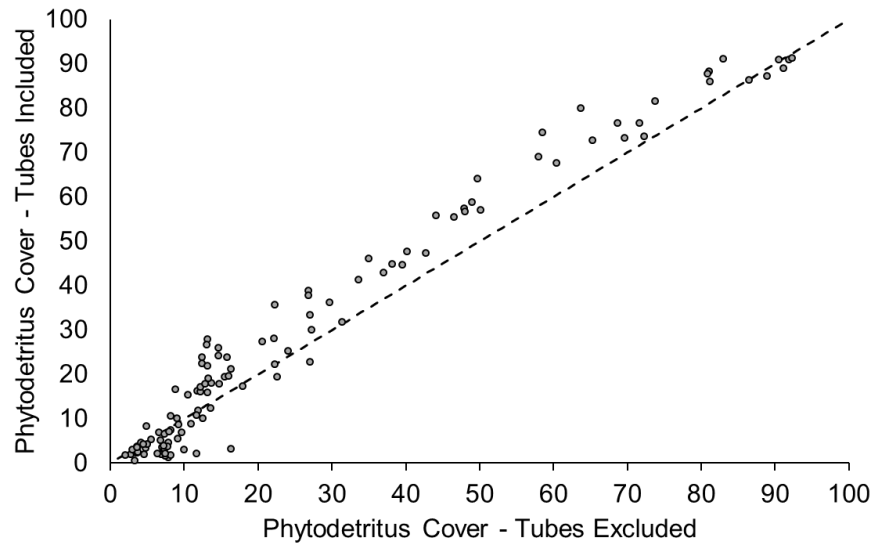


3923

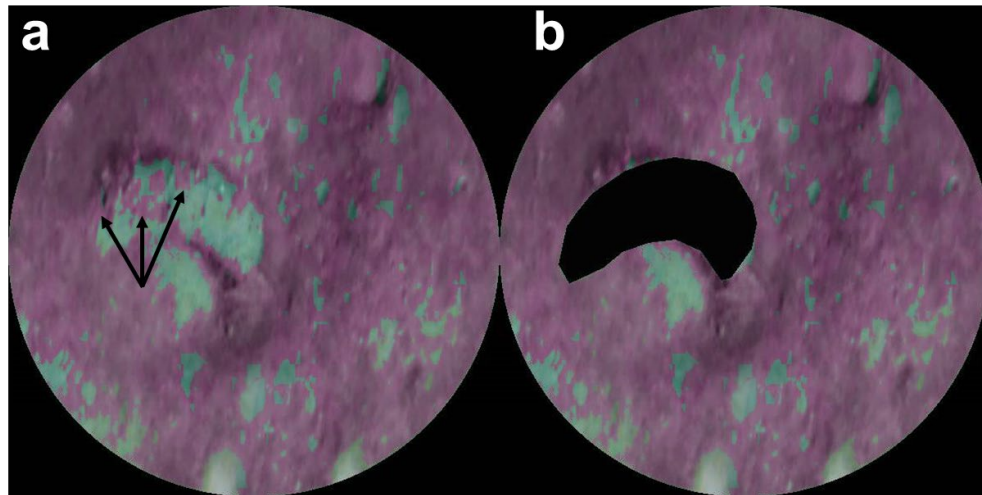
Supplementary Figure 4.3 Example of *A. membranifera* feeding region image including the tube (a) and excluding the tube (b) from which seafloor phytodetritus cover was measured.



Supplementary Figure 4.4 Comparison of the seafloor phytodetritus cover in *Amythas membranifera* feeding regions with (open circles) and without (solid circles) the tube included in the photographs as in Supplementary Figure 4.2.



Supplementary Figure 4.5 Comparison of seafloor phytodetritus cover in *A. membranifera* feeding regions with tubes included (y axis) and tubes excluded (x axis). The dashed line provides the 1:1 relationship. For points above this line, phytodetritus cover was greater with tubes included than with tubes excluded. The mean deviation from this 1:1 relationship was approximately 5 %, and up to 13 %.

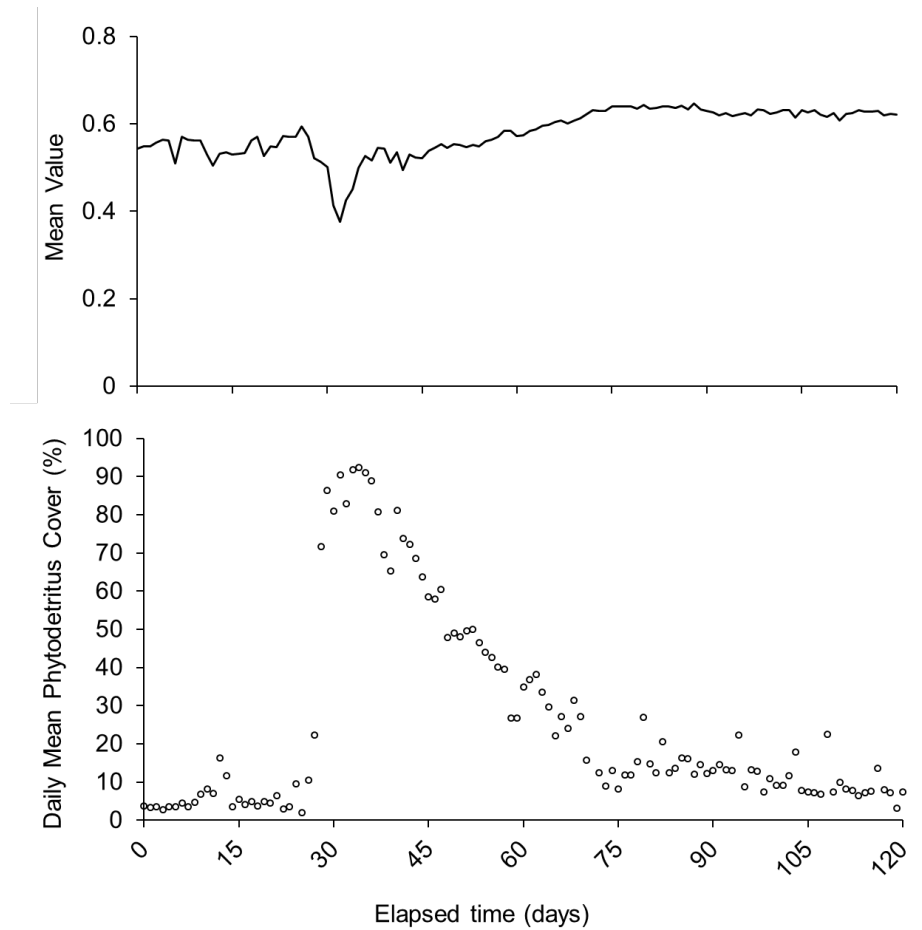


Supplementary Figure 4.6 Comparison of phytodetritus cover in *A. membranifera* feeding region including the tube (a) and excluding the tube (b) from January 5th, 2016. Pixels that were identified as phytodetritus by the algorithm have been colored pink. Note the phytodetritus covering the tube in (a) that is excluded from (b) shown by the black arrows. For reference, the phytodetritus cover in (a) is 71.7% and in (b) 76.7%.

Estimation of phytodetritus thickness

On January 11th, 2016 after 34 days of the camera deployment, phytodetritus reached maximum cover (92.3 %) but continued to accumulate creating a thick carpet of phytodetritus. This accumulation is visually obvious as the seafloor first turns green when phytodetritus covers the seafloor, then darkens as more phytodetritus is deposited on top of it. This is captured by the change in mean value (V in HSV color-space) of *A. membranifera* feeding regions which dramatically decreases (i.e. an increasing

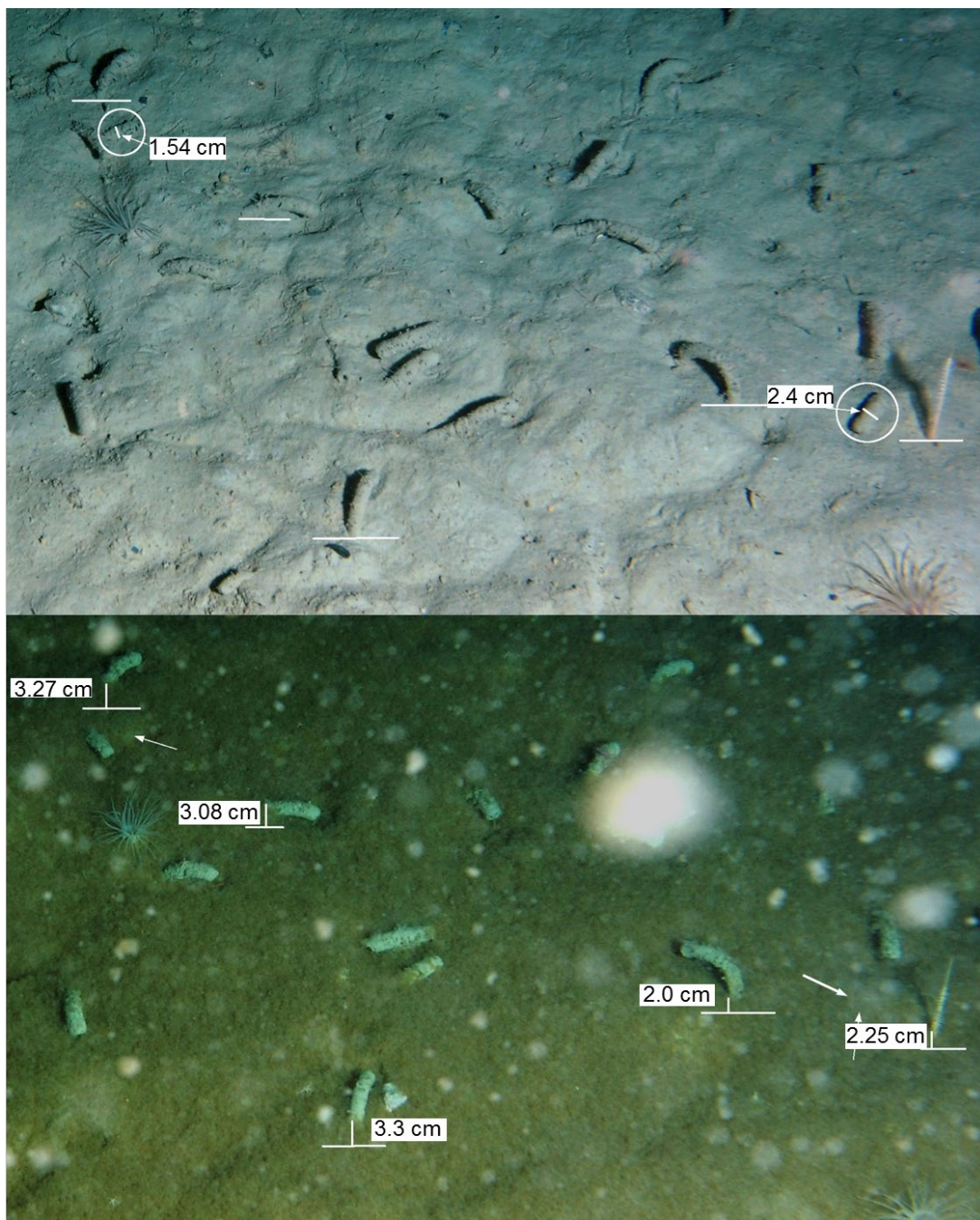
percentage of black in the color) when phytodetritus cover peaks (Supplementary Figure 4.7) and increases steadily after this period. Note that this trend also occurred in control regions of the seafloor indicating an accumulation across the entire seafloor.



Supplementary Figure 4.7 The mean value of *A. membranifera* feeding regions for the first 120 days of the time series compared to the mean seafloor phytodetritus cover within the same regions.

As phytodetritus accumulated on the seafloor, it not only covered the bases of *A. membranifera* tubes but also buried inactive *A. membranifera* tubes. We used these tubes to estimate the thickness of the phytodetritus layer needed to bury them. In the first image of the time series (Dec. 8, 2015) a line delineated the sediment-water interface at the base of *A. membranifera* and a nearly vertical coral (Supplementary Figure 4.7). The positions of these lines were transferred to the photograph from January

11, 2016 when peak phytodetritus accumulation and cover occurred (Supplementary Figure 4.8). The distance from the original sediment-water interface to the top of the phytodetritus layer surface was measured in each location and the mean phytodetritus thickness from these measurements was 2.9 cm. Two inactive *A. membranifera* tubes visible on Dec. 9th, 2015 were completely covered by phytodetritus on Jan. 11, 2016 (white arrows in bottom panel of Supplementary Figure 4.8). Assuming the tubes are cylindrical, the width of each tube should be equal to the minimum height of the tube if lying flat against the seafloor. The widths were 1.54 and 2.4 cm suggesting that 1.5-2.4 cm of phytodetritus at minimum was deposited on the seafloor. This estimate falls within the range measured at the base of other *A. membranifera* tubes and the coral (2.0 - 3.27 cm). Phytodetritus thickness could vary greatly along the seafloor as there are many small-scale topographic features on the seafloor including pits and bioturbation features visible in the photographs. However, our estimates are also consistent with phytodetritus layers collected in megacore samples in other regions of the West Antarctic Peninsula (C. R. Smith, Mincks, and DeMaster 2008) as well as field collections conducted in April 2016 from within Andvord Bay (up to 0.5 cm, C.R. Smith, unpub. data). Therefore, we are confident that approximately 3 cm of phytodetritus was deposited on the seafloor during our study.



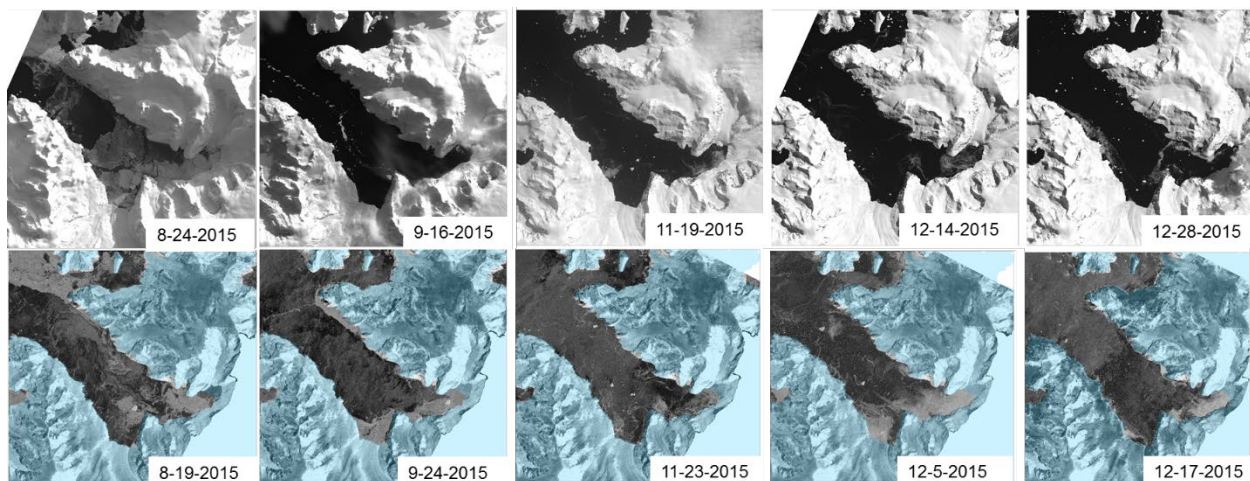
3979

3980 **Supplementary Figure 4.8** Measurement of phytodetritus thickness at bases of *A. membranifera* tubes,
 3981 a nearly vertical coral (far right), and from burial of inactive *A. membranifera* tubes at peak phytodetritus
 3982 cover and accumulation on January 11th, 2016. The first image in the time series (Dec. 8, 2015, top
 3983 panel) was used as a reference for the location of the sediment-water interface (horizontal white lines)
 3984 from which to measure the thickness of phytodetritus (vertical white lines). White circles provide the

location of inactive *A. membranifera* tubes which become completely buried by Jan. 11th, 2016 and are indicated then by white arrows. The diameter of the tube is shown and assumed to equal the height and, thus, the minimum thickness of phytodetritus required to bury the tube.

Andvord Bay sea-ice cover prior to time-lapse camera records

Time-lapse camera records of sea-ice cover began on December 15, 2015. To assess sea ice conditions in Andvord Bay prior to this time period, we utilized Landsat 8 and Sentinel1 (SAR) satellite imagery from August - December 2015. Landsat images suggest that sea ice formation occurred until the end of August as indicated by light and grey patches of ice visible on August 24th, 2015 (Figure 4.9). Sea ice was advected into and out of Andvord Bay throughout October. During November, sea-ice concentration was low and declined to essentially 0% cover by early December. The reduction in sea ice cover within the fjord would allow for ample light conditions in the surface ocean promoting phytoplankton growth over weeks to months prior to the sedimentation event we observe in the seafloor time-lapse camera record.



Supplementary Figure 4.9 Satellite imagery showing sea-ice cover in Andvord Bay from August-December 2015. Top row: Landsat 8 satellite images on cloud-free days. Sea ice appears to be forming in August (8-24-2015 image) and the fjord clears in early September with no new ice formation visible in following months. Bottom row: Sentinel1 satellite imager showing sea-ice cover in Andvord Bay on cloud-free days. Advected sea ice present throughout August-October with loose ice cover present in December.

4004 *References*

4005 Barbour, J. A., Parker, R. L. and Kennel, J. (2019) 'Package "psd", pp. 1–52.

4006 Smith, Craig R., Sarah Mincks, and David J. DeMaster. 2008. "The FOODBANCS Project: Introduction
4007 and Sinking Fluxes of Organic Carbon, Chlorophyll-a and Phytodetritus on the Western Antarctic
4008 Peninsula Continental Shelf." *Deep-Sea Research Part II: Topical Studies in Oceanography* 55
4009 (22–23): 2404–14. <https://doi.org/10.1016/j.dsr2.2008.06.001>.